

Chemistry on Unnatural Amino acid Peptide Building Blocks and Bioinspired Peptide Synthesis

**A thesis
Submitted in partial fulfilment of the requirements
of the degree of
Doctor of Philosophy**

**By
Sachitanand M. Mali**

ID: 20083014



Indian Institute of Science Education and Research, Pune

2014



Dedicated to My Beloved Family....
And
My Mentor

CERTIFICATE

This is to certify that the work incorporated in the thesis entitled “**Chemistry on Unnatural Amino acid Peptide Building Blocks and Bioinspired Peptide Synthesis**” submitted by Sachitanand M. Mali carried out by the candidate at the Indian Institute of Science Education of Research (IISER), Pune, under my supervision. The work presented here or any part of it has not been included in any other thesis submitted previously for the award of any degree or diploma from any other University or institution.

19th February, 2014

Dr. Hosahudya N. Gopi
(Research Supervisor)
Associate Professor, IISER, Pune
Pune-411008, India

Declaration

I hereby declare that the thesis entitled “**Chemistry on Unnatural Amino acid Peptide Building Blocks and Bioinspired Peptide Synthesis**” submitted for the degree of Doctor of Philosophy in Chemistry at Indian Institute of Science Education of Research (IISER), Pune has not been submitted by me to any other University or Institution. This work was carried out at the, Indian Institute of Science Education of Research (IISER), Pune, India under supervision of Dr. Hosahudya N. Gopi.

19th February, 2014

Sachitanand M. Mali
ID: 20083014
Senior Research Fellow
Dept. of Chemistry, IISER-Pune
Pune - 411008

Acknowledgements

My first debt of gratitude must go to my advisor, Dr. Hosahudya N. Gopi. He patiently provided the vision, encouragement and advice necessary for me to proceed through the doctoral program and complete my dissertation. Sir, I want to present my deepest appreciation for your unflagging encouragement and serving as a role model mentor. You have been a strong and supportive adviser to me throughout my PhD tenure. Your principles of life and dedication to work have always inspired me during my graduate studies. Thank you sir for your valuable guidance and developing me as researcher.

I would like to extend my sincere thank to our Director Prof K. N. Ganesh for providing such excellent infrastructure and research facility here at IISER Pune. His enthusiasm about science was always source of inspiration.

I am sincerely thankful to my research advisory committee members Dr. Ramakrishna G. Bhat (RGB) and Dr. Srinivas Hotha for their valuable suggestions during my RAC meetings which helped me a lot to shape my research projects. I also present my sincere appreciation to all chemistry faculties of IISER, Pune for their cooperation and guidance. I would like to acknowledge CSIR India for providing research fellowship during the last five years.

I thanks to Dr. K. M. P. Raja (Madurai Kamaraj University) for NMR modelling structures and Dr. T. S. Mahesh for his help in 2D NMR experiments. I would like to extend my sincere thanks to Dr. H. V. Thulasiram (NCL, Pune) and his lab for their kind cooperation during my PhD. I also acknowledge Prof. Daniel Werz (Technical University of Braunschweig, Germany) for the theoretical calculation studies.

I am fortunate to work with excellent blend of talented and unique labmates who helped me a lot in solving my research problems. Their moral support and helping nature gave me strength to move forward during my critical time. I have very special appreciation to the Dr. Anupam Bandyopadhyay and Sandip Jadhav. With these two guys I started my research carrier and shared every moment of frustration as well as joy. I am very much thankful to Ganesh and Sushil for their kind hearted selfless helping attitude. There was time being funny and playful with Rajkumar (Razz). I am indebted to shiva shankar for his cooperation during my research. I enjoyed working with all my junior labmates Rupal, Sumit, Anindita, Rahi, Ankita, Mona, Viresh, Varsha and shivani and present my sincere thank for their several kind of research support. The Dr. Gopi's lab will be unforgettable place in my life.

I must acknowledge the help from Puja Lunawat for NMR analysis, Archana for X-ray instrument, Swati Dixit for MALDI TOF/TOF mass analysis. My Special thank to Mr. Nitin Dalvi for assisting my research with purchase orders and other help. I thankful to Mahesh and Mayuresh for the administrative help.

Life becomes boring if I would not have met wonderful friends Prakash and Nitin (Nana). As we have been together for long time and shared every moment and experience of life. They were always there for me whenever I required. Their kind and helping attitude always supported me in my difficult time. I present my deepest thank for you both guys for bearing me for such a long time. I have very deep gratitude to my friends from Dr. BAMU, Aurangabad Dr. Santosh Katkar and Dr. Jawale Patil for being with me at every moment.

Further I would like to extend my special thank to Dr. Amar, Deepak, Pramod (Nandu), Arun (Sir), Vijay, Maroti, Shekhar, Gopal, Biplap, Arvind, Shamaprasad Nandi, Dnyaneshwar, Sharad, Tribak, Satish, Prabhakar, Shahaji, Anupam Sawant, Abhik, Madan, Sanjog, Kundan and all friend from chemistry department as well as the friend from NCL Pune, Prakash Chavan, Kishor Harale, Harshal, Rahul Patil, Kailas, Manoj, Kiran Patil, Rahul Kavthe, Valmik, Ganesh shitre for their cooperation.

It would have difficult to complete my PhD work without support from my family. I present my deepest gratitude to my family especially to my parents for their unconditional love and support. The care by my sisters and their love was always behind me during my PhD tenure. My brother Shiva always insisted me to do better, I present my thanks for believing in me. Most importantly I would like express my heartfelt thank to my beloved wife Chaitanya for her encouragement, support and patience during the last days of my PhD. Her love and helpful spirit have made this dissertation possible. Thank you Chaitanya for being too supportive and understanding.

Finally I would like to pray Lord Ganesh for giving me strength and his blessing to complete my research work and submit this thesis.

Sachitanand M. Mali

Contents

Abbreviations	vii
Abstract of thesis	x
Publications	xi

Chapter 1: Exploring the reactivity of E-vinylogous amino acids and their utility in the design of stable β -hairpins

1.1 Introduction	2
1.1.1 Beta amino acids in hybrid foldamers	4
1.1.2 Vinylogous amino acids in biologically active natural products	6
1.1.3 Earlier synthetic protocols for the synthesis of vinylogous amino acids	7
1.2 Aim and rational of present work	7
<u>Section 1A</u>	
1A.3 Results and Discussions	8
1A.3.1 Racemization study for vinylogous amino acid by Chiral HPLC	12
1A.3.2 Crystal structure analysis of the vinylogous amino esters and dipeptides	13
1A.3.3 CD analysis for the vinylogous amino acid containing hybrid peptides	18
<u>Section 1B</u>	
1B.1 Introduction	19
1B.2 Results and discussion	21

1B.2.1 Crystal structure analysis for the β-OBt substituted γ-amino esters	23
1B.2.2 Synthesis of β-OBt substituted γ-amino acid containing peptides	25
1B.2.3 Elimination reaction of OBt-substituted γ-amino esters and amides to unsaturated γ-amino acids and amides	27
<u>Section 1C</u>	
1C.1 Introduction	28
1C.2 Result and discussion	30
1C.2.1 Synthesis of <i>ortho</i>-nitro benzyl protected thiostatines	30
1C.2.2 Synthesis of thiostatines containing peptide P1 and peptides P2	33
1C.2.3 Solution structure analysis of peptide P3	35
1C.2.4 Solution structure of thiostatine bridged β-hairpin peptide P4	40
1.2 Conclusions	45
1.3 Experimental Section	46
1.3.2 Synthesis procedure and compound characterization for Section 1A	47
1.3.3 Synthesis procedure and compound characterization for Section 1B	61
1.3.4 Synthesis procedure and compound characterization for Section 1C	77
1.4 References	86
1.5 Appendix I: Characterization data of synthesized compounds	95

Chapter 2: Utilization of thioacids in copper (II) mediated mild and fast peptide synthesis and N-acylation of amines

Section 2A

2A.1 Introduction	106
2A.1.1 Overview of peptide synthesis	107
2A.1.2 Solid phase peptide synthesis	109
2A.1.3 New approach for peptide construction: Chemical Ligation	109
2A.1.4 Native chemical ligation	111
2A.1.5 Other approaches for chemical ligation	112
2A.1.6 Thioacid in origin of life	113
2A.1.7 Versatile reactivity of thioacid with different functional groups	113
2A.2 Aim and rational of present work	114
2A.3 Results and discussion	116
2A.3.1 Powder XRD study of the byproduct obtained in the reaction mixture	119
2A.3.2 Racemization studies by using peptides, D1 = Boc-^LAla-Leu-OMe, D2 = Boc-^DAla-Leu-OMe, D3= Boc-(±)Ala-Leu-OMe	119
2A.3.3 Possible mechanism for CuSO₄·5H₂O mediated peptides synthesis	122
2A.4 Conclusions	123

Section 2B

2B.1 Introduction	123
2B.2 Aim and rational of the present work	124
2B.3 Results and discussion	124

2B.3.1 Benzoylation of aliphatic and aromatic amines using thiobenzoic acids	128
2B.3.2 N-Acylation of fatty acids using thiooctanoic and thiododecanoic Acids	129
2B.4 Conclusions	131
2.2 Experimental section	131
2.2.1 Synthesis procedure and compound characterization for Section 2A	132
2.2.2 Synthetic procedure and compound characterization for Section 2B	135
2.3 References	157
2.4 Appendix I: Characterization data of synthesized compounds	160

Chapter 3: Synthesis of N-protected amino thioacids and their utilization in thioacid oxidative dimers and peptide synthesis

3.1 Introduction	168
3.1.1 Reported protocols for the synthesis of N-protected amino thioacids	169
3.2 Aim and rational of present work	171
3.3 Results and discussion	171
3.3.1 Crystal structure of thioacid oxidative dimers of N-Boc-Ala and N-Boc-Aib	175
3.3.2 Possible mechanism of the synthesis of N-protected amino thioacids from thioacetic acid and NaSH	175
3.3.3 Utilization of thioacid oxidative dimers in peptide synthesis	177
3.3.4 Racemization study of peptides, P5 = Boc-Phe-^LVal-OMe, P6 = Boc-Phe-^DVal-OMe and P5 & P6 = Boc-Phe-(±)Val-OMe	179

3.3.5 Utilization of <i>N</i>-protected amino thioacids in peptide synthesis	179
3.3.6 Amino thioacids mediated synthesis of other <i>N</i>-protected amino thioacids and its subsequent utilization in peptide synthesis	181
3.3.7 Amino thioacid mediated polypeptide library synthesis in aqueous condition	185
3.4 Conclusions	187
3.5 Experimental	187
3.6 References	203
3.7 Appendix I: Characterization data of synthesized compounds	205

Chapter 4: Utilization of thiazole δ -amino acids in the design of cyclic peptide self assemblies

4.1 Introduction	212
4.1.1 Chalcogen-Chalcogen interactions in mediating the organic Transformations	214
4.1.2 Chalcogen-Chalcogen interactions in biological system	214
4.2 Aim and rationale of the present work	215
4.3 Result and discussion	216
4.3.1 Crystal structure and self assembly analysis of the structure obtained from methanol	217
4.3.2 Crystal and self assembly analysis of the structure obtained from toluene	220

4.3.3 Crystal and self assembly analysis of the structure obtained from Chlorobenzene	223
4.3.4 Crystal and self assembly analysis of the structure obtained from ethyl acetate	225
4.3.5 Crystal structure and self assembly analysis of the peptide structure 6 obtained from Ethyl acetate	226
4.3.6 Theoretical studies of S...O interactions using MP2/6-311G++(3df,3dp) level of theory	229
4.4 Conclusions	231
4.5 Experimental section	231
4.6 References	243
4.7 Appendix I: Characterization data of synthesized compounds	247

Abbreviations

Ac = Acyl

Ac₂O = Acetic anhydride

ACN = Acetonitrile

Aib = α -Amino isobutyric acid

Ar = Aryl

Bn = Benzyl

Boc = tert-Butoxycarbonyl

(Boc)₂O = Boc anhydride

Bu = Butyl

Buⁱ- = Isobutyl

Bu^t- = Tertiary butyl

Calcd. = Calculated

Cbz = Benzyloxycarbonyl

CD = Circular Dichroism

COSY = Correlation spectroscopy

dg = dehydro gamma

DCC = *N, N'*-Dicyclohexylcarbodiimide

DCM = Dichloromethane

DiPEA = Diisopropylethyl Amine

DMF = Dimethylformamide

DMSO = Dimethylsulfoxide

DNA = Deoxyribonucleic acid

EDC = Ethyl-*N, N*-dimethyl-3-aminopropylcarbodiimide

EtOH = Ethanol

EtOAc = Ethyl acetate

Fmoc = 9-Fluorenylmethoxycarbonyl

Fmoc-OSu = *N*-(9-Fluorenylmethoxycarbonyloxy) succinimide

g = gram

hrs = hours

HBTU = O-Benzotriazole-*N,N,N,N'*-tetramethyluronium hexafluorophosphate

HCl = Hydrochloric acid

HOBt = Hydroxybenzotriazol

HPLC = High Performance Liquid Chromatography

IBX = 2-Iodoxybenzoic acid

LAH = Lithium Aluminium Hydride

MALDI-TOF/TOF = Matrix-Assisted Laser Desorption /Ionization – Time of Flight

Me = Methyl

MeOH = Methanol

mg = miligram

min = Minutes

μ L = Microliter

μ M = Micromolar

mL = milliliter

mM = millimolar

mmol = millimoles

m.p. = Melting Point

MS = Mass Spectroscopy

N = Normal

NHS = *N*-hydroxysuccinimide

NMP = *N*-methyl pyrrolidone

NMR = Nuclear Magnetic Resonance

NOE = Nuclear Overhauser Effect

PG = Protecting Group

ppm = Parts per million

Py = Pyridine

R_f = Retention factor

RMS = Root Mean Square

ROESY = Rotating Frame NOE Spectroscopy

RT = Room Temperature

TFA = Trifluoroacetic acid

THF = Tetrahydrofuran

TOCSY = Total Correlation Spectroscopy

S-ONB = S-*ortho* Nitro Benzyl

UV = Ultra Violet

Abstract

Non-ribosomal *E*-vinylogous γ -amino acids and the thiazole δ -amino acids are widely present in many peptide natural products. Many of these peptide natural products display broad spectrum biological activities including anti-cancer and anti-microbial activities. We sought to investigate the chemical reactivity of conjugated double bonds in *E*-vinylogous amino acids and their incorporation into peptides. Utilizing *E*-vinylogous amino acids, we developed novel thiostatines as H-bond surrogates to staple the two anti-parallel β -sheets in the designed β -hairpin structures. Though there are numerous strategies existed for the stapling of α -peptide helices, this is the first strategy that β -sheet or β -hairpin structures can be stapled through the backbone disulfide bonds of thiostatines. Further, the α , β -unsaturated acids have been scarcely explored as Michael acceptors in the conjugate addition reactions due to their poor reactivity, however, here we proved that unsaturated acids can be used as Michael acceptors in the presence of HBTU and developed a new strategy for the HOBt substituted γ -amino acids and peptides. Inspired by the serendipity of S- to N-acetyl group migration in the synthesis of thiostatines and the involvement of acyl-CoA in various acylation reactions in biology led us to investigate the thioacids mediated peptides synthesis in the presence of metal salts. We discovered that peptides can be synthesized in methanol using thioacids in the presence of copper sulfate. In addition, we have also demonstrated the selective *N*-acylation of various aliphatic and aromatic amines using thioacetic acid and copper sulfate. Inspired by the versatile reactivity of sulfur, persulfide and thioacids, we have developed a new synthetic strategy for the synthesis of *N*-protected thioacids and showed their utility in peptide synthesis in the presence and absence of metal salts. Overall these results demonstrate that peptides can be synthesized without using standard coupling agents. In addition, these results also support the speculation of thioacids as possible precursors in the synthesis of polypeptides in the prebiotic era. Finally, we investigated the involvement of sulfur in thiazole amino acids in the solvent dependent intermolecular chalcogen-chalcogen interactions. On the basis of these investigations we divided this thesis into four chapters. The summary of these investigations are given in this synopsis and details are provided in the main chapters of the thesis.

Publications

1. Thioacetic acid/NaSH mediated synthesis of *N*-protected amino thioacids and their utility in peptide synthesis.
Mali, S. M.; Gopi, H. N. *J. Org. Chem.* **2014**, *79*, 2377-2383.
2. Thioacids mediated selective and mild *N*-acylation of amines.
Mali, S. M.; Bhaisare, R. D.; Gopi, H. N. *J. Org. Chem.* **2013**, *78*, 5550-5555.
3. Copper (II) mediated facile and ultrafast peptide synthesis in methanol.
Mali, S. M.; Jadhav, S. V.; Gopi, H. N. *Chem. Commun.* **2012**, *48*, 7085-7087.
4. Thiazole–Carbonyl Interaction: A case study using phenylalanine thiazole cyclic tripeptides.
Mali, S. M.; Schneider, T. F.; Bandyopadhyay, A.; Jadhav, S. V.; Werz, D. B.; Gopi, H. N. *Crystal Growth & Design*, **2012**, *12*, 5643–5648.
5. Synthesis of α , β -unsaturated γ -amino esters with unprecedented high (*E*)-stereoselectivity and their conformational analysis in peptides.
Mali, S. M.; Bandyopadhyay, A.; Jadhav, S. V.; Kumar, M. G.; Gopi, H. N. *Org. Biomol. Chem.* **2011**, *9*, 6566-6574.
6. Synthesis and stereochemical analysis of β -nitromethane substituted γ -amino acids and peptides.
Kumar, M. G.; **Mali, S. M.**; Gopi, H. N. *Org. Biomol. Chem.* **2013**, *11*, 803-813.
7. Synthesis and structural investigation of functionalizable hybrid β -hairpin.
Bandyopadhyay, A.; **Mali, S. M.**; Lunawat, P.; Raja, K. M. P.; Gopi, H. N. *Org. Lett.* **2011**, *13*, 4482-4485.
8. Facile synthesis and crystallographic analysis of *N*-protected β -amino alcohols and short peptidebols.
Jadhav, S. V.; Bandyopadhyay, A.; Benke, S. N.; **Mali, S. M.**; Gopi, H. N. *Org. Biomol. Chem.* **2011**, *9*, 4182-4187.
9. Tin(II) chloride assisted synthesis of *N*-protected γ -amino β -keto esters through semipinacol rearrangement.
Bandyopadhyay, A.; Agrawal, N.; **Mali, S. M.**; Jadhav, S. V.; Gopi, H. N. *Org. Biomol. Chem.* **2010**, *8*, 4855-4860.

10. HBTU mediated 1-Hydroxybezotriazole (HOBt) conjugate addition: Synthesis and stereochemical analysis of β -OBt substituted γ -amino acids and hybrid peptides
Mali, S. M.; Kumar, M. G.; Gopi, H. N. (Manuscript submitted).
11. Synthesis and utilization of novel thiostatines in the design of stable β -hairpins and β -sheets through disulfide stapling.
Mali, S. M. and Gopi, H. N. (Manuscript under preparation)

Chapter 1

Exploring the reactivity of *E*-vinylogous amino acids and their utility in the design of stable β -hairpins

1.1 Introduction

Amino acids are the building blocks of polypeptides and proteins. By utilizing 20 ribosomally encoded amino acids, nature has produced a variety of proteins which are unique in their structure and functions. The function of proteins mainly depends on their three-dimensional structures. The sequences of the amino acids in the polypeptide chain are responsible for the three-dimensional protein structures. In spite of these ribosomal amino acids, which are responsible for protein structure and functions, there is a myriad of non-proteinogenic amino acids present in nature.¹ As these amino acids are not taking part in proteins they also defined as unnatural amino acids or non-ribosomal amino acids. These unnatural amino acids can be classified based on the position of the amino group on the carbon chain.

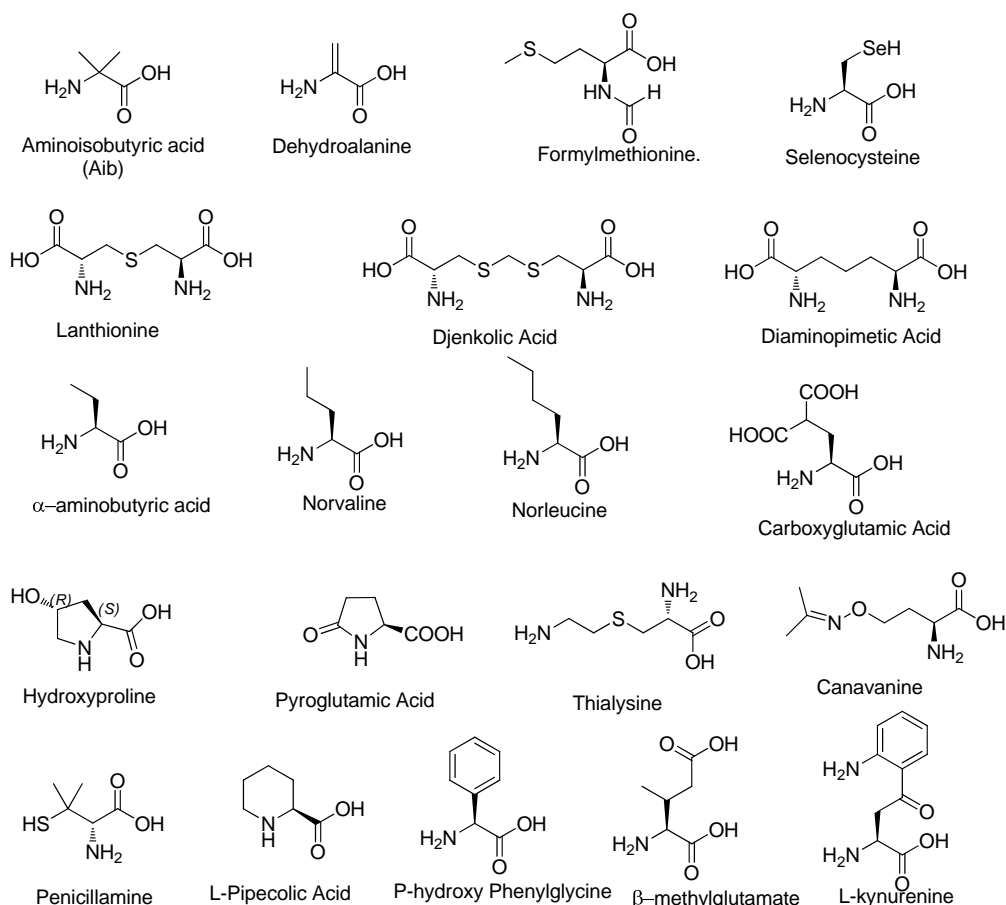


Figure 1: List of the non-ribosomal amino acids present in various natural products

Many α -amino acids with D-configuration, amino acids with gem-dialkyl substitutions, α , β -unsaturated α -amino acids, amino acids with cyclic constraints have been present in peptide natural products.² Some of these unnatural amino acids present in peptide natural products are shown in Figure 1. In addition, chemists have developed a variety of synthetic non-natural amino acids. Research involving the incorporation of these naturally occurring non-ribosomal amino acids and synthetic unnatural amino acids in peptides revealed wide array of applications in biomedical research as well as in drug discovery.³ Some of the biologically active peptide natural products containing these non-ribosomal amino acids are shown in Figure 2. Research involving the incorporation of these non-ribosomal amino acids in peptide and proteins revealed a wide array of applications in biochemical research as well as in drug discovery.

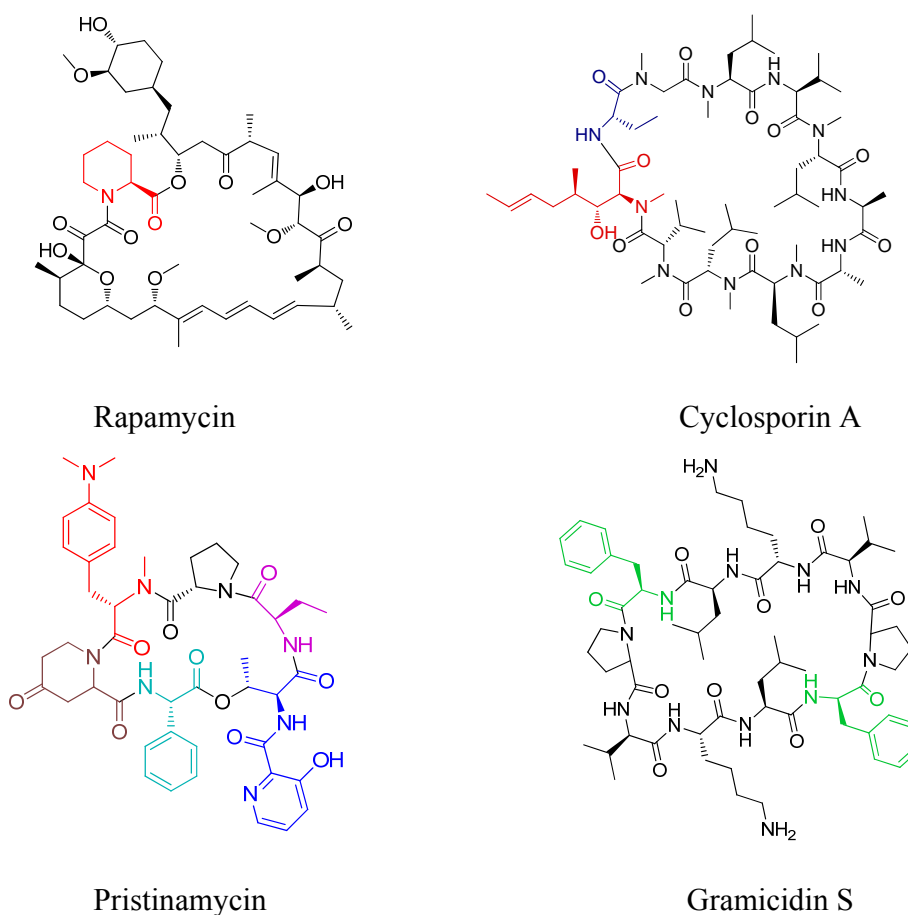


Figure 2: Bioactive natural products containing non-ribosomal amino acids

Further, unnatural amino acids also served as crucial building blocks for the construction of peptidomimetics and the conformational constraints in the design of molecular scaffolds.⁴ Additionally, many of these unnatural amino acids also served as pharmacologically active products.⁵ Thus, unnatural amino acids represent a nearly infinite array of diverse structural elements for the development of new structures and therapeutic leads.

1.1.1 Beta amino acids in hybrid foldamers

The *de novo* design of folded oligomers from different sources of monomers is a very interesting field in the perspective of designing biologically relevant protein and peptidomimetics.⁶ This endeavor has been elegantly described in the design of the structured peptides from recently emerged homologated synthetic derivatives of α -amino acids such as β -, γ - and ω -amino acids.⁷ In addition to the unnatural α -amino acids, β -amino acids and β -peptides are found to be very promising tools in medicinal chemistry. The β -amino acids are homologated species of α -amino acids. Depending on the position of the side chain, they are classified as β^3 - and β^2 -amino acids (Figure 3). Double homologation of α -amino acids leads to γ^2 -, γ^3 -, and γ^4 -amino acids.

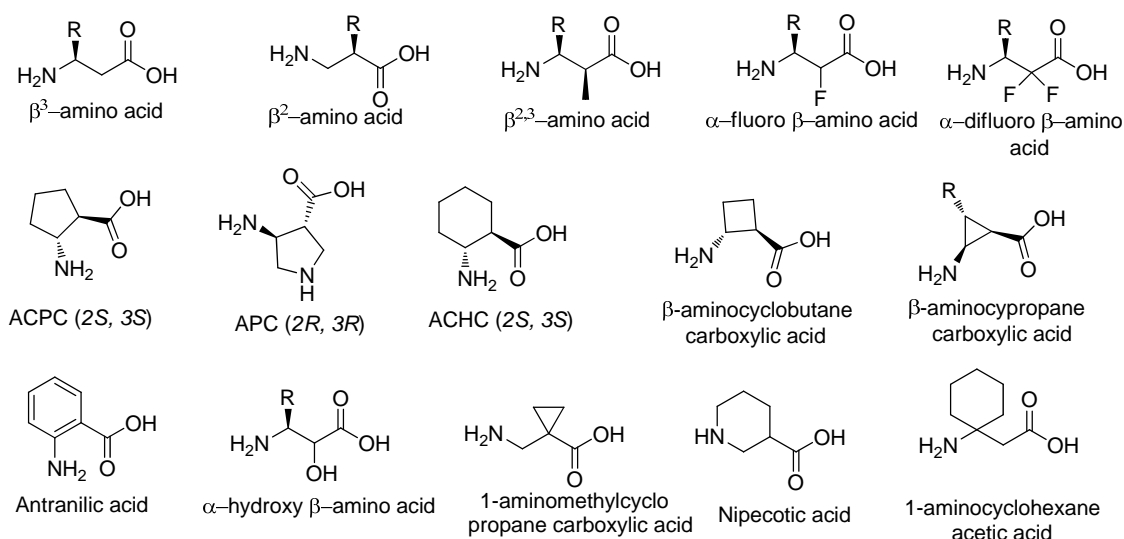


Figure 3: List of substituted β -amino acids

In contrast to α -peptides, β -peptides and higher homologue oligomers have proved the proteolytic and metabolic stability and the prospect of intracellular delivery.⁸ These properties make β -peptides and higher homologue oligomers very attractive from a biomedical perspective.

Extensive investigation from Seebach, Gellman and other groups on the peptides assembled from β -amino acid units are again classified as helices, sheets and reverse turns, however, with different H-bonding patterns. β - and γ -peptides produced a variety of helical secondary structures which are not seen in the α -peptides. The helices produced by the oligomers of β - and γ -amino acids are recognized as C_{14} -, C_{12} -, C_{10} - C_9 - and C_8 -helices. The helices from β -peptides have different polarities with respect to their C and N-termini. The C_8 - and C_{12} -helices have a hydrogen bond direction ($C \leftarrow N$), which is the same as that observed in α -peptides, whereas in the C_{10} - and C_{14} - structures the hydrogen bond directions ($N \leftarrow C$) are reversed. The stability of the helices increases upon progressing from α - to β - to γ -peptides. The γ -peptides form a right handed C_{14} -helix with 2.6 residues per turn. Similar to α -peptides, β -peptides also produced parallel and antiparallel sheets with change in the polarity and net dipole. Besides these synthetic β - and γ -amino acids, a variety of non-ribosomal γ -amino acids such as *E*-vinyllogous γ -amino acids, β -hydroxy- γ -amino acids, β -keto- γ -amino acids and the thiazole δ -amino acids are widely present in many peptide natural products. Many of these peptide natural products display broad spectrum biological activities including anti-cancer and anti-microbial activities. However, the conformational properties of these natural γ -amino acids and their oligomers have not been well explored. Out of all these naturally occurring functionalizable γ -amino acids, α , β -unsaturated γ -amino acids have a particular appeal, because they are unsaturated version of γ -amino acids. Nevertheless, preliminary work by Schreiber and colleagues gave an insight into the structures that can be formed by the vinyllogous amino acids with *E*-double bond.⁹ Grison *et al.* and others reported the β -turn mimetics with a nine-membered hydrogen bond using *Z*-vinyllogous amino acids.¹⁰ Recently, Hofmann *et al.* provided an overview of the helical structures formed by the vinyllogous amino acids using *ab initio* MO theory.¹¹ These systematic conformational analyses are elucidated based on the *trans* and *cis* geometry of the double bonds. As we have been interested in the conformational analysis of the γ - and hybrid γ -peptides, we sought to

investigate the facile synthesis and conformational properties of naturally occurring non-ribosomal α , β -unsaturated γ -amino acids.

1.1.2 Vinylogous amino acids in biologically active natural products

α , β -Unsaturated γ -amino acids (insertion of $-\text{CH}=\text{CH}-$ between C_αH and CO of α -amino acids, vinylogous amino acids) have been frequently found in many peptide natural products,¹² such as Gallinamide A, Cyclotheonamide (A, B, C, D and E), Miraziridine A etc. These peptide natural products also displayed potent inhibitory properties against various proteases including cysteine, serine and aspartic acid proteases. The cyclic peptides Cyclotheonamide A and B are shown potent thrombin inhibiting activities. Further, cyclotheonamides have also shown strong inhibitory profiles against trypsin and other serine proteases. Schreiber and colleagues reported the detailed mechanism of the action of Cyclotheonamide A against serine protease bovine β -trypsin^{12f}. Miraziridine A, another naturally occurring hybrid peptide showed inhibition of the proteolytic activity of trypsin-like serine proteases, papain-like cysteine proteases, and pepsin-like aspartyl proteases.^{12c} In addition to the potent anti-malarial properties, the natural product Gallinamide A isolated from marine cyanobacteria has also showed potent and selective inhibition against the human cathepsin L. Further, Milamides (A, B, C and D) composed of *E*-vinylogous amino acids showed potent cytotoxic activities and microtubule depolymerization.

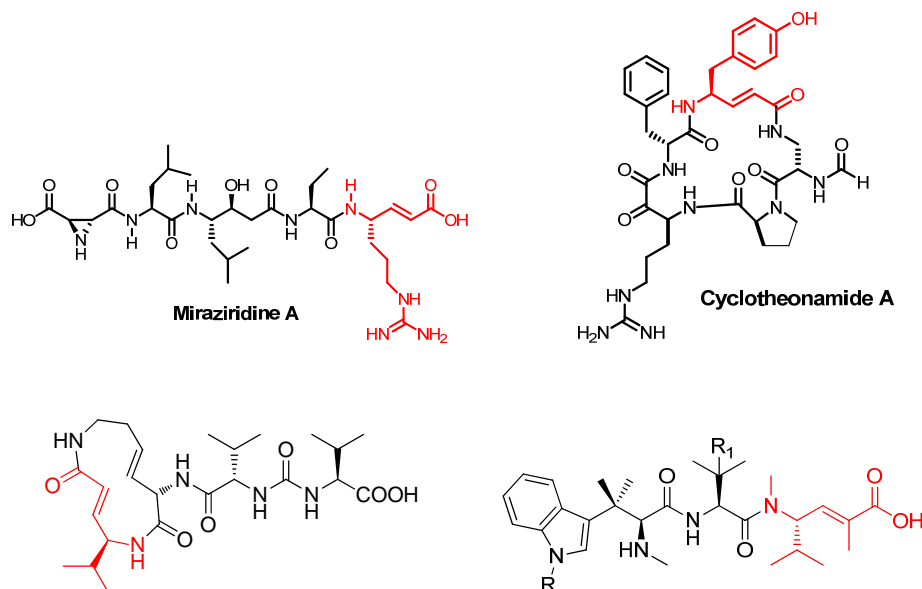


Figure 4: Peptide natural products containing *E*-vinylogous amino acids.

In addition, criamides A and B analogues of milamides displayed potent cytotoxic activities against human cancer cell lines such as ovarian carcinoma, murine leukemia, breast cancer and human lung. Some of the representative examples of peptide natural products containing *E*-vinylogous amino acid residues are shown in Figure 4. In addition to their biological activities, these unsaturated amino acids have also been used as starting materials for the synthesis of γ -amino acids¹³ as well as substrates in a variety of organic reactions including, 1,4-conjugate addition,¹⁴ epoxidation,¹⁵ dihydroxylation and Diels-Alder reaction¹⁶ to develop the functional derivatives of γ -amino acids.

1.1.3 Earlier synthetic protocols for the synthesis of vinylogous amino acids

A range of methodologies including Wittig,¹⁷ Julia,¹⁸ Horner-Wadsworth-Emmons reaction,¹⁹ and Peterson olefination²⁰ have been reported for the synthesis of α , β -unsaturated esters. However, Horner-Wadsworth-Emmons reaction, a variant of Wittig reaction has been extensively utilized for the synthesis of vinylogous amino acids.²¹ In this reaction, alkali metal bases such as BuLi and NaH are commonly used to generate the reactive metalated phosphonate intermediate and to achieve the high levels of stereoselectivity, reactions are also performed in the presence of metal salts and organic bases.²² Seebach and co-workers reported the synthesis of methyl esters of *N*-Boc-protected α , β -unsaturated γ -amino acids with the *E/Z* ratio of 3:1 to 7:1 *via* Horner-Wadsworth-Emmons reaction using NaH as a base.¹³ Grison and colleagues used Horner reagents as starting materials for the stereoselective synthesis of *E* and *Z* vinylogous amino acids.^{10a,b} To achieve the major *E* selectivity, lithiated dianion derivative of 2-diethylphosphonopropanoic acid has been used, while *Z* stereoselectivity has been achieved by KH/ethyl 2-bis(trifluoroethyl)-phosphonopropanoate or BuLi/ethyl 2-diethyl phosphonopropanoate. However, these procedures may not be compatible for the synthesis of vinylogous amino acids containing commonly used base labile Fmoc-protecting group.

1.2 Aim and rationale of the present work

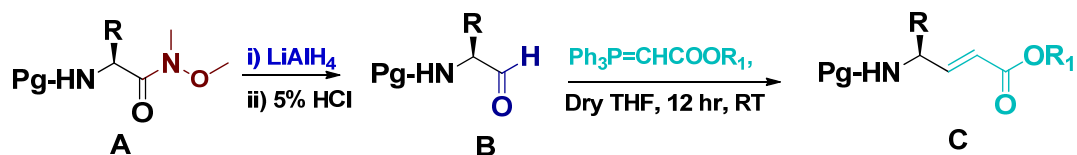
α , β -Unsaturated γ -amino acids containing peptide natural products have displayed excellent biological activities. In addition, they also serve as intermediates for the synthesis of various substituted γ -amino acids as well as saturated γ -amino acids. Here in this chapter we

sought to investigate the facile synthesis and conformational analysis and the reactivity of the conjugated double bonds, thiol conjugate addition to the double bonds and their utility in stapling of the β -strands. For the simplicity, we divided these investigations under three subsections 1A, 1B and 1C. Under the subsection 1A, we report the synthesis and conformational analysis of *E*-vinylogous amino acids and peptides. In the subsection 1B, we are providing the detail investigation regarding the unprecedented HOBt conjugate addition to α , β -unsaturated carboxylic acids. Further, subsection 1C deals with the thiol conjugate addition on *E*-vinylogous amino esters and their utility in stabilization of β -sheets through back-bone disulfide formation.

Section 1A: Synthesis and conformational analysis of *E*-vinylogous amino acids and peptides

1A.3 Results and Discussions

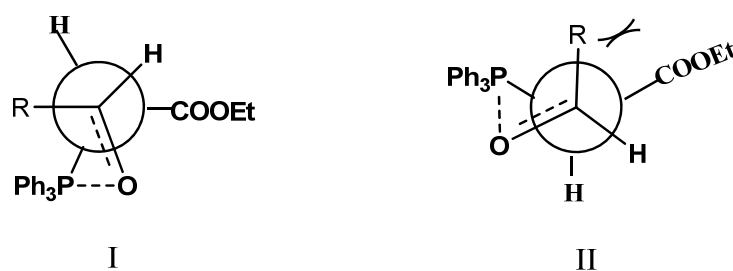
As a part of our investigation to understand the structural features of vinylogous peptides, we sought to utilize the Wittig reaction, since the target vinylogous amino acids can be obtained at neutral conditions and it can be compatible with a variety *N*-protecting groups including base labile Fmoc- group. To understand the efficacy and the stereochemical output of the Wittig reaction in the synthesis of vinylogous amino acids, initially, the Boc-alanal was subjected to the olefination reaction using the ylide, ethyl (triphenylphosphoranylidene) acetate in dry THF (Tetrahydrofuran) at room temperature. The schematic representation of the synthesis is shown in Scheme 1. The Boc-amino aldehyde was synthesized from the LAH (Lithium aluminium hydride) reduction of the corresponding Weinreb amide and subjected immediately to the Wittig reaction.²³ Surprisingly, no trace of *Z* product was observed in the reaction, while 100% *E*-isomer (**1C**) was isolated in high yield (93%).



Where Pg= Boc or Fmoc- ; R₁= Ethyl or benzyl

Scheme 1: Synthesis of α , β -unsaturated γ -amino esters using Wittig reaction.

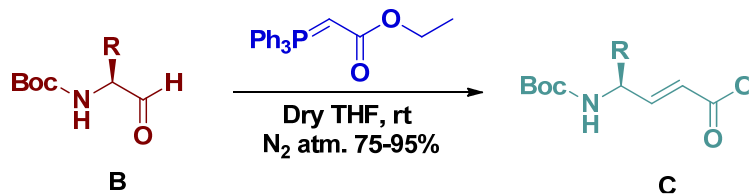
We speculate that there may be a chance of *cis/trans* isomerisation during the column chromatography, which may lead to the conversion of *Z* into *E* product.²⁴ To further confirm the *E*-selectivity, we subjected the crude Wittig product before the column purification to the ¹H NMR to observe the *cis* couplings of vinylic protons. The ¹H NMR shows the *trans* coupling of vinylic protons, indicating the presence of only *E*- product (**1C**) in the reaction mixture. Though it has been reported that the *E*- double bond is a major product in a variety of Wittig reactions, we are surprised to see unprecedented *E*-selectivity in the synthesis of vinylogous amino acids. To further, understand whether the *E*-selectivity is depending upon the amino acid side chain, we subjected a variety amino aldehydes (**2B-8B**), including proline, Ser(OBu^t) and α -aminoisobutyric acid (Aib) to the Wittig reaction. In all these cases, we observed only the *E*-selectivity. In addition, except dialkyl amino acid and proline, all Wittig products (**2C-8C**) were isolated in high yields (>88%) and are given in the Table 1. All Wittig reactions of Boc-aminoaldehydes proceeds very smoothly at room temperature in dry THF. To further, verify whether or not this method can be applicable to the synthesis of *N*-



Scheme 2: Schematic representation of the transition states of the formation of *trans* (I) and *cis* (II) products.

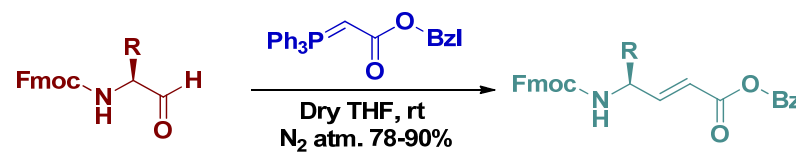
Fmoc-protected vinylogous amino acids, we subjected a variety of *N*-Fmoc-amino aldehydes (**9B-14B**) to the Wittig reaction. The *N*-Fmoc-amino aldehydes were synthesized using the corresponding Weinreb amides as described earlier. The Fmoc-amino aldehydes with a variety of orthogonal side chain protecting groups were subjected to the Wittig reaction using the ylide, benzyl (triphenylphosphoranylidene) acetate. The pure products of benzyl esters of *N*-Fmoc-vinylogous amino esters (**9C-14C**) were isolated after the column chromatography

Table 1: Synthesis of *N*-Boc- α , β -dehydro γ -amino esters (dg) using Wittig reaction



Entry	Aldehyde(B)	Product (C)	%yield
1			93
2			90
3			95
4			92
5			75
6			83
7			88
8			81

Table 2: Synthesis of *N*-Fmoc- α , β -unsaturated γ -amino esters using Wittig reaction



Entry	Aldehyde(B)	Product (C)	%yield
9			78
10			90
11			80
12			90
13			80
14			83

Overall, both *N*-Boc-/Fmoc-protected vinylogous amino esters were isolated in good yields with exceptional *E*-selectivity using the Wittig reaction. We speculate that the formation of *E*-product may adapted a planer transition state that leads to the less steric clash between the amino acids side-chains/NHX (**I**), while the formation of *Z*-product should adapt a energetically unfavourable puckered transition state, that leads to the steric clash between

the amino acid side chains/NHX (**II**) and the incoming ethyloxycarbonyl group as shown in Scheme 2.

1A.3.1 Racemization study for *E*-vinylogous amino acid by chiral HPLC

To further understand the chiral integrity in the synthesis of vinylogous amino esters, we synthesized *N*-Boc-protected L, D and (\pm) DL mixture of valinals using the protocol described earlier and then subjected to the Wittig reaction using the ylide, ethyl (triphenylphosphoranylidene) acetate. The pure ethyl esters of *N*-Boc-vinylogous amino acids were subjected to the chiral HPLC using Daicel CHIRALPAK-AI column. However, all amino acid enantiomers gave a single peak with the same retention time (t_R). Since all amino acids gave the same t_R , we further synthesized three dipeptides, Boc-Ala-dgV-OEt (**D1**), Boc-Ala-(D)dgV--OEt (**D2**) and Boc-Ala-(\pm DL)dgV-OEt (**D3**) by coupling of the vinylogous

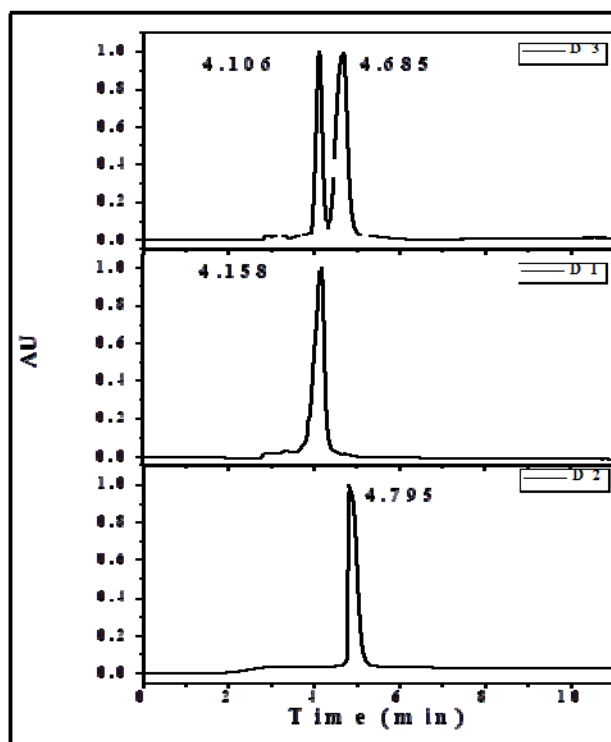


Figure 5: Chiral HPLC of dipeptides **D1**, **D2**, and **D3**. The HPLC was performed on Daicel CHIRALPAK-AI column using 20% isopropanol in *n*-hexane as a solvent system at isocratic mode with the flow rate of 1 mL/ min.

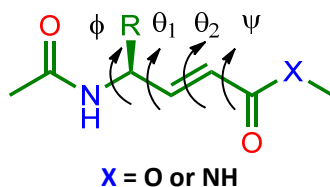
amino esters to the Boc-alanine using the standard DCC/HOBt coupling reaction and subjected to the chiral HPLC. The HPLC profiles of these dipeptides are shown in Figure 5.

Single peaks were observed for the dipeptides **D1** and **D2** at t_R 4.158 and 4.795 min. respectively, whereas dipeptide **D3** showed two peaks with t_R 4.105 and 4.685 min., corresponding to the individual dipeptides **D1** and **D2**, respectively. These results indicate that the synthesis of vinylogous amino acids from Wittig reaction is free from the racemization. Further, out of all vinylogous amino esters in the Tables 1 and 2, and the dipeptides, we were able to obtain the single crystals for the amino esters **2C**, **3C**, **4C**, **5C** and the dipeptide **D1** after slow evaporation of ethyl acetate, ethyl acetate/hexane solution as well as upon standing the pure gummy products. The crystal structure analysis of these vinylogous residues are described below.

1A.3.2 Crystal structure analysis of the vinylogous amino esters and dipeptides

Crystal structures of all vinylogous residues are shown Figure 6. The local conformations of these vinylogous residues are determined by introducing the additional torsional variables θ_1 (N-C ^{γ} -C ^{β} -C ^{α}) and θ_2 (C ^{γ} -C ^{β} =C ^{α} -C) as described by the Hofmann and colleagues.¹¹

Table 3: The torsional angles ($^\circ$) of vinylogous amino esters and the dipeptide D4



Compound	Residues	ϕ	θ_1	θ_2	ψ
2C	dgV	-90	0	179	177
3C	dgL	-91	-1	-179	178
		-(85)	(-4)	(-179)	(-178)
4C	dgI	-94	0	180	-179
5C	dgU	-63	-10	-179	-3
Boc-dgL-dgL-OEt					
D4	dgL1	-107	116	179	171
	dgL2	-137	0	179	180

The torsional variables of all vinylogous residues are summarized in Table 3. In the case of **3C**, two molecules are appeared in the asymmetric unit with a slight variation in the torsional values. The vinylogous residues **2C** and **5C** adapted orthorhombic crystal systems, while **3C** and **4C** exhibited monoclinic crystal systems. Examination of the crystal structures of all vinylogous amino esters reveals that the torsional angle θ_1 is 0° or close to 0° suggesting the eclipsed conformation of the double bond with the N-C γ bond. In addition, the local *s-cis* conformation of the conjugated ester is observed in **2C**, **3C**, and **4C**, whereas *s-trans* is observed in the dialkyl amino acid residue **5C**. The ϕ and ψ angles are found to be $\sim -90^\circ$ and $\sim (\pm)180^\circ$, respectively, in the vinylogous residues **2C**, **3C** and **4C**, while in the case of **5C**, the ϕ and ψ angles -63° and -3° , respectively, are observed. The torsional angle θ_2 is having

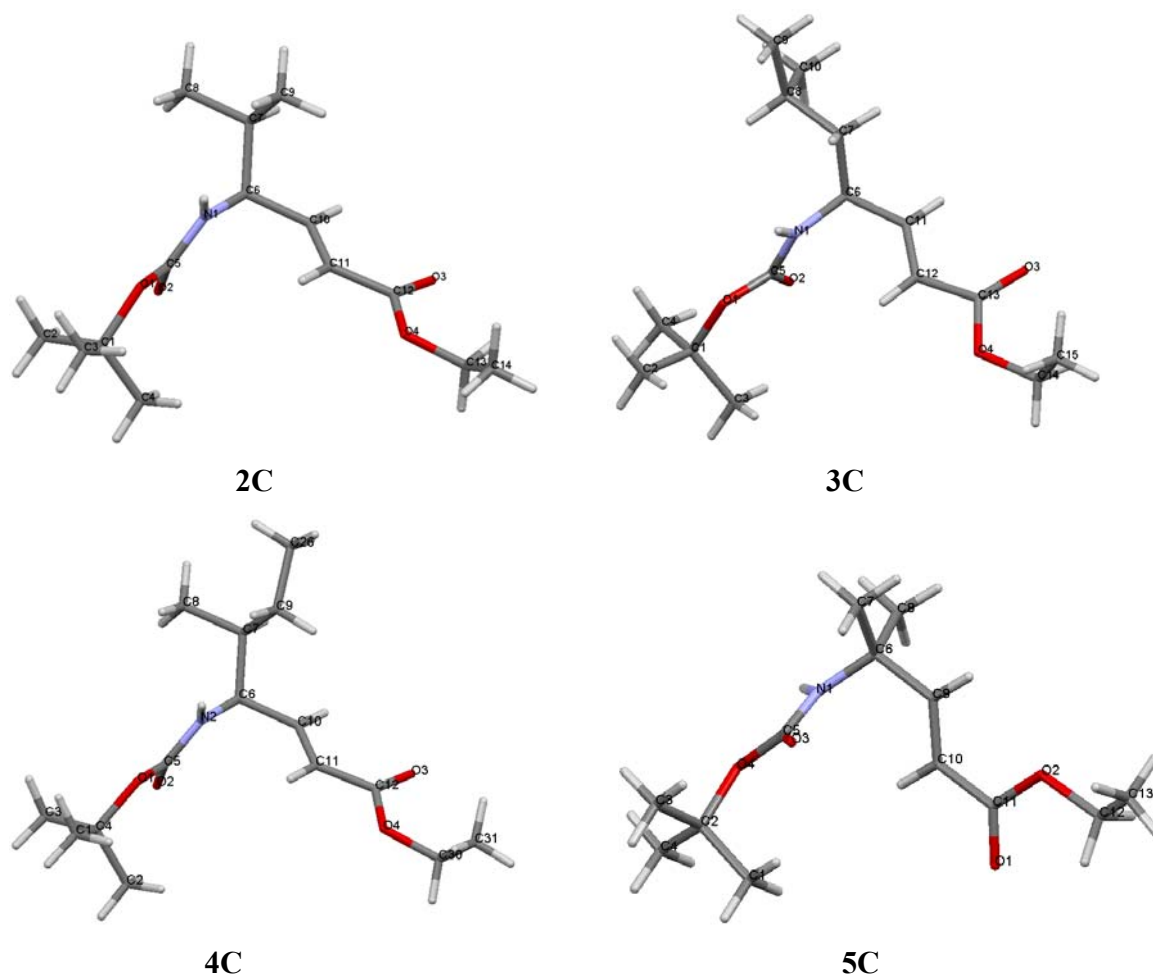


Figure 6: Crystal structures of vinylogous amino acids, Boc-(*S, E*)-dgV-OEt (**2C**), Boc-(*S, E*)-dgL-OEt (**3C**), Boc-(*S, E*)-dgI-OEt (**4C**) and Boc-(*E*)-dgU-OEt (**5C**).

the value $\sim -180^\circ$ in all vinylogous residues. It should be noted that the ψ value in dialkyl vinylogous amino acid is close to 0° , whereas in the other vinylogous residues it is close to 180° , indicating the rotation around the single bond in the conjugated ester is possible.

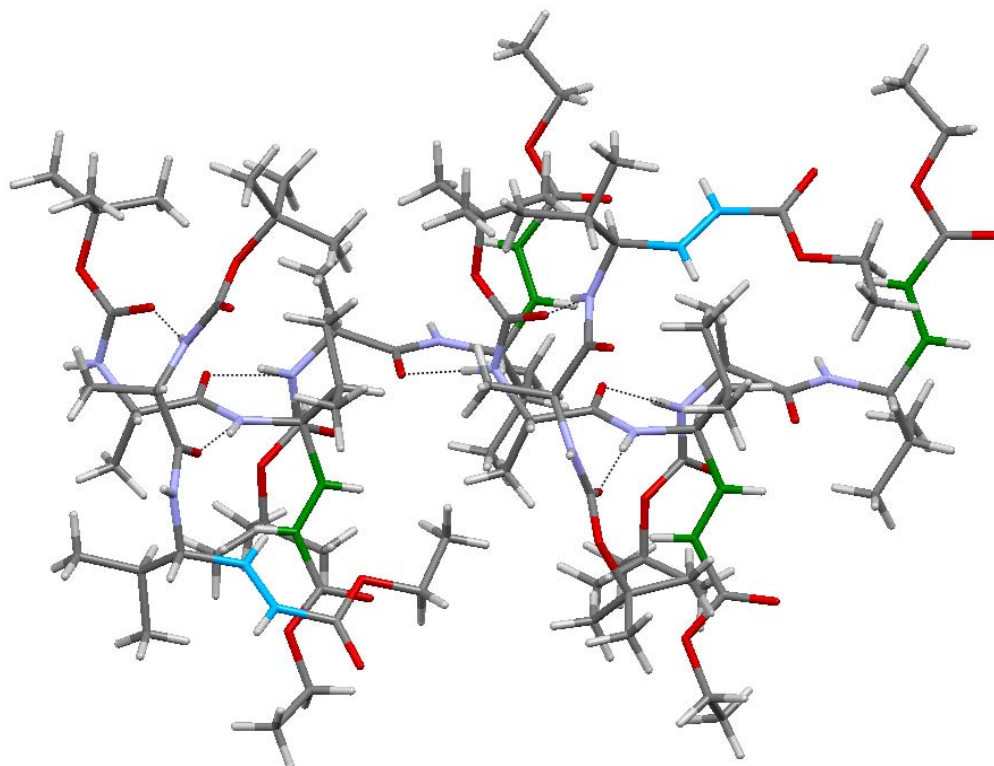
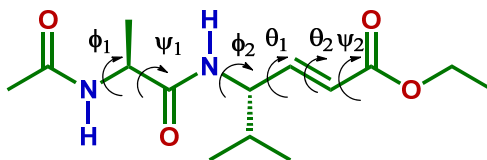


Figure 7: Crystal structure of dipeptide Boc-Ala-dgV-OEt (**D1**). Six molecules are appeared in the asymmetric unit. The intermolecular H-bonding between the dipeptide units are shown in dotted lines. The types of conformations with significant variation in the torsional values of vinylogous residues are highlighted in different colors.

Crystals of Boc-Ala-dgV-OEt (**D1**) were obtained after slow evaporation of ethyl acetate solution and the crystal structure is shown in Figure 7. Surprisingly, six dipeptide molecules are observed in the asymmetric unit with a significant variation in the torsional angles. The torsional values are tabulated in the Table 4. The six molecules in the asymmetric unit are held together by intermolecular H-bonds. The analysis of the torsional variables reveals the conformational flexibility of vinylogous residue in the hybrid dipeptide. Instructively, molecules **a**, **c**, **e** and **f** in the Table 4 adapted a very similar conformations in

the crystals with slight variations in the torsional values (highlighted in green in Fig.7), while dipeptides **b** and **d** adapted similar conformations different from the other four dipeptides (highlighted in blue, Fig.7). In the case of **a**, **c**, **e** and **f**, the Ala adapted a semi-extended conformation by having ϕ_1 and ψ_1 angles $\sim -60^\circ$ and $\sim 140^\circ$, respectively. In addition, the vinylogous residues adapted extended conformations by having $\phi_2 \sim -120^\circ$, however, θ_1 is found to be close to 0° . Further, the local *s-cis* conformation of the conjugated esters is observed with the ψ_2 values $\sim 180^\circ$. Interestingly, in the case of **b** and **d**, the Ala adapted extended conformations with the ϕ_1 and ψ_1 value approximately -120° and 155° , respectively. In addition, the ϕ_2 is found to be 69° and θ_1 is having the values close to 130° . Further, the local *s-trans* conformation of the conjugated ester is observed with the ψ_2 close to 0° . It should be noted that the values of ϕ_2 , θ_1 and ψ_2 are different for the two sets of the peptides in the crystals, indicating that the rotations around the single bonds are possible. In contrast to the all unsaturated γ -amino ester structures (Table 3), the θ_1 of the dipeptides **b** and **d** is having the value close to 130° .

Table 4: Torsional angles ($^\circ$) of the dipeptide Boc-Ala-dgV-OEt (**D1**)



	ϕ_1	ψ_1	ω	ϕ_2	θ_1	θ_2	ψ_2
a	-57	140	173	-123	9	-180	-175
b	-122	157	173	69	127	175	9
c	-60	141	169	-115	-9	179	175
d	-116	155	166	69	129	175	10
e	-61	139	177	-122	7	-179	-179
f	-60	134	175	-112	-3	177	-173

Further, inspired by the interesting results obtained from the dipeptide **D1**, we sought to investigate the conformational behaviour of the vinylogous residues in homo-dipeptides. The dipeptide Boc-dgL-dgL-OEt (**D4**), was synthesized by coupling of *N*-Boc-vinylogous

acid and the free amine of **3C** obtained after the saponification and the Boc-deprotection, respectively. The coupling reaction was mediated by DCC and HOBt. Crystals of homodipeptide **D4** obtained after the slow evaporation of ethyl acetate solution yield the structure shown in Figure 8A.

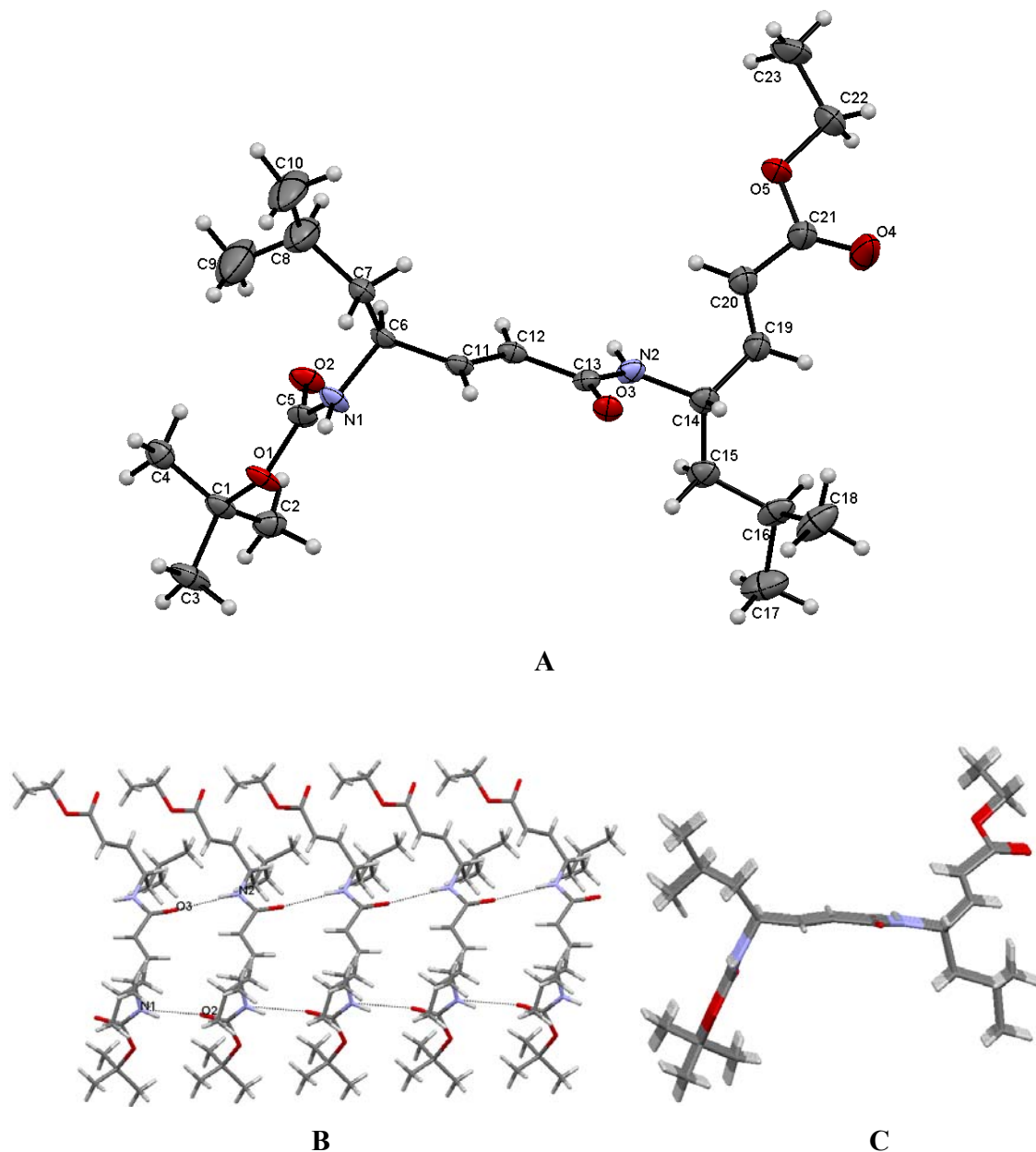


Figure 8: Crystal structure of dipeptide Boc-dgL-dgL-OEt (**D4**). **A.** The ORTEP diagram of the dipeptide. **B.** The partial β -sheet of character exhibited by the dipeptide in crystals. **C.** The side view of the β -sheet.

In contrast to the dipeptide **D1**, single dipeptide molecule is observed in the asymmetric unit. Interestingly, the dipeptide **D4** adapted a partial parallel β -sheet character in the crystal structure (Figure 8B). The torsional values are given in the Table 3. Analysis of the crystal structure reveals that the dipeptide molecules are held together by two intermolecular H-bonding between the C=O and NH groups with N-H---O distances 2.066 [N1H---O2, (N1---O2, 2.872 Å)] and 2.165Å [N2H---O3, (N2---O3, 3.012 Å)] with N-H---O angles 156 and 168°, respectively (Fig. 8B). A fully extended conformation is observed in dgL1 of the dipeptide with ϕ , θ_1 , θ_2 and ψ values -107, 116, 178 and 171°, respectively, whereas in the second residue dgL2, θ_1 is having the eclipsed conformation with the N-C γ bond (θ_1 is 0°), leads to the deviation from the β -sheet structure. However, the other torsional variables ϕ , θ_2 and ψ showing the extended conformations with the angles of -137, 179 and 180°, respectively.

1A.3.3 CD analysis for the vinylogous amino acid containing hybrid peptides

Further, to understand their conformational signature in solution, we subjected the dipeptides **D1**, **D2** and **D4** for CD analysis. The CD spectra of the dipeptides are shown Figure 9. Instructively, dipeptide **D4** showed the CD negative maxima at 228 nm, indicating a β -sheet character in solution, while the other dipeptides **D1** and **D2** exhibiting strange characteristics by giving almost two mirror image spectra with the CD positive and negative maxima at around 205 and 202 nm, respectively. For a comparison, the CD spectrum of the α -dipeptide, Boc-Leu-Leu-OMe (**D5**) is also shown in Figure 9. The CD analysis, however, suggests that the lack of secondary structural elements in dipeptide **D5**. We speculate that the red shift of the CD negative maxima at 228 nm for the dipeptide **D4** and the anomalous CD spectra of the dipeptides **D1** and **D2** may be due to the conjugated enamides and esters of vinylogous residues.

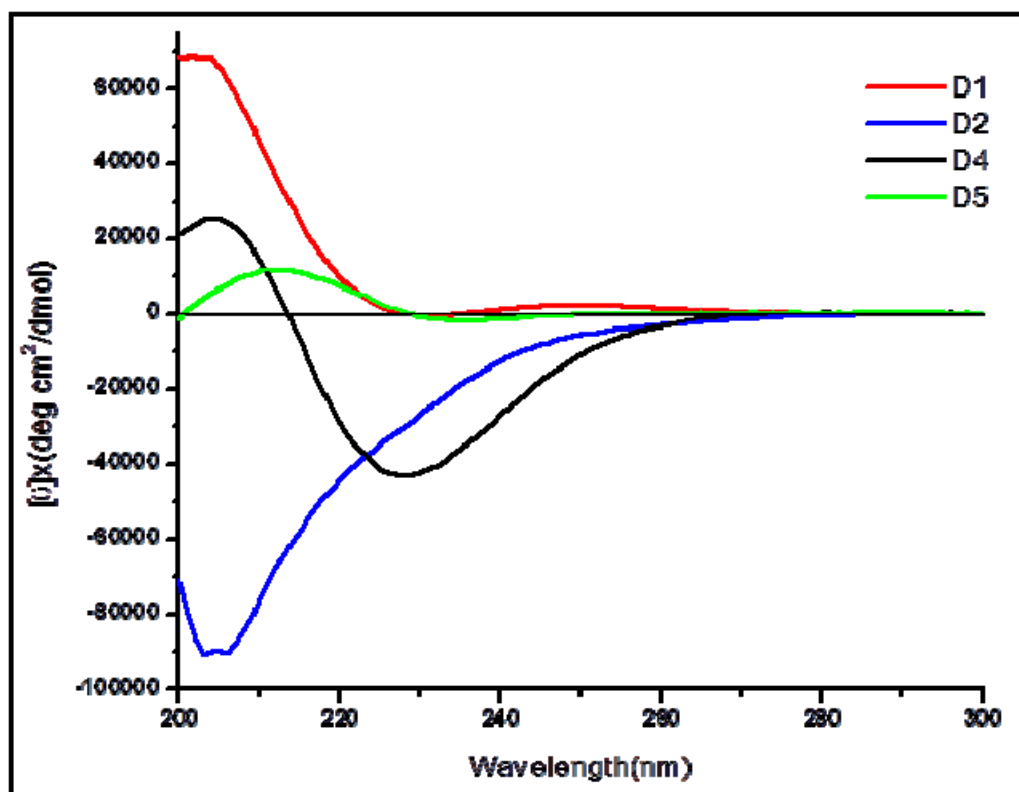


Figure 9: Circular Dichroism spectra of dipeptides **D1**, **D2**, **D4** and **D5** in methanol.

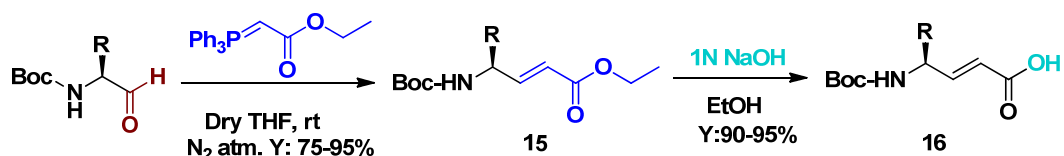
Section 1B: Unusual HOBt conjugate addition on *E*-vinylogous amino acids during the coupling reactions in the absence of free amine coupling partner

1B.1 Introduction

Nucleophilic conjugate addition is one of the most widely explored reactions in synthetic organic chemistry. The conjugate addition offers direct access to a variety of organic compounds through the C-X (X = C, N, O, S etc) bond formation.²⁵ The regiochemistry of 1, 2 or 1, 4- nucleophilic addition to the α , β -unsaturated carbonyl compounds is generally controlled by the relative electrophilicity of the carbonyl group, steric interactions of both electrophile and nucleophile as well as hard and soft nature of the nucleophiles. Besides the organocopper reagents,²⁶ the utility of various other transition metals catalyzed selective conjugate addition reactions has been well documented.²⁷ In contrast to the α , β -unsaturated aldehydes, ketones, esters and amides, the utility of unsaturated carboxylic acids as precursors

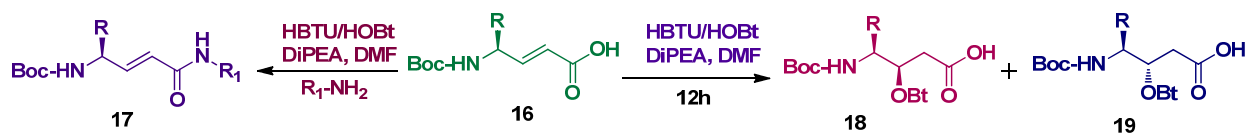
in the conjugate addition reactions have not been well explored. However, the literature survey reveals that the strong alkylating agents such as organolithium²⁸ and organomagnesium reagents,²⁹ copper reagents,³⁰ rhodium(I) catalyzed arylboronic acids,³¹ and gold(III) catalysts,³² have been reported in selective 1, 4 additions to α , β -unsaturated acids.

As described earlier, coupling reactions of *E*-vinylogous peptides were generally performed using the coupling reagent HBTU in the presence of coupling additive HOBt. No HOBt conjugate addition products have been observed while performing the synthesis of hybrid peptides composed of *E*-vinylogous amino acids. However, in an accidental encounter in the absence of free amine coupling partner, we observed HOBt conjugate addition product of the *E*- α , β -unsaturated γ -amino acid. As unsaturated carboxylic acids have been proved difficult to undergo conjugate addition reactions at mild conditions, the unexpected 1, 4 addition products motivated us to investigate the HOBt conjugate addition in detail. Herein, we are reporting the 1, 4 conjugate addition of HOBt to various *E*- α , β -unsaturated γ -amino acids, stereochemical analysis of the conjugate addition products and their utility in the synthesis of peptides.



R= **a**, $-\text{CH}_2\text{-Ph}$; **b**, $-\text{CH}(\text{CH}_3)_2$; **c**, $-\text{CH}_2\text{-CH}(\text{CH}_3)_2$; **d**, $-\text{CH}_2\text{-C}_6\text{H}_4\text{-OBu}^t$; **e**, $-\text{CH}(\text{CH}_3)\text{-CH}_2\text{-CH}_3$; **f**, α , β -unsaturated γ -proline

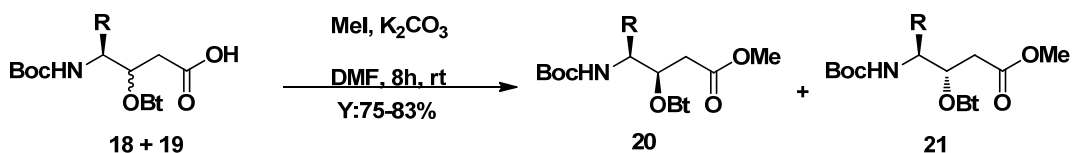
Scheme 3: Synthesis of α , β -unsaturated γ -amino acids



Scheme 4: Amide coupling and conjugate addition of HOBt with *E*-vinylogous amino acids

1B.2 Results and discussion

Ethyl esters of *E*-vinylogous amino acids (**15**) were synthesized starting from α -amino aldehydes using the Wittig reaction as reported section 1A (Scheme 3).³³ All *E*-vinylogous amino acids (**16**) were obtained after the saponification using 1*N* NaOH and used for the conjugate addition without further purification. The schematic representation of the HOBt conjugate addition in the absence and the presence of free amine coupling partner is shown in Scheme 4. In the absence of free amine coupling partner, we isolated the diastereomeric mixture of HOBt conjugate addition products (**18** + **19**) in moderate to good yields from the α , β -unsaturated γ -amino acids, **16a-f** (Scheme 4). Instructively, no HOBt conjugate addition product was observed with HBTU alone suggesting the requirement of additional equivalent HOBt for the conjugate addition. Though the β -OBt substituted γ -amino acids, (**18** + **19**) **a-f**, were isolated after the simple aqueous work-up, we found it difficult to separate the diastereomeric carboxylic acids **18** and **19** using column chromatography. In order to understand the diastereomeric ratio in the conjugated addition, we subjected all HOBt substituted diastereoisomeric mixtures, (**18** + **19**) **a-f**, to the esterification reaction using methyl iodide and potassium carbonate in DMF to give methyl esters **20** and **21** as shown in Scheme 5.



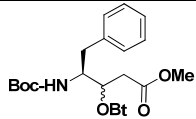
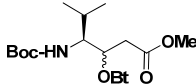
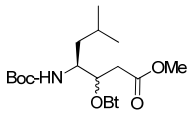
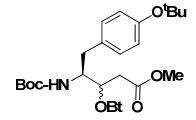
R= **a**, $-\text{CH}_2\text{-Ph}$; **b**, $-\text{CH}(\text{CH}_3)_2$; **c**, $-\text{CH}_2\text{-CH}(\text{CH}_3)_2$; **d**, $-\text{CH}_2\text{-C}_6\text{H}_4\text{-OBu}^\dagger$; **e**, $-\text{CH}(\text{CH}_3)\text{-CH}_2\text{-CH}_3$; **f**, α , β -unsaturated γ -proline

Scheme 5: Esterification of HOBt conjugate addition product of γ -amino acids

Out of all methyl esters of diastereoisomers in Scheme 5, we were able to separate the diastereoisomers **20a-d** and **21a-d** using silica gel column chromatography. We found it difficult to separate the diastereoisomers **20e** and **21e** as well as **20f** and **21f** using column

chromatography. The yields and the diastereomeric ratio of the products are given in the Table 5. We observed moderate diastereoselectivity in the conjugate addition and based on the earlier reports,³⁴ we anticipate that *anti* addition product (**21**) may be the major product compared to the *syn* addition product (**20**). To further understand whether the conjugate addition to *E*- vinylogous amino acids is specific to the coupling additive HOBt, we performed two, individual control reactions using other coupling additives, pentafluorophenol and *N*-hydroxysuccinimide in the presence HBTU.

Table 5: List of β -OBt substituted γ -amino acid methyl ester and their diastereomeric ratios.

AA	20+21	% Yield (20+ 21)	% <i>syn</i> (20)	% <i>anti</i> (21)
a		75	39	61
b		80	37	63
c		83	41	59
d		70	40	60

The mass spectral analysis of the products reveals no conjugate addition from both pentafluorophenol as well as *N*-hydroxysuccinimide rather we isolated corresponding active esters.

1B.2.1 Crystal structure analysis for the β -OBt substituted γ -amino esters.

In order to understand the stereochemistry and the diastereoselectivity, we subjected all major (**21**) and minor (**20**) diastereoisomers for crystallization. Out of all major and minor diastereoisomers, we were able to get the single crystals for minor (**20a**) and major (**21a**) diastereoisomers of β -OBt substituted γ -phenylalanine, and the minor isomer of β -OBt-substituted γ -leucine (**20c**). The crystal structures of these diastereoisomers are shown in Figure 10.

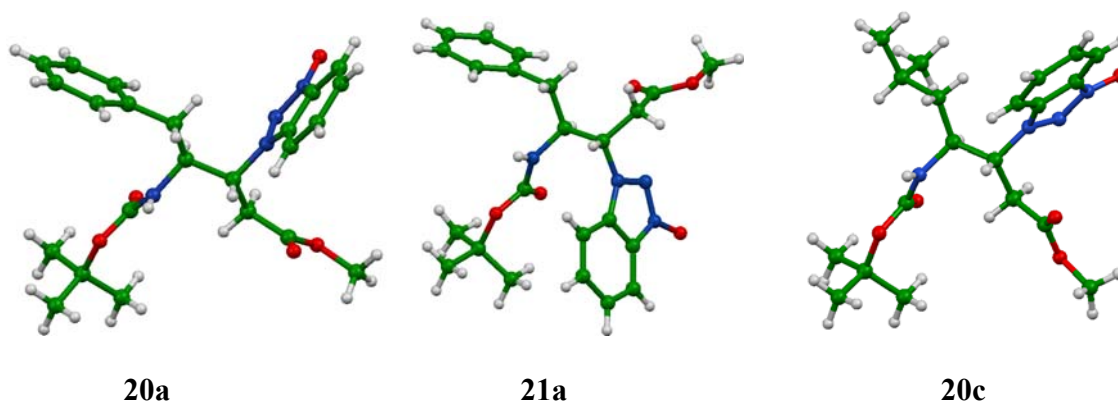
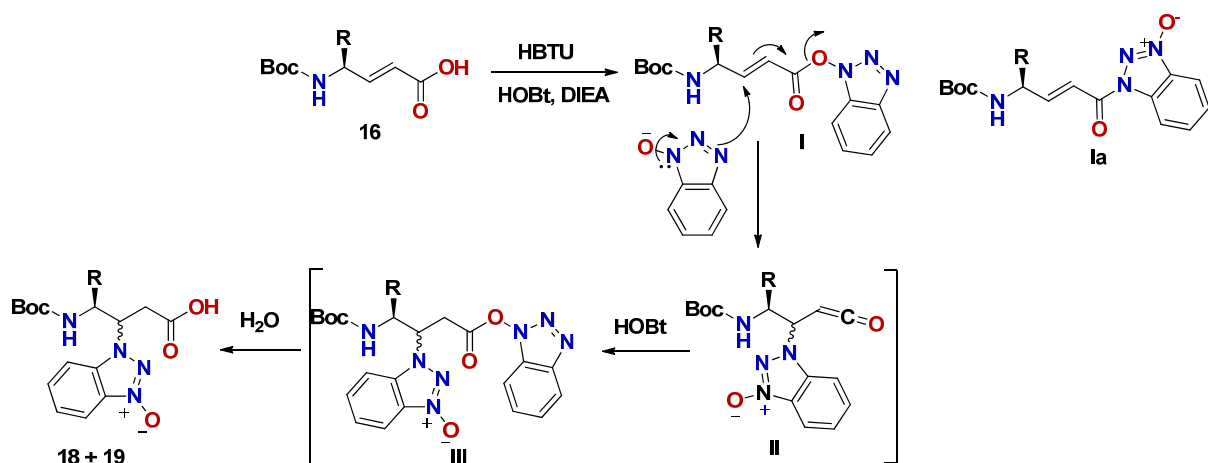


Figure 10: X-ray structures of **20a**, **21a** and **20c**.

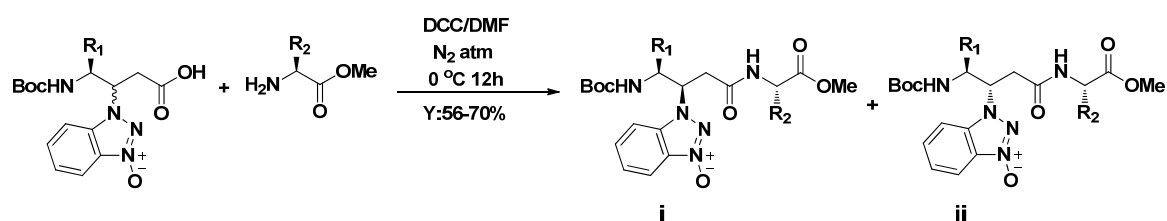
The crystal structure analysis reveals that as anticipated *anti* (**21**) is a major product and *syn* addition product (**20**) is a minor. Intriguingly, crystal structures also provide information regarding the involvement of triazole nitrogen (*N*) as a nucleophile in the conjugate addition over the *N*-hydroxyl (*N*-OH) group of HOBt. All three structures displayed *N*-alkylated benzotriazole *N*-oxides. The participation of the triazole *N* in the conjugate addition instead of free *N*-OH group of the HOBt is not surprising as enormous attention has been paid over the decades regarding the ambidentate reactivity of HOBt. A survey of the literature reveal that both *N*-acylation and *O*-acylation properties of HOBt and their solvent dependent equilibrium properties.³⁵ Further, the crystal structures of HBTU, TBTU and HAPyU also suggest the formation of *N*-oxide derivatives over their uronium salts. Most of these studies convincingly suggest the *N*-acylation is an intermolecularly driven process. Based on these experimental evidences the possible reaction mechanism of the HOBt conjugate addition is outlined in the Scheme 6.



Scheme 6: Schematic representation of the conjugate addition of HOBT

We anticipate that the active ester (**I**) and/or amide (**Ia**) obtained after the treatment of HBTU in the presence of a base, will react further with the HOBT leading to the formation of diastereomeric mixture **II** which will immediately react further with HOBT to give active ester **III**. The hydrolysis of the active ester **III** during the aqueous work-up gave the diastereomeric conjugate addition products **18** and **19**. Further, we speculate that the soft nucleophilic nature of triazole nitrogen (N) may be preferred for the conjugate addition over the hard nucleophilic nature of the oxygen in *N*-OH. This was further supported by the 1, 2 addition of pentafluorophenol and *N*-hydroxysuccinimide. Similarly, intramolecular *N*-alkylation of unsaturated acids with various carbodiimides leading to the multisubstituted hydantoins have been recently reported.³⁶

Table: 6. List of the peptides synthesized by using β -OBt substituted γ -amino acids



Entry	Peptides (P)	% Yield	% i	% ii
22		70	41	59
23		62	38	62
24		67	37	63
25		58	41	59
26		56	39	61

1B.2.2 Synthesis of β -OBt substituted γ -amino acid containing peptides

Based on the encouraging results from the methyl esters of HOBT conjugate addition products, we subjected β -OBt substituted diastereomeric mixture of **18** and **19** directly to the peptide synthesis, anticipating that it may be possible to separate the diastereomeric dipeptides once they coupled to the α -amino acid esters. In this regard, the conjugate addition products

of **16c** (**18c** + **19c**) were directly coupled with methyl ester of Ala in the presence of DCC. The two diastereomeric dipeptides **22i** and **22ii** were isolated with 70% yield and were separated using column chromatography in the ratio of 41 and 59%, respectively (Table 6). The dipeptides **23i** and **23ii** were synthesized after coupling with methyl ester of Leu with the diastereomeric mixture of the conjugate addition products **18e** and **19e**, respectively. Similarly, dipeptides **24** (**i** and **ii**), **25** (**i** and **ii**) and **26** (**i** and **ii**) were synthesized using the diastereomeric mixtures OBt conjugate addition products obtained from **16b**, **16f** and **16a**, respectively, by direct coupling with leucine methyl ester. Overall yield and the diastereomeric ratios of dipeptides are given in the Table 6.

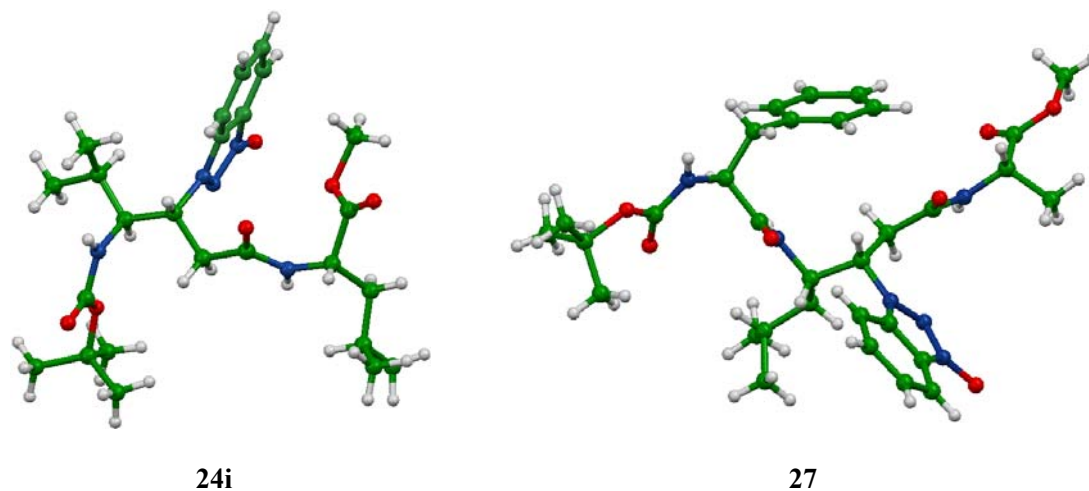


Figure 11: The X-ray structures of Boc- γ Val(β -OBt)-Leu-OMe(**24i**) and Boc-Phe- γ Leu(β -OBt)-Ala-OMe (**27**).

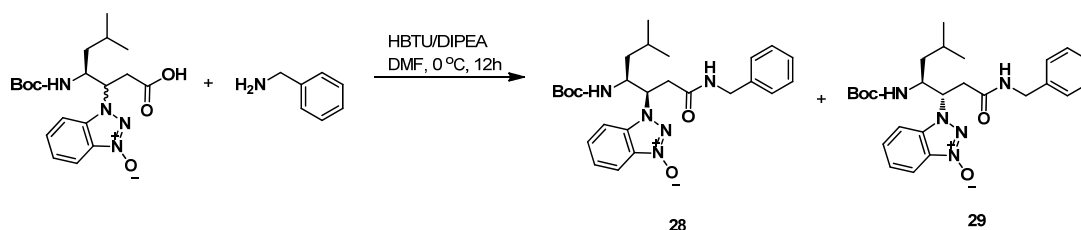
We further subjected dipeptide **22ii** for the synthesis of the tripeptide Boc-Phe- γ Leu(β -OBt)-Ala-OMe (**27**). The Boc- group of the dipeptide was deprotected using TFA and the isolated free amine was coupled to the Boc-Phe using DCC/HOBt to give tripeptide in good yield. Out of all the HOBt substituted peptides, we were able to get single crystals of dipeptide **24i** and tripeptide **27** and their X-ray structures are shown in Figure 11. Instructively, similar to methyl esters, the peptide crystal structures also revealed *N*-substituted conjugate addition products in the peptides.

Crystal structure analysis of methyl esters of major (**21a**, *anti*) and minor (**20a**, *syn*) products from *N*-Boc- α , β -unsaturated γ -phenylalanine reveal that both molecules adopted

unfavorable staggered conformation along the C^β-C^γ bond. The molecule **21a** adopted *t* and *g*⁻ conformations, while **20a** displayed *g*⁺ and *t* conformation along C^β-C^γ and C^β-C^α bonds, respectively. Similarly, *syn* addition products **20b** and γVal(OBt) in the dipeptide (**24i**) showed *g*⁺ and *t* conformations. In contrast, *anti* γLeu(OBt) in the tripeptide **27** follow the general trend of tetra alkyl substituted ethane by adopting the *gauche* conformations³⁷ along C^β-C^γ bond and displayed *anti* (*t*) conformation along the backbone C^β-C^α bond.

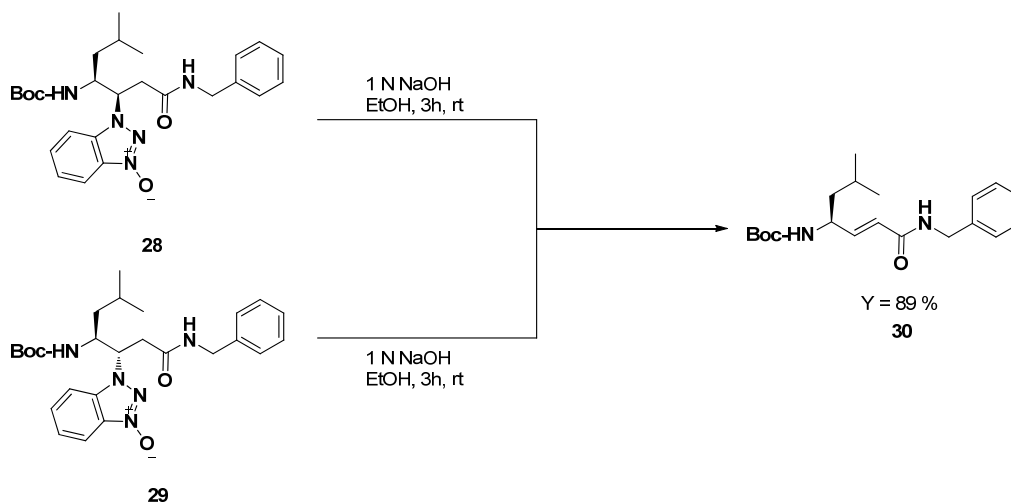
1B.2.3 Elimination reaction of OBt-substituted γ-amino esters and amides to unsaturated γ-amino acids and amides

In order to understand the stability of the β-OBt substituted γ-amino acids towards aqueous base, we treated methyl esters of **20a** with 1*N* NaOH in methanol. Surprisingly, both diastereomers gave starting material *E*-vinylogous γ-amino acid (**16a**) in quantitative yield through elimination reaction as well as ester hydrolysis. To further understand whether the elimination of OBt products are also possible even in the case of amides, we coupled the diastereomeric acids of **18c** + **19c** with benzyl amine using HBTU (Scheme 7).



Scheme 7: Coupling of benzyl amine with diastereomeric mixture of **18c** & **19c**

The diastereomeric amides **28** and **29** were separated using column chromatography and individually treated with the 1*N* NaOH. Instructively, both **28** and **29** gave α, β-unsaturated amide **30** (Scheme 8). Results of these investigations suggest that the reactivity of double bond can be masked in unsaturated acid or ester or amides through OBt conjugate addition. The double bonds can be re-generated after the treatment of 1*N* NaOH. In addition irrespective of the stereochemistry at OBt substituted γ-amino acid residues, we observed only *trans* double bonds in products.



Scheme 8: Schematic representation for the OBt elimination from **28** and **29** after treatment with 1N NaOH

Section 1C: Conjugate addition of thiols: Synthesis of novel thiostatine and their utility in the design of stable β -hairpin mimetics

1C.1 Introduction

Enormous amount of literature is documented towards the design and stabilization of protein secondary structures. Stabilizing the protein secondary structures is of paramount importance in the designing the structure based inhibitors for protein-protein interactions.³⁸ The protein-protein interactions are responsible for most of biological functions and also responsible for the diseases and infections. A variety of strategies have been developed to mimic the short and stable α -peptide helices including covalent cross-linkage of amino acids side-chains,³⁹ utilization of C-C covalent bond as intramolecular H-bond surrogate,⁴⁰ non-peptidic organic templates,⁴¹ metal induced helices⁴² and so on. The schematic representation of the stapled helices is shown in the Figure 12.

In contrast to the helical secondary structures, very little is known in the stabilization of other predominant protein secondary structures, β -sheets and β -hairpins. Unlike α -helical peptides, where structure is stabilized by local C13 H-bonds, β -strand requires a structural context for stabilization. The design of β -hairpins with stabilized β -strands is a formidable task. The β -strand residues that modulate the β -hairpin stability depending upon their intrinsic β -sheet propensities through both cross strand and diagonal side chain-side chain interaction.⁴³

The β -sheets are generally stabilized by the intermolecular H-bonds between the two β -strands and the van der Waals interactions between the side chains. The stabilities of the antiparallel β -strands were further improved by incorporating Trp-Trp residues at opposite faces,⁴⁴ ionic interactions⁴⁵ as well as cation- π interactions.⁴⁶ Many examples in the protein structures suggests the stabilization of anti-parallel β -sheets through disulfide bond formation through cysteine residues positioned at the non-hydrogen bonding positions.⁴⁷ These types of disulfide stabilization are rarely observed in the parallel β -sheets.⁴⁸ However, Gellman and colleagues recently reported that disulfide mediated stabilization of the two parallel β -strands in a designed β -hairpin conformation.⁴⁹ Except the disulfide bond stabilization through the side-chains of the cysteine residues, no attempts have been made to covalently link two β -strands together. Many examples in the literature also suggest macrocyclization of peptides through the disulfide formation,⁵⁰ instead of β -hairpin.

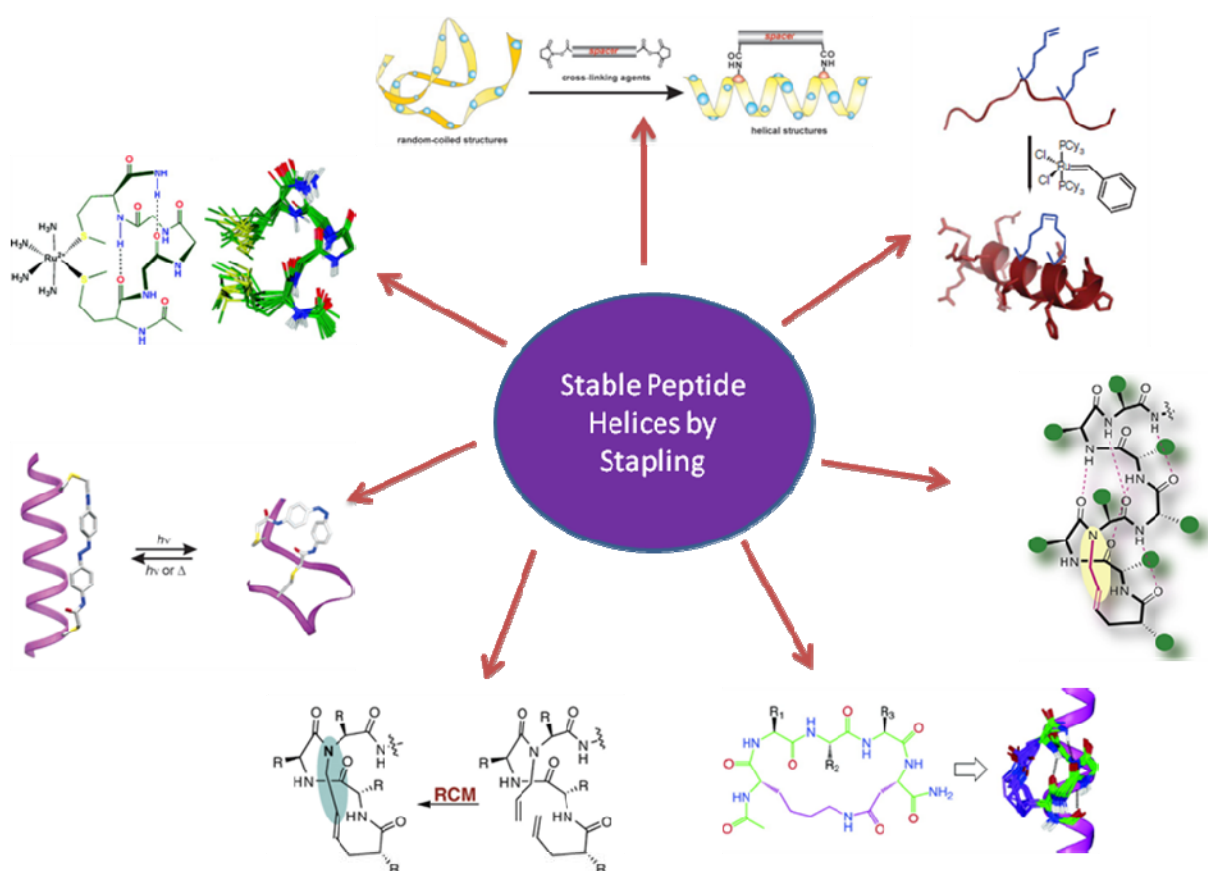


Figure 12: Various reported protocols for generating stable helices through stapling

1C.2 Results and discussion

We anticipate that β -sheet structures can be stabilized through the incorporation of –SH directly to the back-bone carbon atom instead of the side-chains of cysteine residues. However, Erlenmeyer's rule suggests that these kinds of heteroatom substitution at the α -carbon atom of the α -amino acids would lead to a hydrolytically labile N-C bond (Figure 13). We anticipate that heteroatoms such as O, S or N can be easily introduced into the carbon backbone using α , β -unsaturated carbonyl compounds residues through 1, 4-conjugate addition. The conjugate addition provides an excellent opportunity to synthesize diverse molecular scaffolds through the reaction between the nucleophiles and the α , β -unsaturated carbonyl compounds. Here we sought to exploit the chemical reactivity of the double bond in *E*-vinylogous γ -amino acids through conjugate addition using thiols and their utility in stapling the β -sheets and β -hairpin through disulfide formation.

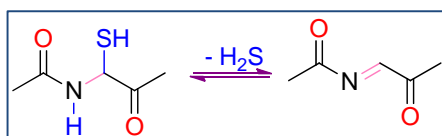
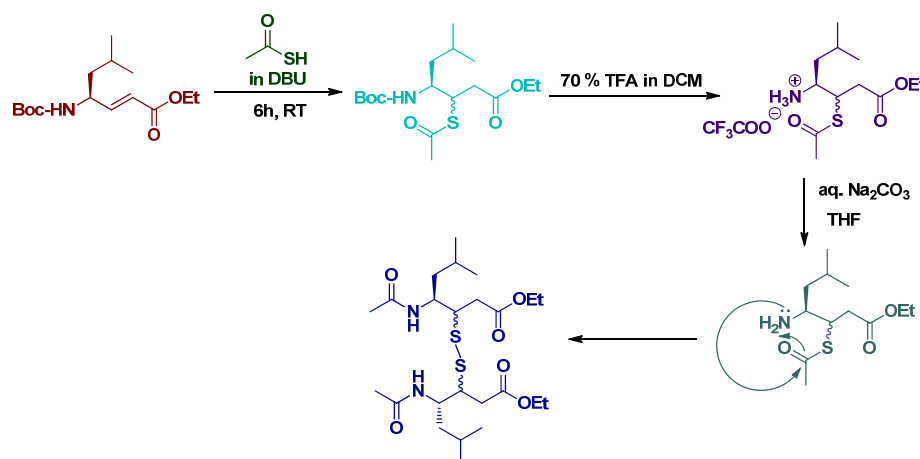


Figure 13: Representative example for hydrolytically labile N-C bond and elimination

1C.2.1 Synthesis of *ortho*-nitro benzyl protected thiostatines

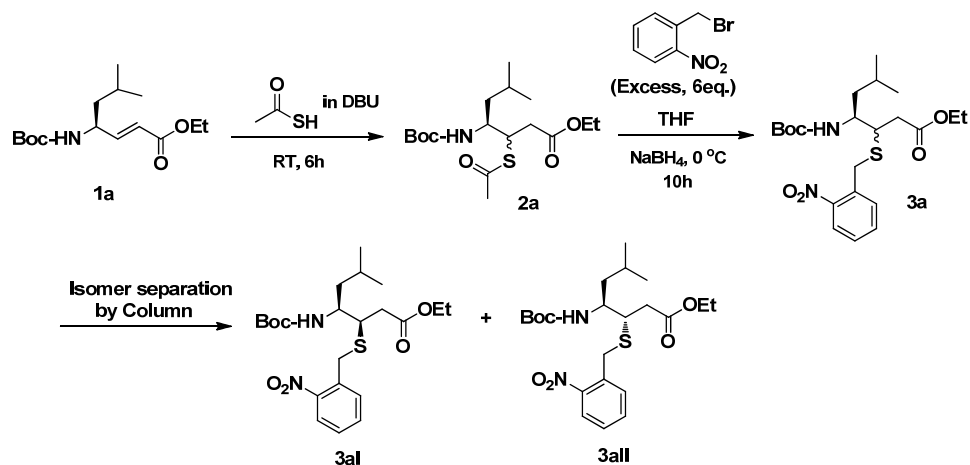
We speculated that conjugate addition of thioacetic acid to the α , β -unsaturated γ -amino esters would lead to the orthogonally protected β -thiol substituted γ -amino acids and the acetate protecting groups can be removed after the synthesis of peptides through mild sodium borohydride reduction. In this regard, we subjected ethyl ester of α , β -unsaturated γ -amino acid to the conjugate addition using thioacetic acid in the presence of DBU. The reaction mixture was stirred for about 6 hr. at room temperature. The progress of the reaction was monitored by TLC. The thioacetic acid conjugate addition product was isolated in 70% yield after the aqueous work-up. Further, we found it difficult to separate the diastereomeric mixture of thiol conjugate addition products. We anticipate that these amino acids can be separated as dipeptides after coupling to the other amino acids. We subjected the thioacetic acid substituted γ -amino ester for the *N*-terminal Boc- deprotection using 70% TFA

in DCM. Surprisingly, we found that the rearranged product through the S→N-acyl transfer similar to the native chemical ligation. The schematic representation of the reaction is shown in Scheme 9. This S→N-acyl transfer was found to trace less and the product was isolated in quantitative yield.



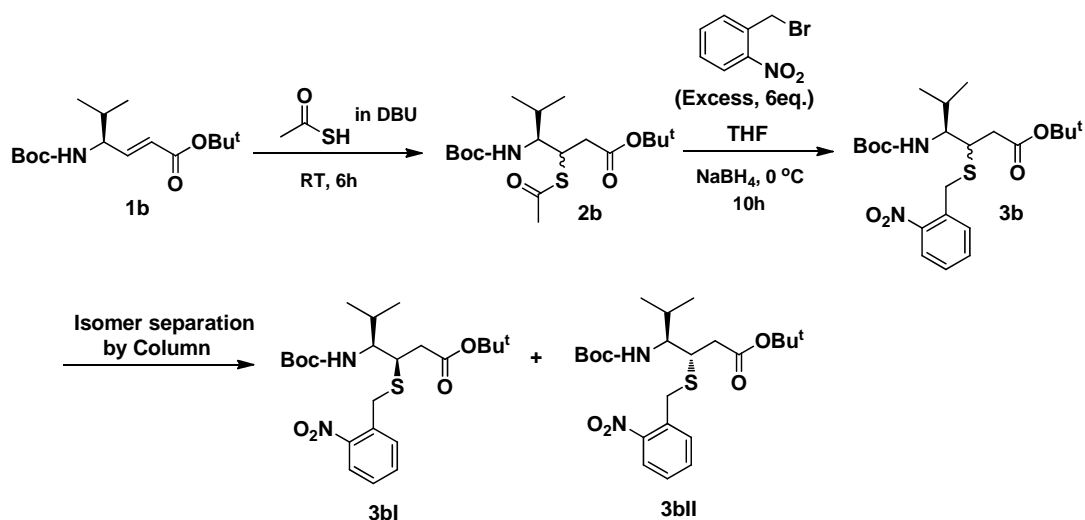
Scheme 9: Schematic representation of S-N acyl transfer during thiostatine isolation

We speculate that if we reduce the thioester to thiol and protect the thiol with suitable orthogonal protecting groups before the deprotection of *N*-Boc group it will be possible to synthesize orthogonally protected thiostatines which can be used in the peptide synthesis. The modified reaction is shown in Scheme 10.

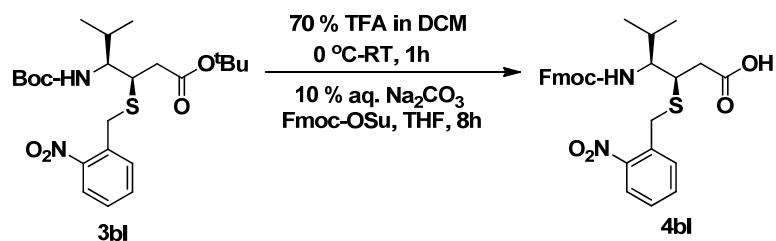


Scheme 10: Schematic representation for synthesis of orthogonally protected thiostatine

The thioacetic acid conjugate addition product was reduced using NaBH₄ in THF in the presence of excess *o*-nitrobenzyl bromide. We anticipate that the liberated free thiol after the reduction can be protected with *o*-nitrobenzyl bromide, which can be removed after the peptide synthesis through UV-irradiation at 365nm.⁵¹ As anticipated both the thioester reduction and thiol protection were achieved in a single step. In contrast to the thioacid conjugated addition products, the *S*-nitrobenzyl protected thiostatine products were separated using column chromatography. Both *syn* and *anti* diastereoisomers with respect to the amino acid side chains were obtained in 60:40 ratio after the column purification. Unfortunately, similar to the methyl ester of β -OBt substituted γ -amino acids, we also observe elimination products in the saponification of ethyl ester of thiostatine derivatives. In this regard, we further modified the protecting group strategy. Instead of ethyl esters, we used *tert*-butyl ester of *E*-vinylogous amino acids for the thioacetic acid conjugate addition. After the conjugate addition, the thioacetate was reduced to thiol in the presence *o*-nitrobenzyl bromide and both *syn* and *anti* diastereomers were separated using column chromatography (Scheme 11). Both Boc- and *tert*-butyl groups were deprotected using 70% TFA in DCM and the free amine was further protected with solid phase compatible Fmoc-group. The schematic representation of the reaction is shown in Scheme 12.



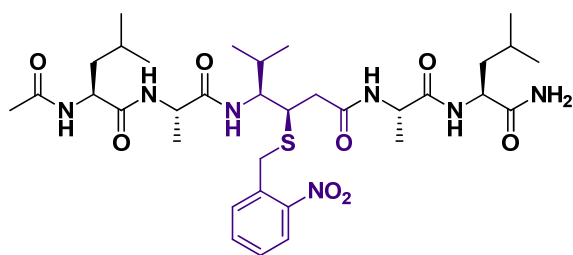
Scheme 11: Schematic representation for the synthesis of orthogonally protected thiostatine



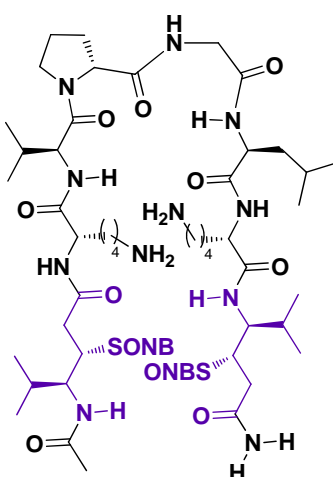
Scheme 12: Synthesis protocol for Fmoc- γ Val β -(S-ONB)-OH

1C.2.2 Synthesis of thiostatines containing peptide P1 and peptides P2

In order to understand whether these thiostatines can be utilized to synthesize the stable β -sheets and β -hairpins, we designed two model peptides **P1** and **P2** by incorporating thiostatine amino acids. The sequences of the peptides are given in the Scheme 13.



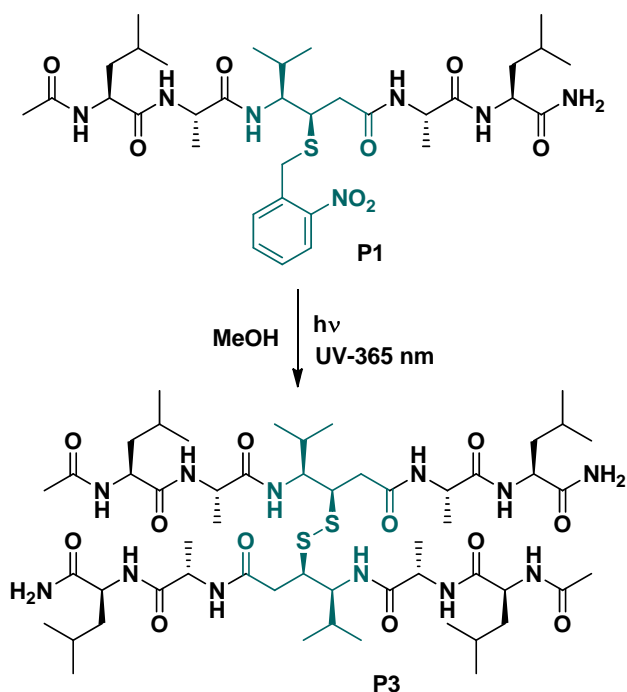
P1: Ac-Leu-Ala- γ Val β -(S-ONB)-Ala-Leu-CONH₂



P2: Ac- γ Val β -(S-ONB)-Lys-Val-^DPro-Gly-Leu-Lys- γ Val β -(S-ONB)CONH₂

Scheme 13: Designed sequence of the peptide **P1** and **P2** containing thiostatine amino acids.

In case of **P1** only one thioistatine was incorporated at the third position, anticipating after the deprotection of the *o*-nitrobenzyl group, the free thiol group can undergo oxidative dimerization. In case of the **P2**, the thioistatines were incorporated at the N- and C-terminals of the β -hairpin. We hypothesized that after deprotection of the thiol protecting groups, the intramolecular oxidative disulfide formation leads to the formation of stable β -hairpin structure. To induce the reverse turn in peptide **P2**, we used the ^DPro-Gly at the turn segment. The dipeptide ^DPro-Gly has been extensively utilized as a β -turn inducer in the synthetic β -hairpin designs.⁵² The hydrophilic residue Lys was incorporated at the positions 2 and 7 of the anti-parallel β -strands to induce the solubility of the peptide in aqueous solution. Both peptide **P1** and **P2** were synthesized using solid phase method by standard Fmoc- chemistry on Rink amide resin at 0.2 mmol scale. The coupling reactions were performed using standard HBTU/HOBt coupling conditions. After completion of the synthesis, peptides were cleaved from resin using TFA/water cocktail mixture and isolated as solid white crude product after precipitation with DCM/pet-ether or diethyl ether. The peptide **P1** was purified using reverse phase HPLC on C18 column using MeOH/H₂O and as solvent systems, while **P2** was purified using acetonitrile/water solvent systems. The pure peptides were subjected to the UV-light irradiation at 365 nm in the methanol solution to deprotect the *o*-nitrobenzyl group. The reaction was monitored using the mass spectral analysis and HPLC. Complete deprotection of *o*-nitrobenzyl group and concomitant disulfide formation were achieved in a single step. The schematic representation of the reaction is shown in Scheme 14. The disulfide bridged peptides **P3** and **P4** were further purified using HPLC and pure peptides were subjected to the 2D NMR and CD analysis to understand solution conformations of these peptides.



Scheme 14: Schematic representation for deprotection of photo labile group and simultaneous dimerization through disulfide bond of peptide **P1**

1C.2.3 Solution structure analysis of peptide **P3**

The ^1H NMR of **P3** in CD_3OH reveals that the wide dispersion of backbone NH and C^αH along with C^γH signalling a well structured peptide in solution. Interestingly, we observed one set of ^1H NMR signals for the two β -strands in the disulfide bridged β -sheet, suggesting the highly symmetric nature of the β -strands. The fully assigned ^1H NMR of **P3** is shown in the Figure 13. Further, we subjected **P3** to the 2D NMR analysis. Partial TOCSY spectrum of the **P3** is given Figure 14. Using the sequential proton interactions from TOCSY, amino acid residues were identified. The sequence of amino acid residues of the peptide **P3** was established using ROESY spectrum.

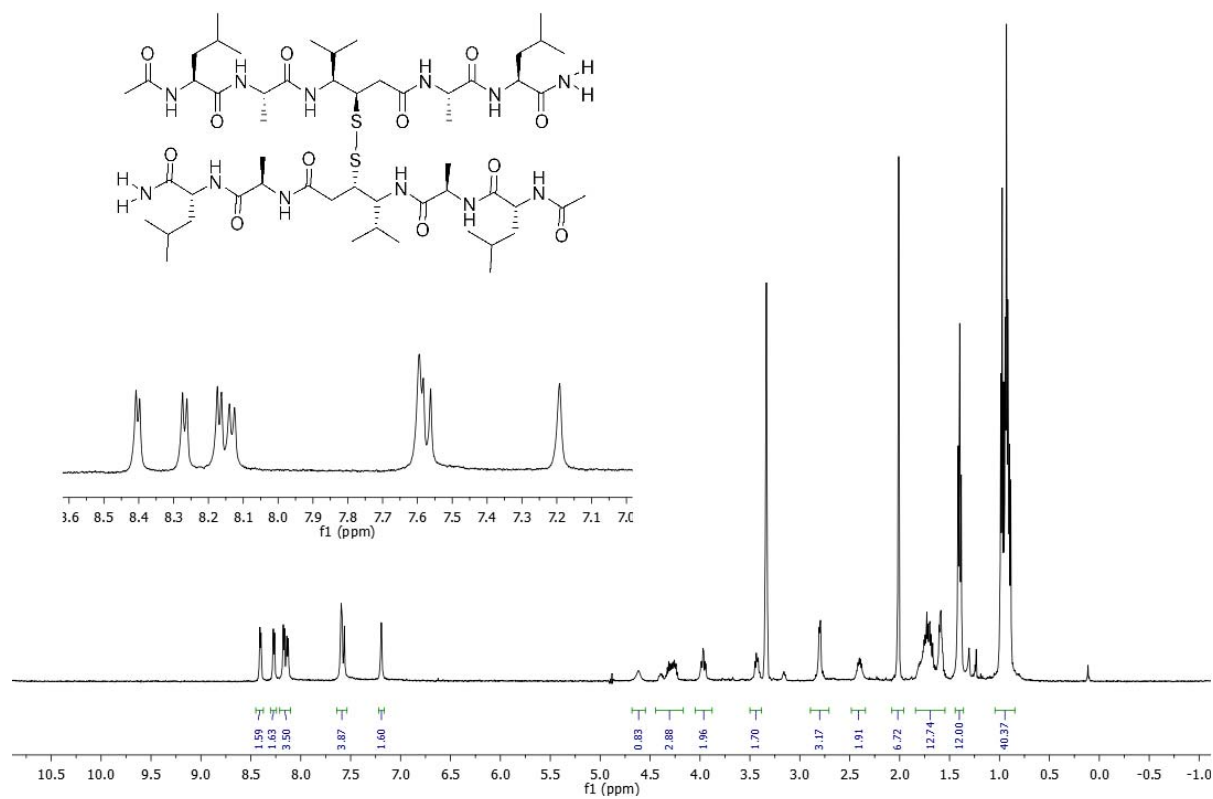


Figure 13: ^1H NMR of stapled peptide **P3**

The wide dispersion of amide NH protons in ^1H NMR spectra reveals the extended structure of the peptide. The analysis of the ROESY spectrum reveals the strong $\text{C}^\alpha\text{H} \leftrightarrow \text{NH}$ protons of i to $i-1$ residues indicating the extended β -sheet character of the peptide. The partial ROESY spectrum highlighting these interactions is shown in Figure 15 and 16. In addition, we also observed the $\text{NH} \leftrightarrow \text{NH}$ interactions between the residues Ala2 to γ Val NH and the terminal amide to Leu 5 NH (Figure 17). These sequential $\text{NH} \leftrightarrow \text{NH}$ interactions are generally observed in the helix and reverse turns and are not observed in the β -sheet structures. All observed NOEs in the ROESY spectrum is given in the Figure 18.

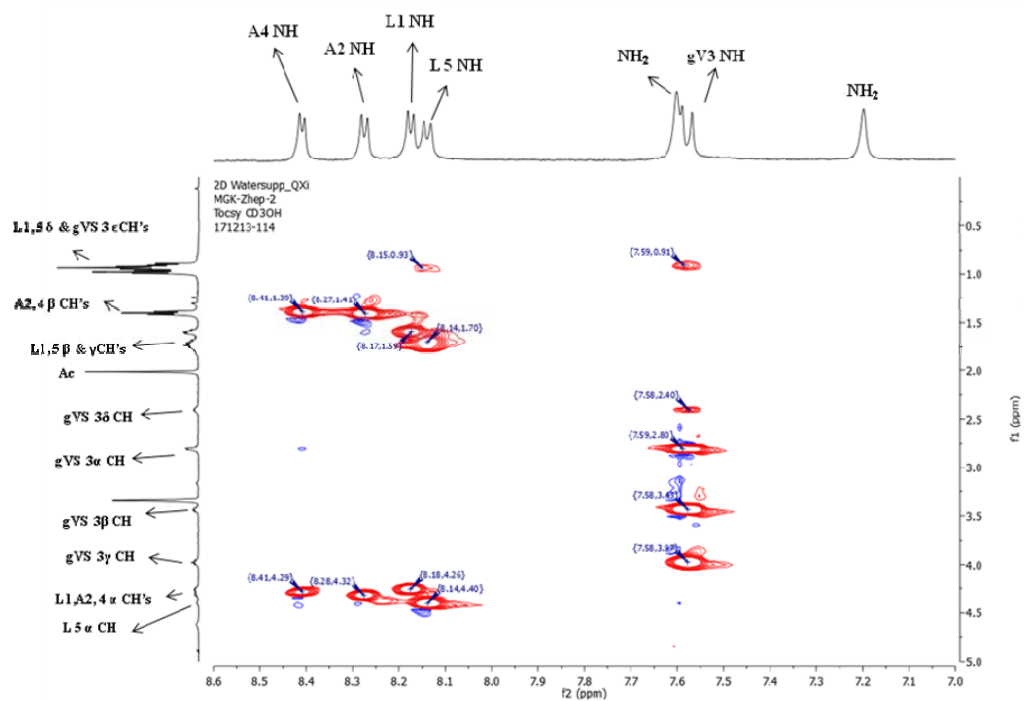


Figure 14: Partial TOCSY spectrum of the peptide P3

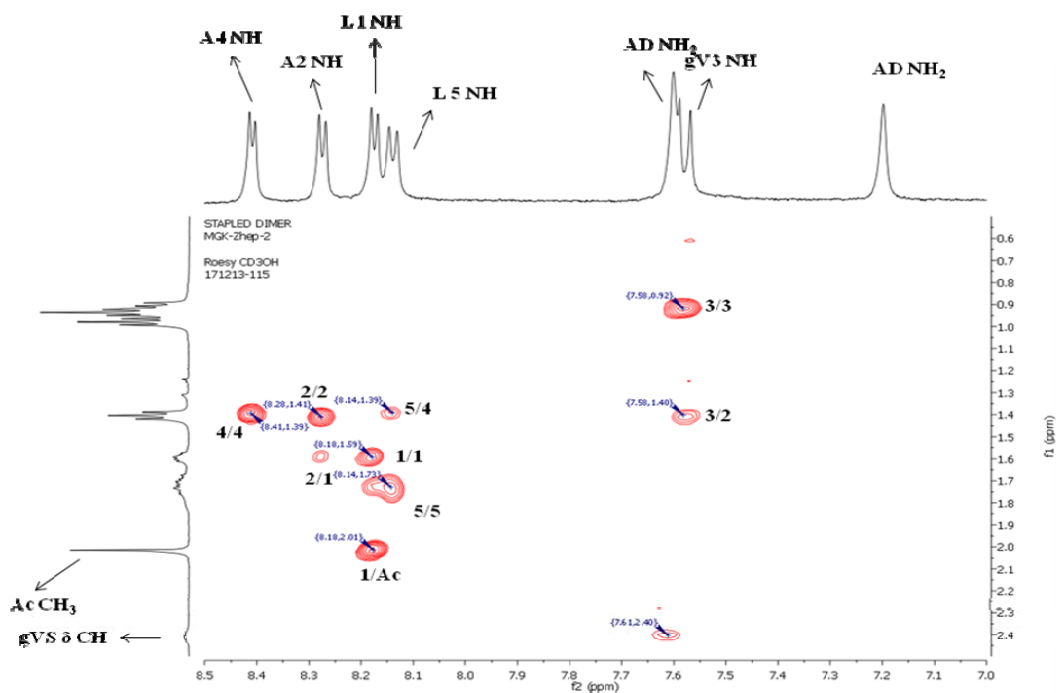


Figure 15: Partial ROESY spectrum of peptide P3, highlighting the NH ↔ CH interactions.

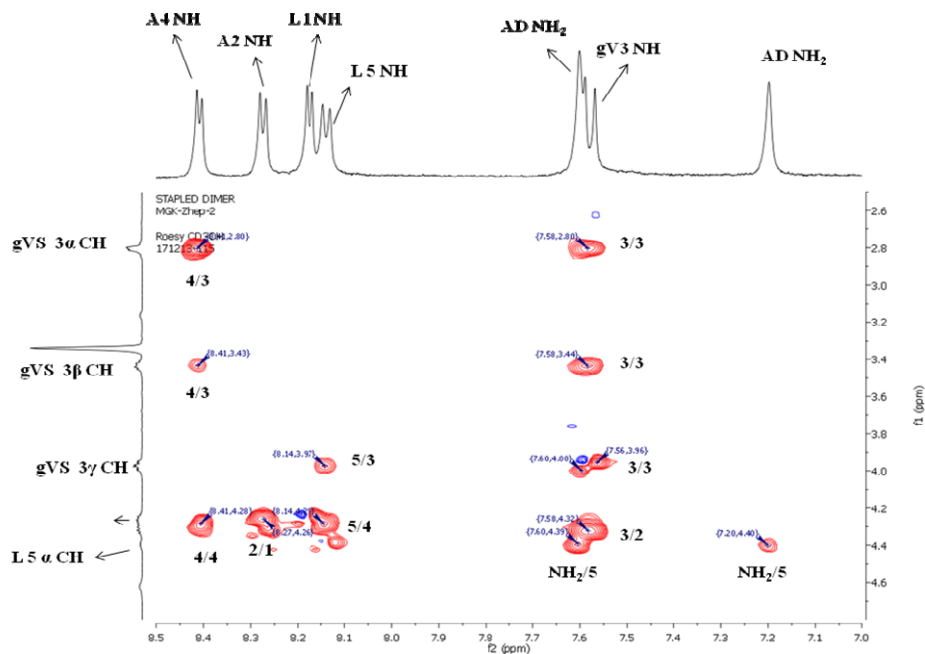


Figure 16: Partial ROESY spectrum of peptide P3, highlighting the NH \leftrightarrow CH interactions.

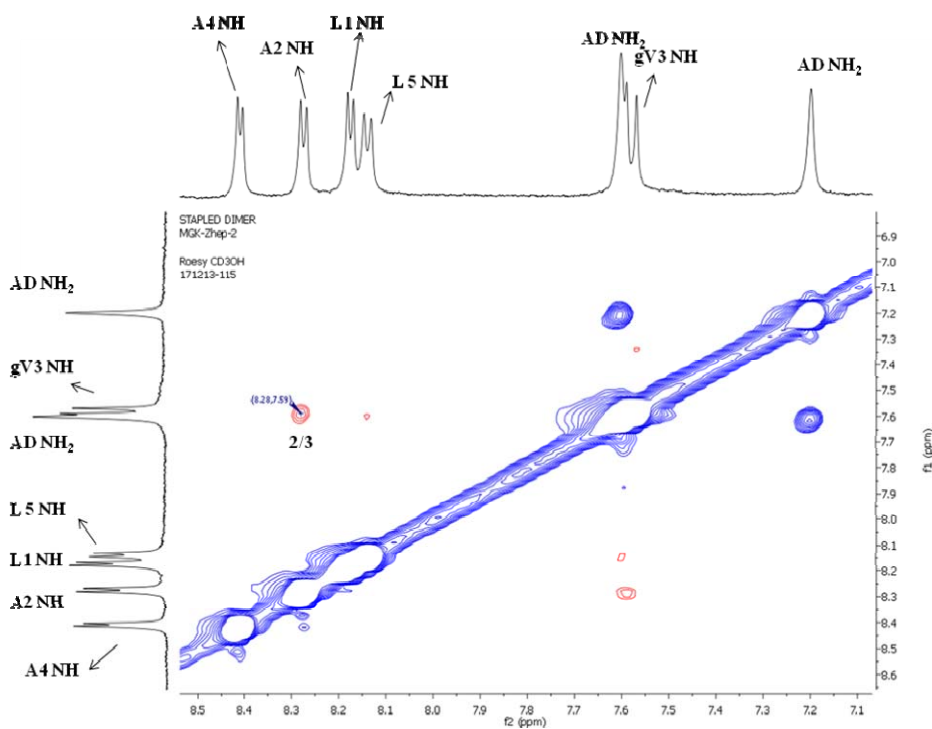


Figure 17: Partial ROESY spectrum of peptide P3, depicting the NH-NH NOEs.

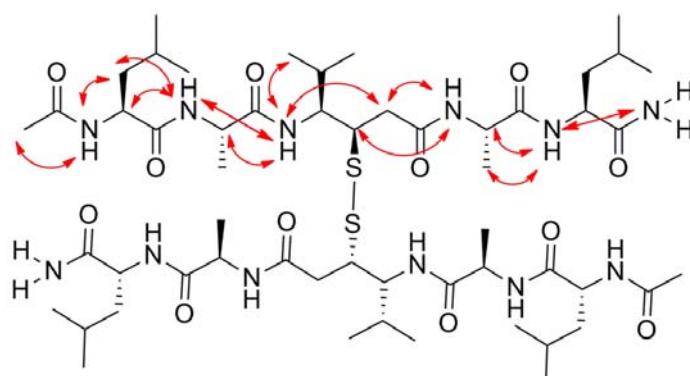


Figure 18: All observed NOEs for peptide **P3** in the ROESY spectrum are highlighted in the peptide sequence .

Further, we subjected the peptide **P3** for the temperature dependent ^1H NMR to understand the involvement of amide protons in the intermolecular H-bonds. The experiments were performed from 250 K to 325 K with 10K intervals. A graph depicting the temperature vs amide chemical shift is shown in Figure 19.

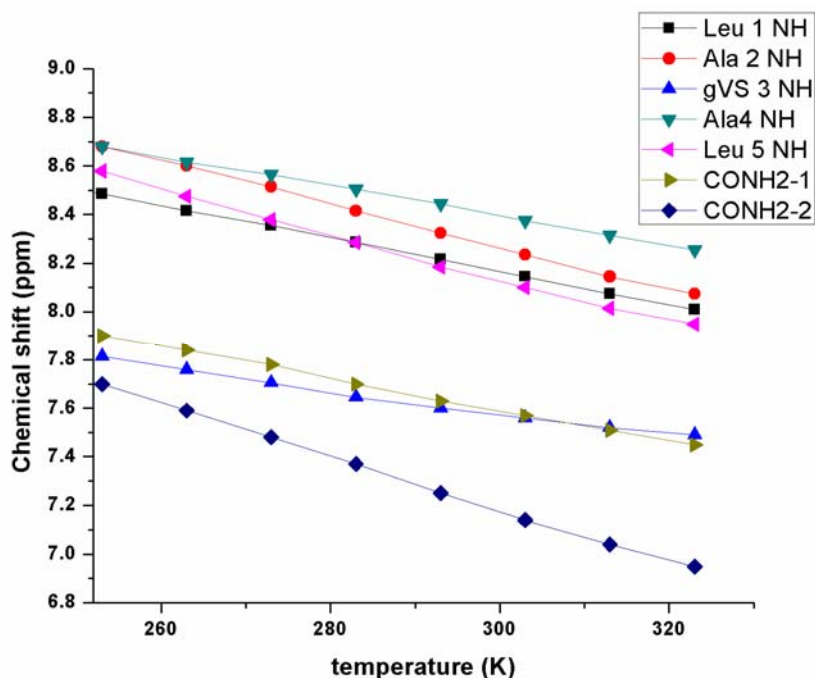


Figure 19: Plot of amide shift with the various temperatures for peptide **P3**

Analysis of the results reveal that in contrast to the amide protons of Leu1, γ Val3 and Ala4, the amide protons of the Ala2, Leu5 and C-terminal amide protons showed strong upfield shift with increase in temperature. However, gradual upfield shift is observed in all amide NHs with increase in temperature. Based on the 2D NMR NOEs constraints, the solution structure of **P3** was calculated using software Insight II⁵⁵ and energy minimized structure is given in the Figure 20.

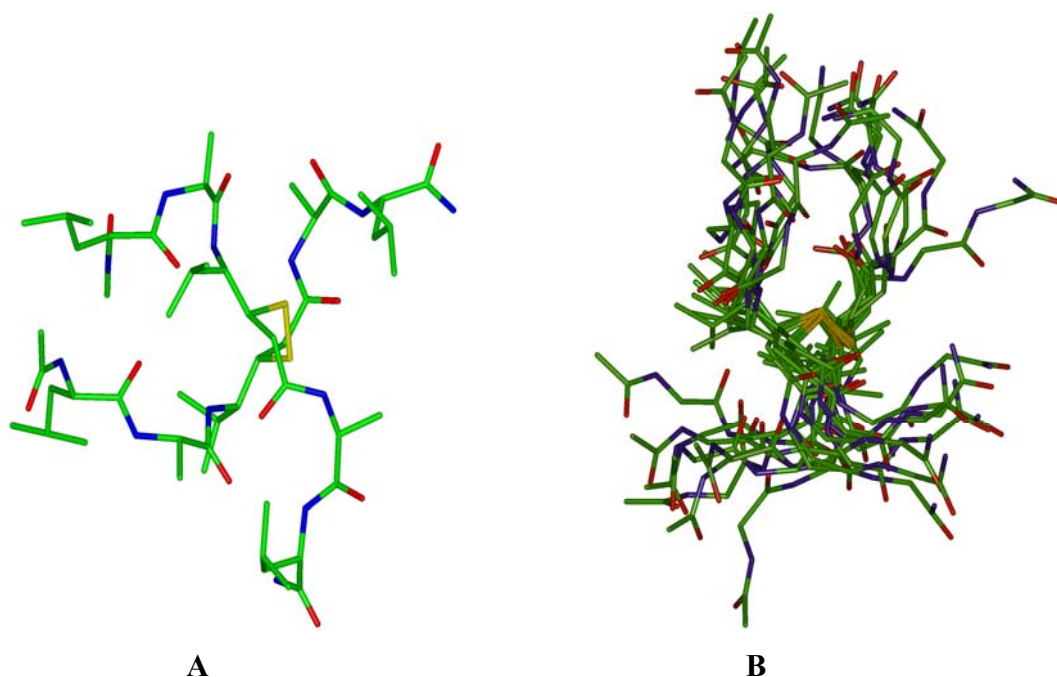


Figure 20: A) The NMR model solution structure of disulfide stapled peptide **P3** B) The ensemble of ten low energy structures are calculated based on the observed NOEs.

1C.2.4 Solution structure of thiostatine bridged β -hairpin peptide **P4**

Similar to the peptide **P1**, concomitant *o*-nitrobenzyl deprotection and oxidative disulfide formation of peptide **P2** was achieved through UV-irradiation in water. The disulfide stapled peptide **P4** was subjected to ^1H and 2D NMR analysis in water to understand its solution structure. The wide dispersion of both amide NHs and C^αH in ^1H NMR spectrum signaling a well ordered structure of the peptide in solution. The fully assigned ^1H NMR of peptide **P4** is shown in Figure 21.

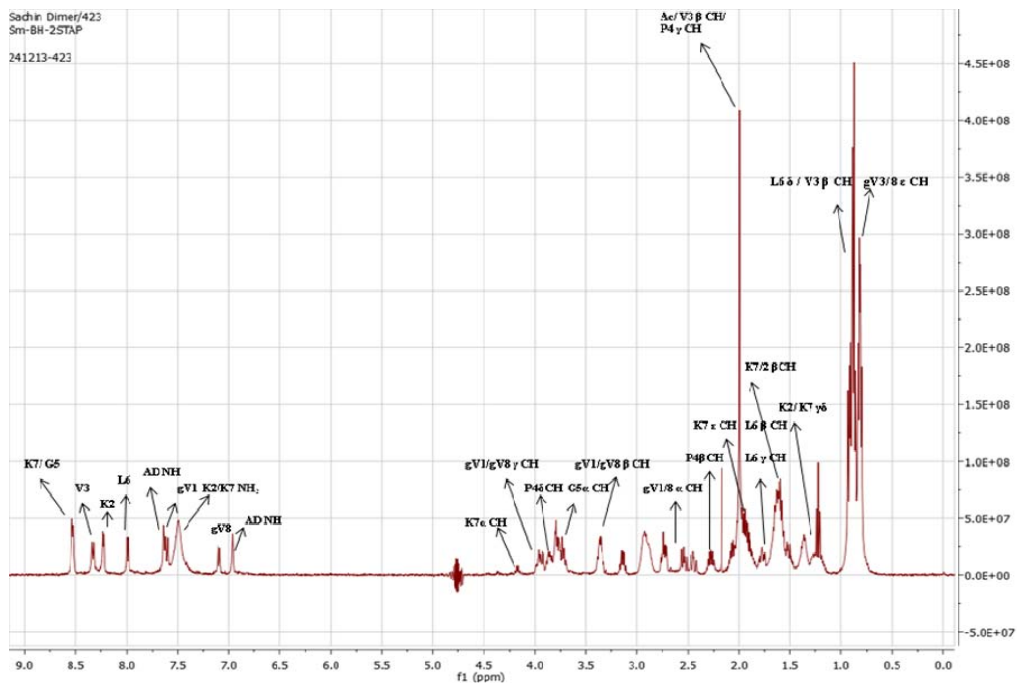


Figure 21: Fully assigned ^1H NMR of disulfide stapled peptide P4

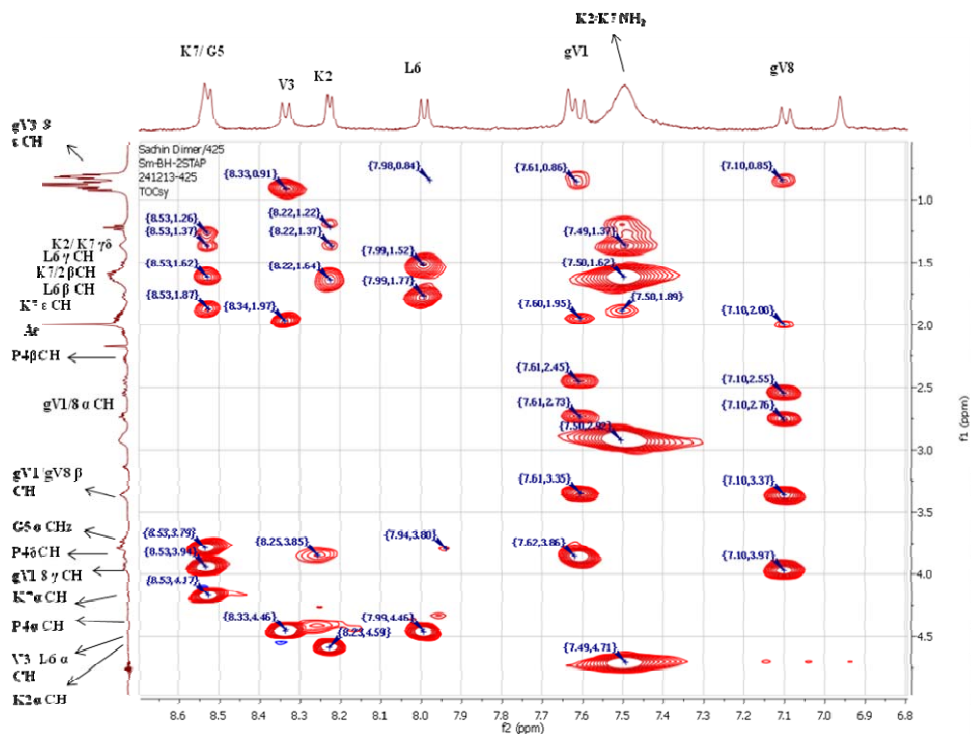


Figure 22: Partial TOCSY spectrum of the peptide P4

Partial TOCSY spectrum of the **P4** is given Figure 22. Using the sequential proton interactions from TOCSY the amino acid residues in the β -hairpin were identified. The sequence of amino acid residues were further established using ROESY spectrum. As anticipated, the 2D NMR (ROESY) analysis showed the characteristic turn and the cross-strand NOEs of antiparallel β -strands confirming a β -hairpin structure in solution. The critical NOEs observed in the ROESY spectrum are illustrated in the schematic diagram shown in Figure 23.

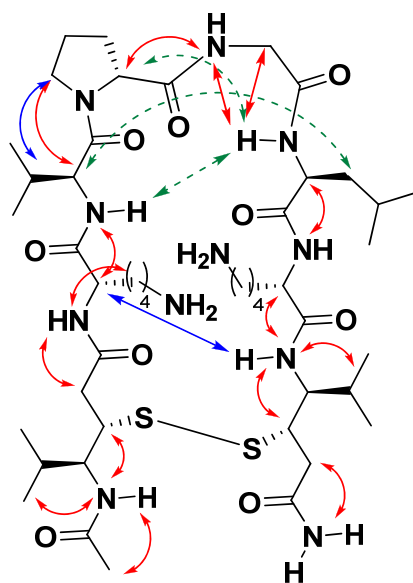


Figure 23: NOEs observed in the ROESY spectrum are highlighted as red (strong), blue (medium) and green (weak) in double headed arrows.

The characteristic sequential $\text{NH} \leftrightarrow \text{C}^\alpha \text{H}$, cross-strand $\text{NH} \leftrightarrow \text{NH}$ and $\text{C}^\alpha \text{H} \leftrightarrow \text{C}^\gamma \text{H}$ NOEs of facing β -strands in the ROESY spectrum are shown in Figure 24, 25 and 26. The long range NOEs between the Lys2 $\text{C}^\alpha \text{H}$ and NH of γ Val 8 ($\text{C}^\alpha \text{H} \leftrightarrow \text{HN}$) and $\text{NH} \leftrightarrow \text{NH}$ NOEs between the residues Val3 and Lue6 indicating the stable and the well folded antiparallel β -sheet character in aqueous solution. The strong NOEs between the δ protons of $^{\text{D}}$ Pro4 and Val $\text{C}^\alpha \text{H}$ suggesting the *trans* conformation Pro amide bond.

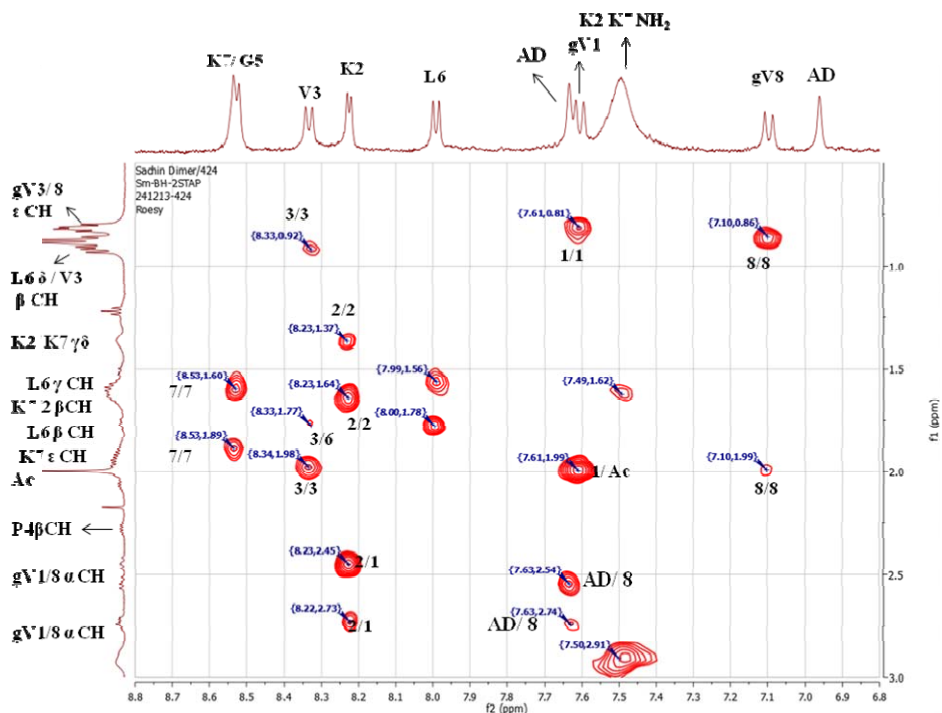


Figure 24: Partial ROESY spectrum of peptide P4 showing NH↔CH NOEs

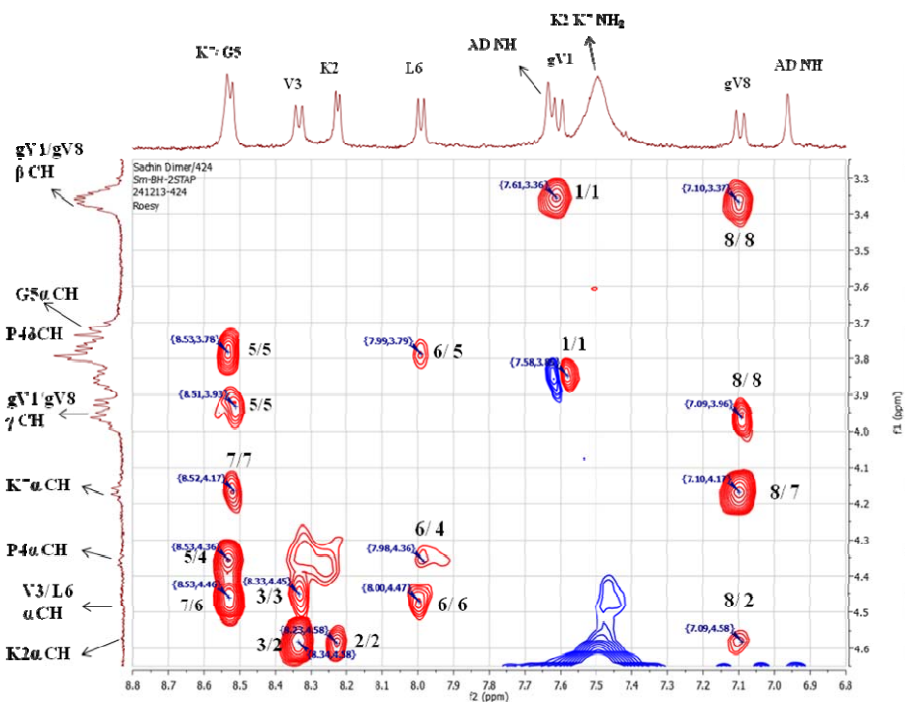


Figure 25: Partial ROESY spectrum of peptide P4 showing NH↔CH NOEs

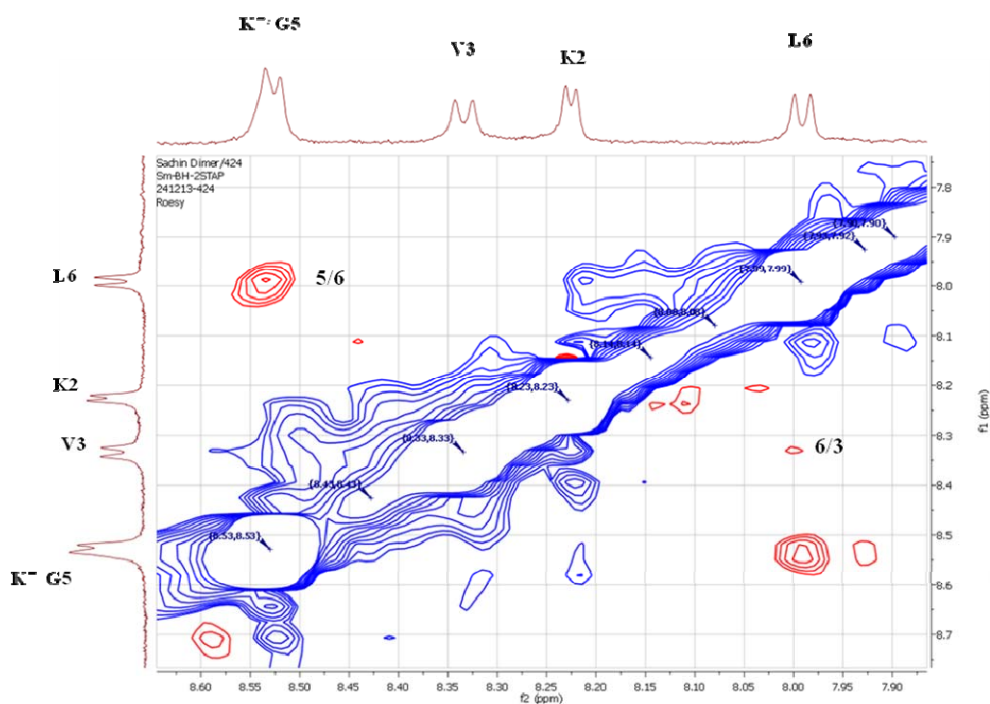


Figure 26: Partial ROESY spectrum of peptide **P4** depicting the NH↔NH NOEs

Interestingly, we did not observe any characteristic cross-strand NH↔NH and CH↔CH interactions between the terminal thiostatines residues. Using the experimentally deduced NOEs for peptide **P4**, the ensemble of structures is obtained by distance restrained molecular dynamic simulations (Insight II 2005, Accelrys Inc.).⁵⁵ The overlay of ten low energy conformers of NMR calculated structures are shown in Figure 27. The NMR model reveals that **P4** adapted a folded β -hairpin conformation in solution. These results suggesting that thiostatines can be used to stabilized the frying terminal strands in β -hairpins. Another very interesting point here to note that the side-chain functionalities of cysteine and other amino acids can be merged into a single thiostatine residue.

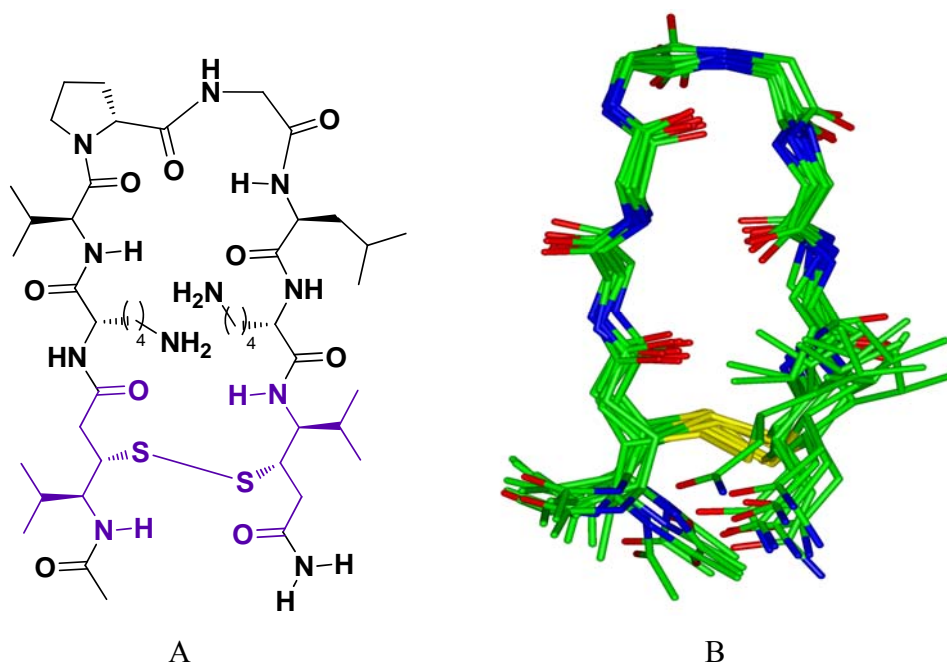


Figure 27: A) Disulfide stapled structure of β -hairpin peptide **P4**. B) The ensemble of ten low energy structures of β -hairpin peptide **P4** are calculated based on the observed NOEs (except terminal thioestatin side chains of all other amino acid residues are omitted for clarity)

1.2 Conclusions

Overall, we have demonstrated the facile and racemization-free synthesis of α , β -unsaturated γ -amino esters with exceptional high *E*-stereoselectivity using Wittig reaction and their utility in the conjugate addition of HOBT and thiols. Although both reactions are 1, 4-conjugate additions the mechanism of the conjugate addition is different. Wittig reaction was found to be compatible with Boc-, Fmoc- and other side chain protecting groups in the synthesis of *E*-vinylogous amino acids. The crystal conformations of *E*-vinylogous amino acids and peptides suggest that they prefer to adopt extended β -sheet type of the structures. The HBTU mediated HOBT conjugate addition to the α , β -unsaturated γ -amino acids in the absence of free amine coupling partner showed the flexible reactivity of the unsaturated carbonyl compounds. This provides a mild and facile methodology for the synthesis of various β -OBT substituted γ -amino acids. The stereochemistry of the novel β -OBT substituted γ -amino acids were analyzed using single crystal X-ray structures from both the monomers as well as in peptides. The elimination products observed after the treatment of β -OBT substituted γ -amino acids and

peptides with NaOH, suggests that this methodology can be used to mask the reactivity of the conjugated double bonds. As conjugate addition of unsaturated carboxylic acids has scarcely studied due to their inherent limitations, the results reported here may provide an opportunity to extend this methodology to other α , β -unsaturated acids. Further, we developed novel thiostatine with photolabile, solid phase compatible protecting groups. The synthesis of thiostatines was achieved through the conjugate addition of thioacetic acid on *E*-vinylogous amino acids. In contrast to the side-chain disulfides of cysteine residues, the back-bone disulfides from the thiostatines may lead to the more compact β -hairpins and β -sheets within the distance of H-bond. As β -hydroxy- γ -amino acids (statines) have been extensively used as inhibitors of various aspartic acid proteases, anti-cancer and other properties, we believe that novel thiostatines discovered here may find applications in various fields of chemical biology, medicinal chemistry and biomaterials. The S \rightarrow N-acyl transfer during the synthesis of the thiostatines in this chapter motivated us to explore the reactivity of thioacids as coupling reagents in the peptides synthesis. Details of this investigation are given in Chapter 2.

1.3 Experimental Section

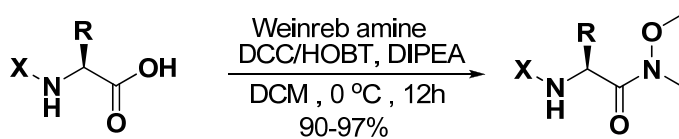
1.3.1 General Information

All amino acids, Weinreb amine hydrochloride salt, DCC, LAH, DIPEA, PPh₃ were purchased from Aldrich. The solvents THF, DCM, toluene were purchased from Merck. THF and DIPEA was dried over sodium and distilled prior to use. Ethyl bromoacetate, di-*tert*-butyl dicarbonate, Fmoc-OSu were purchased from Spectrochem and used without further purification. Column chromatography was performed on Merck silica gel (100-200 mesh). ¹H NMR spectra were recorded on *Jeol* 400 MHz and ¹³C NMR on 100 MHz spectrometer using residual solvent as internal standard (CDCl₃ δ_{H} , 7.24 ppm, δ_{C} 77.0 ppm). The chemical shifts (δ) were reported in ppm and coupling constant (*J*) in Hz. Specific rotations were recorded using methanol and DMF (Rudolph Analytical Research). Mass spectra were obtained from MALDI-TOF/TOF (Applied Biosystem).

1.3.2 Synthesis procedure and compound characterization for Section 1A

General Procedure for the Synthesis of Boc/Fmoc-amino Weinreb Amide

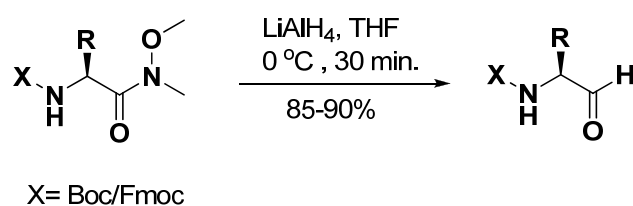
In a typical experimental procedure, protected amino acid (20 mmol) was dissolved in a DCM and to this solution hydrochloride salt of Weinreb amine (30 mmol) was added. The reaction mixture was then cooled at 0 °C. This reaction mixture was treated with DIPEA, DCC and HOBT. The progress of the reaction was monitored by TLC. After the completion of reaction (12 h) DCM was evaporated and residue was diluted with 150 mL of ethyl acetate and washed with 5% aqueous HCl (50 mL), 10% aqueous Na₂CO₃ (50 mL) followed by brine solution. The organic layer was then dried over the anhydrous Na₂SO₄ and the product was concentrated under reduced pressure. The pure Weinreb amide of *N*-protected amino acid was isolated after the column chromatography using EtOAc/ petroleum ether (60-80 °C) solvent system.



X= Boc/Fmoc

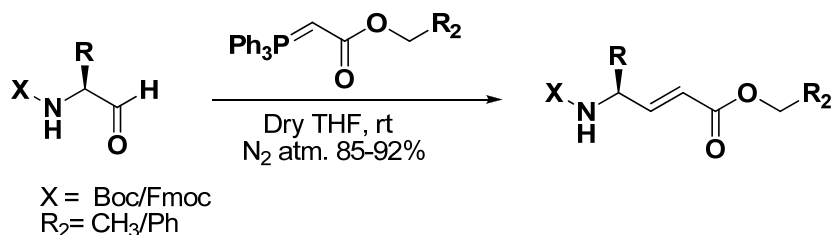
General Procedure for Synthesis of Synthesis of Boc/Fmoc Amino Aldehyde

The *N*-Protected Weinreb amide (20 mmol) was dissolved in 130 mL of dry THF under N₂ atmosphere, cooled to 0 °C, and then LiAlH₄ (22 mmol) was added slowly during 10 min. Reaction mixture was stirred for another 20 min. After completion, the reaction was quenched with 5% HCl (5 % by volume in water) very slowly in ice cool condition (pH~3). THF was evaporated from the reaction mixture and the *N*-protected amino aldehyde was extracted with ethyl acetate (3 × 80 mL). Combined organic layer was washed with brine (40 mL) and dried over anhydrous Na₂SO₄. Organic layer was concentrated under reduced pressure to get oily product and immediately used for next step without purification.



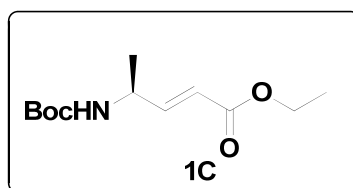
General Procedure for Synthesis of Boc/Fmoc Vinylogous Amino Ester

The *N*-protected amino aldehyde (10 mmol) was dissolved in dry THF (40 mL) under the N₂ atmosphere. To this solution Wittig ylide (11.5 mmol) was added. The progress of reaction was monitored by TLC. After the completion of reaction (8h) the THF was evaporated and product was purified by column chromatography using 5:95 ethyl acetate /pet ether solvent system.

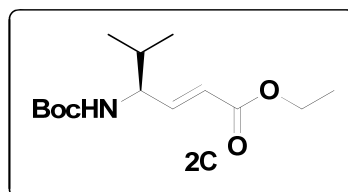


Spectroscopic data for *N*-protected vinylogous amino esters

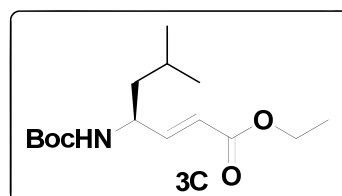
(*S, E*)-Ethyl 4-(tert-butoxycarbonylamino)pent-2-enoate (1C); Colorless Oil (Yield 2.25 g, 93%); $[\alpha]_D^{25} = -20.8$ (c = 1, MeOH) ¹H NMR (400 MHz, CDCl₃) δ 6.876-6.827 (dd, 1H vinylic β proton), 5.898-5.859 (d, 1H vinylic α proton), 4.5 (br., NH), 4.38 (br., α proton), 4.198-4.144 (q, *J* = 7.3 Hz, OCH₂), 1.432 (s, 9H, C(CH₃)₃ Boc), 1.265-1.247 (m, 6H, (CH₃)₂); ¹³C NMR (100 MHz CDCl₃) 166.4, 154.9, 120.2, 79.8, 60.5, 47.0, 28.4, 20.4, 14.3; **MALDI TOF/TOF** m/z Calcd. for C₁₂H₂₁NO₄ (M + Na) 266.1368 Observed = 266.1365.



(S, E)-Ethyl 4-(tert-butoxycarbonylamino)-5-methylhex-2-enoate (2C) Colorless solid (2.43 g, 90%); $[\alpha]_D^{25} = -3.40$ ($c = 1$, MeOH); $^1\text{H NMR}$ (400 MHz, CDCl_3) δ 6.855-6.816 (dd, 1H vinylic β proton) 5.924-5.880 (d, $J = 15.6$ Hz, 1H, vinylic α proton), 4.55 (d, 1H, NH), 4.187-4.168 (q, $J = 6.88$ Hz, 2H, OCH_2), 1.862-1.84 (m, 1H, γ proton), 1.429 (s, 9H, $\text{C}(\text{CH}_3)_3$ Boc), 1.292-1.256 (t, $J = 7.32$ Hz, 3H, CH_3), 0.932-0.885 (q, $J = 6.4$ Hz, $\text{C}(\text{CH}_3)_2$); $^{13}\text{C NMR}$ (100 MHz, CDCl_3); 166.2, 155.3, 147.3, 121.4, 79.6, 60.3, 56.6, 32.1, 28.2, 18.8, 17.9, 14.1 **MALDI TOF/TOF** Calcd. for $\text{C}_{14}\text{H}_{25}\text{NO}_4$ ($\text{M} + \text{Na}$) = 294.1681 Observed = 294.1686.

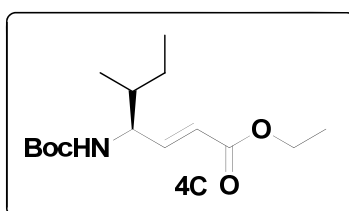


(S, E)-Ethyl 4-(tert-butoxycarbonylamino)-6-methylhept-2-enoate (3C); Colorless crystalline solid (2.70 g, 95%); $[\alpha]_D^{25} = -25.50$ ($c = 1$, MeOH); $^1\text{H NMR}$ (500 MHz, CDCl_3) δ 6.854-6.811 (dd, $J = 16$ Hz, $J = 5.5$ Hz, 1H, $\text{CH}=\text{CHCO}_2\text{Et}$), 5.936-5.904 (d, $J = 16$ Hz, 1H, $\text{CH}=\text{CHCO}_2\text{Et}$), 4.451 (br., 1H, NH), 4.334 (br., 1H, $\text{CH}-\text{CH}=\text{CH}$), 4.215-4.172 (q, $J = 7$ Hz, 2H, $-\text{OCH}_2$), 1.726-1.671 (m, 1H, $\text{CH}-(\text{CH}_3)_2$), 1.446 (s, 9H, $-(\text{CH}_3)_3$ Boc), 1.400-1.372 (t, $J = 7$ Hz, 2H, $\text{CH}_2\text{CH}-(\text{CH}_3)_2$), 1.304-1.276 (t, $J = 7$ Hz, 3H, $-\text{OCH}_2\text{CH}_3$), 0.945-0.932 (d, $J = 6.5$ Hz, 6H, $\text{CH}-(\text{CH}_3)_2$); $^{13}\text{C NMR}$ (100 MHz, CDCl_3) δ 166.4, 155.0, 148.8, 120.3, 79.6, 60.4, 49.7, 43.7, 28.3, 24.6, 22.6, 22.1476, 14.2; **MALDI TOF/TOF** m/z Calcd. For $\text{C}_{15}\text{H}_{27}\text{NO}_4$ ($\text{M} + \text{Na}$) = 308.1838, Observed = 308.1840.

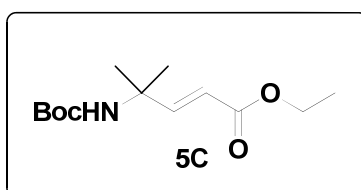


(4S, 5R)-Ethyl 4-(tert-butoxycarbonylamino)-5-methylhept-2-enoate (4C); Colorless solid, (yield 2.62 g, 92%); $[\alpha]_D^{25} = -11.20$ ($c = 1$, MeOH); $^1\text{H NMR}$ (400 MHz, CDCl_3) δ

6.858-6.819 (d, 1H vinylic β proton), 5.917-5.878 (d, $J = 14.36$ Hz, 1H, vinylic α proton), 4.568 (br, 1H, NH), 4.255 (br., 1H, α proton), 4.197-4.161 (q, $J = 6.88$ Hz, 2H, OCH₃), 1.655-1.595 (br., 2H, CH₂), 1.421 (s, 9H, C(CH₃)₃, Boc), 1.284-1.248 (t, $J = 6.88$ Hz, 3H, CH₃), 0.9152-0.8659 (m, 6H, (CH₃)₂); ¹³C NMR (100 MHz, CDCl₃) δ 166.3, 155.3, 147.1, 121.6, 79.651, 60.4, 55.7, 39.0, 28.4, 25.3, 15.3, 14.2, 11.6; **MALDI TOF/TOF** m/z Calcd. for C₁₅H₂₇NO₄ (M + Na) = 308.1838 Observed = 308.1837

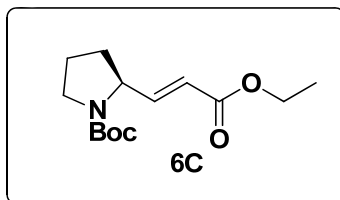


(Ethyl 4-(tert-butoxycarbonylamino)-4-methylpent-2-enoate (5C)); Colorless solid (1.92 g, 75%); ¹H NMR (400 MHz, CDCl₃) δ 7.020-6.980 (d, $J = 16.04$ Hz, 1H, vinylic β proton), 5.860-5.820 (d, $J = 16.04$ Hz, 1H, vinylic α proton), 4.710 (br., 1H, NH), 4.216-4.164 (q, $J = 6.88$ Hz, 2H, OCH₂), 1.428 (s, 9H, C(CH₃)₃, Boc), 1.408 (s, 6H, C(CH₃)₂), 1.306-1.270 (t, $J = 6.88$ Hz, 3H, CH₃); ¹³C NMR (100 MHz, CDCl₃) 166.7, 154.2, 153.6, 118.5, 79.4, 60.4, 52.9, 29.7, 28.4, 27.4, 14.3; **MALDI TOF/TOF** m/z Calcd. for C₁₃H₂₃NO₄ (M + Na) = 280.1525 Observed = 280.1526.

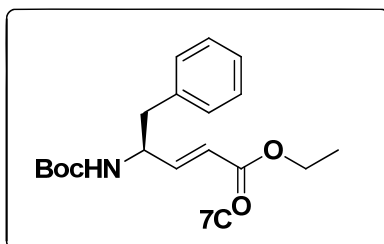


(S, E)-tert-Butyl2-(3-ethoxy-3-oxoprop-1-enyl)pyrrolidine-1-carboxylate (6C); Colorless oil (2.23 g, 83%) [α]_D²⁵ = -72 (c = 1, MeOH); ¹H NMR (400 MHz, CDCl₃) δ 6.836-6.783 (dd, $J = 15.6$ Hz, 1H, CH vinylic β proton), 5.838-5.800 (d, $J = 15.2$ Hz, 1H, CH vinylic α proton), 4.514&4.373 (br., 1H CH γ proton), 4.213-4.179 (q, $J = 6.4$ Hz, 2H OCH₂), 3.446-3.431 (t, $J = 6$ Hz, 2H, CH₂), 2.146-2.056 & 1.892-1.821 (m, 4H, β & γ CH₂), 1.421 (s, 9H C(CH₃)₃ Boc) 1.313-1.279 (t, $J = 6.8$ Hz, 3H, CH₃); ¹³C NMR (100 MHz, CDCl₃) δ 172.1,

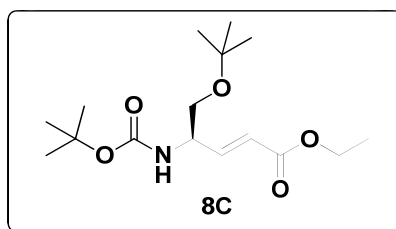
154.3, 148.5, 120.4, 79.631, 60.3, 57.8, 46.2, 31.7, 28.3, 22.9, 14.2; **MALDI TOF/TOF** m/z Calcd. for C₁₄H₂₃NO₄ (M + Na) = 292.1525 Observed = 292.1520.



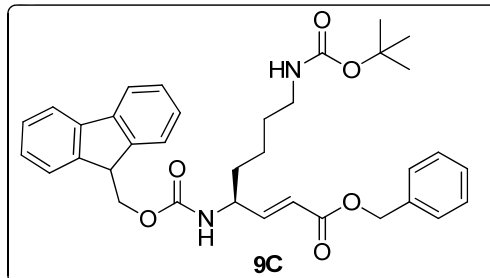
(S, E)-Ethyl 4-(tert-butoxycarbonylamino)-5-phenylpent-2-enoate (7C); White powder (2.67 g, 88%), ¹H NMR (400 MHz, CDCl₃) : δ 7.30-7.14 (m, 5H, -Ph), 6.91-6.86 (dd, *J* = 5.04, *J* = 11, 1H, CH=CHCO₂Et), 5.85-5.81 (d, *J* = 17.4, 1H, CH=CHCO₂Et), 4.59 (b, 1H, NH), 4.52 (b, 1H, CH-CH=CH), 4.18-4.13 (q, *J* = 6.88, 2H, -OCH₂), 2.92-2.85 (m, 2H, CH₂-Ph), 1.37 (s, 9H, -(CH₃)₃ Boc), 1.27-1.23 (t, *J* = 7.3, 3H, -OCH₂CH₃). ¹³C NMR (100MHz, CDCl₃) δ 166.14, 154.91, 147.56, 136.33, 129.36, 128.54, 126.83, 121.04, 79.83, 60.44, 52.16, 40.82, 28.26, 14.18; **MALDI TOF/TOF** m/z Calcd. [M+Na]⁺ 342.1681, observed 342.1657.



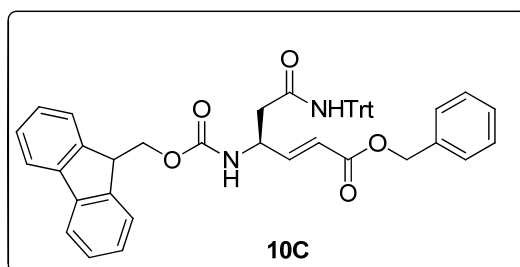
(R, E)-Ethyl 5-tert-butoxy-4-(tert-butoxycarbonylamino)pent-2-enoate (8C); Colorless oil (2.55 g, 81%); [α]_D²⁵ = +4.4 (c = 1, MeOH); ¹H NMR (400 MHz, CDCl₃) δ 6.918-6.866 (dd, *J* = 15.6 Hz, 1H, CH vinylic β proton), 5.948-5.909 (d, *J* = 15.6 Hz, 1H, CH vinylic α proton), 5.012 (br., 1H, NH), 4.355 (br., 1H, CH γ proton), 4.191-4.137 (q, *J* = 7.2 Hz, 2H, OCH₂), 3.478-3.445 (d, *J* = 4.4 Hz, 2H, CH₂), 1.423 (s, 9H, C(CH₃)₃, Boc), 1.135 (s, 9H, C(CH₃)₃, OtBu); ¹³C NMR (100 MHz, CDCl₃) δ 166.3, 155.3, 146.9, 121.7, 79.7, 73.4, 63.2, 60.4, 51.7, 28.4, 27.391, 14.2; **MALDI TOF/TOF** m/z Calcd for C₁₆H₂₉NO₅ (M+Na) = 338.1943 Observed = 338.1904.



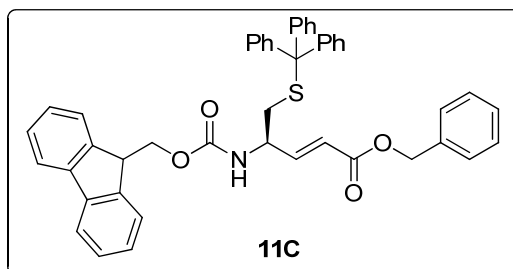
Benzyl 4-(((9H-fluoren-9-yl)methoxy)carbonylamino)-8(tert-butoxycarbonylamino)oct-2-enoate (9C); White solid, (4.55 g, 78%); $[\alpha]_D^{25} = -9.30$ ($c = 1$, MeOH); $^1\text{H NMR}$ (400 MHz, CDCl_3) δ 7.773-7.755 (d, $J = 7.2$ Hz, 2H, aromatic Fmoc-), 7.603-7.585 (d, $J = 7.2$ Hz, 2H, aromatic Fmoc-), 7.391-7.300 (m, 9H aromatic Fmoc & benzylic), 6.909-6.858 (dd, $J = 15.6$ Hz 1H, vinylic β proton), 5.967-5.928 (d, $J = 15.6$ Hz, 1H, vinylic α proton), 5.186 (s, 2H, benzylic), 4.460-4.429 (t, $J = 6.4$ Hz 1H, CH Fmoc-), 4.975 (br., 2H, CH_2), 4.225-4.193 (m, 1H, γ proton), 3.121-3.106 (t, $J = 6$ Hz, 2H, CH_2), 1.620-1.543 (m, 4H, β CH_2 δ CH_2), 1.392-1.356 (m, 2H, γ CH_2), 1.438 (s, 9H, $\text{C}(\text{CH}_3)_3$, Boc); $^{13}\text{C NMR}$ (100 MHz, CDCl_3) δ 166.1, 155.8, 148.57, 143.8, 141.4, 135.8, 128.6, 128.4, 127.8, 127.1, 125.0, 120.7, 120.0, 79.3, 67.2, 66.7, 66.5, 52.02, 47.3, 40.0, 33.9, 31.0, 29.8, 29.8, 28.5, 22.7; **MALDI TOF/TOF** m/z Calcd. For $\text{C}_{35}\text{H}_{40}\text{N}_2\text{O}_6$ ($M + \text{Na}$) = 607.2784 Observed = 607.2787.



(S, E)-Benzyl 4-(((9H-Fluoren-9-yl)methoxy)carbonylamino)-6-amino-6-oxohex-2-enoate (10C); Colorless solid (6.4 g, 90%), $[\alpha]_D^{25} = -3.7$ ($c = 1$, MeOH); $^1\text{H NMR}$ (400 MHz, CDCl_3) δ 7.773-7.755 (d, $J = 7.2$ Hz, 2H, aromatic Fmoc-), 7.591-7.572 (d, $J = 7.6$ Hz, 2H, aromatic Fmoc-), 7.391-7.142 (m, 24H, aromatic protons), 7.049-6.999 (dd, $J = 15.6$ Hz, 1H, vinylic β proton), 6.450-6.429 (b, 1H, NH amide), 6.052-6.013 (d, $J = 15.6$ Hz, 1H, vinylic α proton), 5.23 (s, 2H, CH_2 benzylic), 4.695 (b, 1H, NH Boc), 4.390-4.301 (m, $J = 7.2$ Hz, 1H, CH γ proton), 4.190-4.154 (t, $J = 6.8$ Hz, 1H, Fmoc), 2.688 (b, 2H, β CH_2); $^{13}\text{C NMR}$ (100 MHz, CDCl_3) 178.7, 169.4, 165.9, 155.9, 147.0, 144.1, 141.3, 135.8, 128.7, 128.1, 127.3, 125.2, 120.0, 71.0, 67.1, 66.5, 49.5, 47.2, 40.1, 33.9, 25.6; **MALDI TOF/TOF** m/z Calcd. for $\text{C}_{47}\text{H}_{40}\text{N}_2\text{O}_5$ ($M + \text{Na}$) = 735.2835 Observed = 735.2889.

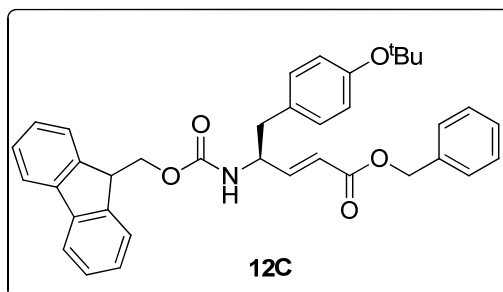


(R, E)-Benzyl 4-(((9H-fluoren-9-yl)methoxy)carbonylamino)-5-(tritylthio)pent-2-enoate (11C); Colorless solid (5.6 g, 80%); $[\alpha]_D^{25} = +6.70$ ($c = 1$, MeOH); $^1\text{H NMR}$ (400 MHz, CDCl_3) δ 7.747-7.732 (d, $J = 6.4$ Hz, 2H, aromatic Fmoc), 7.573-7.555 (d, $J = 7.2$ Hz, 2H, aromatic Fmoc), 7.388-7.347 (t, $J = 7.2$ Hz, 2H, aromatic Fmoc) 7.334-7.186 (m, 17H, aromatic Ph), 6.717-6.69 (dd, $J = 15.6$ Hz, 1H, vinylic β proton), 5.820-5.782 (d, $J = 15.2$ Hz, 1H, vinylic α proton), 5.140 (s, 1H, benzylic), 4.850-4.805 (t, 1H, CH Fmoc), 4.407-4.391 (d, $J = 6.4$ Hz, 2H, OCH_2), 4.222-4.160 (m, 1H, γ proton), 2.449-2.436 (d, $J = 5.2$ Hz, 2H, βCH_2); $^{13}\text{C NMR}$ (100 MHz, CDCl_3) 165.8, 155.5, 146.8, 144.3, 143.8, 141.4, 135.8, 129.6, 128.2, 127.0, 125.0, 121.5, 120.116, 98.5, 82.0, 68.0, 67.4, 66.5, 65.3, 51.5, 50.4, 47.3, 35.9, 34.3, 33.3, 31.0, 30.4, 25.7; **MALDI TOF/TOF** m/z Calcd. for $\text{C}_{46}\text{H}_{39}\text{NO}_4\text{S}$ ($\text{M} + \text{Na}$) = 724.2497 Observed = 724.2491.

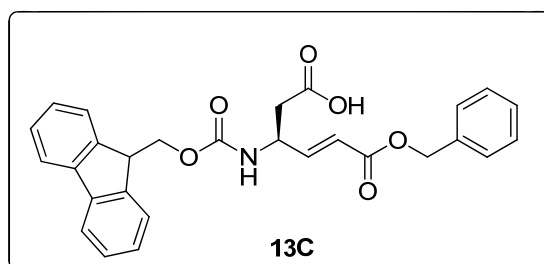


(S, E)-Benzyl 4-(((9H-fluoren-9-yl)methoxy)carbonylamino)-5-(4-tert-butoxyphenyl)pent-2-enoate (12C); Colorless solid (5.3 g, 93%); $[\alpha]_D^{25} = -28.6$ ($c = 1$, MeOH); $^1\text{H NMR}$ (400 MHz, CDCl_3) δ 7.775-7.757 (d, $J = 7.2$ Hz, 2H, aromatic Fmoc), 7.560-7.529 (t, $J = 6.4$ Hz, 2H, aromatic Fmoc-), 7.415-7.397 (d, $J = 7.2$ Hz, 2H, aromatic Fmoc-), 7.385-7.289 (m, 11H, aromatic proton), 6.996-6.913 (dd, 1H, vinylic β proton), 5.914-5.875 (d, $J = 15.6$ Hz, 1H, vinylic α proton), 5.186 (s, 2H, CH_2 benzylic), 4.790-4.769 (d, $J = 8.4$ Hz, 1H, CH), 4.453-4.353 (m, 1H, CH γ proton), 4.200-4.167 (t, $J = 6.4$ Hz, 2H, OCH_2), 2.885-2.850 (t, $J = 7.2$ Hz, 2H, βCH_2), 1.327 (s, 9H, $\text{C}(\text{CH}_3)_3$ ^tBu); $^{13}\text{C NMR}$ (100 MHz, CDCl_3) 164.1, 155.5, 151.2, 147.8, 144.5, 143.8, 141.3, 132.9, 132.2, 131.8, 128.5,

128.3, 127.7, 127.6, 127.1, 126.7, 124.3, 124.054, 120.1, 68.0, 66.4, 65.2, 47.2, 33.9, 31.0, 28.8, 25.6; **MALDI TOF/TOF** m/z Calcd. for C₃₇H₃₇NO₅ (M + Na) = 598.2569 Observed = 598.2574.

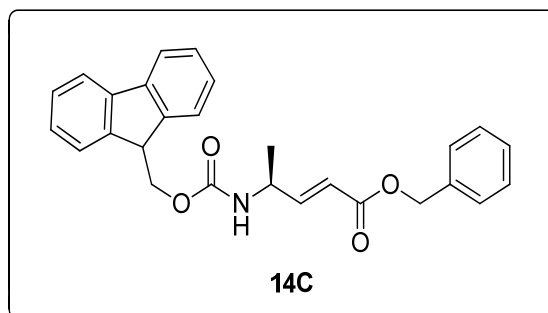


(S, E)-3-(((9H-Fluoren-9-yl)methoxy)carbonylamino)-6-(benzyloxy)-6-oxohex-4-enoic acid (13C); Colorless solid (3.76 g, 80%); $[\alpha]_D^{25} = -16.60$ (c = 1, MeOH) **¹H NMR** (400 MHz, CDCl₃) δ 7.760-7.742 (d, *J* = 7.2 Hz, 2H aromatic Fmoc-), 7.583-7.564 (d, *J* = 7.6 Hz, 2H, aromatic Fmoc-) 7.395-7.297 (m, 9H, aromatic), 6.993-6.941 (dd, *J* = 15.6 Hz, 1H, vinylic β proton), 6.038-6.001 (d, *J* = 14.8 Hz, 1H vinylic α proton), 5.568-5.545 (d, *J* = 9.2 Hz, 1H, NH), 5.185 (s, 2H, benzylic), 4.768 (b, 1H, Fmoc), 4.439-4.423 (d, *J* = 6.4 Hz, 2H, -OCH₂), 4.223-4.188 (m, 1H, CH γ proton), 2.764-2.725 (m, *J* = 4.8 Hz, 2H, β CH₂); **¹³C NMR** (100 MHz, CDCl₃) δ 174.5, 166.0, 155.7, 146.3, 143.7, 141.3, 135.6, 132.9, 128.7, 127.2, 125.1, 121.9, 120.1, 67.1, 66.7, 48.3, 47.2, 37.9, 31.0); **MALDI TOF/TOF** m/z Calcd. for C₂₈H₂₅NO₆ (M + Na) = 494.1580 Observed = 494.1555.



(S, E)-Benzyl 4-(((9H-fluoren-9-yl)methoxy)carbonylamino)pent-2-enoate (14C); White solid (4 g, 94 %); $[\alpha]_D^{25} = -16.0$ (c = 1, MeOH); **¹H NMR** (400 MHz, CDCl₃) δ 7.762-7.743 (d, *J* = 7.6 Hz, 2H aromatic Fmoc-), 7.583-7.565 (d, *J* = 7.2 Hz, 2H, aromatic Fmoc-) 7.416-7.300 (m, 9H, aromatic Fmoc & benzylic), 6.941-6.890 (dd, *J* = 16 Hz, 1H vinylic β proton), 5.955-5.916 (d, *J* = 15.6 Hz, 1H vinylic α proton), 5.178 (s, 1H benzylic), 4.782-4.762 (d, *J* =

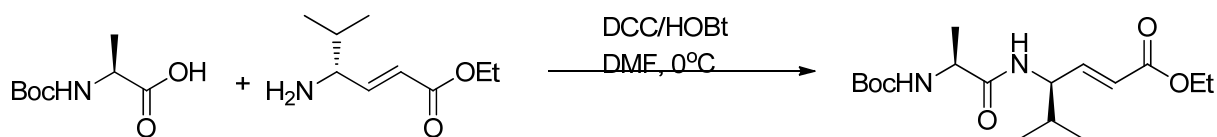
8Hz, 1H, NH), 4.507-4.490 (d, $J = 6.8$ Hz, 2H, OCH₂), 4.445-4.429 (t, $J = 6.4$ Hz, 1H, CH Fmoc), 4.215-4.182 (m, 1H γ proton), 1.292-1.275 (d, $J = 6.8$ Hz, 3H, CH₃); ¹³C NMR (100 MHz, CDCl₃) 166.1, 155.5, 149.4, 143.8, 141.4, 135.8, 133.8, 128.7, 128.6, 128.4, 127.1, 125.0, 124.9, 120.2, 120.0, 66.7, 66.5, 47.6, 47.3, 31.0, 20.3; **MALDI TOF/TOF** m/z Calcd. for C₂₇H₂₅NO₄ (M + Na) = 450.1681 Observed = 450.1641.



Synthesis of dipeptide Boc-Ala-(D)dgVal-OEt (D2)

Boc-Ala-OH (0.129 g 0.68 mmol) and NH₂-dg^DVal-OEt (0.185 g, 0.68 mmol) were dissolved in dissolved in DMF (1.5 mL). The reaction mixture was cooled at 0 °C. Then DCC (0.141 g, 0.68 mmol), HOBT (0.092 g, 0.68 mmol) were added together. The reaction mixture was then allowed to stir for further 12 h. After the completion of reaction, the reaction mixture was diluted with ethyl acetate and DCU generated in the reaction mixture was filtered and the filtrate was then washed with 5 % aqueous HCl, 10% aqueous Na₂CO₃ and dried over anhydrous Na₂SO₄. The organic layer was then concentrated under reduced pressure. The dipeptide was purified using ethyl acetate/pet ether solvent system (1:3). The pure dipeptide Boc-Ala-dg^DV-OEt obtained as colorless oil (0.250 g, 75%). $[\alpha]_D^{25} = +2.7$ (c = 1, MeOH); ¹H NMR (400 MHz, CDCl₃) δ 6.893-6.842 (dd, $J = 15.6$ Hz, 1H, CH vinylic β proton), 6.60 (br., 1H, NH), 5.891-5.852(d, $J = 15.6$ Hz, 1H, vinylic α proton), 5.037-5.020 (d, $J = 6.8$ Hz, 1H, NH Boc), 4.529-4.476 (m, CH γ proton Val), 4.202-4.150 (q, $J = 6.8$ Hz, 2H, OCH₂), 1.953-1.871(m, CH α proton Ala), 1.457(s, 9H, C(CH₃)₃ Boc), 1.380-1.363(d, $J = 6.8$ Hz, 3H, CH₃ Ala), 1.293-1.257(t, $J = 7.2$ Hz, 3H, CH₃), 0.955-0.907(dd, $J = 6.8$ Hz, 6H, (CH₃)₂); ¹³C NMR (100 MHz, CDCl₃) δ 172.3, 166.2, 155.9, 146.7, 121.6, 80.5, 60.5, 55.0, 53.5, 50.1,

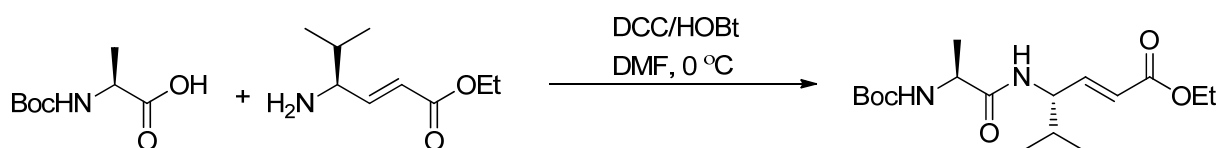
32.0, 28.3, 19.0, 17.943, 14.2; **MALDI TOF/TOF** m/z Calcd. for C₁₇H₃₀N₂O₅ (M + Na) = 365.2052 observed = 365.2050.



Dipeptide D2

Synthesis of Boc-Ala-dgVal-OEt (D1)

Same protocol described above was used for the synthesis of dipeptide Boc-Ala-dg^DVal-OEt. (0.392 g, 93%); $[\alpha]_D^{25} = -50.8$ (c = 1, MeOH); ¹H NMR (400 MHz, CDCl₃) δ 6.891-6.338 (dd, *J* = 15.6 Hz, 1H, CH vinylic β proton), 6.637 (br, 1H, NH), 5.919-5.879 (d, *J* = 16 Hz, 1H, CH vinylic α proton), 5.042-5.024 (d, *J* = 7.2 Hz, 1H, NH Boc), 4.527-4.477 (m, 1H, CH α proton Val), 4.205-4.152 (q, *J* = 7.2 Hz, 2H, OCH₂), 1.915-1.851 (m, 1H, CH α proton), 1.444 (s, 9H, C(CH₃)₃ Boc), 1.368-1.350 (d *J* = 7.2 Hz, 3H, CH₃ Ala), 1.293-1.254 (t, *J* = 8Hz, 3H, CH₃), 0.929-0.894 (t, *J* = 7.2 Hz, 6H, (CH₃)₂ Val); ¹³C NMR (100 MHz, CDCl₃) δ 172.3, 166.2, 155.9, 146.7, 121.7, 80.4, 60.5, 55.0, 53.5, 32.1, 28.3, 21.1, 19.0, 17.8, 14.2; **MALDI TOF/TOF** m/z Calcd. for C₁₇H₃₀N₂O₅ (M + Na) = 365.2052 Observed = 365.2057.



Dipeptide D1

Synthesis of d Dipeptide Boc-dgL-dgL-OEt (D4)

(S, E)-4-(tert-Butoxycarbonylamino)-6-methylhept-2-enoic acid(Boc-dgL-OH); Boc-dgL-OEt, **4C** (1.86 g 6.8 mmol) was dissolved in 4 mL of ethanol followed by 10 mL of 1N NaOH was added slowly to the solution. The reaction mixture was then stirred for about 8h. The progress of reaction was monitored by TLC. After completion of the reaction, the solvent

was evaporated under reduced pressure. The aqueous layer was diluted with water (50 mL) and then acidified (~pH 3.0) with 5% HCl and extracted with ethyl acetate (3 x 50 mL). The combined organic layer was then washed with brine and dried over anhydrous Na₂SO₄. Product was concentrated under reduced pressure to get 1.67g (95%) of oily Boc-dgL-OH.

(S, E)-Ethyl 4-amino-6-methylhept-2-enoate (H₂N-dgL-OEt): The solution of Boc-dgL-OEt (1.95 g, 7.2 mmol) in 5mL of DCM was cooled to 0 °C followed by 5 mL of neat TFA was added. The reaction mixture was stirred for about 1.5 h at the same temperature. The progress of the reaction was monitored by TLC. After completion of the reaction (1.5 h), the solvent was evaporated under reduced pressure. The residue was then treated with saturated Na₂CO₃ solution in cold condition. This aqueous layer was extracted with ethyl acetate (3 x 50 mL). The combined organic layer was washed with brine and dried over anhydrous Na₂SO₄. The organic layer was concentrated under reduced pressure to 4 mL.

The solution of H₂N-dgL-OEt in ethyl acetate (4 mL) was added to the ice-cold solution of Boc-dgL-OH (1.67 g, 6.5 mmol) in DMF (4 mL). The reaction mixture was then treated with DCC (1.34 g, 6.5 mmol) followed by HOBT (0.884 g, 6.5 mmol). The reaction mixture was stirred for about 12 h at room temperature and the progress of the reaction was monitored by TLC. After completion of reaction, the reaction mixture was diluted with ethyl acetate (100 mL) and DCU formed in reaction was filtered. This filtrate was washed with brine (3 x 50 mL), 5% HCl (3 x 50 mL), 10% Na₂CO₃ (3 x 50 mL), brine (30 mL) and dried over Na₂SO₄. The organic layer was concentrated under reduced pressure and the crude product was purified by column chromatography using ethyl acetate/ pet ether to get 1.2 g (40%) of the pure dipeptide D4.



Dipeptide **D4**

¹H NMR (400 MHz, CDCl₃); δ 6.858-6.805 (dd, *J* = 15.6 Hz, 1H vinylic β CH=CH-CO₂Et), 6.709-6.656 (dd, *J* = 15.2 Hz, 1H vinylic β CH=CH-CONH), 5.924-5.885(d, *J* = 15.6 Hz, 2H

vinyllic α CH=CH-CO), 5.655(br., 1H NH amide), 4.773-4.737(m, $J=7.2$ Hz, 1H γ proton), 4.547(br., 1H NH Boc), 4.297(m, 1H, γ proton), 4.205-4.151(q, $J=7.2$ Hz, 2H, OCH₂CH₃), 1.696-1.630(m, $J=6.8$ Hz, 2H, CH₃CHCH₃), 1.464-1.43(t, $J=6.8$ Hz, 2H, CH-CH₂-CH), 1.439(s, 9H, (CH₃)₃, Boc), 1.398-1.363(t, $J=6.8$ Hz, 2H CH-CH₂-CH), 1.294-1.258(t, $J=6.8$ Hz, 3H, OCH₂CH₃), 0.934-0.918(d, $J=6.4$ Hz 12H, (CH₃)₄); ¹³C NMR (100 MHz, CDCl₃) 166.4, 164.9, 147.9, 145.2, 122.7, 120.9, 60.5, 49.9, 48.4, 44.0, 43.5, 28.4, 24.7, 22.796, 14.3; **MALDI TOF/TOF** m/z Calcd. for C₂₃H₄₀N₂O₅ (M + K) = 463.2574 Observed = 463.1999.

Data Collection

A colorless crystal with diffractable dimensions was selected under oil under ambient conditions and attached on nylon CryoLoops with Paraton-N (Hampton Research). The crystal was mounted in a stream of cold nitrogen at 100(2) K and centered in the X-ray beam by using a video camera.

The crystal evaluation and data collection were performed on a Bruker KAPPA APEX II CCD Duo diffractometer (operated at 1500 W power: 50 kV, 30 mA) with Mo K α ($\lambda = 0.71073$ Å) radiation and the diffractometer to crystal distance of 6.0 cm.

The initial cell constants were obtained from three series of ω scans at different starting angles. Each series consisted of 12 frames collected ω with the exposure time of 10-20 seconds per frame. Obtained reflections were successfully indexed by an automated indexing routine built in the SMART program.

The data were collected by using the full sphere data collection routine to survey the reciprocal space to the extent of a full sphere to a resolution of 0.75 Å, with an exposure time 10-20 sec per frame. The data integration and reduction were processed with SAINT⁵³ software. A multi-scan absorption correction was applied to the collected reflections.

Structure Solution and Refinement

The systematic absences in the diffraction data were yielded chemically reasonable and computationally stable results of refinement.⁵⁴

A successful solution by the direct methods provided most non-hydrogen atoms from the *E*-map. The remaining non-hydrogen atoms were located in an alternating series of least-squares cycles and difference Fourier maps. All non-hydrogen atoms were refined with anisotropic

displacement coefficients. All hydrogen atoms were included in the structure factor calculation at idealized positions and were allowed to ride on the neighbouring atoms with relative isotropic displacement coefficients.

Crystal structure analysis of Boc-dgV-OEt: Crystals of peptide were grown by slow evaporation from a solution of EtOAc and Hexane. A single crystal (0.50 × 0.35 × 0.20 mm) was mounted on loop with a small amount of the paraffin oil. The X-ray data were collected at 200K temperature on a Bruker APEX DUO CCD diffractometer using Mo K_α radiation (λ = 0.71073 Å), ω-scans (2θ = 55.84), for a total of 3650 independent reflections. Space group P2(1), 2(1), 2(1), a = 9.978(4), b = 10.083(3), c = 16.904(6), V = 1700.7(10) Å³, Orthorhombic P, Z=4 for chemical formula C₁₄H₂₅NO₄, with one molecule in asymmetric unit; ρ Calcd = 1.060 gcm⁻³, μ = 0.077 mm⁻¹, F(000) = 592, R_{int} = 0.0268. The structure was obtained by direct methods using SHELXS-97.¹ The final R value was 0.0581 (wR2 = 0.1589) 1978 observed reflections (F_o ≥ 4σ (|F_o|)) and 178 variables, S = 1.011. The largest difference peak and hole were 0.344 and -0.160 eÅ³, respectively.

Crystal structure analysis of Boc-dgL-OEt: Crystals of peptide were grown by slow evaporation from a solution of EtOAc and Hexane. A single crystal (0.45 × 0.34 × 0.24 mm) was mounted on loop with a small amount of the paraffin oil. The X-ray data were collected at 296K temperature on a Bruker APEX DUO CCD diffractometer using Mo K_α radiation (λ = 0.71073 Å), ω-scans (2θ = 48.56), for a total of 2788 independent reflections. Space group P2(1), a = 10.340(3), b = 9.733(3), c = 18.073(5), β = 106.331(5), V = 1700.7(10) Å³, Monoclinic P, Z=2 for chemical formula C₃₀H₅₄N₂O₈, with two molecule in asymmetric unit; ρ Calcd = 1.086 gcm⁻³, μ = 0.078 mm⁻¹, F(000) = 624, R_{int} = 0.0277. The structure was obtained by direct methods using SHELXS-97.¹ The final R value was 0.0341 (wR2 = 0.0804) 2413 observed reflections (F_o ≥ 4σ (|F_o|)) and 373 variables, S = 0.985. The largest difference peak and hole were 0.110 and -0.130 eÅ³, respectively.

Crystal structure analysis of Boc-dgU-OEt: Crystals of peptide were grown by slow evaporation from a solution of EtOAc and Hexane. A single crystal (0.45 × 0.30 × 0.23 mm) was mounted on loop with a small amount of the paraffin oil. The X-ray data were collected at

296K temperature on a Bruker APEX DUO CCD diffractometer using Mo K α radiation ($\lambda = 0.71073 \text{ \AA}$), ω -scans ($2\theta = 60.56$), for a total of 4448 independent reflections. Space group P 21/c, $a = 10.669(2)$, $b = 9.092(2)$, $c = 15.882(4)$, $\beta = 90.923(5)$, $V = 1540.3(6) \text{ \AA}^3$, Monoclinic P, $Z=4$ for chemical formula $C_{30} H_{54} N_2 O_8$, with one molecule in asymmetric unit; ρ Calcd = 1.114 g cm^{-3} , $\mu = 0.082 \text{ mm}^{-1}$, $F(000) = 564$, $R_{\text{int}} = 0.0579$. The structure was obtained by direct methods using SHELXS-97.¹The final R value was 0.0651 ($wR_2 = 0.1879$) 1713 observed reflections ($F_0 \geq 4\sigma(|F_0|)$) and 169 variables, $S = 1.031$. The largest difference peak and hole were 0.303 and $-0.283 \text{ e \AA}^{-3}$, respectively.

Crystal structure analysis of Boc-dgI-OEt: Crystals of peptide were grown by slow evaporation from a solution of EtOAc and Hexane. A single crystal ($0.54 \times 0.43 \times 0.32 \text{ mm}$) was mounted on loop with a small amount of the paraffin oil. The X-ray data were collected at 200K temperature on a Bruker APEX DUO CCD diffractometer using Mo K α radiation ($\lambda = 0.71073 \text{ \AA}$), ω -scans ($2\theta = 59.20$), for a total of 3650 independent reflections. Space group P2(1), 2(1), 2(1), $a = 10.153(3)$, $b = 10.273(3)$, $c = 16.191(5)$, $V = 1688.8(9) \text{ \AA}^3$, Orthorhombic P, $Z=4$ for chemical formula $C_{15} H_{27} N O_4$, with one molecule in asymmetric unit; ρ calcd = 1.122 g cm^{-3} , $\mu = 0.080 \text{ mm}^{-1}$, $F(000) = 624$, $R_{\text{int}} = 0.0265$. The structure was obtained by direct methods using SHELXS-97.¹The final R value was 0.0378 ($wR_2 = 0.0912$) 3750 observed reflections ($F_0 \geq 4\sigma(|F_0|)$) and 188 variables, $S = 1.023$. The largest difference peak and hole were 0.185 and $-0.190 \text{ e \AA}^{-3}$, respectively.

Crystal structure analysis of Boc-Ala-dgVal-OEt : Crystals of peptide were grown by slow evaporation from a solution of ethylacetate. A single crystal ($0.25 \times 0.24 \times 0.20 \text{ mm}$) was mounted on loop with a small amount of the paraffin oil. The X-ray data were collected at 100K temperature on a Bruker APEX DUO CCD diffractometer using Mo K α radiation ($\lambda = 0.71073 \text{ \AA}$), ω -scans ($2\theta = 56.56$), for a total of 25408 independent reflections. Space group P1, $a = 13.3376(19)$, $b = 14.030(2)$, $c = 17.956(3)$, $\alpha = 88.064(5)$, $\beta = 70.670(4)$, $\gamma = 73.874(5)$, $V = 3039.6(7) \text{ \AA}^3$, Triclinic P, $Z= 1$ for chemical formula $C_{102} H_{180} N_{12} O_{30}$, with six molecule in asymmetric unit; ρ Calcd = 1.122 g cm^{-3} , $\mu = 0.082 \text{ mm}^{-1}$, $F(000) = 1116$, $R_{\text{int}} = 0.0718$. The structure was obtained by direct methods using SHELXS-97.¹The final R value

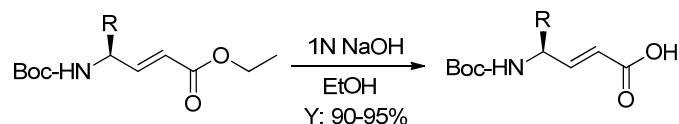
was 0.0881 ($wR_2=0.1946$) 12742 observed reflections ($F_0 \geq 4\sigma(|F_0|)$) and 1339 variables, $S = 0.990$. The largest difference peak and hole were 0.587 and $-0.334e\text{\AA}^3$, respectively.

Crystal structure analysis of Boc-dgLeu-dgLeu-OEt: Crystals of peptide were grown by slow evaporation from a solution of EtOAc. A single crystal ($0.35 \times 0.25 \times 0.11$ mm) was mounted on loop with a small amount of the paraffin oil. The X-ray data were collected at 200K temperature on a Bruker APEX DUO CCD diffractometer using Mo K_α radiation ($\lambda = 0.71073 \text{\AA}$), ω -scans ($2\theta = 58.26$), for a total of 5271 independent reflections. Space group P1, $a = 5.053(2)$, $b = 9.812(5)$, $c = 13.498(6)$, $\alpha = 73.640(9)$, $\beta = 84.653(9)$, $\gamma = 78.566(9)$, $V = 628.8(5) \text{\AA}^3$, Triclinic P, $Z=1$ for chemical formula $C_{23} H_{40} N_2 O_5$, with one molecule in asymmetric unit; ρ calcd = 1.121gcm^{-3} , $\mu = 0.078 \text{mm}^{-1}$, $F(000) = 232$, $R_{\text{int}} = 0.0613$. The structure was obtained by direct methods using SHELXS-97.¹ The final R value was 0.0663 ($wR_2 = 0.1509$) 3557 observed reflections ($F_0 \geq 4\sigma(|F_0|)$) and 305 variables, $S = 1.036$. The largest difference peak and hole were 0.575 and $-0.373e\text{\AA}^3$, respectively.

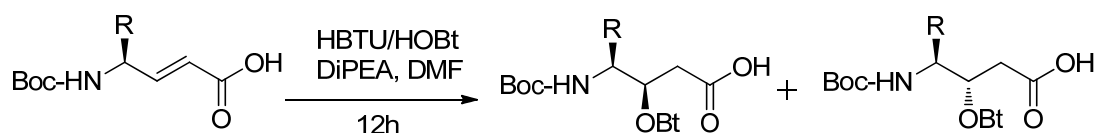
1.3.3 Synthesis procedure and compound characterization for Section 1B

Saponification of *N*-Protected α , β -Unsaturated γ -Amino Esters:

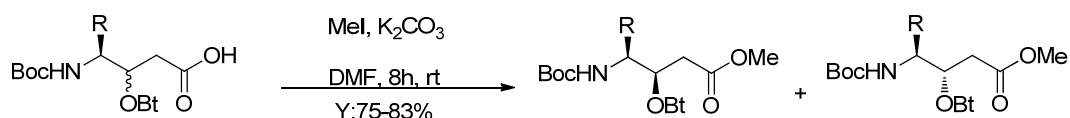
The *N*-protected vinylogous amino ester (10 mmol) was dissolved in 15 ml of ethanol. To this solution 1N NaOH (10 ml) was added drop wise. The reaction mixture was allowed to stir for further 3h. The progress of reaction was monitored by TLC. After completion of reaction (3h) the solvent ethanol was evaporated and the aqueous layer was acidified with 5% aq. HCl to make $pH \sim 2$. This aqueous solution was then extracted with ethyl acetate ($30 \text{ ml} \times 3$). The organic layer was washed with brine dried over anhydrous Na_2SO_4 and concentrated under reduced pressure to give *N*-protected vinylogous amino acid in average 95% yield.



General procedure for synthesis of β -OBt substituted γ -amino acids through Michel addition of HOBt to *N*-protected α , β unsaturated γ -amino acids: In 10 ml RB flask *N*-protected vinylogous amino acid (1.6 mmol) was dissolved in 2 ml of dry DMF under N_2 atmosphere. To this solution HBTU (1.6 mmol) and HOBt (1.6 mmol) were added. The reaction mixture was cooled at $0^\circ C$ prior to the addition of DIPEA (3.2 mmol). This reaction mixture was allowed to stir for another 12h. After 12h, the reaction mixture was diluted with ethyl acetate and acidified by 5% HCl to make pH~2. This reaction mixture was transferred to the separating funnel and organic layer was separated. The aqueous layer was further extracted with ethyl acetate (2 x 20 ml). The combined organic layer was then washed with brine dried over anhydrous Na_2SO_4 and concentrated under reduced pressure. This product was used as such for methyl ester and dipeptide synthesis without purification.

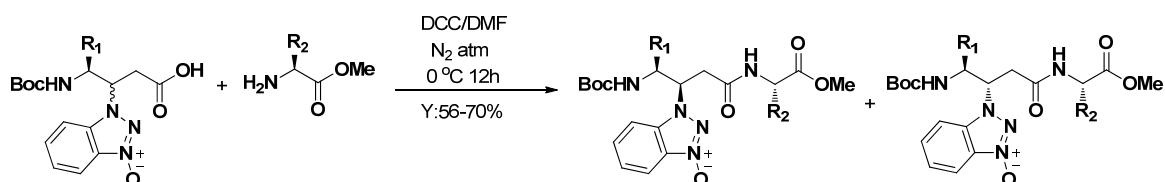


General procedure for synthesis of methyl ester of β -OBt substituted *N*-protected γ -amino acids. HOBt conjugate addition product of vinylogous amino acid (1.6 mmol) was dissolved in dry DMF (2 mL). To this solution K_2CO_3 (1.6 mmol) and methyl iodide (3.2 mmol) were added. This reaction mixture was further stirred for 8h. After completion of reaction (8h), the reaction mixture was poured in ice cold water and extracted with ethyl acetate (25 mL \times 3). The combined organic layer was washed with saturated solution of $Na_2S_2O_3$, brine and dried over anhydrous Na_2SO_4 . The two diastereoisomers of methyl ester of β -OBt substituted *N*-protected γ -amino acid were isolated by concentrating the organic layer under reduced pressure. This two diastereoisomers were then separated by using 70:30 (EtOAc : Pet Ether) solvent system.



General procedure for synthesis of β -OBt substituted *N*-protected γ -amino acids containing dipeptides: The HCl.H₂N-Ala/Leu-OMe salt (3 mmol) was dissolved in water and was added Na₂CO₃ to make P_H ~12 in cold condition. This aqueous solution was then extracted with ethyl acetate (30 ml \times 3). The combined organic layer was then washed with brine and dried over anhydrous Na₂SO₄. This organic layer was concentrated up to ~2 ml.

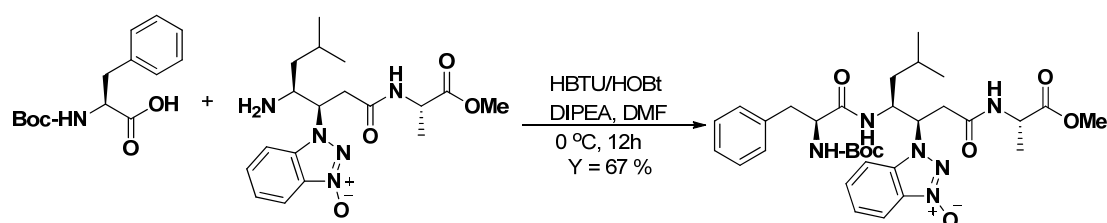
In another 10 ml RB flask, β -OBt substituted *N*-protected γ -amino acid (2 mmol) was dissolved in dry DMF under N₂ atmosphere. To this solution NH₂-Ala/Leu-OMe (with ~2 ml of EtOAc) was added. The reaction mixture was cooled to 0 °C and DCC (2 mmol) was added. This reaction mixture was allowed to stir for another 12h and progress of reaction was monitored by TLC. After completion of reaction, reaction mixture was diluted with ethyl acetate (50 ml) and DCU generated in the reaction was filtered through sintered funnel. The filtrate was then washed with 5% HCl (20 ml) and 10% Na₂CO₃ (20 ml). This organic layer was treated with brine and dried over Na₂SO₄. The organic layer was concentrated under reduced pressure to get two diastereomers of dipeptide. These two diastereomers of dipeptide were purified using 2:98 (MeOH : DCM) solvent system.



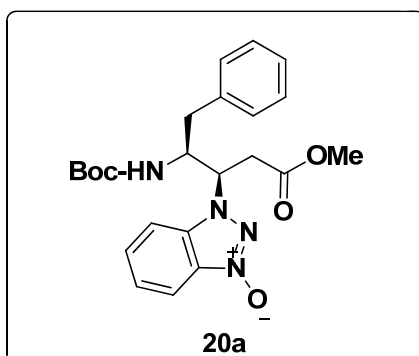
Procedure for Synthesis of Tripeptide Boc-Phe- γ Leu(β -OBt)-Ala-OMe (28P); NH₂- γ Leu(β -OBt)-Ala-OMe: Boc- γ Leu(β -OBt)-Ala-OMe (200 mg, 0.4 mmol) was dissolved in 2 ml DCM and cooled at 0 °C. To this solution TFA (4 ml) was added. After the completion of reaction (1h) (monitored by TLC), TFA was evaporated under reduced pressure. Residue was dissolved in water and added Na₂CO₃ to make P_H~12 in ice cold condition. This aqueous solution was then extracted with ethyl acetate (25 ml \times 3), washed with brine dried over Na₂SO₄. The organic layer was concentrated under reduced pressure up to ~2 ml.

The Boc-Phe-OH (110 mg, 0.4 mmol) was dissolved in dry DMF under N₂ atmosphere. To this solution NH₂- γ Leu(β -OBt)-Ala-OMe (with ~2 ml EtOAc) was

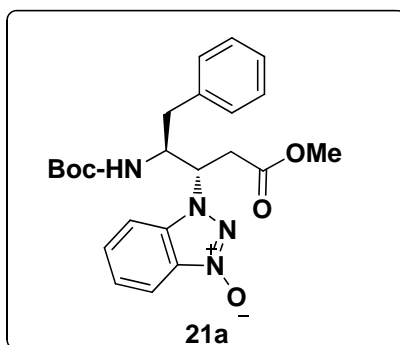
added. The reaction mixture was cooled to 0 °C and treated with HBTU (158 mg, 0.4 mmol), HOBt (56 mg, 0.4 mmol), DIPEA (0.144 ml, 0.8 mmol). This reaction mixture was allowed to stir for another 12h. After completion of reaction (12h), the reaction mixture was diluted with ethyl acetate (75 ml), washed with 5% HCl, 10% Na₂CO₃ and brine, dried over anhydrous Na₂SO₄. The organic layer was concentrated under reduced pressure. Tripeptide Boc-Phe- γ Leu(β -OBt)-Ala-OMe was obtained as white solid in 67 % yield after purification in 80:20 (Ethyl acetate : Pet ether) solvent system.



1-((3*R*,4*S*)-4-(tert-Butoxycarbonylamino)-1-methoxy-1-oxo-5-phenylpentan-3-yl)-1*H*-benzo[*d*][1,2,3]triazole 3-oxide (Boc- γ Phe(β -OBt)-OMe) (20a)^{syn}; White solid, (0.204 g, 30%); The diastereomeric ratio of 6a:7a is 39:61 respectively; $[\alpha]_D^{25}$ -7.4 (*c* 0.1, MeOH); UV(λ_{max}) 323 nm, 274 nm; IR (neat) ν (cm⁻¹) 3362, 2973, 2928, 1736, 1604, 1504, 1458, 1425, 1306, 1208, 1134, 748; ¹H NMR (400 MHz, CDCl₃) δ 7.99 (d, *J* = 8 Hz, 1H), 7.55 (t, *J* = 8 Hz, 1H), 7.42 (t, *J* = 6 Hz, 1H), 7.24-7.21 (m, 4H), 6.91 (dd, *J* = 4 Hz, 2H), 5.54 (d, *J* = 8 Hz, 1H), 5.16-5.12 (m, 1H), 4.57-4.49 (m, 1H), 3.51 (s, 3H), 3.21 (dd, *J* = 4 Hz & 12 Hz, 1H), 2.98 (dd, 4 Hz & 12 Hz, 1H), 2.76 (t, *J* = 8 Hz, 1H), 2.41 (dd, *J* = 4 Hz & 8 Hz, 1H), 1.42 (s, 9H); ¹³C NMR (100 MHz, CDCl₃) 170.7, 155.7, 136.3, 130.5, 129.5, 128.7, 127.0, 124.9, 115.3, 111.7, 56.8, 54.7, 52.2, 38.5, 36.9, 29.7, 28.3 **HRMS (ESI) *m/z*** calcd. for C₂₃H₂₈N₄O₅ [M + H] is 441.2138 Observed = 441.2134.

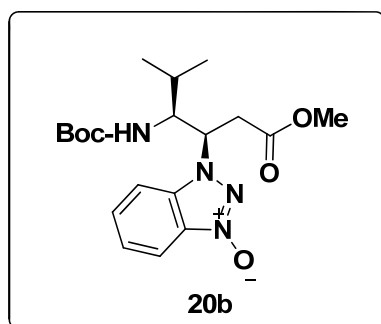


1-((3S,4S)-4-(tert-Butoxycarbonylamino)-1-methoxy-1-oxo-5-phenylpentan-3-yl)-1H-benzo[d][1,2,3]triazole 3-oxide (Boc- γ Phe(β -OBt)-OMe) (21a)^{anti}; White solid, (0.320 g, 45%); $[\alpha]_D^{25}$ -0.2 (*c* 0.1, MeOH); UV (λ_{\max}) 323 nm, 274 nm; IR (neat) ν (cm^{-1}) 3360, 2971, 2921, 1736, 1604, 1507, 1458, 1425, 1367, 1311, 1209, 1167, 1024, 747; $^1\text{H NMR}$ (400 MHz, CDCl_3) δ 7.99 (d, *J* = 12 Hz, 1H), 7.74-7.70 (m, 1H), 7.62-7.61 (m, 2H), 7.54 (dd, *J* = 4 Hz, 1H), 7.43-7.39 (m, 1H), 7.29 (d, *J* = 8 Hz, 1H), 7.23 (d, *J* = 6 Hz, 2H), 7.11 (d, *J* = 8 Hz, 2H), 5.57 (br., 1H), 5.02-4.92 (m, 1H), 4.22 (t, *J* = 6 Hz, 1H), 3.57 (s, 3H), 3.33 (dd, *J* = 8 Hz, 1H), 3.03 (dd, *J* = 16 Hz & *J* = 4 Hz, 1H), 2.89-2.77 (m, 2H), 1.35 (s, 9H); $^{13}\text{C NMR}$ (100 MHz, CDCl_3) 170.6, 155.4, 136.7, 135.6, 130.5, 128.9, 128.6, 126.8, 124.7, 115.3, 111.1, 80.1, 57.9, 55.3, 52.2, 35.7, 29.7, 28.3; HRMS (ESI) *m/z* calcd. for $\text{C}_{23}\text{H}_{28}\text{N}_4\text{O}_5$ [*M* + *H*] is 441.2138 Observed = 441.2138.

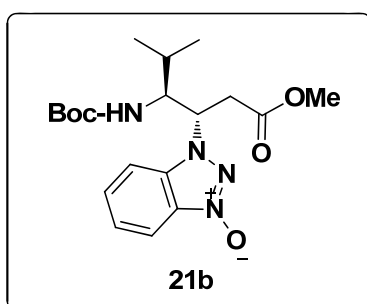


1-((3R,4S)-4-(tert-Butoxycarbonylamino)-1-methoxy-5-methyl-1-oxohexan-3-yl)-1H-benzo[d][1,2,3]triazole 3-oxide (Boc- γ Val(β -OBt)-OMe) (21b)^{syn} White powder, (0.185 g, 32%); The diastereomeric ratio of 6b:7b is 37:63 respectively $[\alpha]_D^{25}$ -1.0 (*c* 0.1, MeOH); UV (λ_{\max}) 323 nm; IR (neat) ν (cm^{-1}) 2968, 1736, 1707, 1605, 1503, 1460, 1423, 1390, 1366, 1303, 1241, 1199, 1165, 1109, 1022, 749; $^1\text{H NMR}$ (400 MHz, CDCl_3) δ 7.98 (d, *J* = 8 Hz, 1H), 7.70-7.63 (m, *J* = 8 Hz, 2H), 7.42 (t, *J* = 8 Hz, 1H), 5.5 (d, *J* = 12 Hz, 1H), 5.40-5.3 (m,

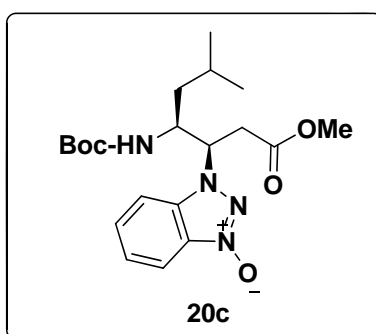
1H), 3.90-3.8 (m, 1H), 3.54 (s, 3H), 3.18 (dd $J = 10$ Hz & $J = 3.6$ Hz, 1H), 2.96 (dd, $J = 4$ Hz & 12 Hz, 1H) 1.47 (s, 9H), 0.89 (dd, $J = 4$ Hz, 6H); ^{13}C NMR (100 MHz, CDCl_3) 173.0, 168.9, 156.6, 135.0, 130.9, 129.3, 124.8, 115.3, 111.6, 59.1, 57.4, 52.4, 50.8, 40.9, 40.3, 30.7, 28.4, 24.6, 22.7, 21.2, 20.1, 19.4. HRMS (ESI) m/z calcd. for $\text{C}_{19}\text{H}_{28}\text{N}_4\text{O}_5$ [M + H] is 393.2138 Observed = 393.2147.



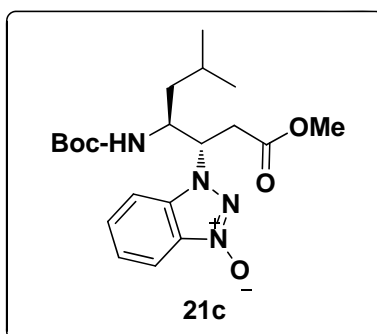
1-((3*S*,4*S*)-4-(tert-Butoxycarbonylamino)-1-methoxy-5-methyl-1-oxohexan-3-yl)-1*H*-benzo[*d*][1,2,3]triazole 3-oxide(Boc- γ Val(β -OBt)-OMe) (21b)^{anti}; White powder, (0.315 g, 48%); $[\alpha]_{\text{D}}^{25}$ -7.2 (c 0.1, MeOH); UV (λ_{max}) 323 nm; IR (neat) ν (cm^{-1}) 3272, 2966, 2928, 1738, 1690, 1606, 1506, 1423, 1394, 1308, 1250, 1167, 1033; ^1H NMR (400 MHz, CDCl_3) δ 7.99 (d, $J = 8.8$ Hz, 1H), 7.64-7.63 (m, 2H), 7.43-7.38 (m, 1H), 5.09-5.03 (m, 1H), 4.53(d, $J = 12$ Hz, 1H), 4.27-4.21 (m, 1H), 3.58 (s, 3H), 3.22-3.07 (m, 3H), 1.45 (s, 9H), 0.86 (dd, $J = 6.8$ Hz, 6H); ^{13}C NMR (100 MHz, CDCl_3) 171.4, 155.8, 139.3, 134.3, 130.7, 124.6, 115.8, 110.8, 57.8, 57.2, 52.2, 36.1, 31.9, 29.7, 28.3, 22.7, 20.1, 15.8, 14.1. HRMS (ESI) m/z calcd. for $\text{C}_{19}\text{H}_{28}\text{N}_4\text{O}_5$ [M + H] is 393.2138 Observed = 393.2143.



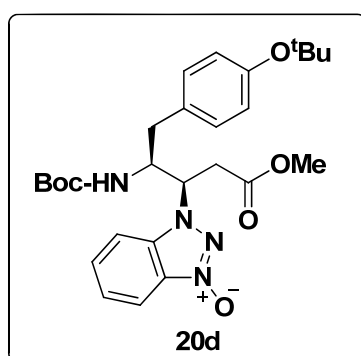
1-((3*R*,4*S*)-4-(tert-Butoxycarbonylamino)-1-methoxy-6-methyl-1-oxoheptan-3-yl)-1H-benzo[d][1,2,3]triazole 3-oxide (Boc- γ Leu(β -OBt)-OMe) (20c)^{syn}; White solid, (0.220 g, 33%); The diastereomeric ratio of 6*c*:7*c* is 41:59 respectively; $[\alpha]_D^{25}$ -7.0 (*c* 0.1, MeOH); UV (λ_{\max}) 323 nm; IR (neat) ν (cm⁻¹) 3360, 3267, 2957, 1735, 1704, 1605, 1510, 1460, 1398, 1366, 1317, 1248, 1167, 1035, 749; ¹H NMR (400 MHz, CDCl₃) δ 7.97 (d, *J* = 8 Hz, 1H), 7.69-7.62(m, 2H), 7.41 (t, *J* = 6 Hz, 1H), 5.20-5.15 (m, 2H), 4.25-4.19 (m, 1H), 3.55 (s, 3H), 3.23 (dd *J* = 8 Hz, 1H), 3.02 (dd, *J* = 4 Hz & 12 Hz, 1H), 1.62-1.56 (m, 1H), 1.43 (s, 9H), 1.02 (t, *J* = 6 Hz, 2H), 0.81 (dd, *J* = 4 Hz, 6H); ¹³C NMR (100 MHz, CDCl₃) 170.9, 155.8, 135.3, 130.9, 129.5, 124.7, 115.5, 111.0, 79.9, 59.1, 52.1, 51.5, 40.940, 36.1, 29.7, 28.3, 24.7, 23.1, 21.7; HRMS (ESI) *m/z* calcd. for C₂₀H₃₀N₄O₅ [M + H] is 407.2294 Observed = 407.2300.



1-((3*S*,4*S*)-4-(tert-Butoxycarbonylamino)-1-methoxy-6-methyl-1-oxoheptan-3-yl)-1H-benzo[d][1,2,3]triazole 3-oxide (Boc- γ Leu(β -OBt)-OMe) (21c)^{anti}; White solid, (0.317 g, 50%); $[\alpha]_D^{25}$ -1.6 (*c* 0.1, MeOH); UV (λ_{\max}) 323 nm; IR (neat) ν (cm⁻¹) 3360, 3270, 2956, 2927, 2863, 2315, 1737, 1702, 1607, 1506, 1460, 1424, 1394, 1367, 1262, 1167, 1115, 1038, 749; ¹H NMR (400 MHz, CDCl₃) δ 7.89 (d, *J* = 4 Hz, 1H), 7.61-7.54 (m, 2H), 7.34 (t, *J* = 6 Hz, 1H), 5.40 (br, 1H), 4.72 (br, 1H), 4.03-4.00 (m, 1H), 3.50 (s, 3H), 3.29 (dd, *J* = 4 Hz & 8 Hz, 1H), 2.87 (dd, *J* = 4 Hz, 12 Hz, 1H), 1.60-1.58 (m, 1H), 1.39 (s, 9H), 0.83 (t, *J* = 4 Hz, 8H) ¹³C NMR (100 MHz, CDCl₃) 170.5, 155.4, 135.7, 130.4, 129.8, 124.5, 115.3, 111.1, 58.3, 52.1, 38.0, 35.1, 29.7, 28.3, 24.7, 23.6, 21.1; HRMS (ESI) *m/z* calcd. for C₂₀H₃₀N₄O₅ [M + H] is 407.2294 Observed = 407.2303.

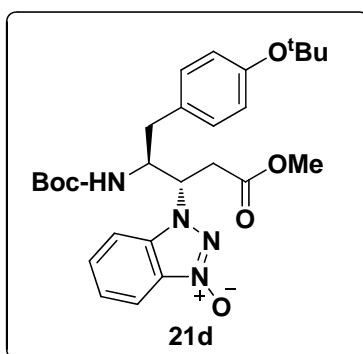


1-((3*R*, 4*S*)-5-(4-(tert-butoxy)phenyl)-4-((tert-butoxycarbonyl)amino)-1-methoxy-1-oxopent-3-yl)-1H-benzod[1,2,3]triazole 3-oxide (Boc-Tyr(β -OBt)-OMe) (20d**)^{syn}**
 :Yellowish oil; (0.152 g, 28%); The diastereomeric ratio of 6d:7d is 40:60 respectively; $[\alpha]_{25}^D$ -7.0 (*c* 0.1, MeOH); UV (λ_{max}) 219 nm, 273 nm, 280 nm, 323 nm; IR (neat) ; **¹H NMR (400 MHz, CDCl₃)** δ 7.95 (d, *J* = 8 Hz, 1H), 7.61-7.56 (m, 2H), 7.39-7.36 (m, 1H), 6.99-6.87 (m, 4H), 5.54-5.49 (m, 1H), 4.62-4.57 (m, 1H), 4.24-4.18 (m, 1H), 3.54 (s, 3H), 3.36-2.95 (m, 2H), 2.82-2.71 (m, 2H), 1.33 (s, 9H), 1.30 (s, 9H); **¹³C NMR (100 MHz, CDCl₃)** δ 170.6, 155.4, 154.3, 1135.7, 131.4, 130.6, 130.0, 129.4, 124.7, 124.5, 115.5, 111.2, 80.3, 78.6, 57.7, 55.3, 52.3, 35.5, 35.0, 29.8, 28.9, 28.3; **HRMS (ESI) *m/z*** calculated for [C₂₇H₃₆N₄O₆ +H⁺] 513.2713, observed 513.2717.

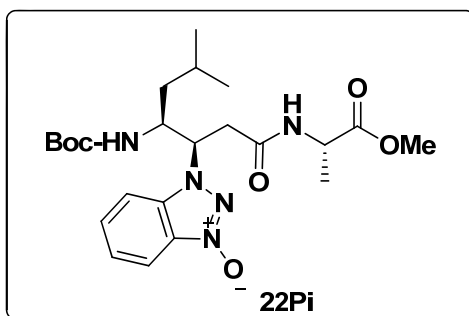


1-((3*S*, 4*S*)-5-(4-(tert-butoxy)phenyl)-4-((tert-butoxycarbonyl)amino)-1-methoxy-1-oxopent-3-yl)-1H-benzod[1,2,3]triazole 3-oxide (Boc-Tyr(β -OBt)-OMe) (21d**)^{anti}**
 :Yellowish oil; (0.240 g, 42%); $[\alpha]_{25}^D$ + 0.2 (*c* 0.1, MeOH); UV (λ_{max}) 219 nm, 273 nm, 280

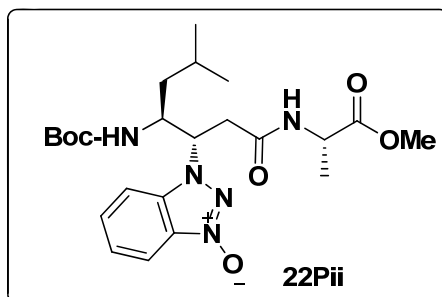
nm, 323 nm; IR (neat) ; $^1\text{H NMR}$ (400 MHz, CDCl_3) δ 7.98 (d, $J = 8$ Hz, 1H), 7.55-7.39 (m, 2H), 7.24-7.19 (m, 1H), 6.89-6.77 (m, 4H), 5.52 (d, $J = 8$ Hz, 1H), 5.12 (m, 1H), 4.51 (m, 1H), 3.51 (s, 3H), 3.10 (m, 2H), 2.54 (m, 2H), 1.42 (s, 9H), 1.33 (s, 9H); $^{13}\text{C NMR}$ (100 MHz, CDCl_3) δ 170.7, 155.7, 154.3, 135.4, 131.1, 130.5, 129.4, 124.8, 124.5, 115.3, 111.8, 80.1, 78.6, 56.7, 54.6, 52.1, 37.9, 36.9, 29.7, 28.8, 28.3; HRMS (ESI) m/z calculated for $[\text{C}_{27}\text{H}_{36}\text{N}_4\text{O}_6 + \text{H}^+]$ 513.2713, observed 513.2730.



1-((4*S*,8*R*,9*S*)-9-Isobutyl-4,13,13-trimethyl-3,6,11-trioxo-2,12-dioxa-5,10-diazatetradecan-8-yl)-1*H*-benzo[d][1,2,3]triazole 3-oxide (Boc- γ Leu(β -OBt)-Ala-OMe) (22Pi**);** White solid, (0.273 g, 28%); The diastereomeric ratio of 8Pi:8Pii is 41:59 respectively UV(λ_{max}) 323 nm; IR (neat) ν (cm^{-1}) 3281, 2960, 2378, 2312, 2112, 1741, 1668, 1525, 1458, 1423, 1367, 1208, 1164, 1114, 1052, 996, 748; $^1\text{H NMR}$ (500 MHz, CDCl_3) 7.91 (d, $J = 4$ Hz, 1H), 7.68 (d, $J = 8$ Hz, 1H), 7.59 (t, $J = 6$ Hz, 1H), 7.38 (t, $J = 8$ Hz, 1H), 6.85 (d, $J = 8$ Hz, 1H), 5.26 (d, $J = 8$ Hz, 1H), 5.24-5.21 (m, 1H), 4.35-4.30 (m, 1H), 4.29-4.25 (m, 1H), 3.66 (s, 3H), 3.03-2.93 (m, 2H), 1.61-1.54 (m, 1H), 1.41 (s, 9H), 1.07 (d, $J = 4$ Hz, 3H), 0.79 (t, $J = 4$ Hz, 6H); $^{13}\text{C NMR}$ (100 MHz, CDCl_3) 173.1, 168.7, 155.1, 135.3, 130.8, 129.4, 124.8, 115.2, 111.4, 60.0, 52.5, 51.6, 48.1, 41.2, 38.5, 28.3, 24.8, 23.1, 21.7, 17.5; MALDI TOF/TOF m/z Calculated for $\text{C}_{23}\text{H}_{35}\text{N}_5\text{O}_5$ $[\text{M} + \text{Na}]$ is 500.2485. Observed = 500.2491.

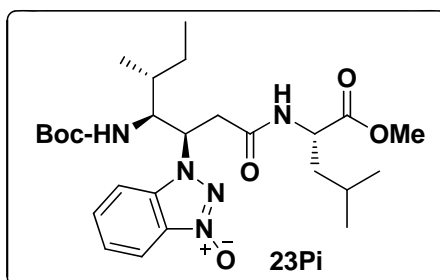


1-((4*S*,8*S*,9*S*)-9-Isobutyl-4,13,13-trimethyl-3,6,11-trioxo-2,12-dioxa-5,10-diazatetradecan-8-yl)-1H-benzo[d][1,2,3]triazole 3-oxide (Boc- γ Leu(β -OBt)-Ala-OMe) (22Pii); White solid, (0.393 g, 42%); UV (λ_{max}) 323 nm; IR (neat) ν (cm^{-1}) 3276, 2958, 2873, 2313, 1740, 1710, 1661, 1532, 1458, 1423, 1368, 1208, 1166, 1114, 953, 749; ^1H NMR (400 MHz, $\text{DMSO-}d_6$) δ 8.52 (d, $J = 8$ Hz, 1H), 7.85 (d, $J = 8$ Hz, 1H), 7.67 (t, $J = 8$ Hz, 1H), 7.60 (d, $J = 8$ Hz, 1H), 7.41 (t, $J = 8$ Hz, 1H), 6.94(d, $J = 8$ Hz, 1H), 5.17-5.13 (m, 1H), 3.95-3.88 (m, 1H), 3.23 (s, 3H), 3.03 (dd, $J = 4$ Hz & 12 Hz, 1H), 2.75 (dd $J = 4$ Hz & 12 Hz, 1H), 1.36 (s, 9H), 1.12(d, $J = 8$ Hz, 3H), 0.77 (t, $J = 8$ Hz, 6H); ^{13}C NMR (100 MHz, $\text{DMSO-}d_6$) 173.0, 169.1, 155.8, 135.3, 130.6, 129.6, 124.5, 115.1, 112.0, 78.5, 59.7, 51.7, 48.0, 36.1, 28.6, 24.7, 23.9, 21.4, 17.1; **MALDI TOF/TOF m/z** Calculated for $\text{C}_{23}\text{H}_{35}\text{N}_5\text{O}_5$ [M + Na] is 500.2485 Observed = 500.3464.

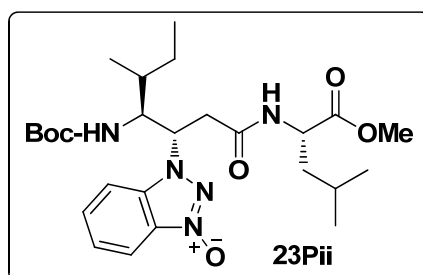


1-((4*S*,8*R*,9*S*)-9-sec-Butyl-4-isobutyl-13,13-dimethyl-3,6,11-trioxo-2,12-dioxa-5,10-diazatetradecan-8-yl)-1H-benzo[d][1,2,3]triazole 3-oxide (Boc- γ Ile(β -OBt)-Leu-OMe) (23Pi); White solid, (0.254 g, 25%); The diastereomeric ratio of 9Pi:9Pii is 39:61 respectively UV (λ_{max}) 323 nm; IR (neat) ν (cm^{-1}) 2963, 2381, 2313, 2112, 1738, 1660, 1509, 1459, 1424, 1368, 1310, 1207, 1167, 749; ^1H NMR (400 MHz, CDCl_3) δ 7.96 (d, $J = 8$ Hz, 1H), 7.66-7.58 (m, 2H), 7.39 (t, $J = 8$ Hz, 1H), 6.08 (d, $J = 8$ Hz, 1H), 5.47-5.43 (m, 2H), 4.42-4.36 (m, 1H), 4.01-3.95 (m, 1H), 3.44 (s, 3H), 2.99 (dd, $J = 4$ Hz & 12 Hz, 1H), 2.87 (dd, $J = 4$ Hz & $J = 12$ Hz, 1H), 1.61-1.50 (m, 2H), 1.45 (s, 9H), 1.17-1.11 (m, 2H), 0.89 (d,

$J = 4$ Hz, 6H), 0.76 (dd, $J = 8$ Hz, 6H); ^{13}C NMR (100 MHz, CDCl_3) 172.4, 168.7, 156.3, 135.1, 130.8, 129.5, 124.6, 115.4, 111.3, 57.3, 52.2, 50.9, 41.2, 39.6, 36.6, 29.7, 28.4, 26.3, 24.8, 22.7, 21.8, 14.9, 10.6; MALDI TOF/TOF m/z Calculated for $\text{C}_{26}\text{H}_{41}\text{N}_5\text{O}_6$ [M + Na] is 542.2955 Observed = 542.2957.

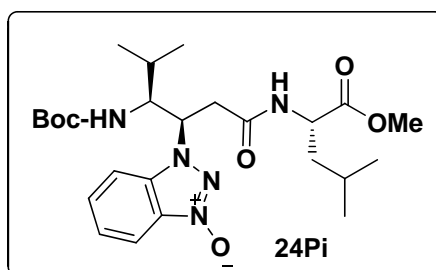


1-((4S,8S,9S)-9-sec-Butyl-4-isobutyl-13,13-dimethyl-3,6,11-trioxo-2,12-dioxa-5,10-diazatetradecan-8-yl)-1H-benzo[d][1,2,3]triazole 3-oxide (Boc- γ Ile(β -OBt)-Leu-OMe) (23Pii); White solid, (0.397 g, 37%); UV (λ_{max}) 323 nm; IR (neat) ν (cm^{-1}) 2964, 2875, 2314, 2259, 2124, 1740, 1707, 1664, 1545, 1460, 1425, 1369, 1207, 1168, 1022, 992, 825, 754; ^1H NMR (400 MHz, $\text{DMSO}-d_6$) δ 8.49 (d, $J = 8$ Hz, 1H), 7.84 (d, $J = 8$ Hz, 1H), 7.67 (d, $J = 4$ Hz, 2H), 7.42-7.38 (m, 1H), 7.03 (d, $J = 8$ Hz, 1H), 5.28-5.22 (m, 1H), 4.05-4.0 (m, 1H), 3.86-3.80 (m, 1H), 3.22 (s, 3H), 3.05 (dd, $J = 4$ Hz & 12 Hz, 1H), 2.69 (dd, $J = 4$ Hz & 12 Hz, 1H), 1.33 (s, 9H), 0.84 (d, $J = 8$ Hz, 3H), 0.73 (dd, $J = 4$ Hz & 12 Hz, 6H), 0.56 (t, $J = 8$ Hz, 3H) ^{13}C NMR (100 MHz, $\text{DMSO}-d_6$) 172.8, 169.5, 156.1, 134.5, 130.6, 129.7, 124.5, 115.2, 112.0, 78.4, 57.5, 51.9, 50.8, 35.7, 35.2, 28.6, 24.5, 23.1, 21.5, 16.5, 11.4. MALDI TOF/TOF m/z Calculated for $\text{C}_{26}\text{H}_{41}\text{N}_5\text{O}_6$ [M + Na] is 542.2955 Observed = 542.2950.

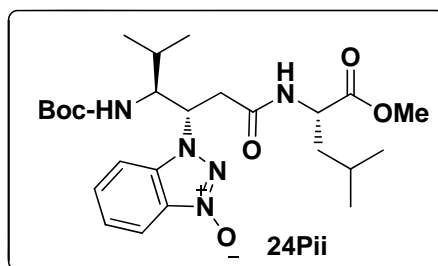


1-((4S,8R,9S)-4-Isobutyl-9-isopropyl-13,13-dimethyl-3,6,11-trioxo-2,12-dioxa-5,10-diazatetradecan-8-yl)-1H-benzo[d][1,2,3]triazole 3-oxide (Boc- γ Val(β -OBt)-Leu-OMe) (24Pi); White solid, (0.249 g, 26%); The diastereomeric ratio of 10Pi:10Pii is 37:63 respectively; UV (λ_{max}) 323 nm; IR (neat) ν (cm^{-1}) 2964, 2312, 2117, 1740, 1542, 1425, 1368, 1311, 1210, 1092, 748; ^1H NMR (400 MHz, CDCl_3) δ 7.95 (d, $J = 8$ Hz, 1H), 7.70 (d, $J = 8$

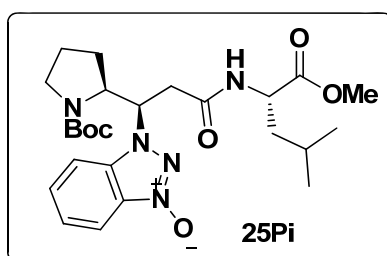
Hz, 1H), 7.62 (t, $J = 8$ Hz, 1H), 7.40 (t, $J = 8$ Hz, 1H), 6.54 (d, $J = 8$ Hz, 1H), 5.55 (d, $J = 12$ Hz, 1H), 5.46-5.42 (m, 1H), 4.39-4.33 (m, 1H), 3.99-3.93 (m, 1H), 3.70 (s, 3H), 2.89 (d, $J = 8$ Hz, 2H), 1.48 (s, 9H), 1.28-1.24 (m, 2H), 0.90 (t, $J = 8$ Hz, 6H), 0.69 (d, $J = 8$ Hz, 3H) 0.53 (d, $J = 4$ Hz, 3H); ^{13}C NMR (100 MHz, CDCl_3) δ 173.0, 168.9, 156.6, 135.0, 130.9, 129.3, 124.8, 115.3, 111.6, 59.1, 57.4, 52.4, 50.8, 40.9, 40.3, 30.7, 28.4, 24.6, 22.7, 21.2, 20.1, 19.4
MALDI TOF/TOF m/z Calculated for $\text{C}_{25}\text{H}_{39}\text{N}_5\text{O}_6$ $[\text{M} + \text{Na}]$ is 528.2798 Observed = 528.2780.



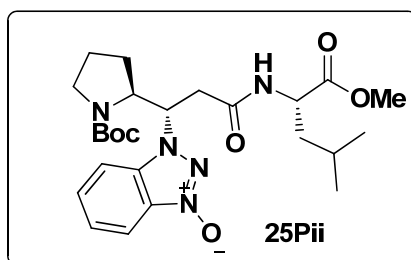
1-((4S,8S,9S)-4-Isobutyl-9-isopropyl-13,13-dimethyl-3,6,11-trioxo-2,12-dioxa-5,10-diazatetradecan-8-yl)-1H-benzo[d][1,2,3]triazole 3-oxide (Boc- γ Val(β -OBt)-Leu-OMe) (24Pii); White solid (0.425 g, 41%); UV (λ_{max}) 323 nm; IR (neat) ν (cm^{-1}) 2962, 2928, 2314, 1737, 1543, 1459, 1424, 1368, 1310, 1208, 1169, 1089, 1038, 747; ^1H NMR (400 MHz, $\text{DMSO-}d_6$) δ 8.47 (d, $J = 8$ Hz, 1H), 7.84 (d, $J = 8$ Hz, 1H), 7.697-7.662 (m, 2H), 7.40 (t, $J = 8$ Hz, 1H), 7.08 (d, $J = 8$ Hz, 1H), 5.17 (t, $J = 8$ Hz, 1H), 4.032-3.98 (m, 1H), 3.91-3.86 (m, 1H), 3.19 (s, 3H), 3.00 (t, $J = 12$ Hz, 1H), 2.70 (d, $J = 20$ Hz, 1H), 1.37 (s, 9H), 0.91-0.85 (m, 2H) 0.82 (d, $J = 8$ Hz, 3H), 0.75 (d, $J = 4$ Hz, 3H), 0.71 (d, $J = 4$ Hz, 6H); ^{13}C NMR (100 MHz, $\text{DMSO-}d_6$) 172.7, 169.5, 156.3, 134.6, 130.7, 129.6, 124.5, 115.2, 112.1, 78.5, 57.8, 51.9, 50.8, 36.5, 28.6, 24.5, 23.1, 21.6, 20.4, 17.2
MALDI TOF/TOF m/z Calculated for $\text{C}_{25}\text{H}_{39}\text{N}_5\text{O}_6$ $[\text{M} + \text{Na}]$ is 528.2798 Observed 528.2535.



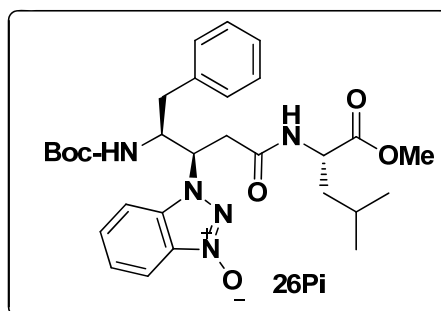
1-((R)-1-((S)-1-(tert-Butoxycarbonyl)pyrrolidin-2-yl)-3-((S)-1-methoxy-4-methyl-1-oxopentan-2-ylamino)-3-oxopropyl)-1H-benzo[d][1,2,3]triazole 3-oxide (Boc-γPro(β-OBt)-Leu-OMe) (25Pi); White solid, (0.242 g, 23%); The diastereomeric ratio of 11Pi:11Pii is 41:59 respectively; UV (λ_{\max}) 323 nm; IR (neat) ν (cm^{-1}) 2966, 2313, 1740, 1687, 1544, 1507, 1455, 1368, 1210, 1164, 907, 748; $^1\text{H NMR}$ (400 MHz, CDCl_3) δ 7.94 (d, $J = 8$ Hz, 1H), 7.62 (d, $J = 8$ Hz, 1H), 7.52 (t, $J = 6$ Hz, 1H), 7.37 (t, $J = 8$ Hz, 1H), 6.39 (d, $J = 8$ Hz, 1H), 5.87-5.83 (m, 1H), 4.41-4.36 (m, 1H), 4.27-4.23 (m, 1H), 3.40 (s, 3H), 3.23-3.21 (m, 2H), 2.87 (dd, $J = 4$ Hz & 12 Hz, 1H), 2.24-2.20 (m, 1H), 2.05-2.00 (m, 4H), 1.45 (s, 9H), 0.88 (t, $J = 4$ Hz, 6H); $^{13}\text{C NMR}$ (100 MHz, CDCl_3) 172.6, 168.5, 157.0, 155.2, 139.3, 135.7, 130.3, 124.6, 115.0, 114.1, 111.6, 60.5, 57.0, 52.1, 51.0, 47.0, 41.0, 37.4, 33.8, 31.9, 29.7, 28.4, 25.8, 24.8, 22.8, 21.8, 14.1; **MALDI TOF/TOF m/z** Calculated for $\text{C}_{25}\text{H}_{37}\text{N}_5\text{O}_6$ [$\text{M} + \text{Na}$] is 526.2642 Observed = 526.2652.



1-((S)-1-((S)-1-(tert-Butoxycarbonyl)pyrrolidin-2-yl)-3-((S)-1-methoxy-4-methyl-1-oxopentan-2-ylamino)-3-oxopropyl)-1H-benzo[d][1,2,3]triazole 3-oxide (Boc-γPro(β-OBt)-Leu-OMe) (25Pii); White solid, (0.349 g, 35%); UV (λ_{\max}) 323 nm; IR (neat) ν (cm^{-1}) 3023, 2967, 2129, 1739, 1653, 1509, 1443, 1368, 1221, 1022, 990, 763; $^1\text{H NMR}$ (400 MHz, $\text{DMSO-}d_6$) δ 8.50 (d, $J = 8$ Hz, 1H), 7.79 (br. 2H), 7.63 (t, $J = 8$ Hz, 1H), 7.36 (t, $J = 8$ Hz, 1H), 5.12-5.05 (br. 1H), 4.11-4.09 (m, 2H), 3.53 (s, 3H), 3.19 (dd, $J = 12$ Hz, 1H), 2.84 (d, $J = 16$ Hz, 1H), 1.97-1.81 (m, 4H), 1.08 (s, 9H), 0.71 (d, $J = 4$ Hz, 3H), 0.33 (d, $J = 4$ Hz, 3H); $^{13}\text{C NMR}$ (100 MHz, $\text{DMSO-}d_6$) 173.2, 169.0, 135.1, 124.4, 114.9, 111.9, 58.7, 52.2, 50.2, 31.8, 29.5, 28.0, 24.3, 24.2, 20.7 **MALDI TOF/TOF m/z** Calculated for $\text{C}_{25}\text{H}_{37}\text{N}_5\text{O}_6$ [$\text{M} + \text{Na}$] is 526.2642 Observed = 526.2639.

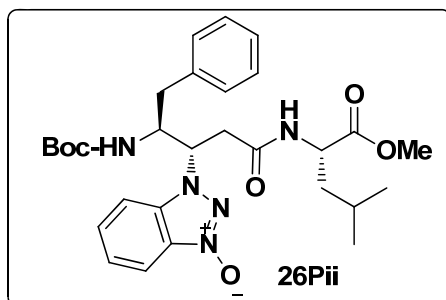


1-((4S,8R,9S)-9-Benzyl-4-isobutyl-13,13-dimethyl-3,6,11-trioxo-2,12-dioxo-5,10-diazatetradecan-8-yl)-1H-benzo[d][1,2,3]triazole 3-oxide (Boc- γ Phe(β -OBt)-Leu-OMe) (26Pi) ; White solid, (0.240 g, 23%); The diastereomeric ratio of 12Pi:12Pii is 39:61 respectively; UV (λ_{max}) 323 nm, 274; IR (neat) ν (cm^{-1}) 2960, 2130, 1739, 1655, 1526, 1505, 1458, 1425, 1368, 1209, 1164, 1022, 991, 749; $^1\text{H NMR}$ (400 MHz, $\text{DMSO-}d_6$) δ 8.50 (d, $J = 8$ Hz, 1H), 7.86 (d, $J = 8$ Hz, 1H), 7.70-7.61 (m, 2H), 7.42 (t, $J = 8$ Hz, 1H), 7.25-7.16(m, 5H), 7.07-7.05 (d, $J = 8$ Hz 1H), 5.33-5.28 (m, 1H), 4.14-4.05 (m, 2H), 3.54 (s, 3H), 3.18 (dd, $J = 4$ Hz & 12 Hz, 1H), 2.88 (dd, $J = 4$ Hz, & $J = 12$ Hz, 1H), 2.69-2.66 (m, 2H), 1.25 (s, 9H), 0.67 (d, $J = 8$ Hz, 3H) 0.28 (d, $J = 8$ Hz, 3H) $^{13}\text{C NMR}$ (100 MHz, $\text{DMSO-}d_6$) 173.2, 169.1, 155.4, 138.9, 135.3, 130.3, 129.5, 128.4, 126.5, 124.4, 114.9, 112.6, 78.1, 60.2, 55.9, 52.2, 50.2, 28.4, 24.3, 23.3, 20.6, 14.5. **MALDI TOF/TOF m/z** Calculated for $\text{C}_{29}\text{H}_{39}\text{N}_5\text{O}_6$ [$\text{M} + \text{Na}$] is 576.2798 Observed = 576.2814.

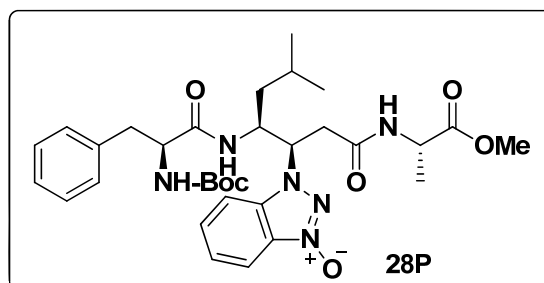


1-((4S,8S,9S)-9-Benzyl-4-isobutyl-13,13-dimethyl-3,6,11-trioxo-2,12-dioxo-5,10-diazatetradecan-8-yl)-1H-benzo[d][1,2,3]triazole 3-oxide (Boc- γ Phe(β -OBt)-Leu-OMe) (26Pii) ; White solid, (0.377 g, 33%); UV (λ_{max}) 323 nm, 274 nm; IR (neat) ν (cm^{-1}) 3026, 2966, 2313, 1739, 1653, 1542, 1524, 1456, 1425, 1368, 1210, 1022, 992, 757; $^1\text{H NMR}$ (400 MHz, $\text{DMSO-}d_6$) δ 8.53 (d, $J = 8$ Hz, 1H), 7.86 (d, $J = 8$ Hz, 1H), 7.69-7.61 (m, 2H), 7.42 (t, $J = 6$ Hz, 1H), 7.23 (t, $J = 8$ Hz, 3H), 7.16 (d, $J = 4$ Hz, 4H), 7.03 (d, $J = 12$ Hz, 1H), 5.34-

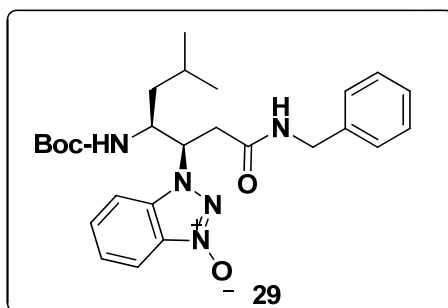
5.29 (m, 1H), 4.10.4.06 (m, 2H), 3.28 (s, 3H), 3.16 (dd, $J = 4$ Hz & 12 Hz, 1H), 2.94 (dd, $J = 4$ Hz & 12 Hz, 1H), 2.73-2.65 (m, 2H), 1.24 (s, 9H), 0.79 (d, $J = 8$ Hz, 3H), 0.74 (d, $J = 8$ Hz, 3H); ^{13}C NMR (100 MHz, DMSO- d_6) 172.9, 169.3, 155.6, 138.9, 135.3, 130.5, 129.4, 128.5, 126.5, 124.4, 115.2, 112.0, 78.5, 60.2, 59.4, 55.3, 52.0, 50.8, 36.0, 35.5, 28.6, 24.5, 23.2, 21.5, 14.5. MALDI TOF/TOF m/z Calculated for $\text{C}_{29}\text{H}_{39}\text{N}_5\text{O}_6$ [M + Na] is 576.2798 Observed = 576.4337.



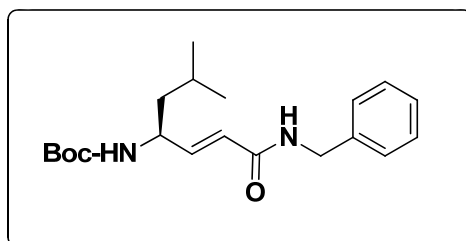
1-((4*S*,8*S*,9*S*,12*S*)-12-Benzyl-9-isobutyl-4,16,16-trimethyl-3,6,11,14-tetraoxo-2,15-dioxo-5,10,13-triazaheptadecan-8-yl)-1H-benzo[d][1,2,3]triazole 3-oxide (Boc-Phe- γ Leu(β -OBt)-Ala-OMe) (27P); White solid, (0.175 g, 67%); UV (λ_{max}) 323 nm; IR (neat) ν (cm^{-1}) ^1H NMR (400 MHz, DMSO- d_6) δ 8.52 (d, $J = 8$ Hz, 1H), 7.91 (d, $J = 8$ Hz, 2H), 7.80 (d, $J = 8$ Hz, 1H), 7.68 (t, $J = 8$ Hz, 1H), 7.35 (t, $J = 6$ Hz, 1H), 7.22 (t, $J = 8$ Hz, 3H), 7.15 (d, $J = 8$ Hz, 1H), 6.93 (d, $J = 8$ Hz, 1H), 5.15-5.10 (m, 1H), 4.27 (d, $J = 8$ Hz, 1H), 4.06-4.99 (m, 1H), 3.86-3.80 (m, 1H), 3.50 (s, 3H), 3.17-3.03 (m, 1H), 2.79 (dd, $J = 4$ Hz & 12 Hz, 1H), 2.38 (dd, $J = 4$ Hz & 12 Hz, 1H), 2.07 (dd, $J = 4$ Hz & 8 Hz, 1H), 1.67-1.59 (m, 1H), 1.27 (s, 9H), 1.10 (d, $J = 4$ Hz, 3H), 0.82 (d, $J = 4$ Hz, 3H), 0.74 (d, $J = 8$ Hz, 3H); ^{13}C NMR (100 MHz, DMSO- d_6) 173.3, 172.2, 168.9, 155.7, 138.8, 135.3, 129.5, 128.4, 124.5, 115.0, 112.6, 78.4, 59.8, 56.5, 48.0, 36.1, 28.5, 24.1, 21.3 MALDI TOF/TOF m/z Calculated for $\text{C}_{32}\text{H}_{44}\text{N}_6\text{O}_7$ [M + Na] is 647.3169 Observed = 647.3171.



1-((3*R*,4*S*)-1-(Benzylamino)-4-(tert-butoxycarbonylamino)-6-methyl-1-oxoheptan-3-yl)-1*H*-benzo[d][1,2,3]triazole 3-oxide (Boc- γ Leu(β -OBt)-NHBn) (28); White solid, (0.223 g, 62 %); $^1\text{H NMR}$ (400 MHz, CDCl_3) δ 7.96 (d, $J = 8$ Hz, 1H), 7.70 (d, $J = 8.4$ Hz, 1H), 7.63 (t, $J = 8$ Hz, 1H), 7.42 (t, $J = 6$ Hz, 1H), 7.20-7.18 (m, 3H), 6.99 (br., 2H), 6.25-6.19 (m, 1H), 5.32-5.29 (m, 1H), 5.21 (d, $J = 8$ Hz, 1H), 4.24 (d, $J = 8$ Hz, 3H), 2.99-2.96 (m, 2H), 1.63-1.56 (m, 1H), 1.44 (s, 9H), 1.05 (t, $J = 8$ Hz, 2H), 0.83 (t, $J = 6$ Hz, 6H); $^{13}\text{C NMR}$ (100 MHz, CDCl_3) 168.7, 156.0, 137.5, 135.3, 130.9, 128.6, 127.5, 124.8, 115.3, 111.4, 79.9, 60.2, 51.6, 43.7, 41.3, 38.9, 29.7, 28.4, 24.8, 23.1, 21.7. MALDI TOF/TOF m/z Calculated for $\text{C}_{26}\text{H}_{35}\text{N}_5\text{O}_4$ $[\text{M} + \text{Na}] = 504.2587$ observed $[\text{M} + \text{Na}] = 504.2202$.



(*S*, *E*)-tert-Butyl 1-(benzylamino)-6-methyl-1-oxohept-2-en-4-ylcarbamate (Boc-dgL-NHBn) (30); White solid, (0.142 g, 89%); $^1\text{HNMR}$ (400 MHz, CDCl_3) δ 7.36-7.29 (m, 5H), 6.72 (dd, $J = 8$ Hz & 8 Hz, 1H), 5.90 (d, $J = 16$ Hz, 1H), 5.86-5.81 (m, 1H), 4.51 (d, $J = 8$ Hz, 2H), 4.47 (d, $J = 8$ Hz, 1H), 4.30(t, $J = 8$ Hz 1H), 1.71-1.65 (m, 1H), 1.44 (s, 9H), 1.38 (t, $J = 6$ Hz, 2H), 0.93 (dd, $J = 4$ Hz, 6H); $^{13}\text{CNMR}$ (100 MHz, CDCl_3) 165.4, 155.2, 144.9, 138.1, 128.8, 128.0, 127.6, 122.9, 114.9, 79.7, 49.9, 44.0, 43.8, 32.0, 29.7, 28.4, 24.7, 22.6, 14.2; MALDI TOF/TOF m/z Calculated for $\text{C}_{20}\text{H}_{30}\text{N}_2\text{O}_3$ $[\text{M} + \text{Na}] = 369.2154$ observed $[\text{M} + \text{Na}] = 369.1958$.



1.3.4 Synthesis procedure and compound characterization for Section 1C

NMR spectroscopy: All NMR studies were carried out by using a Bruker AVANCE^{III}-500 MHz spectrometer at a probe temperature of 300 K. Resonance assignments were obtained by TOCSY and ROESY analysis. All two-dimensional data were collected in phase-sensitive mode, by using the time-proportional phase incrementation (TPPI) method. Sets of 1024 and 512 data points were used in the t_2 and t_1 dimensions, respectively. For TOCSY and ROESY analysis, 32 and 72 transients were collected, respectively. A spectral width of 6007 Hz was used in both dimensions. A spin-lock time of 256 ms was used to obtain ROESY spectra. Zero-filling was carried out to finally yield a data set of $2\text{ K} \times 1\text{ K}$. A shifted square-sine-bell window was used before processing.

Molecular Dynamics: Model building and molecular dynamics simulation of P2 was carried out using Insight II (97.0) / Discover program on a Silicon Graphics Octane workstation.⁵⁶ The cvff force field with default parameters was used throughout the simulations. Minimization's were done first with steepest decent, followed by conjugate gradient methods for a maximum of 1000 iterations each or RMS deviation of 0.001 kcal/mol, whichever was earlier. The energy-minimized structures were then subjected to MD simulations. A number of inter atomic distance constraints obtained from NMR data were used as restraints in the minimization as well as MD runs. For MD runs, a temperature of 300 K was used. The molecules were initially equilibrated for 50 ps and subsequently subjected to a 1 ns dynamics with a step size of 1 fs, sampling the trajectory at equal intervals of 10 ps. In trajectory 50 samples were generated and the best structures were again energy minimized with above protocol and superimposed these structures.

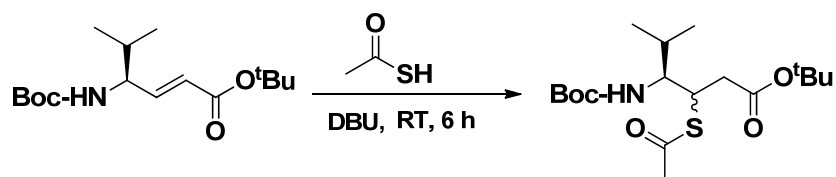
Circular dichroism (CD) spectroscopy:

CD spectrometry study was carried out on JASCO J-815 spectropolarimeter using cylindrical, jacketed quartz cell (1 mm path length), which was connected to Julabo-UC-25 water circulator. Spectra were recorded with a spectral resolution of 0.05 nm, band width 1 nm at a

scan speed of 50nm/min and a response time 1 sec. All the spectra were corrected for methanol solvent and are typically averaged over 3 scans.

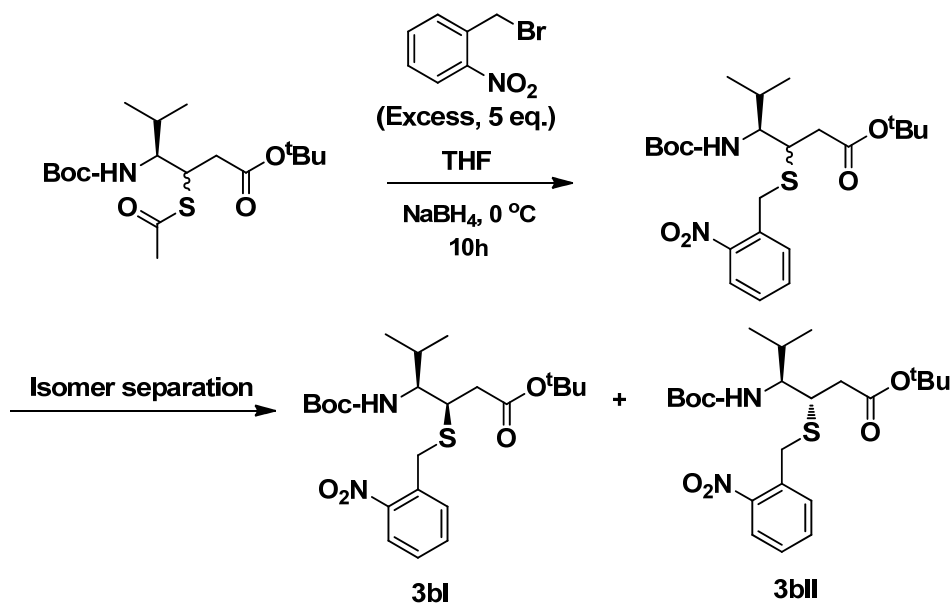
Procedure for conjugate addition of thioacetic acid to Boc-dgVal-O^tBu

In 50 mL RB flask, Boc-dgVal-O^tBu (1.49 g, 5mmol) was treated with mixture of DBU (0.228 g, 1.5mmol) and thioacetic acid (2.28 g, 30 mmol). The reaction mixture was vigorously stirred for another 6h. The progress of reaction was monitored by the TLC. After the completion of reaction, the thioacetic acid was evaporated under reduced pressure and residue was dissolved in 70 mL of ethyl acetate. The organic layer was treated 5 % aqueous HCl, 5 % aqueous Na₂CO₃ and brine. The organic layer was dried over anhydrous Na₂SO₄ evaporated under reduced pressure. The diastereomeric mixture of Boc-γValβ-(SAC)-O^tBu was obtained after column chromatography in 70 % (1.3 g) yield.



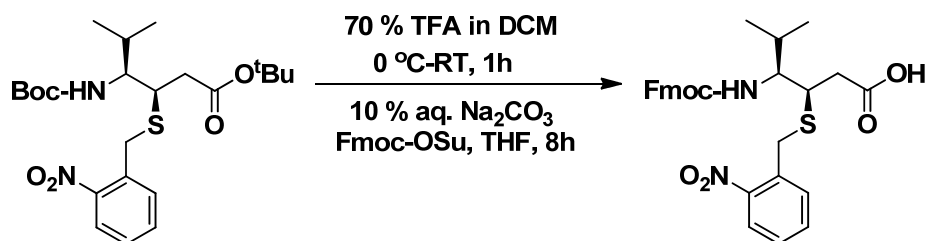
Procedure for orthogonal protection of thiol by *ortho*-nitro benzyl group

The diastereomeric mixture of Boc-γValβ-(SAC)-O^tBu (1.3 g, 3.4 mmol) was dissolved in THF (25 mL). To this, *ortho*-nitro benzyl bromide (3.74 g, 17 mmol) was added. The reaction mixture was cooled to 0 °C and treated with NaBH₄ (1.29 g, 34 mmol) in water (4 mL). The reaction was allowed to stir for another 12 h. After completion of reaction (monitored by TLC and mass analysis) the excess NaBH₄ was quenched with 5 % aqueous HCl and the solvent THF was evaporated under reduced pressure. Further, the residue was dissolved in ethyl acetate (75 mL) washed with brine, dried over anhydrous Na₂SO₄ and concentrated under reduced pressure to get crude diastereomeric mixture of Boc-γValβ-(S-ONB)O^tBu. The crude product was purified through silica gel column chromatography using 5 % ethyl acetate in petroleum ether to get pure diastereomers (3bI and 3bII) in 40 % yield (0.64 g)

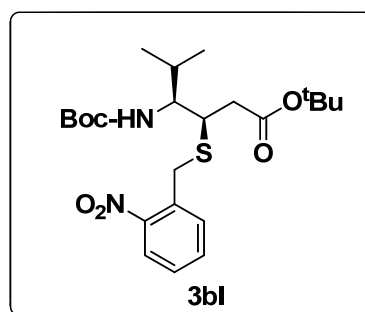


Procedure for synthesis of Fmoc- γ Val β -(S-ONB)-OH

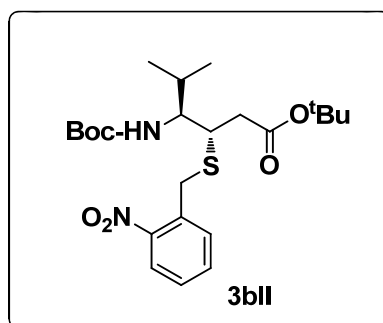
The pure diastereomer Boc- γ Val β -(S-ONB)O^tBu (0.384 g, 0.8 mmol) was dissolved in DCM (3 mL). The solution was cooled to 0 °C and to this added TFA (3mL). The reaction mixture was stirred for another 1h. The progress of reaction was monitored by TLC. After completion of reaction (indicated by TLC) the solvent DCM and TFA was evaporated under reduced pressure and residue was co-evaporated with DCM (three times). Further residue was dissolved in 10 % aqueous Na₂CO₃ (10 mL) and added THF (3mL). To this reaction mixture Fmoc-OSu (0.276 g, 0.8 mmol) in THF (3 mL) was added. The reaction mixture was stirred for another 8h. After the completion of reaction, solvent THF was evaporated and residue was treated with 5 % aqueous HCl to make pH~2. The aqueous layer was extracted with ethyl acetate (30mL \times 3) washed with brine dried over anhydrous Na₂SO₄ concentrated under reduced pressure to give Fmoc- γ Val β -(SONB)-OH in 90 % yield (0.394 g) which was used for solid phase peptide synthesis.



(3*S*, 4*S*)-*tert*-Butyl 4-((*tert*-butoxycarbonyl)amino)-5-methyl-3-((2-nitrobenzyl)thio)hexanoate (Boc- γ Val β -(S-ONB)O^tBu) (**3bI**); Gummy oil (0.256 g, 16 %) ¹H NMR (400 MHz, CDCl₃) δ 7.97 (d, *J* = 7 Hz, 1H), 7.57-7.50 (m, 2H), 7.44-7.40 (m, 1H), 4.44 (d, *J* = 8 Hz, 1H), 3.39-3.34 (m, 1H), 3.29-3.25 (m, 1H), 2.67-2.53 (m, 2H), 1.69-1.61 (m, 1H), 1.46 (s, 9H), 1.41 (s, 9H); ¹³C NMR (100 MHz, CDCl₃) δ 171.0, 155.9, 148.6, 134.0, 133.07, 128.3, 125.4, 80.9, 79.1, 60.36, 59.7, 44.8, 41.3, 33.7, 28.2, 28.0, 19.7, 19.1; HRMS (ESI) *m/z* calcd. for C₂₃H₃₆N₂O₆S [M + Na] is 491.2192 Observed = 491.2226.

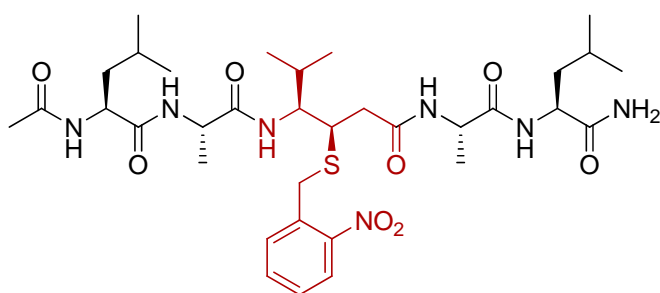


(3*R*, 4*S*)-*tert*-Butyl 4-((*tert*-butoxycarbonyl)amino)-5-methyl-3-((2-nitrobenzyl)thio)hexanoate (Boc- γ Val β -(S-ONB)O^tBu) (**3bII**); Gummy oil (0.384 g, 24 %) ¹H NMR (400 MHz, CDCl₃) δ 7.97 (d, *J* = 8.4 Hz, 1H), 7.56-7.49 (m, 2H), 7.43-7.39 (m, 1H), 4.45 (d, *J* = 10.8 Hz, 1H), 3.57-3.51 (m, 1H), 3.09-3.01 (m, 1H), 2.65-2.47 (m, 2H), 2.13-2.08 (m, 1H), 1.45 (s, 9H), 1.42 (s, 9H); ¹³C NMR (100 MHz, CDCl₃) 171.4, 158.0, 148.6, 133.9, 132.9, 128.2, 125.3, 81.0, 79.2, 60.8, 57.6, 43.8, 39.5, 32.4, 28.9, 28.3, 28.0, 20.3, 16.0; HRMS (ESI) *m/z* calcd. for C₂₃H₃₆N₂O₆S [M + Na] is 491.2192 Observed = 491.2236.



Solid Phase Peptide Synthesis of **P1**: Ac-Leu-Ala- γ Val(β -S-ONB)-Ala-Leu-CONH₂

Peptide **P1** was synthesized at 0.2 mmol scales on Rink Amide resin using standard Fmoc-chemistry. HBTU/HOBT was used as coupling agents. Fmoc deprotections were facilitated using 20% piperidine in DMF. The coupling reactions were monitored by Kaiser Test. *N*-terminal of peptide was capped with acetyl group. After completion of the synthesis, peptide was cleaved from the resin using 15 mL of TFA/H₂O (99:1) cocktail mixture. After cleavage, the resin was filtered and washed with TFA. The cleavage mixture was evaporated under reduced pressure to give gummy product. Peptide was further recrystallized using EtOAc/Hexane. Peptide was filtered and finally it was purified on reverse phase HPLC (Waters 600), with C₁₈ column (XBridge™ Prep BEH 130, C₁₈ 5 μ m, dimension 10 \times 250 mm column) using MeOH/H₂O (system MeOH/H₂O 50:50- 95:5 as gradient, 3 mL flow per min) gradient system. The mass of the peptide **P1** was confirmed by MALDI TOF/TOF mass analysis.



Peptide **P1** synthesized by using solid phase method

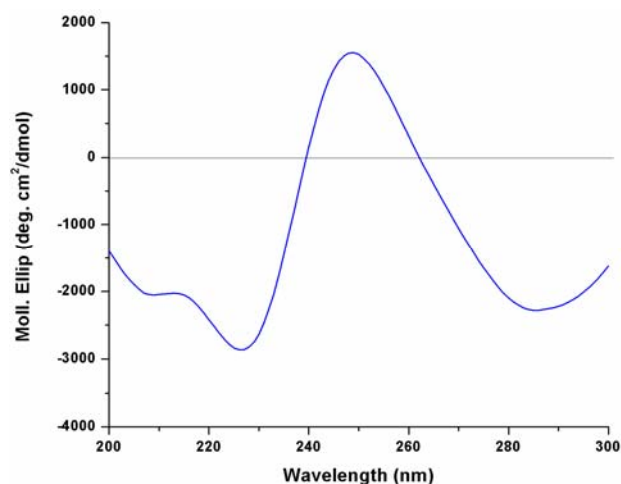
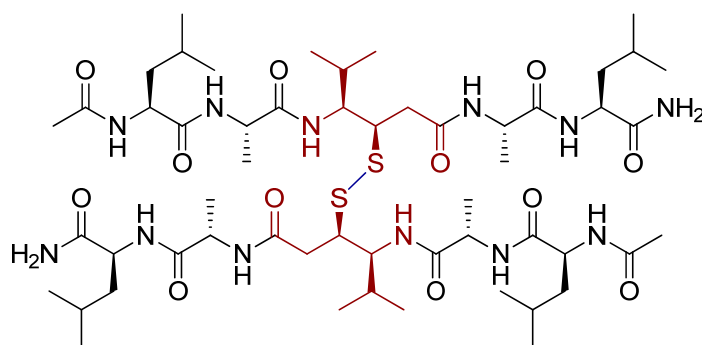


Figure 28: Circular Dichroism spectra for the peptide **P1**

Transformation of peptide P1 (Ac-Leu-Ala- γ Val(β -S-ONB)-Ala-Leu-CONH₂) into stapled peptide P3 [Ac-Leu-Ala- γ Val(β -S)-Ala-Leu-CONH₂]₂

In 50 mL beaker, Peptide **P1** Ac-Leu-Ala- γ Val(β -S-ONB)-Ala-Leu-CONH₂ (10 mg, 0.014 mmol) was dissolved in 5mL of distilled methanol. The solution was exposed to the UV irradiation of 365 nm wavelength with constant stirring. The reaction mixture was stirred for another 24 h. Progress of reaction was monitored by MALDI TOF/TOF mass analysis. After completion of reaction solution was concentrated under reduced pressure up to 2 mL. The peptide was purified through reverse phase HPLC using MeOH/H₂O solvent system. The stapled peptide **P3** was obtained in 85% yield (7 mg, 0.006 mmol). The mass of the peptide was confirmed using MALDI TOF/TOF m/z Calcd. For C₅₄H₉₈N₁₂O₁₂S₂ 1193.6766 Da Observed 1193.6713 Da.



Disulfide stapled peptide P3

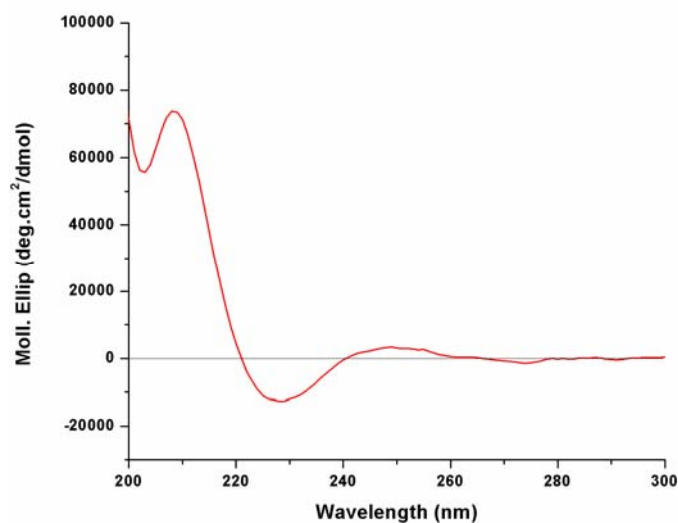


Figure 29: CD spectra for the disulfide stapled Peptide **P3**

Solid phase peptide synthesis of P2: Ac- γ Val(β -S-ONB)-Lys-Val-^DPro-Gly-Leu-Lys- γ Val(β -S-ONB)CONH₂

Peptide **P2** was synthesized at 0.2 mmol scale on Rink Amide resin using standard Fmoc-chemistry. HBTU/HOBT was used as coupling agents. The coupling reactions were monitored by Kaiser Test. After completion of the synthesis, peptide was cleaved from the resin using 15 mL of TFA/H₂O (99:1) cocktail mixture. After cleavage, the resin was filtered and washed with TFA. The cleavage mixture was evaporated under reduced pressure to give gummy product. Peptide was further recrystallized using cold diethyl ether. Peptide was filtered and purified through reverse phase HPLC on C₁₈ column using acetonitrile/water gradient (System ACN/H₂O 5:95-95:5 in 20 minutes as gradient with 3mL flow/min). Homogeneity of peptide was further confirmed using analytical C₁₈ column in same acetonitrile/water gradient system. The HPLC profile is shown in Figure 30. The mass of the peptide was confirmed using **MALDI TOF/TOF** Mass Calcd. for C₆₀H₉₅N₁₃O₁₃S₂ [M+H] 1270.6692 Da, Observed 1270.6268 Da.

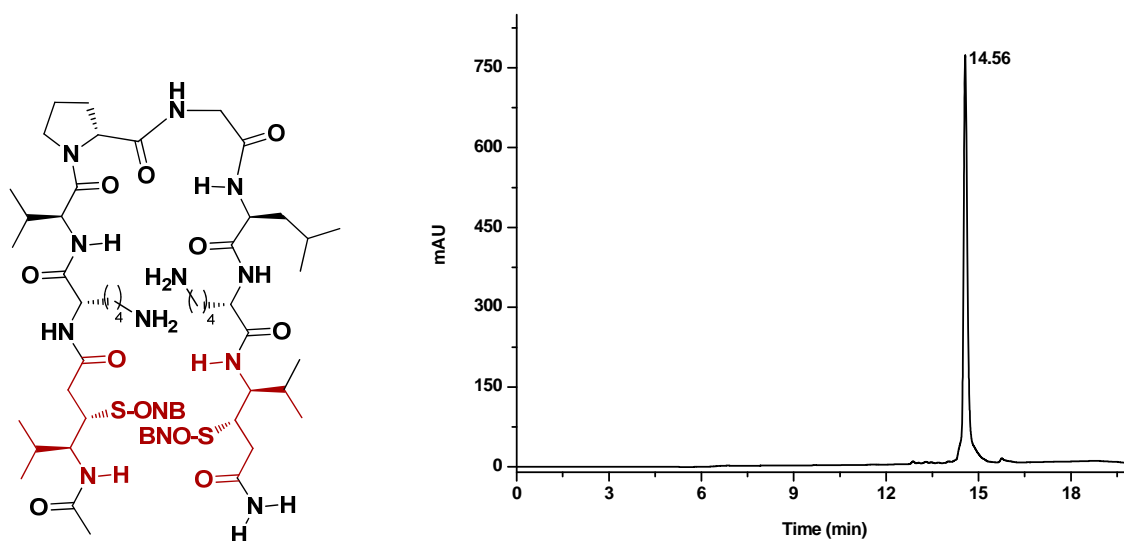


Figure 30: Structure of the peptide **P2** and HPLC profile for pure peptide **P2**

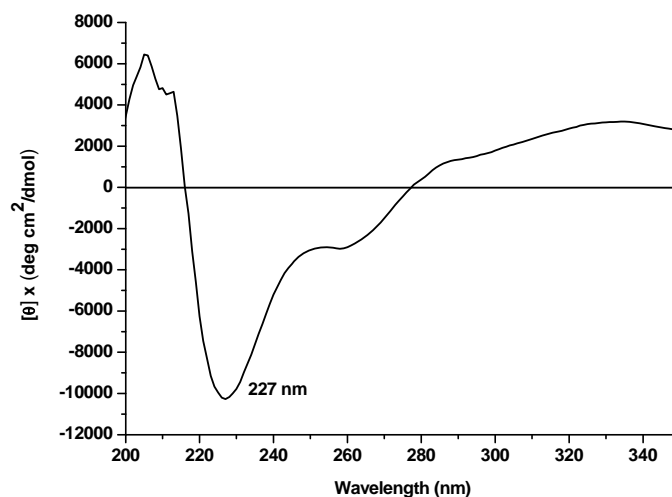


Figure 31: CD spectra for the peptide **P2** in water

Transformation of peptide P2: Ac- γ Val(β -S-ONB)-Lys-Val-^DPro-Gly-Leu-Lys- γ Val(β -S-ONB)CONH₂ in to stapled peptide P4 [Ac- γ Val(β -S)-Lys-Val-^DPro-Gly-Leu-Lys- γ Val(β -S)CONH₂]₂

In 50 mL beaker, Peptide **P2** Ac- γ Val(β -S-ONB)-Lys-Val-^DPro-Gly-Leu-Lys- γ Val(β -S-ONB)CONH₂ (10 mg, 0.008 mmol) was dissolved in 5mL of distilled water. The solution was exposed to the UV irradiation of 365 nm wavelength with constant stirring. The reaction

mixture was stirred for another 24 h. Progress of reaction was monitored by MALDI TOF/TOF mass analysis. After completion of reaction solution was concentrated under reduced pressure up to 2mL. The peptide was purified through reverse phase HPLC using gradient (System ACN/H₂O 5:95-95:5 in 20 minutes as gradient with 3mL flow/min). Homogeneity of peptide was further confirmed using analytical C₁₈ column in same acetonitrile/water gradient system. The HPLC profile is shown in Figure 32. The stapled peptide was obtained in 62% yield (5 mg, 0.005 mmol). The mass of the peptide was conformed using MALDI TOF/TOF m/z Calcd. For C₄₆H₈₃N₁₁O₉S₂ [M + Na] 1020.5714 Da Observed 1020.7676 Da.

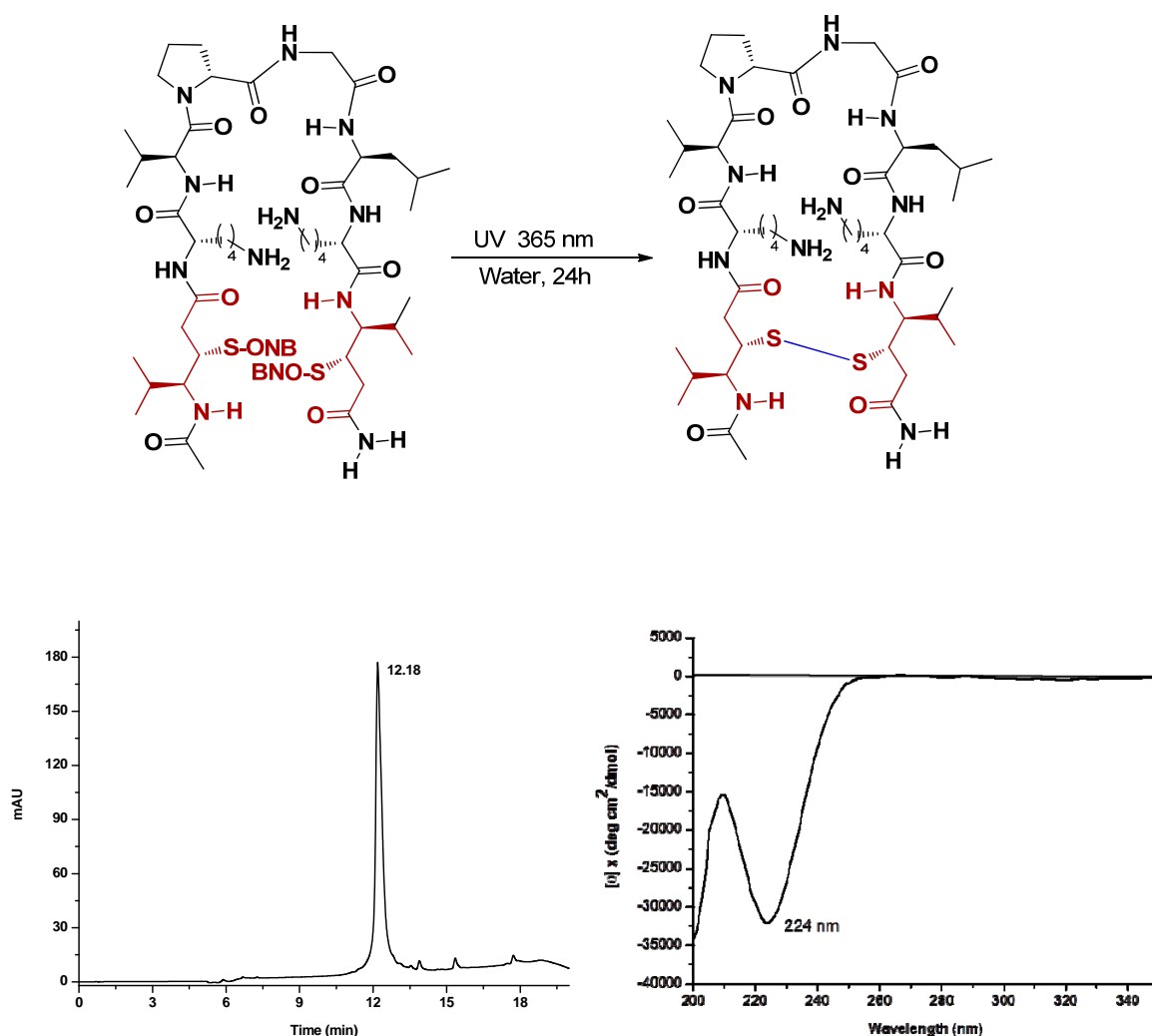


Figure 32: HPLC profile and CD spectra for the disulfide stapled peptide P4

1.4 References

1. a) Ma, J. S. *Chem. Today*, **2003**, 65; b) Ambrogelly, A.; Palioura, S.; Söll, D. *Nat. Chem. Bio.* **2007**, 3, 29; c) Dougherty, D. A. *Curr Opin Chem Biol.* **2000**, 4, 645.
2. a) Schwecke, T.; Aparicio, J. F.; Molnar, I.; Kçnig, A.; Khaw, L. E.; Haydock, S. F.; Oliynyk, M.; Caffrey, P.; Cortes, J.; Lester, B.; Bçhm, G. A.; Staunton, J.; Leadlay, P. F. *Proc. Natl. Acad. Sci. USA* **1995**, 92, 7839; b) Walsh, C. T.; O'Brien, R. V.; Khosla, C. *Angew. Chem. Int. Ed.* **2013**, 52, 7098; c) Mast, Y.; Weber, T.; Gçlz, M.; Ort-Winklbauer, R.; Gondran, A.; Wohlleben, W.; Schinko, E. *Microb. Biotechnol.* **2011**, 4, 192; d) Blanc, V.; Gil, P.; Bamas-Jacques, N.; Lorenzon, S.; Zagorec, M.; Schleuniger, J.; Bisch, D.; Blanche, F.; Debussche, L.; Crouzet, J.; Thibaut, D. *Mol. Microbiol.* **1997**, 23, 191; e) Mast, Y. J.; Wohlleben, W.; Schinko, E. *J. Biotechnol.* **2011**, 155, 63; f) Weber, G.; Leitner, E.; *Curr. Genet.* **1994**, 26, 461; g) Laupacis, A.; Keown, P. A.; Ulan, R. A.; McKenzie, N.; Stiller, C. R. *Can. Med. Assoc. J.* **1982**, 126, 1041; h) Offenzeller, M.; Santer, G.; Totschnig, K.; Su, Z.; Moser, H.; Traber, R.; SchneiderScherzer, E. *Biochemistry* **1996**, 35, 840; i) Keller-Juslen, C.; Kuhn, M.; Loosli, H. R.; Petcher, T. J.; Weber, H. P.; vonWartburg, A. *Tetrahedron Lett.* **1976**, 17, 414; j) Schçnewolf, M.; Rohr, J. *Angew. Chem. Int. Ed. Engl.* **1991**, 30, 183; k) Steenbergen, J. N.; Alder, J.; Thorne, G. M.; Tally, F. P. *J. Antimicrob. Chemother.* **2005**, 55, 283; l) Miao, V.; Coeffet-LeGal, M.-F.; Brian, P.; Brost, R.; Penn, J.; Whiting, A.; Martin, S.; Ford, R.; Parr, I.; Bouchard, M.; Silva, C. J.; Wrigley, S. K.; Baltz, R. H. *Microbiology* **2005**, 151, 1507; m) Gause, G. F.; Brazhnikova, M. G. *Nature* **1944**, 154, 703; n) Stachelhaus, T.; Marahiel, M. A.; Brick, P. *The EMBO Journal* **1997**, 16, 4174.
3. a) Albericio, F.; Kruger, H. G. *Future Med. Chem.* **2012**, 4, 1527; b) Nixon A. E. *Therapeutic Peptides, Methods and Protocols*, **2014**, 1088.
4. a) DeGrado, W. F.; Summa, C. M.; Pavone, V.; Nastro, F.; Lombardi, A. *Annual Review of Biochemistry*, **1999**, 68, 779; b) Hill, R. B.; Raleigh, D. P.; Lombardi, A.; DeGrado, N. F. *Acc. Chem. Res.*, **2000**, 33, 745; c) Gellman, S. H. *Curr. Opin. Chem. Biol.* **1998**, 2, 717 d) Venkatraman, J.; Shankaramma, S. C.; Balaram, P. *Chem. Rev.*

- 2001**, *101*, 3131; e) Lacroix, E.; Kortemme, T.; de la Paz, M. L.; Serrano, L. *Curr. Opin. Struc. Biol.* **1999**, *9*, 487.
5. a) Pless, S. A.; Ahern, C. A. *Annual Review of Pharmacology and Toxicology*, **2013**, *53*, 211; b) Budisa, N.; Minks, C.; Medrano, F. J.; Lutz, J. Huber, R.; Moroder L. *Proc. Natl. Acad. Sci. USA* **1998**, *95*, 455; c) Saladino, R.; Botta, G.; Crucianelli, M. *Mini Rev Med Chem.* **2012**, *12*, 277-300. d) Cavelier F, Marchand D, Martinez J, Sagan S. *J Pept Res.* **2004**, *63*, 290.
 6. a) Hill, D. J.; Mio, M. J.; Prince, R. B.; Hughes, T. S.; Moore, J. S. *Chem Rev.*, **2001**,*101*, 3893-4011. b) Gellman, S. H. *Acc. Chem. Res.*, **1998**, *31*, 173-180. c) Kim, I. C.; Hamilton, A. D. *Org. Lett.*, **2006**, *8*, 1751-1754. d) Brown, N. J.; Wu, C. W.; Seurnyck-Servoss, S. L.; Barron, A. E. *Biochemistry*, **2008**, *47*, 1808-1818.
 7. a) Seebach, D.; Gardiner, J. *Acc. Chem. Res.*, **2008**, *41*, 1366-1375. b) Horne, W. S.; Gellman, S. H. *Acc. Chem. Res.*, **2008**, *41*, 1399-1408. c) Price, J. L.; Horne, W. S.; Gellman, S. H. *J. Am. Chem. Soc.*, **2010**, *132*, 12378-12387. d) Cheng, R. P.; Gellman, S. H.; DeGrado, W. F. *Chem. Rev.*, **2001**, *101*, 3219-3232. e) Vasudev, P. G., Chatterjee, S., Shamala, N., Balaram, P. *Chem. Rev.*, **2011**, *111*, 657-687.
 8. Hook, D.F.; Bindschadler, P.; Mahajan, Y. R.; Sebesta, R.; Kast, P.; Seebach, D. *Chem. Biodiv.* **2005**, *2*, 591.
 9. Hagihara, M.; Anthony, N. J.; Stout, T. J.; Clardy, J.; Schreiber, S. L. *J. Am. Chem. Soc.*, **1992**, *114*, 6568.
 10. a) Grison, C.; Coutrot, P.; Geneve, S.; Didierjean C.; Marraud, M. *J. Org. Chem*, **2005**, *70*,10753; b) Grison, C.; Geneve, S.; Halbin E.; Coutrot, P. *Tetrahedron*, **2001**, *57*, 4903; c) Chakraborty, T. K.; Ghosh, A.; Kumar, S. K.; Kunwar, A. C. *J. Org. Chem*, **2003**, *68*, 6459.
 11. a) Baldauf, C.; Gunther, R.; Hofmann, H. J. *J. Org. Chem*, **2005**, *70*, 5351; b) Baldauf, C.; Gunther, R.; Hofmann, H. J. *Helv. Chim. Acta*, **2003**, *86*, 2573.
 12. a) Linington, R. G.; Clark, B. R.; Trimble, E. E.; Almanza, A.; Uren, L.-D.; Kyle, D. E.; Gerwick, W. H. *J. Nat. Prod.*, **2009**, *72*, 14; b) Coleman, J. E.; de Silva, E. D.; Kong, F.; Andersen, R. J.; Allen, T. M. *Tetrahedron*, **1995**, *51*, 10653; c) Schaschke, N. *Bioorg. Med. Chem. Lett.*, **2004**, *14*, 855; d) Lee, A. Y.; Hagihara, M.; Karmacharya, R.; Albers, M. W.; Schreiber, S. L.; Clardy, J. *J. Am. Chem. Soc.*, **1993**, *115*, 12619; e) Hagihara M.; Schreiber, S. L. *J. Am. Chem. Soc.*, **1992**, *114*, 6570; f)

- Lee, A. Y.; Hagihara, M.; Karmacharya, R.; Albers, M. W.; Schreiber, S. L.; Clardy, J. *J. Am. Chem. Soc.*, **1993**, *115*, 12619 g) Nieman, J. A.; Coleman, J. E.; Wallace, D. J.; Piers, E.; Lim, L. Y.; Roberge, M.; Andersen, R. J. *J. Nat. Prod.*, **2003**, *66*, 183; h) Nakao, Y.; Matsunaga S.; Fusetani, N. *Bioorg. Med. Chem.* **1995**, *3*, 1115; i) Fusetani, N.; Matsunaga, S.; Matsumoto, H.; Takebayashi, H. *J. Am. Chem. Soc.*, **1990**, *112*, 7051.
13. a) Hintermann, T.; Gademann, K.; Jaun, B.; Seebach, D. *Helv. Chim. Acta*, **1998**, *81*, 983; b) Brenner, M.; Seebach, D. *Helv. Chim. Acta*, **2001**, *84*, 1181.
14. a) Santos, M. M. M.; Moreira, R. *Mini-Rev. Med. Chem.* **2007**, *7*, 1040; b) Plummer, J. S.; Emery, L. A.; Stier, M. A.; M.; Suto, M. J. *Tetrahedron Lett.* **1993**, *34*, 7529.
15. Fu, Y.; Xu, B.; Zou, X.; Ma, C.; Yang, X.; Mou, K.; Fu, G.; Lu, Y.; Xu, P. *Bioorg. Med. Chem. Lett.* **2007**, *17*, 1102.
16. Reetz, M. T. *Angew. Chem., Int. Ed.* **1991**, *30*, 1531.
17. a) Wittig, G.; Geissler, G. *Liebigs Ann. Chem.* **1953**, *580*, 44; b) Wittig, G.; Schollkopf, U. *Chem. Ber.* **1954**, *87*, 1318 c) Wittig, G. *Science* **1980**, *210*, 600 d) Maerckar, A. *Org. React.* **1965**, *14*, 270; e) Maryanoff, B. E.; Reitz, A. B.; *Chem. Rev.* **1989**, *89*, 863; f) Kolodiazhnyi, O. I. *Phosphorus Ylides, Chemistry and Application in Organic Synthesis*; Wiley-VCH: Weinheim, Germany, **1999**. g) Vedejs, E.; Marth, C. F. *J. Am. Chem. Soc.* **1990**, *112*, 3905; h) El-Batta, A.; Jiang, C.; Zhao, W.; Anness, R.; Cooksy, A. L.; Bergdahl, M. *J. Org. Chem.*, **2007**, *72*, 5244 and references sited therein.
18. a) Julia, M.; Paris, J. M. *Tetrahedron Lett.* **1973**, *14*, 4833; b) Baudin, J. B.; Hareau, G.; Julia, S. A.; Ruel, O. *Tetrahedron Lett.* **1991**, *32*, 1175; c) Kocienski, P. J. *Phosphorus Sulfur* **1985**, *24*, 97; d) Blakemore, P. R. *J. Chem. Soc., Perkin Trans. 1* **2002**, 2563.
19. a) Rotella, D. P. *J. Am. Chem. Soc.*, **1996**, *118*, 12246; b) Oishi, S.; Kamano, T.; Niida, A.; Odagaki, Y.; Hamanaka, N.; Yamamoto, M.; Ajito, K.; Tamamura, H.; Otaka, A.; Fujii, N. *J. Org. Chem.* **2002**, *67*, 6162; c) Chintareddy, V. R.; Ellern, A.; Verkade, J. G. *J. Org. Chem.* **2010**, *75*, 7166 and references sited therein.
20. a) Peterson, D. J. *J. Org. Chem.* **1968**, *33*, 780 b) Ager, D. J. *Synthesis*, **1984**, 384 c) Ager, D. J. *Org. React.* **1990**, *38*, 1.
21. Blasdel, L. K.; Myers, A. G. *Org. Lett.*, **2005**, *7*, 4281.

22. a) Claridge, T. D. W.; Davies, S. G.; Lee, J. A.; Nicholson, R. L.; Roberts, P. M.; Russell, A. J.; Smith, A. D.; Toms, S. M. *Org Lett*, **2008**, *10*, 5437; b) Blanchette, M. A.; Choy, W.; Davis, J. T.; Essensfeld, A. P.; Masamune, S.; Roush, W. R.; Sakai, T. *Tetrahedron Lett.* **1984**, *25*, 2183; c) Rathke, M. W.; Nowak, M. *J. Org. Chem.* **1985**, *50*, 2624.
23. Bandyopadhyay, A.; Agrawal, N.; Mali, S. M.; Jadhav, S. V.; Gopi, H. N. *Org. Biomol. Chem.* **2010**, *8*, 4855.
24. Dunne, E. C.; Coyne, E. J.; Crowley, P. B.; Gilheany, D. G. *Tetrahedron Lett.* **2002**, *43*, 2449.
25. a) Perlmutter, P. *Conjugate Addition Reactions in Organic Synthesis*; Pergamon: Oxford, 1992. 339; b) Christoffers, J.; Baro, A. *Angew. Chem., Int. Ed.* **2003**, *42*, 1688; c) Alexakis, A.; Benhaim, C. *Eur. J. Org. Chem.* **2002**, 3221; d) Tsogoeva, S.B. *Eur. J. Org. Chem.* **2007**, 1701; e) Kireev, A. S.; Manpadi, M.; Kornienko, A. *J. Org. Chem.* **2006**, *71*, 2630; f) Ballini, R.; Bosica, G.; Fiorini, D.; Palmieri, A.; Petrini, M. *Chem. Rev.* **2005**, *105*, 933; g) Wabnitz, T. C.; Spencer, J. B. *Org. Lett.* **2003**, *5*, 2141.
26. a) Gilman, H.; Jones, R. G.; Woods, L. A. *J. Org. Chem.* **1952**, *17*, 1630; b) Alexakis, A.; Bäckvall, J. E.; Krause, N.; Pàmies, O.; Diéquez, M. *Chem. Rev.* **2008**, *108*, 2796; c) Krause, N.; Hoffmann-Röder, A. *Synthesis* **2001**, 171; d) Feringa, B. L.; Naasz, R.; Imbos, R.; Arnold, L. A. In *Modern Organocopper Chemistry*; Krause, N., Ed.; Wiley-VCH: Weinheim, Germany, **2002**, 224-258; e) Harutyunyan, S. R.; den Hartog, T.; Geurts, K.; Minnaard, A. J.; Feringa, B. L. *Chem. Rev.* **2008**, *108*, 2824; f) Frase, P. K.; Woodward, S. *Chem.-Eur. J.* **2003**, *9*, 776; g) Dambacher, J.; Bergdahl, M. *J. Org. Chem.* **2005**, *70*, 580; h) House, H. I. *Acc. Chem. Res.* **1976**, *9*, 59.
- 27 a) Hargrave, J. D.; Joseph C. Allen, J. C.; Frost, C. G. *Chem. Asian J.* **2010**, *5*, 386; b) Sakai, M.; Hayashi, H.; Miyaoura, N. *Organometallics* **1997**, *16*, 4229; c) Yoshida, K.; Ogasawara, M.; Hayashi, T. *J. Org. Chem.* **2003**, *68*, 1901
- 28 a) Plunian, B.; Vaultier, M.; Mortier, J. *Chem Commun*, **1998**, 81; b) Aurell, M. J.; Domingo, L. R.; Mestres, R.; Muñoz, E.; Zaragoza, R. J. *Tetrahedron*, **1999**, *55*, 815.
- 29 Cooke, Jr., M. P. *J. Org. Chem.* **1987**, *52*, 5729.

- 30 Yamamoto, Y.; Yamamoto, S.; Yatagai, H.; Ishihara, Y.; Maruyama, K. *J. Org. Chem.* **1982**, *47*, 119.
- 31 Vautravers, N. R.; Breit, B. *Synlett*, **2011**, 2517.
- 32 Li, Z.; Shi, Z.; He, C. *J. Organomet. Chem.* **2005**, *690*, 5049.
- 33 Mali, S. M.; Bandyopadhyay, A.; Jadhav, S. V.; Ganesh Kumar, M.; Gopi, H. N. *Org. Biomol. Chem.* **2011**, *9*, 6566.
- 34 a) Ganesh Kumar, M.; Mali, S. M.; Gopi, H. N. *Org. Biomol. Chem.* **2013**, *11*, 803; b) Plummer, J. S.; Emery, L. A.; Stier, M. A.; Suto, M. J. *Tetrahedron Lett.* **1993**, *34*, 7529.
- 35 a) Li, P.; Xu, J. C. *J. Chem. Soc., Perkin Trans. 2*, **2001**, 113; b) Katritzky, A. R.; Malhotra, N.; Fana, W. -Q.; Anders, E. *J. Chem. Soc., Perkin Trans. 2*, **1991**, 1545; c) Boyle, F. T.; Jones, R. A. Y. *J. Chem. Soc., Perkin Trans. 2*, **1973**, 160; d) Carpino, L. A.; Imazumi, H.; El-Faham, A.; Ferrer, F. J.; Zhang, C.; Lee, Y.; Foxman, B. M.; Henklein, P.; Hanay, C.; Mugge, C.; Wenschuh, H.; Klose, J.; Beyermann, M.; Bienert, M. *Angew. Chem. Int. Ed.* **2002**, *41*, 441; e) Carpino, L. A.; Henklein, P.; Foxman, B. M.; Abdelmoty, I.; Costisella, B.; Wray, V.; Domke, T.; El-Faham, A.; Mugge, C. *J. Org. Chem.* **2001**, *66*, 5245; f) Brink, B. D.; DeFrancisco, J. R.; Hillner, J. A.; Linton, B. R. *J. Org. Chem.* **2011**, *76*, 5258; g) Barlos, K.; Papaioannou, D.; Voliotis, S.; Prewo, R.; Bieri, J. H. *J. Org. Chem.* **1985**, *50*, 696; h) Nagarajan, S.; Wilson, S. R.; Rinehart, K. L., Jr. *J. Org. Chem.* **1985**, *50*, 2174; i) Singh, J.; Fox, R.; Wong, M.; Kissick, T. P.; Moniot, J. L.; Gougoutas, J. Z.; Malley, M. F.; Kocy, O. *J. Org. Chem.* **1988**, *53*, 205; j) Coste, J.; Frerot, E.; Patrick, J. *J. Org. Chem.* **1994**, *59*, 2437.
- 36 a) Volonterio, A.; Ramirez de Arellano, C.; Zanda, M. *J. Org. Chem.* **2005**, *70*, 2161; b) Marcelli, T.; Olimpieri, F.; Volonterio, A. *Org. Biomol. Chem.*, **2011**, *9*, 5156.
- 37 Brownstein, S.; Dunogues, J.; Lindsay, D.; Ingold, K. U. *J. Am. Chem. Soc.* **1977**, *99*, 2073.
- 38 a) Fasan, R.; Dias, R. L. A.; Moehle, K.; Zerbe, O.; Obrecht, D.; Mittl, P. R. E.; Grütter, M. G.; Robinson, J. A. *ChemBioChem*, **2006**, *7*, 515; b) Vita, C.; Drakopoulou, E.; Vizzavona, J.; Rochette, S.; Martin, L.; Menez, A.; Roumestand, C.; Yang, Y. S.; Ylisastigui, L.; Benjouad, A.; Gluckman, J. C. *Proc. Natl. Acad. Sci. U. S.*

- A., **1999**, *96*, 13091; c) Wilson, A. J. *Chem. Soc. Rev.*, **2009**, *38*, 3289; d) Stanfield, R. L.; Wilson, I. A. *Curr. Opin. Struct. Biol.*, **1995**, *5*, 103 e) Mahon, A. B.; Arora, P. S. *Future Medicine*, **2013**, 62.
- 39 a) Condon, S. M.; Morize, I.; Darnbrough, S.; Burns, C. J.; Miller, B. E.; Uhl, J.; Burke, K.; Jariwala, N.; Locke, K.; Krolikowski, P. H.; Kumar, N. V.; and Labaudiniere, R. F. *J. Am. Chem. Soc.*, **2000**, *122*, 3007; b) Shepherd, N. E.; Hoang, H. N.; Abbenante, G.; and Fairlie, D.P. *J. Am. Chem. Soc.* **2005**, *127*, 2974; c) Shepherd, N. E.; Abbenante, G.; Fairlie, D. P. *Angew. Chem. Int. Ed.*, **2004**, *43*, 2687; d) Shepherd, N. E.; Hoang, H. N.; Desai, V. S.; Letouze, E.; Young, P. R.; Fairlie, D. P. *J. Am. Chem. Soc.*, **2006**, *128*, 13284.
- 40 a) Blackwell, H. E.; Grubbs, R. H. *Angew. Chem., Int. Ed.*, **1998**, *37*, 3281; b) Blackwell, H. E.; Sadowsky, J. D.; Howard, R. J.; Sampson, J. N.; Chao, J. A.; Steinmetz, W. E.; O'Leary, D. J.; Grubbs, R. H. *J. Org. Chem.*, **2001**, *66*, 5291; c) Schafmeister, C. E.; J. Po, J.; Verdine, G. L. *J. Am. Chem. Soc.*, **2000**, *122*, 5891; d) Venkatraman, J.; Shankarammaand, S. C.; Balaram, P. *Chem.Rev.*, **2001**, *101*, 3131; e) Walensky, L. D.; Korsmeyer, S. J.; Verdine, G.; *Int. Pat.Appl.*, 044839, **2005**; f) Walensky, L. D.; Kung, A. L.; Escher, I.; Malia, T. J.; Barbuto, S.; Wright, R. D.; Wagner, G.; Verdine, G. L.; Korsmeyer, S. J. *Science*, **2004**, *305*, 1466; g) Bernal, F.; Tyler, A. F.; Korsmeyer, S. J.; Walensky, L. D.; Verdine, G. L. *J. Am. Chem. Soc.*, **2007**, *129*, 2456.
- 41 a) Orner, B. P.; Ernst, J. T.; Hamilton, A. D. *J. Am. Chem. Soc.*, **2001**,*123*, 5382; b) Ernst, J. T.; Becerril, J.; Park, H. S.; Yin, H.; Hamilton, A. D.; *Angew.Chem., Int. Ed.*, **2003**, *42*, 535; c) Yin, H.; Lee, G.-i.; Sedey, K. A.; Kutzki, O.; Park, H. S.; Orner, B. P.; Ernst, J. T.; Wang, H.-G.; Sebti, S. M.; Hamilton, A. D. *J. Am. Chem. Soc.*, **2005**, *127*, 10191; d) Chen, L.; Yin, H.; Farooqi, B.; Sebti, S.; Hamilton, A. D.; Chen, J. *Mol. Cancer Ther.*, **2005**, *4*, 1019; e) Yin, H.; Lee, G.; Sedey, K. A.; Rodriguez, J. M.; Wang, H. G.; Sebti, S. M.; Hamilton, A. D. *J. Am. Chem. Soc.*, **2005**, *127*, 5463; f) Davis, J. M.; Truong, A.; Hamilton, A. D. *Org. Lett.*, **2005**, *7*, 5405; g) Yin, H.; Lee, G.-i.; Park, H. S.; Payne, G. A.; Rodriguez, J. M.; Sebti, S. M.; Hamilton, A. D. *Angew. Chem., Int. Ed.*, **2005**, *44*, 2704; h) Rodriguez, J. M.; Hamilton, A. D. *Tetrahedron Lett.*, **2006**, *47*, 7443; i) Kim, I. C.; Hamilton, A. D. *Org. Lett.*, **2006**, *8*, 1751.

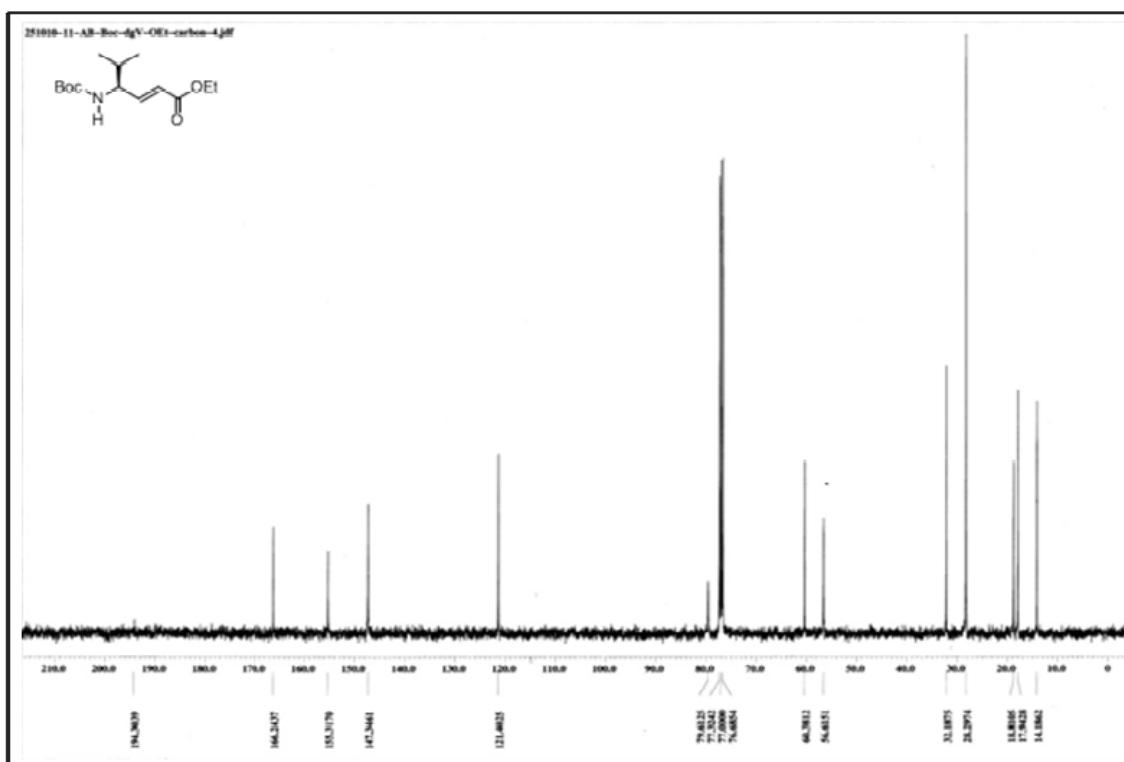
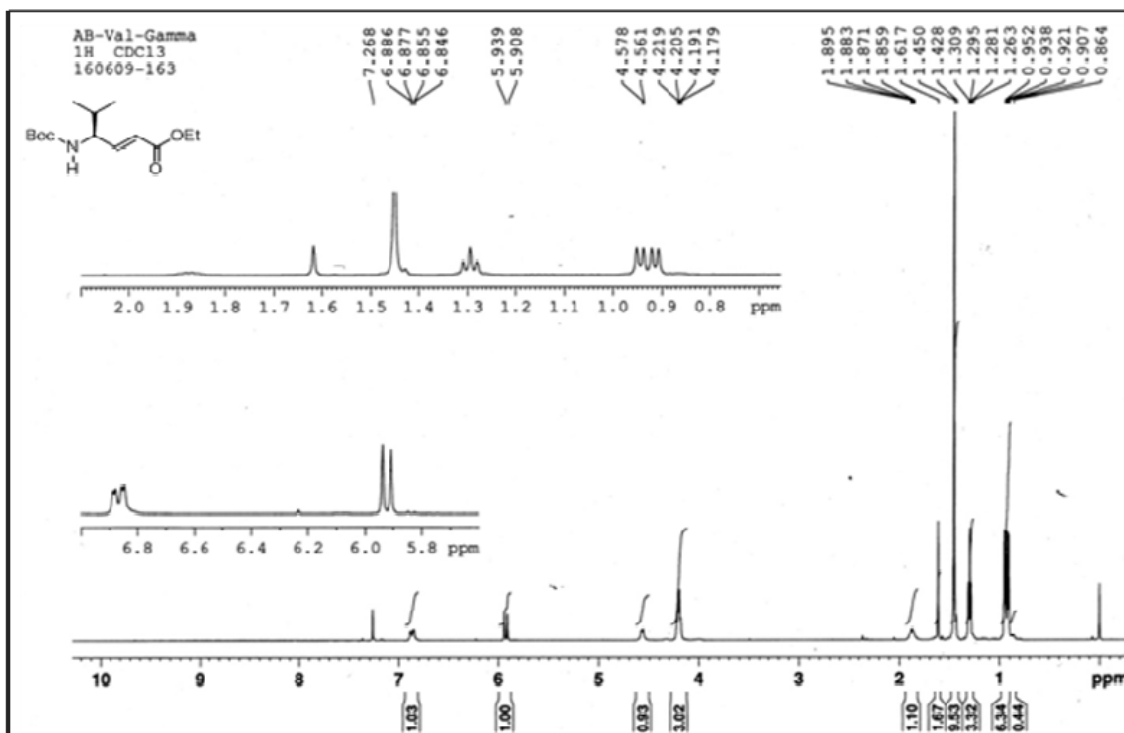
- 42 a) Ghadiri, M. R.; Choi, C. *J. Am. Chem. Soc.*, **1990**, *112*, 1630; b) Ghadiri, M. R.; and Fernholz, A. K. *J. Am. Chem. Soc.*, **1990**, *112*, 9633; c) Kelso, M. J.; Hoang, H. N.; Oliver, W.; Sokolenko, N.; March, D. R.; Appleton, T. G.; Fairlie, D. P. *Angew. Chem., Int. Ed.*, **2003**, *42*, 421; d) Beyer, R. L.; Hoang, H. N.; Appleton, T. G.; Fairlie, D. P. *J. Am. Chem. Soc.*, **2004**, *126*, 15096; e) Kelso, M. J.; Beyer, R. L.; Hoang, H. N.; Lakdawala, A. S.; Snyder, J. P.; Oliver, W. V.; Robertson, T. A.; Appleton, T. G.; Fairlie, D. P.; *J. Am. Chem. Soc.*, **2004**, *126*, 4828; f) Kharenkom, O. A.; Ogawa, M. Y. *J. Inorg. Biochem.*, **2004**, *98*, 1971; g) Ghosh, D.; Pecoraro, V. L. *Inorg. Chem.*, **2004**, *43*, 7902; h) Matzapetakis, M.; Pecoraro, V. L. *J. Am. Chem. Soc.*, **2005**, *127*, 18229.
- 43 a) Gellman, S. H. *Curr. Opin. Chem. Biol.* **1998**, *7*, 717; b) Syud, F. A.; Stanger, H. E.; Gellman, S. H. *J. Am. Chem. Soc.* **2001**, *123*, 8667; c) Searle, M. S. *J. Chem. Soc., Perkin Trans. 2* **2001**, 1011; d) deAlba, E.; Rico, M.; Jimenez, M. A. *Protein Sci.* **1997**, *6*, 2548; e) Ramirez-Alvarado, M.; Blanco, F. J.; Serrano, L. *Nat. Struct. Biol.* **1996**, *3*, 604; f) Regan, L.; Smith, C. K. *Acc. Chem. Res.* **1997**, *30*, 153; g) Wouters, M. A.; Curmi, P. M. *Proteins: Struct., Funct., Genet.* **1995**, *22*, 199; h) Hutchinson, G. E.; Sessions, R. B.; Thornton, J. M.; Woolfson, D. N. *Protein Sci.* **1998**, *7*, 2287.
- 44 a) Russell, S. J.; Cochran, A. G. *J. Am. Chem. Soc.*, **2000**, *122*, 12600; b) Cochran, A. G.; Skelton, N. J.; Starovasnik, M. A. *Proc. Natl. Acad. Sci. U. S. A.*, **2001**, *98*, 5578; c) Fesinmeyer, R. M.; Hudson, F. M.; Andersen, N. H. *J. Am. Chem. Soc.*, **2004**, *126*, 7238; d) Mahalakshmi, R.; Raghothama, S.; Balaram, P. *J. Am. Chem. Soc.*, **2006**, *128*, 1125; e) Jager, M.; Dendle, M.; Fuller, A. A.; Kelly, J. W. *Protein Sci.*, **2007**, *16*, 2306; f) Eidenschink, L.; Kier, B. L.; Huggins, K. N.; Andersen, N. H. *Proteins*, **2009**, *75*, 308; g) Eidenschink, L.; Crabbe, E.; Andersen, N. H. *Biopolymers*, **2009**, *91*, 557; h) Takekiyo, T.; Wu, L.; Yoshimura, Y.; Shimizu, A.; and Keiderling, T. A. *Biochemistry*, **2009**, *48*, 1543; i) Wu, L.; McElheny, D.; Huang, R.; Keiderling, T. A. *Biochemistry*, **2009**, *48*, 10362; j) Mirassou, Y.; Santiveri, C. M.; Perez de Vega, M. J.; Gonzalez-Muniz, R.; Jimenez, M. A. *ChemBioChem*, **2009**, *10*, 902; k) Santiveri, C. M.; Jimenez, M. A. *Biopolymers* **2010**, *94*, 779.
- 45 a) Searle, M. S. *Biopolymers*, **2004**, *76*, 185; b) Ramirez-Alvarado, M.; Blanco, F. J.; Serrano, L. *Protein Sci.* **2001**, *10*, 1381; c) Huyghues-Despointes, B.; Qu, X.; Tsai, J.; Scholtz, J. M. *Proteins*. **2006**, *63*, 1005.

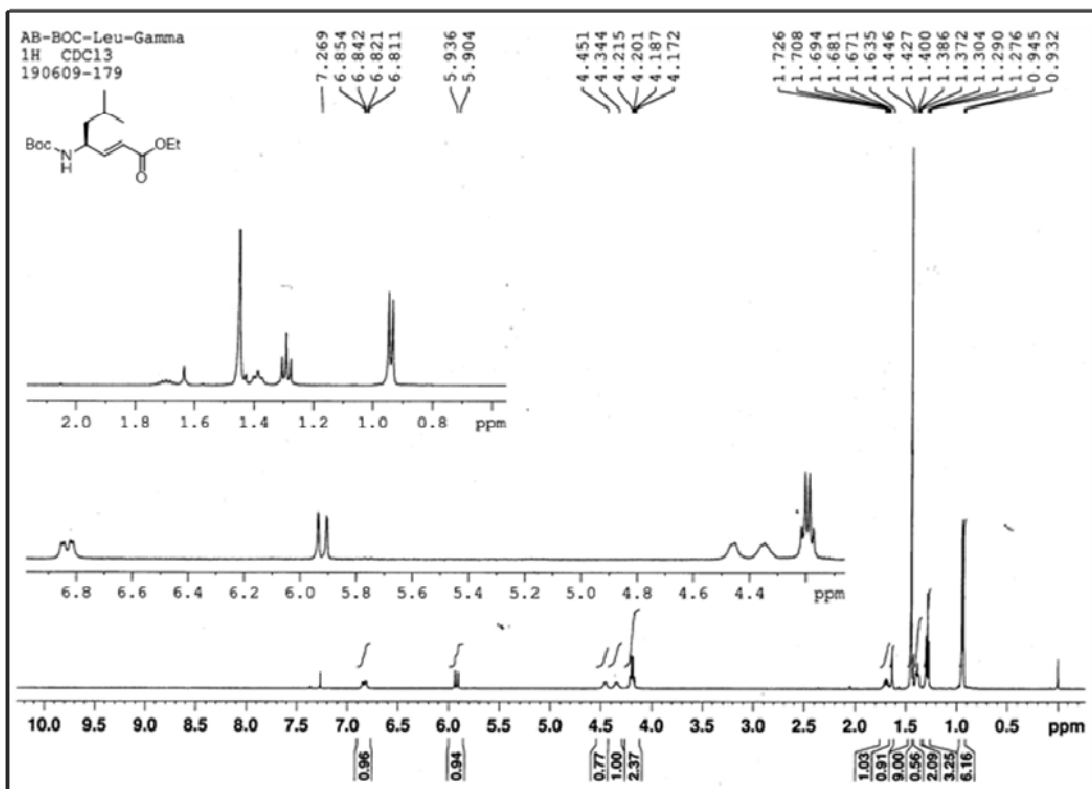
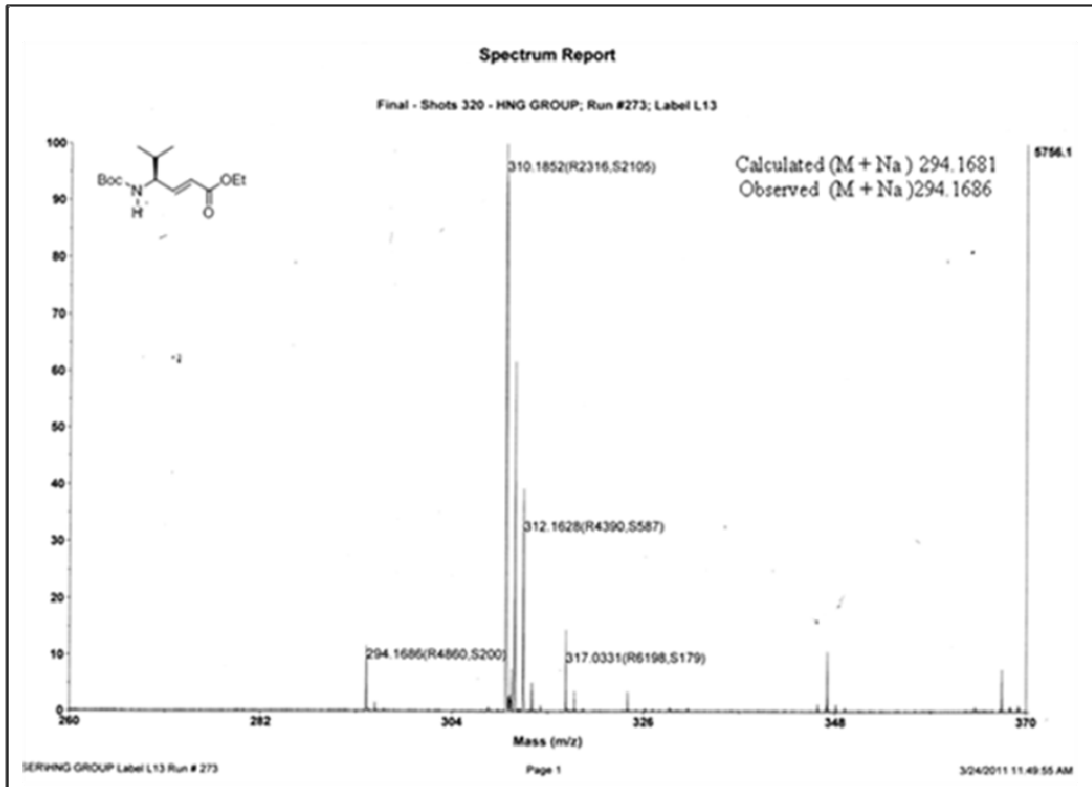
- 46 a) Andrew, C. D.; Bhattacharjee, S.; Kokkoni, N.; Hirst, J. D.; Jones, G. R.; Doig, A. J. *J. Am. Chem. Soc.* **2002**, *124*, 12706; b) Gallivan, J. P.; Dougherty, D. A.P. *Natl. Acad. Sci. U.S.A.* **1999**, *96*, 9459; c) Tsou, L. K.; Tatko, C. D.; Waters, M. L. *J. Am. Chem. Soc.* **2002**, *124*, 14917; d) Tatko, C. D.; Waters, M. L. *Protein Sci.* **2003**, *12*, 2443; e) Rashkin, M. J.; Hughes, R. M.; Calloway, N. T.; Waters, M. L. *J. Am. Chem. Soc.* **2004**, *126*, 13320.
- 47 a) Santiveri, C. M.; Leon, E.; Rico, M.; Jimenez, M. A. *Chem.–Eur. J.*, **2008**, *14*, 488; b) Bulet, P.; Stocklin, R.; Menin, L. *Immunol. Rev.* **2004**, *198*, 169; c) Andreu, D.; Rivas, L. *Biopolymers*, **1998**, *47*, 415; d) Barford, D. *Curr. Opin. Struct. Biol.* **2004**, *14*, 679; e) Hogg, P. J. *Trends Biochem. Sci.* **2003**, *28*, 210; f) McDonald, N. Q.; Hendrickson, W. A. *Cell* **1993**, 421; g) Willey, J. M.; van der Donk, W. A. *Annu. Rev. Microbiol.* **2007**, *61*, 477; h) Ganz, T. *Nat. Rev. Immunol.* **2003**, *3*, 710; i) Cheek, S.; Krishna, S. S.; Grishin, N. V. *J. Mol. Biol.* **2006**, *359*, 215.
- 48 a) Srinivisan, N.; Sowdhamini, R.; Ramakrishnan, C.; Balaram, P. *Int. J. Pept. Protein Res.* **1990**, *36*, 147; b) Mao, B. *J. Am. Chem. Soc.* **1988**, *111*, 6132; (c) Chou, P. Y.; Fasman, G. D. *Biochemistry* **1974**, *13*, 221; d) Fooks, H. M.; Martin, A. C.; Woolfson, D. N.; Sessions, R. B.; Hutchinson, E. G. *J. Mol. Biol.* **2006**, *356*, 32.
- 49 Almeida, A. M.; Li, R.; Gellmann, S. H. *J. Am. Chem. Soc.* **2012**, *134*, 75.
- 50 a) Berman, H. M.; Westbrook, J.; Feng, Z.; Gilliland, G.; Bhat, T. N.; Weissig, H.; Shindyalov, I. N.; Bourne, P. E. *Nucleic Acids Res.* **2000**, *28*, 235; b) Jiang, C.-S.; Muller, W.E.G.; Schroder, H. C.; Guo, Y.-W. *Chem. Rev.* **2012**, *112*, 2179; c) Wen, S.; Packham, G.; Ganesan, A. *J. Org. Chem.* **2008**, *73*, 9353.
- 51 a) Patchornik, A.; Amit, B.; Woodward, R. B. *J. Am. Chem. Soc.* **1970**, *92*, 6333; b) Bayley, H.; Chang, C.-Y.; Miller, W. T.; Niblack, B.; Pan, P. *Methods Enzymol.* **1998**, *291*, 117; c) Givens, R. S.; Kueper, L. W. *Chem. Rev.* **1993**, *93*, 55.
- 52 a) Venkatraman, J.; Shankaramma, S. C.; Balaram, P. *Chem. Rev.* **2001**, *101*, 3131; b) Karle, I. L.; Gopi, H. N.; Balaram, P. *Proc. Natl. Acad. Sci., USA*, **2002**, *99*, 5160.
- 53 *SAINT Plus*, (Version 7.03); Bruker AXS Inc.: Madison, WI, 2004.
- 54 a) SHELXS-97: G. M. Sheldrick, *Acta Crystallogr. Sect A* **1990**, *46*, 467-473, b) G. M. Sheldrick, SHELXL-97, Universität Göttingen (Germany) 1997.

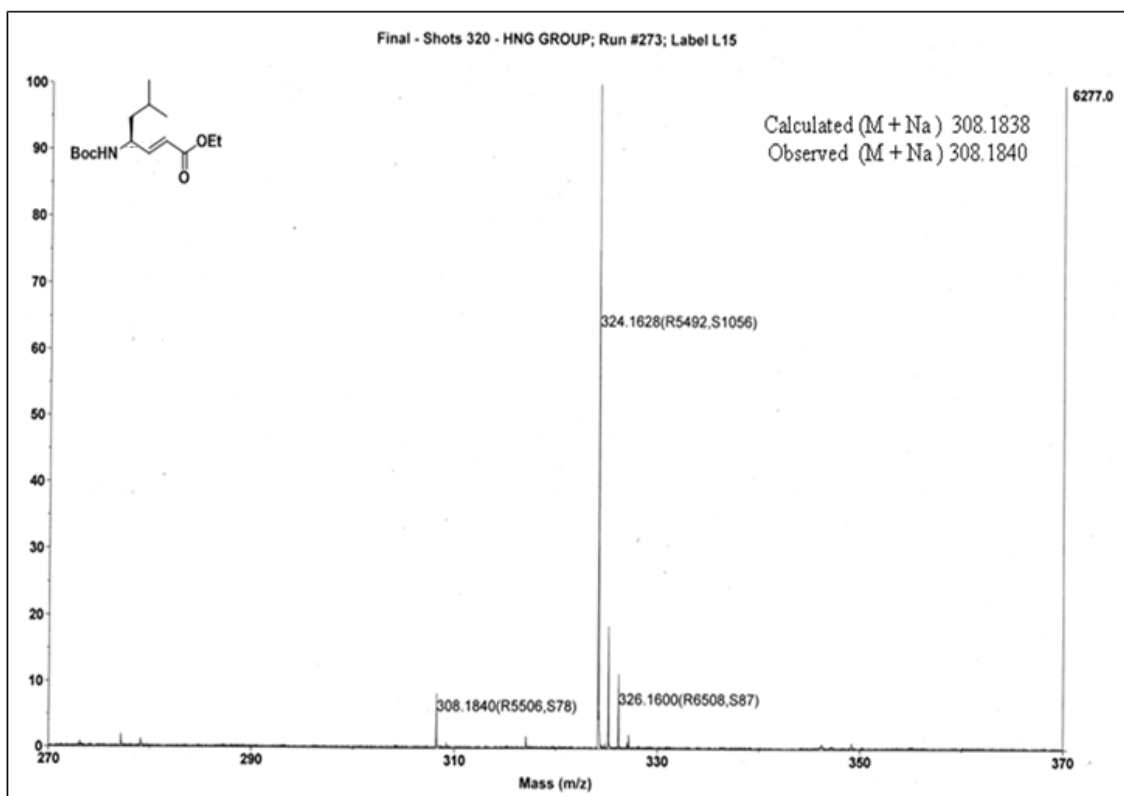
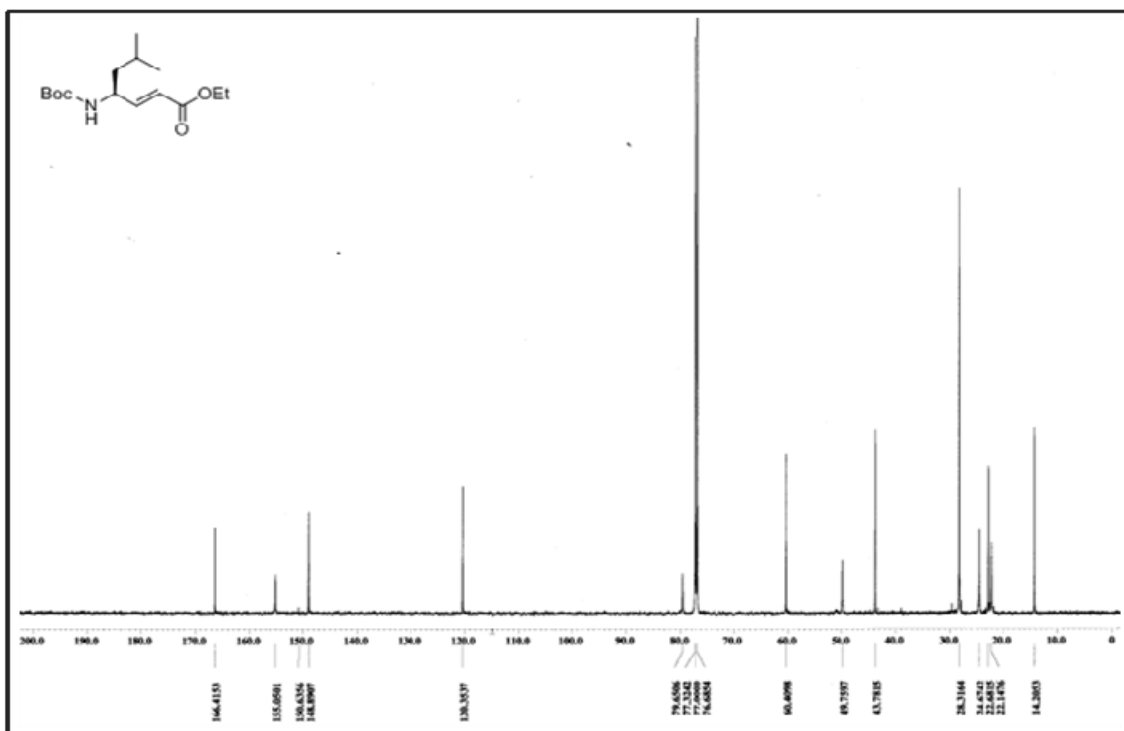
- 55 Shankaramma, S. C.; Kumar Singh, S.; Sathyamurthy, A.; Balaram, P, *J. Am. Chem. Soc.* **1999**, *121*, 5360-5363.
- 56 Betzel, C.; Lange, G.; Pal, G.P.; Wilson, K.S.; Maelicke, A.; Saenger, W. *J. Biol. Chem.* **1991**, *266*, 21530-21536.

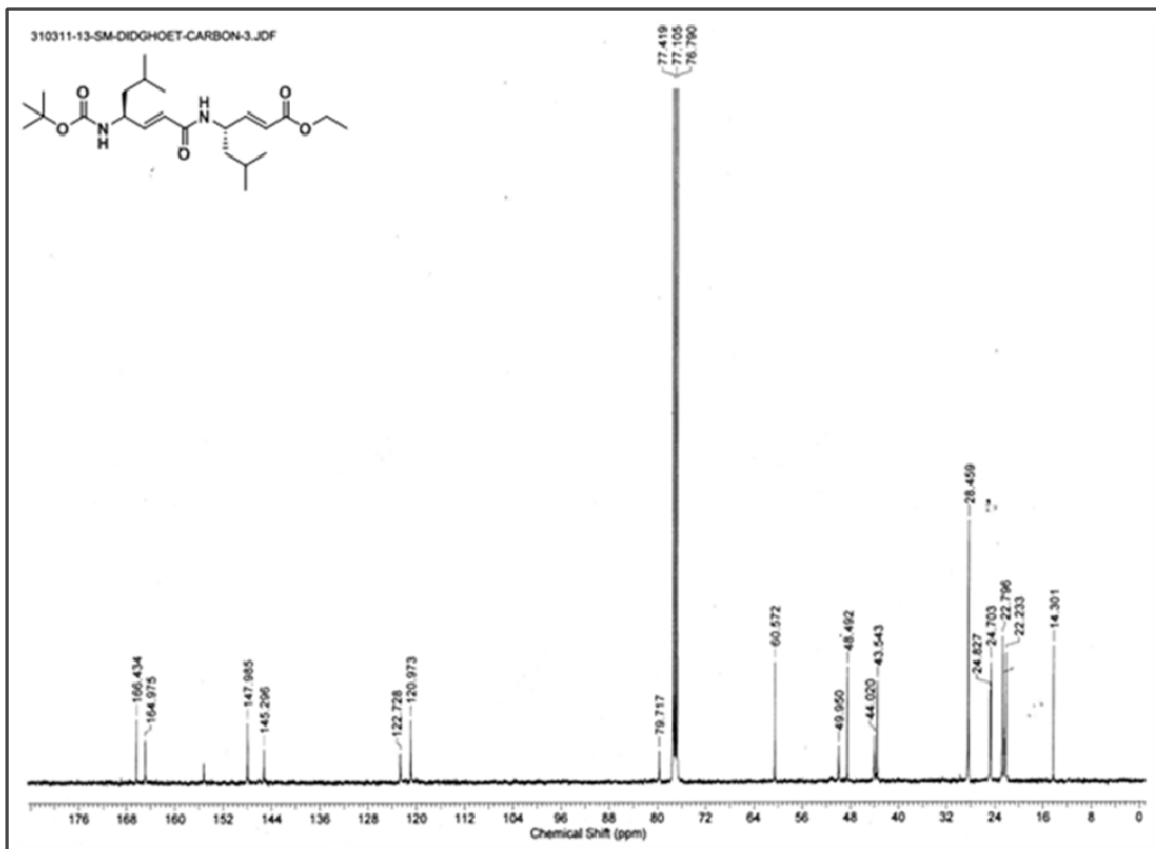
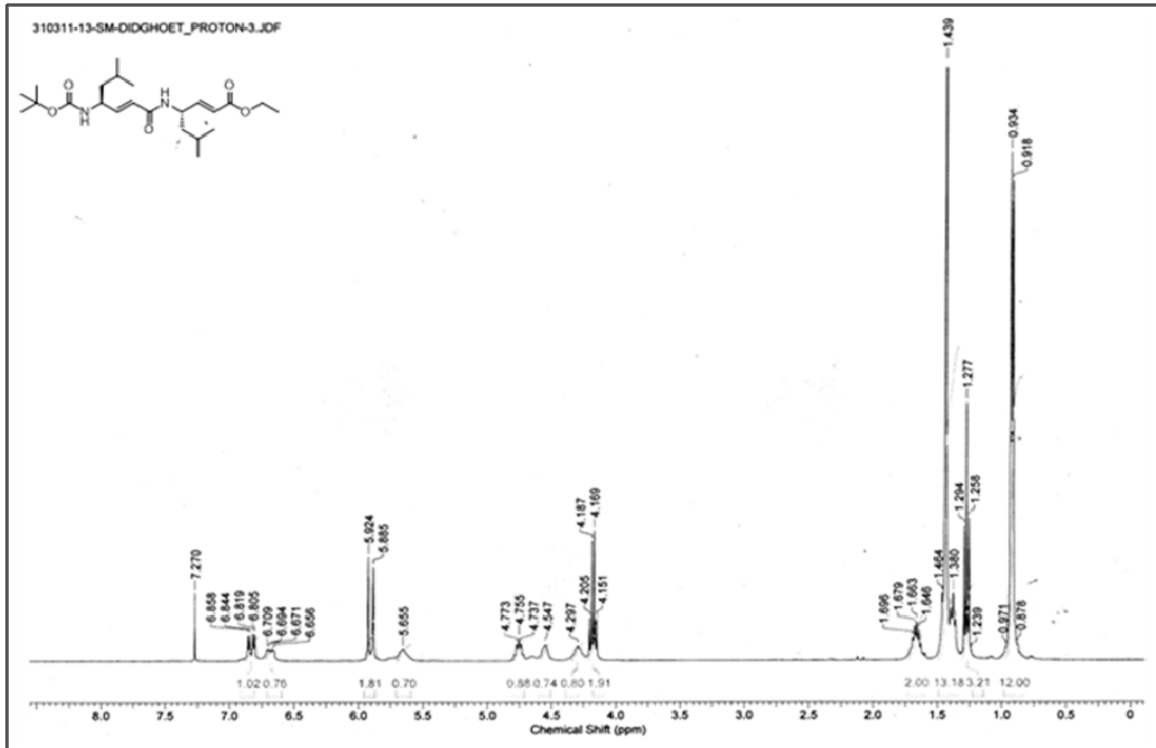
1.5 Appendix I: Representative Characterization Data of Synthesized Compounds

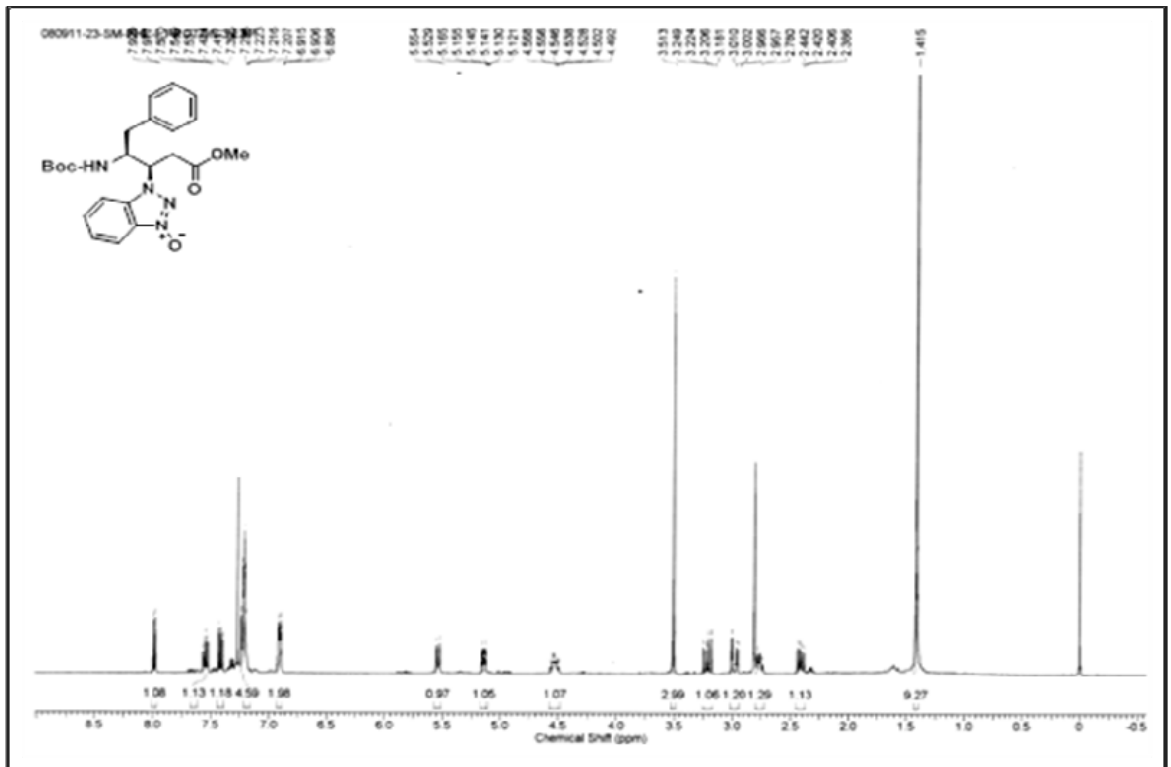
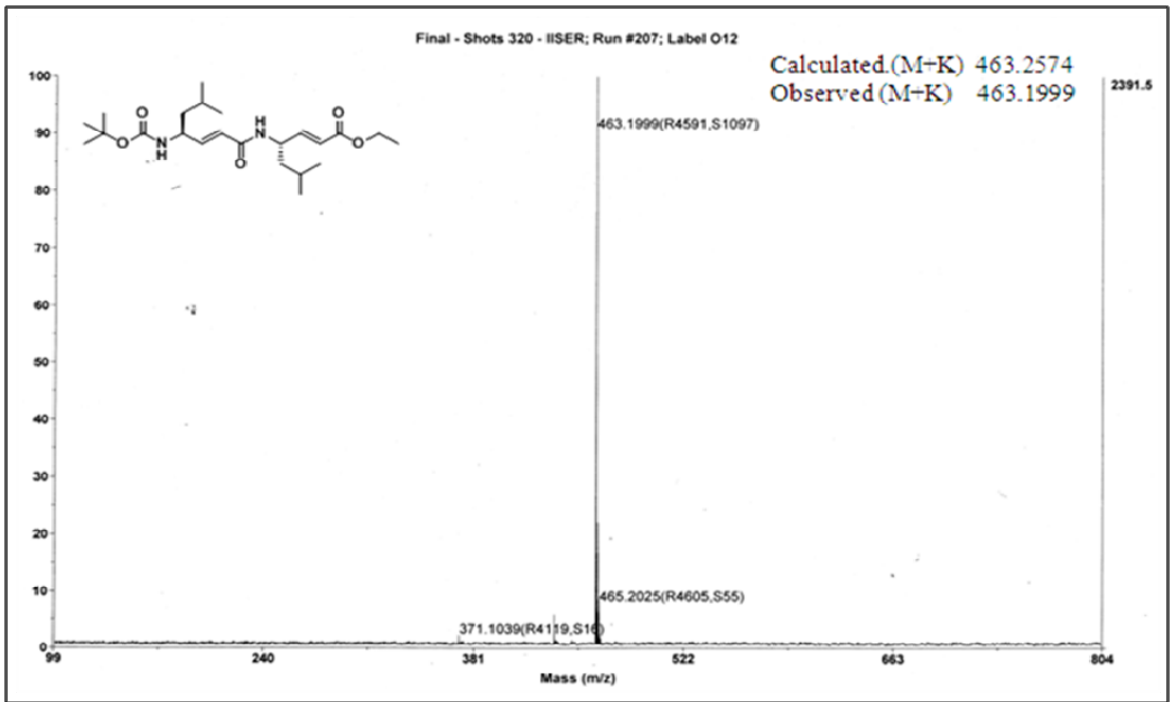
Designation	Description	Page
Boc-dgVal-OEt (2C)	¹ H NMR (400 MHz)	96
Boc-dgVal-OEt (2C)	¹³ C NMR (400 MHz)	96
Boc-dgVal-OEt (2C)	Mass Spectrum	97
Boc-dgLeu-OEt (3C)	¹ H NMR (400 MHz)	97
Boc-dgLeu-OEt (3C)	¹³ C NMR (400 MHz)	98
Boc-dgLeu-OEt (3C)	Mass Spectrum	98
Boc-dgLeu-dgLeu-OEt (D4)	¹ H NMR (400 MHz)	99
Boc-dgLeu-dgLeu-OEt (D4)	¹³ C NMR (400 MHz)	99
Boc-dgLeu-dgLeu-OEt (D4)	Mass Spectrum	100
Boc- γ Phe(β -OBt)-OMe ^{syn} (20a)	¹ H NMR (400 MHz)	100
Boc- γ Phe(β -OBt)-OMe ^{syn} (20a)	¹³ C NMR (400 MHz)	101
Boc- γ Phe(β -OBt)-OMe ^{anti} (21a)	¹ H NMR (400 MHz)	101
Boc- γ Phe(β -OBt)-OMe ^{anti} (21a)	¹³ C NMR (400 MHz)	102
Boc- γ Leu(β -OBt)-Ala-OMe (22Pi)	¹ H NMR (400 MHz)	102
Boc- γ Val β -(S-ONB)O ^t Bu ^{syn} (3bI)	¹ H NMR (400 MHz)	103
Boc- γ Val β -(S-ONB)O ^t Bu ^{syn} (3bI)	¹³ C NMR (400 MHz)	103
Boc- γ Val β -(S-ONB)O ^t Bu ^{anti} (3bII)	¹ H NMR (400 MHz)	104
Boc- γ Val β -(S-ONB)O ^t Bu ^{anti} (3bII)	¹³ C NMR (400 MHz)	104

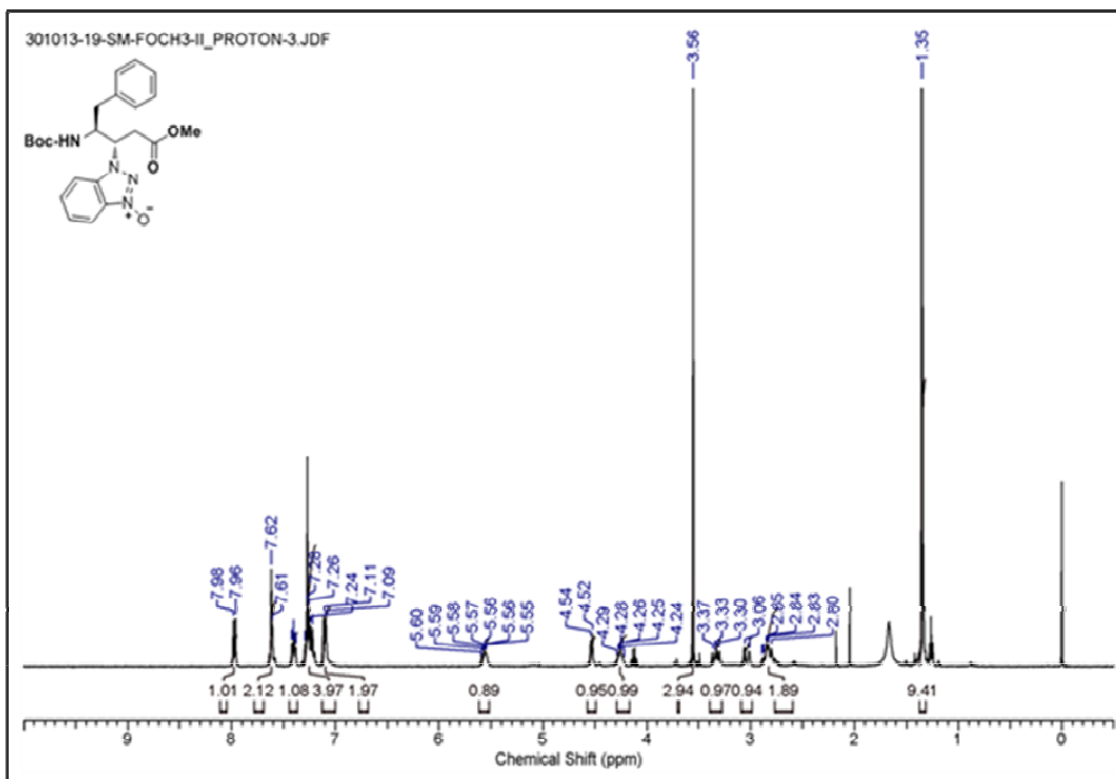
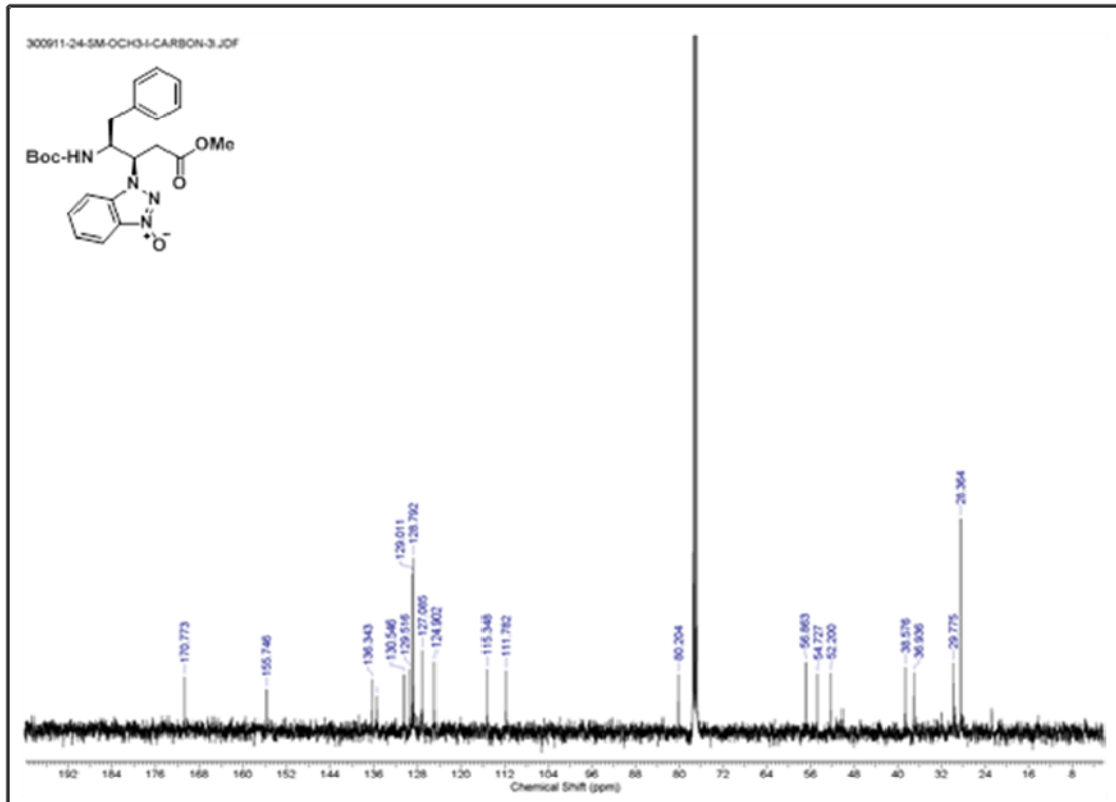


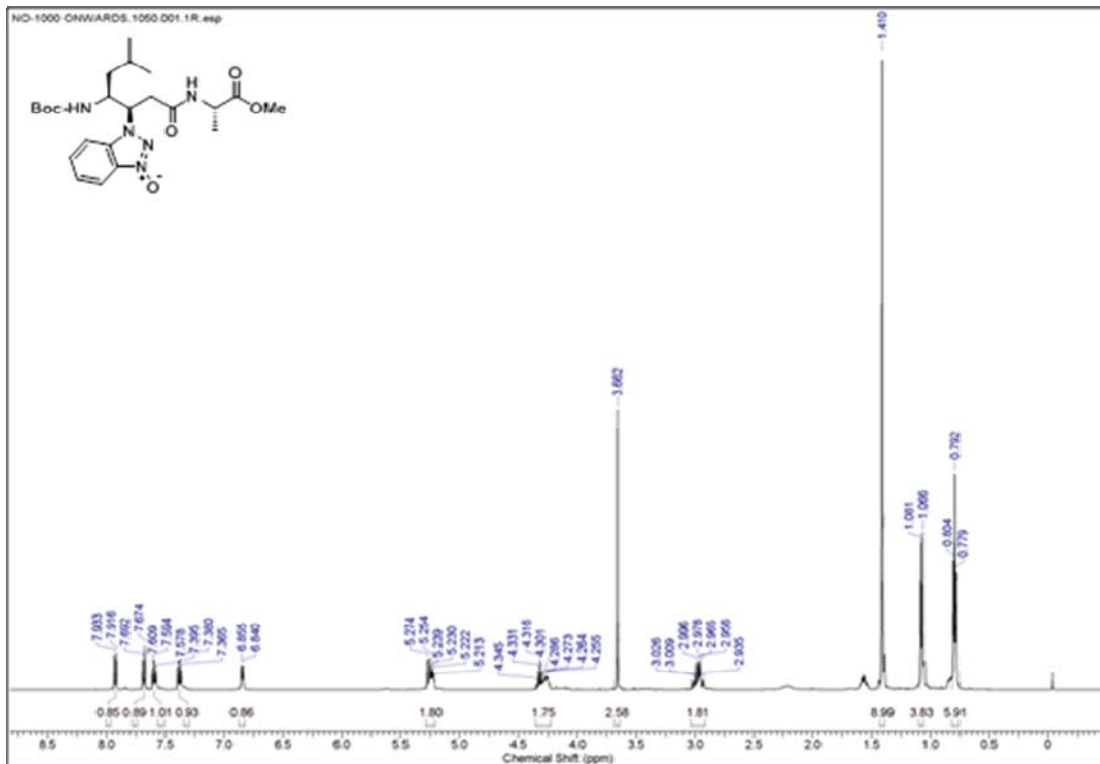
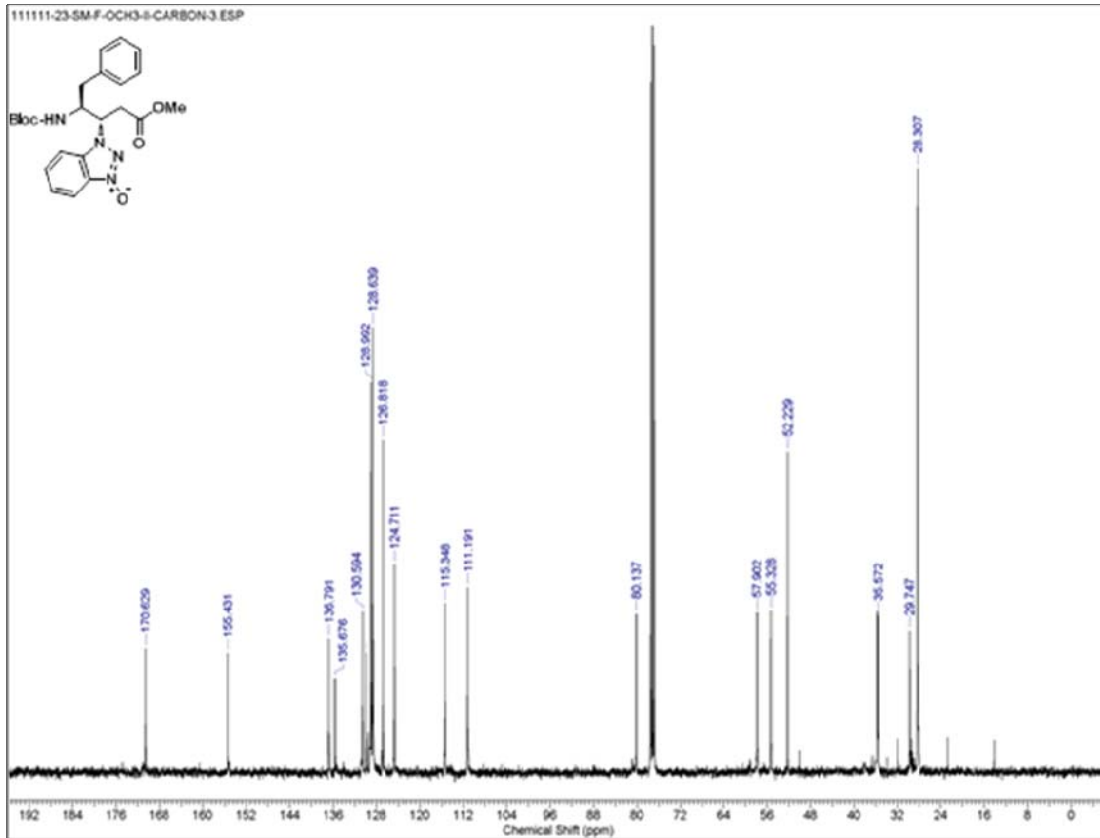


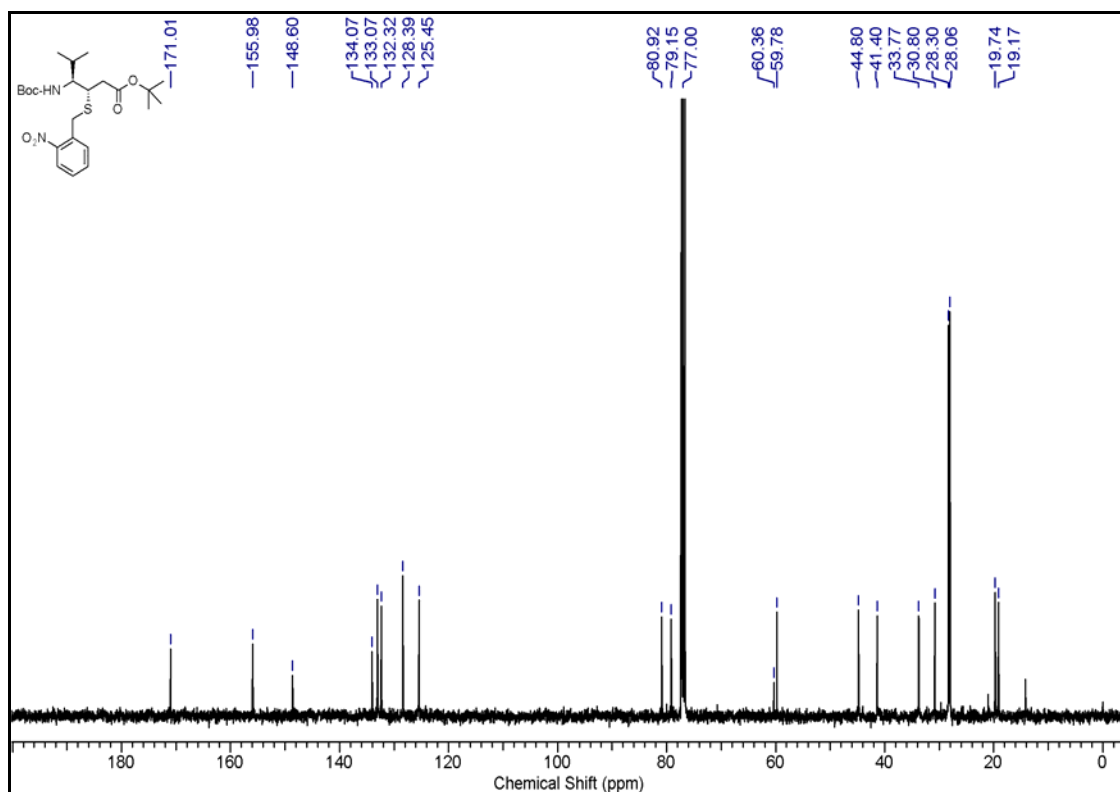
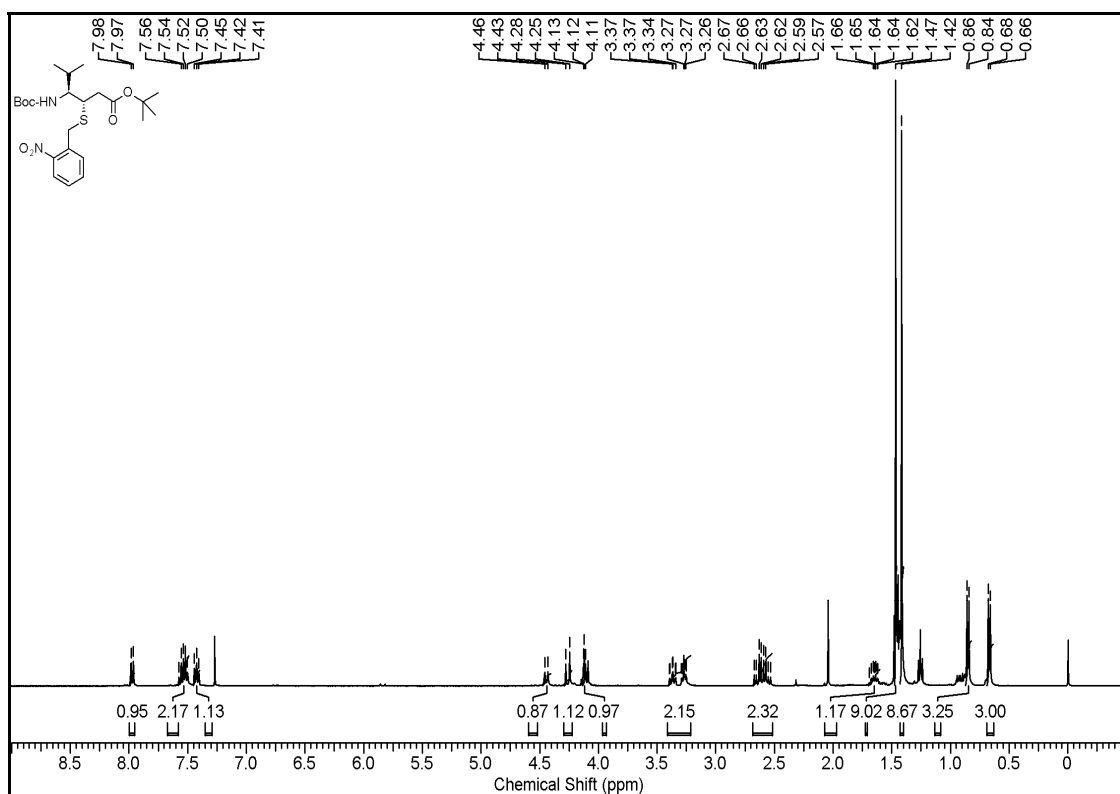


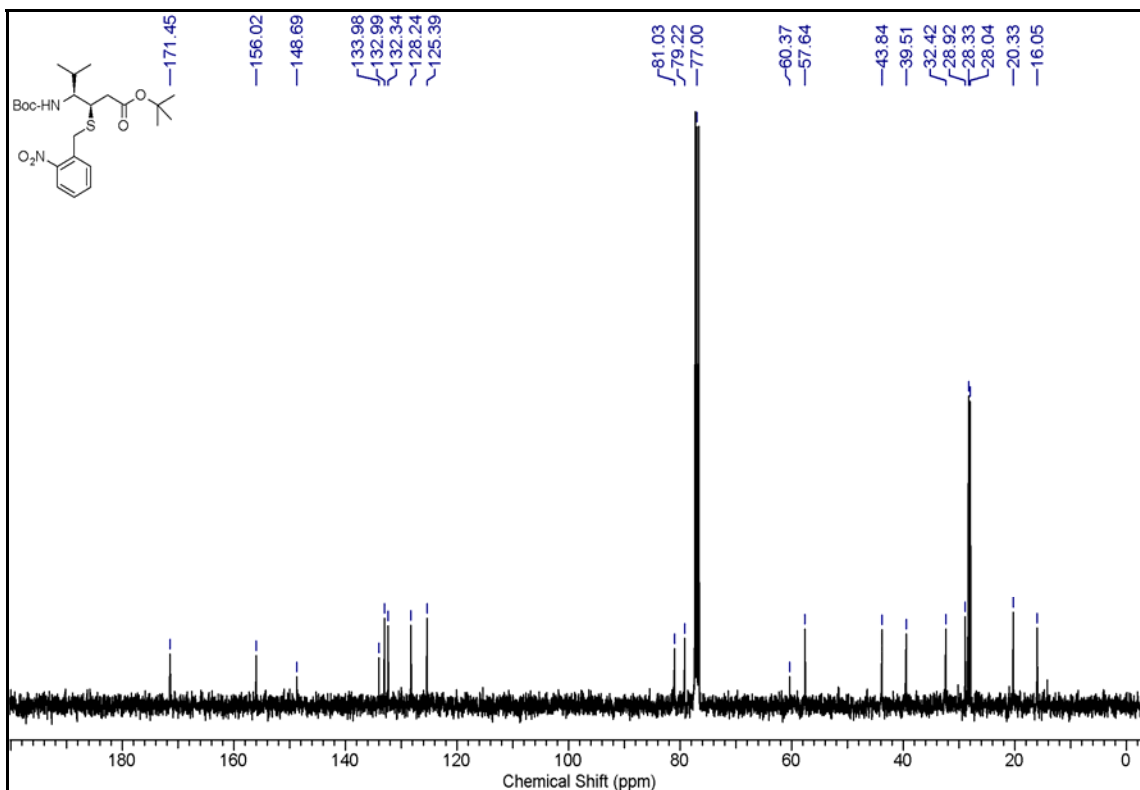
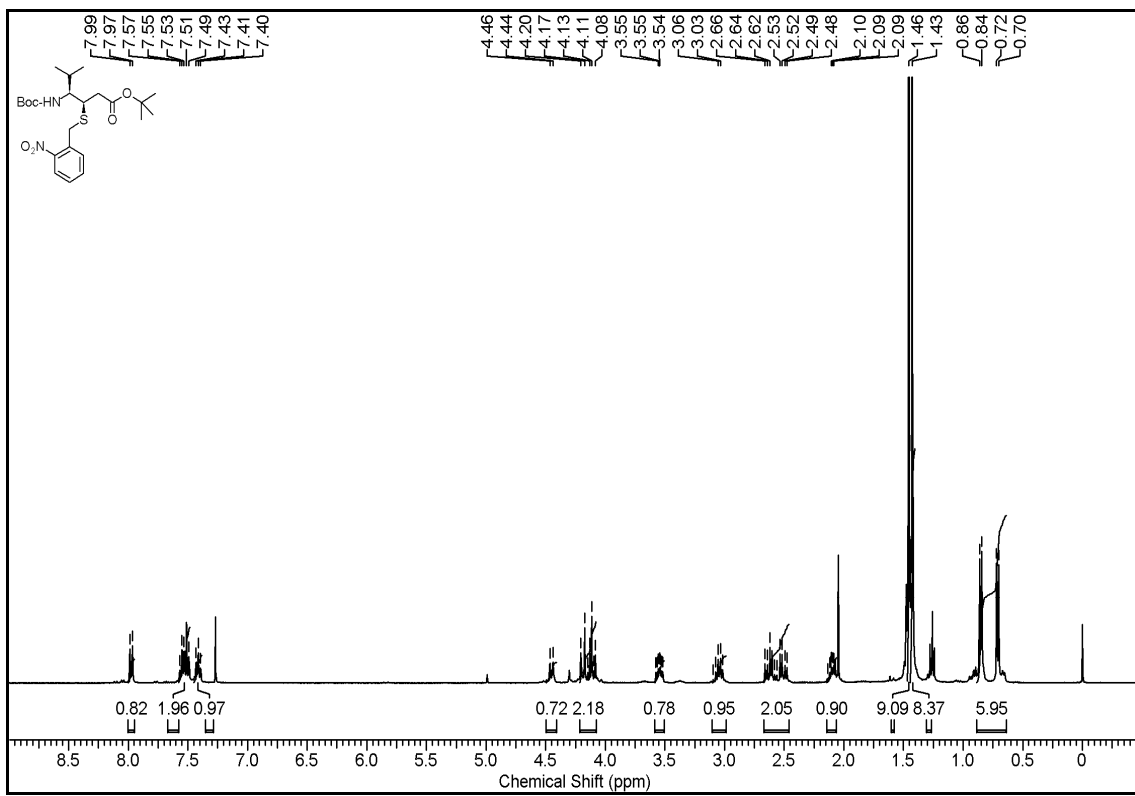












Chapter 2

**Utilization of thioacids in copper(II)
mediated mild and fast peptide
synthesis and *N*-acylation of amines**

Section 2A: Copper (II) Mediated Facile and Fast Peptide Synthesis in Methanol

2A.1 Introduction

Proteins constitute the largest content of cell. Proteins are made up of the coupling of basic units called amino acids. During the peptide synthesis carboxylic acid of one amino acid residue reacts with α -amine functional group of another amino acid residue, resulting in the formation of amide bond. The structure and function of a protein is mainly depends on the primary sequence of that protein. There are twenty naturally occurring α -amino acids, which are covalently connected through amide bonds in various sequence order to form different types of proteins. Nature has its own pathway to construct these polypeptides and proteins. Ribosomal protein synthesis is the leading pathway in higher organisms to construct the polypeptides.¹ In the ribosomal pathway, DNA undergoes transcription to mRNA, which carries the information of amino acids to be incorporated in growing polypeptide chain. The mRNA undergoes translation on ribosome to construct the polypeptide chain (Figure 1). Further, the non ribosomal pathway of peptide synthesis is mainly observed in microorganisms like fungi and bacteria and generally follow the thioester strategy mediated by the complex machinery of proteins.² In comparison to ribosomal peptide synthesis, this non ribosomal approach provides access to diverse class of branched, cyclic and non-proteinogenic amino acids including D amino acids containing peptides. Large number of non ribosomal peptide natural products has also displayed wide variety of biological activities. Through these ribosomal and non ribosomal strategies nature produces polypeptides and proteins which play a crucial role in all activities of life.

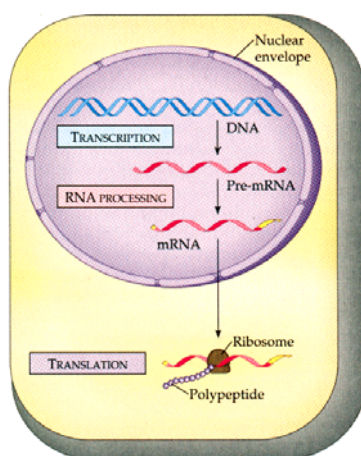


Figure 1: Ribosomal protein synthesis pathway in cell.

2A.1.1 Overview of peptide synthesis

The wide abundance, their structural and biological activities of proteins has attracted chemists over the several decades to chemically synthesize peptides and proteins. A century ago Curtius made first attempt to chemically synthesize a dipeptide benzoyl-Gly-Gly, however, the actual publication reporting the synthesis of Gly-Gly dipeptide came in 1901 by E. Fisher who used diketopiperazine of glycine for synthesis of dipeptide and this was assumed to be the beginning of peptide chemistry.⁴ Later, Curtius developed the azide based peptide synthesis of benzoyl protected glycine peptide with desired length.⁵ On the other hand, Fisher developed the acyl chloride mediated peptide synthesis using amino acid, PCl_5 and acetyl chloride as a solvent.⁶ Due to lack of selective protecting groups for amines and acids, peptide field not progressed much in this period. In 1931, introduction of Cbz (Carboxybenzyl) as a amine protecting group by M. Bergmann and L. Zervas and acid labile *t*-Boc [(*tert*-butyloxycarbonyl)] by L.A Carpino and coworkers in 1957, greatly strengthen the peptide synthesis strategy with the choice of orthogonal protecting groups.^{7a,b} Utilizing this strategy, various bioactive peptides such as glutathione, carnosine; hormones like octapeptide oxytocin, β -corticotropin Adrenocorticotrophic Hormone (ACTH), porcine hormone were synthesized. Further, the introduction of base labile protecting group Fmoc- further strengthens peptides synthesis protocols. In addition, the development of peptide chemistry was also associated with the introduction of new coupling reagents. In 1955, J. C. Sheehan and colleagues introduced the new carbodiimide based coupling reagent DCC (dicyclohexyl carbodiimide).⁸ These carbodiimide based reagent gives very fast coupling product but associated with problem of racemization which in turn was solved by addition of additives (eg. HOBt, HOAt etc) which make the less reactive OBt ester minimizing the risk of racemization. Over the period of time, the combination of carbodiimides and HOBt (HOAt) complex reagents called as “stand-alone coupling reagents” have also been developed.^{9a, b, c} Some of the peptide coupling reagents and coupling additives are shown in Figure 2 and Figure 3, respectively.

Peptide Coupling Reagents

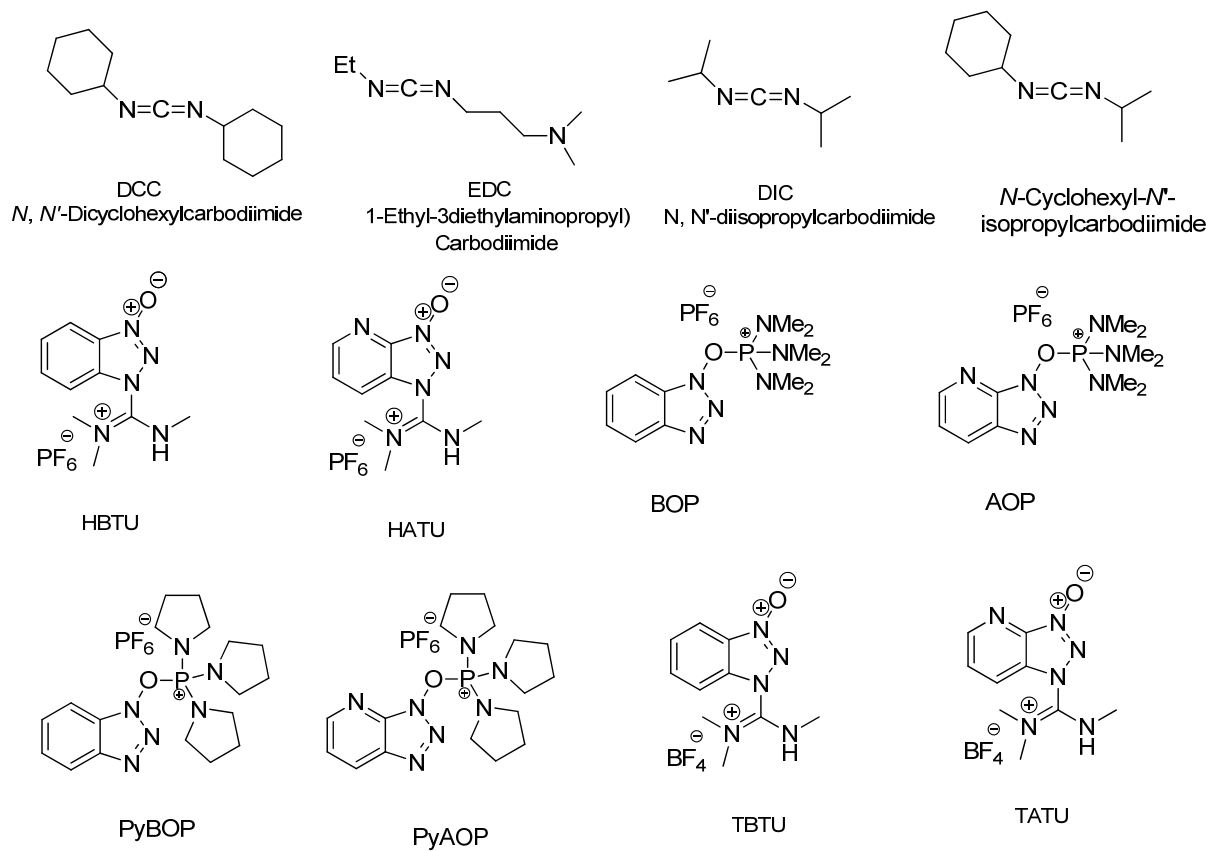


Figure 2: Standard coupling reagents practiced in peptide synthesis

Peptide Coupling Additives

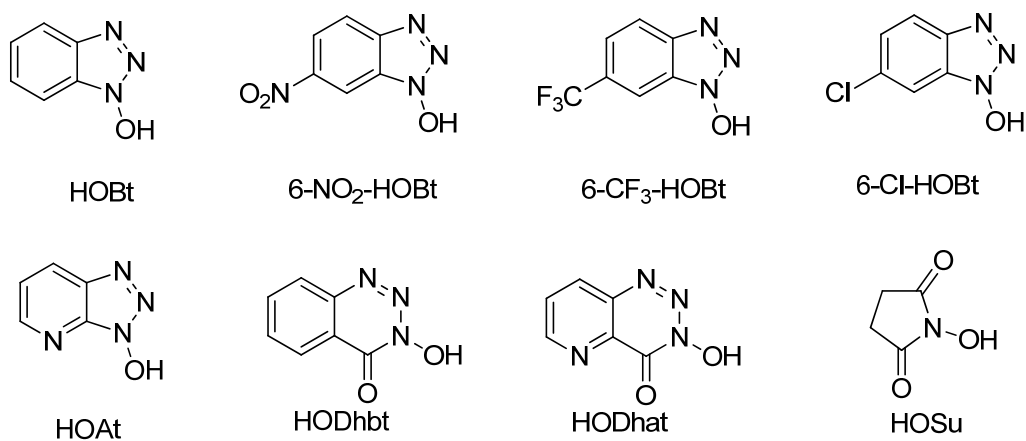


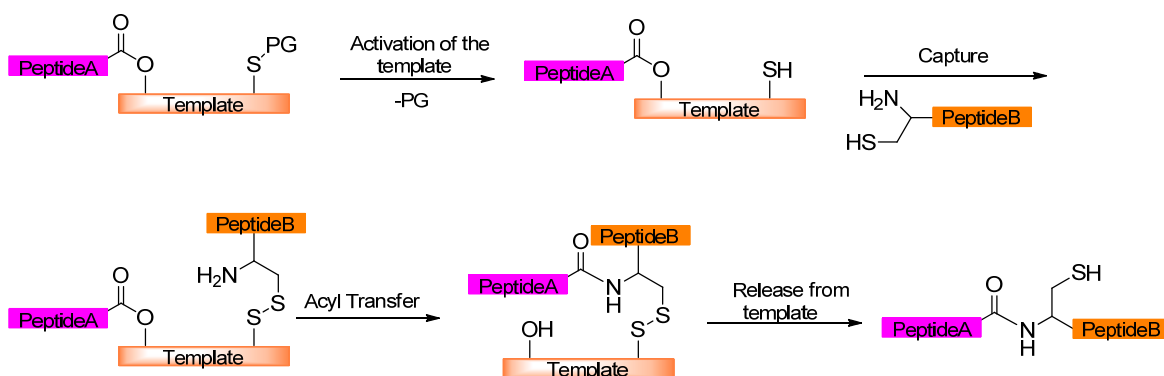
Figure 3: Coupling additives used in peptide synthesis

2A.1.2 Solid phase peptide synthesis

The introduction of solid support for the peptide synthesis has greatly influenced peptide field. The pioneering work by Merrifield in the field of peptide chemistry by introducing the concept of solid phase peptide synthesis gave a new tool to access longer peptides in short period of time.¹⁰ As compared to the solution phase peptide synthesis where it requires the isolation and purification of peptides after each step, the solid phase peptide synthesis where the growing peptide is attached to the polymer bound solid support and after each coupling the excess reagents were removed by simply washing the resin. This method opens new era in the field of peptides and proteins synthesis and proved that longer peptide sequences and peptides having complicated sequences can be synthesized in a short period of time.

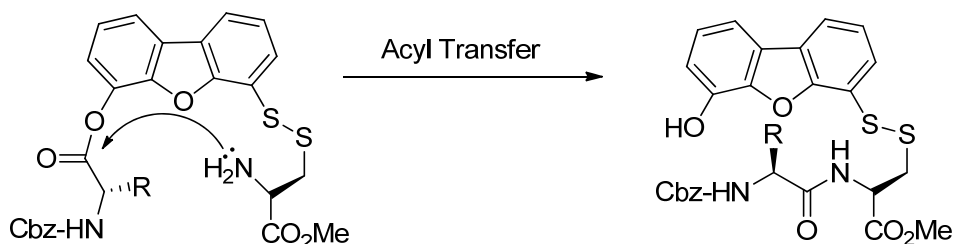
2A.1.3 New approach for peptide construction: Chemical Ligation

Although the invention of solid phase peptide synthesis protocol for peptide synthesis gave a new tool to construct the polypeptides of desired length as well as small proteins, however, there are only few examples which describe the synthesis of polypeptide of length more than 80 residues. The major issues in the solid phase synthesis of higher ordered peptides are the incomplete coupling and deprotection, deletion of amino acid residues from the sequences, aggregation of polypeptides, accumulation of the side products and overall lower yields. To overcome these shortcomings and to achieve desired polypeptides and proteins in good yields scientists started looking for other approaches. In this regard, Kemp and Kerkman in 1981 developed a new approach to get a desired length polypeptide by treating the two unprotected segments of peptide in aqueous solution and this approach called chemical ligation.^{11a, b} This approach is based on the Wieland's finding where he reported an amide bond formation in aqueous solution by intramolecular acyl shift.¹² The protocol described by Kemp and Kerkman also known as prior thiol capture strategy and is shown in Scheme 1.



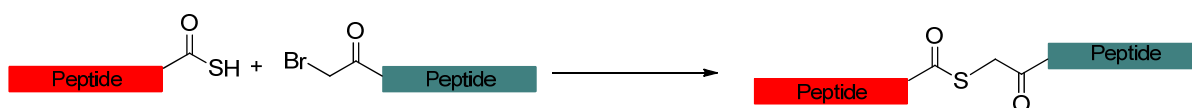
Scheme 1: Prior thiol capture strategy for chemical ligation

Kemp and co-workers achieved the chemical ligation of two polypeptide chains with the help of organic template benzofuran derivative. The schematic representation of the reaction is shown in Scheme 2. The close proximity of the reacting termini helps in the ligation through 12 membered transition state intermediate.



Scheme 2: Benzofuran as a template for prior thiol capture strategy.

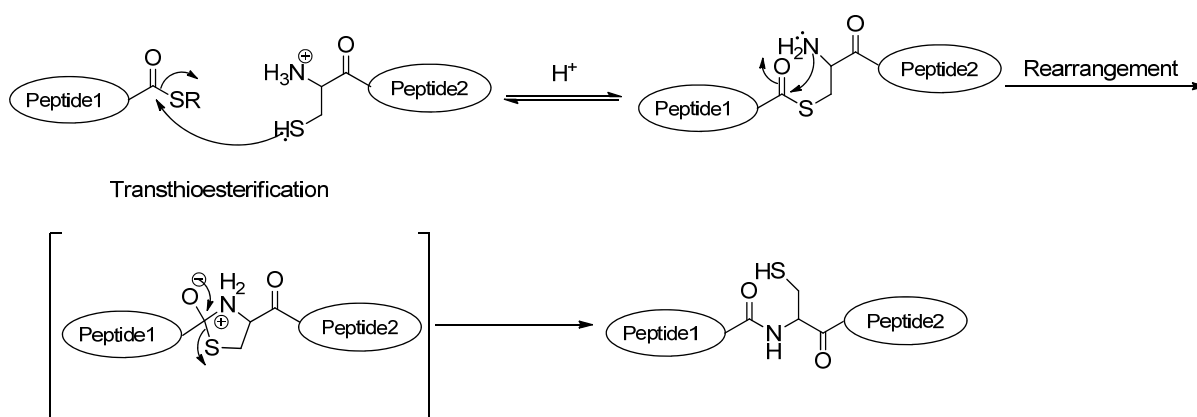
This chemical ligation strategy was further improved by Schnolzer and Kent in 1992 in which the two unprotected fragment of polypeptide in aqueous solution were coupled chemoselectively.¹⁴ The basic principle used in this approach was nucleophilic substitution reaction between the free thiol at C-terminal of one fragment (peptide thioacid) and alkyl bromide of at *N*-terminal of another fragment which results in the thioester linked polypeptide shown in Scheme 3. This new approach enabled to overcome the shortcomings of the conventional solid phase peptide synthesis like incomplete couplings, side product accumulation, difficulties in purification of fully protected peptide, however, the disadvantage of this method is that synthesized polypeptide consists of a thioester linkage at the site of ligation which is quite unnatural.



Scheme 3: Thioester strategy for the chemical ligation

2A.1.4 Native chemical ligation

In order to overcome this limitation, Kent and colleagues put forward the new ligation strategy called native chemical ligation.¹⁵ Similar to the earlier method of ligation this method also provides the access to the fully unprotected peptide and overcome the all problems associated with conventional solid phase peptide synthesis. The advantage of this new native chemical ligation method is that the introduction of native amide bond at the site of ligation. This strategy makes use of thioester at C-terminal of one fragment and cysteine residue at *N*-terminal of another peptide fragment. This thioester was replaced by the attack of cysteine thiol which was then attacked by amine group of cysteine residue to form native amide bond. The detailed mechanism of native chemical ligation is shown in Scheme 4.



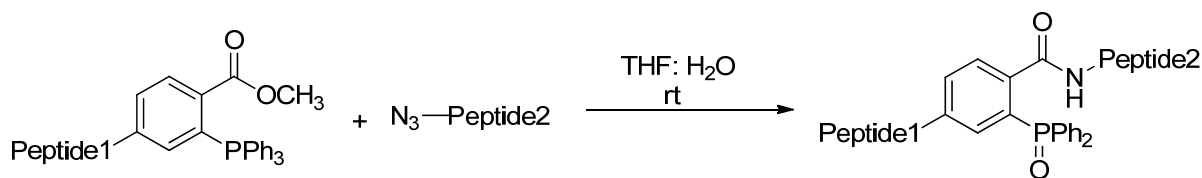
Scheme 4: Native chemical ligation to construct native amide bond at site of ligation

Despite of its success the native chemical ligation method is still fall short due to its requirement of the *N*-terminal cysteine for the ligation and many proteins do not contain the cysteine at the right position. To overcome this drawback, many modifications in the existing NCL method have been made. In that regard, Tam *et al.*,¹⁶ Hilver *et al.*,^{17a, b} van der Donk *et al.*^{18a, b} shown the cysteine can be replaced by various other amino acid like methionine, histidine, selenocysteine, homoselenocysteine at the *N*-terminal of the

fragment peptide. Similarly, Canne *et al.* reported the native chemical ligation using oxyethanethiol-substituted *N*-terminus and after the ligation *N*-(oxyalkyl) substituent was removed using zinc dust.¹⁹

2A.1.5 Other approaches for chemical ligation

In addition to the native chemical ligation, Raines^{20a, b, c, d} and Bertozzi^{21a, b} have developed different strategy by utilizing Staudinger reaction in which requirement of *N*-terminal cysteine was omitted. In this technique, they used the C-terminal phosphinothioester group and azido group at *N*-terminal. These groups then undergo staudinger reaction and amine anion generated replaces the thioester to give native amide bond and amidophosphonium salt was then hydrolyzed to phosphine oxide (Scheme 5). The drawback in this ligation is the high reactivity of azide.



Scheme 5: Staudinger ligation for peptide synthesis

In addition to the native chemical ligation, many groups have made use of the thioacids and thioesters for the synthesis of various other peptidomimetics and glycopeptides. As earlier thioester ligation method used to construct the longer peptide sequence and at ligation site, introduction of *N*-terminal cysteine and other selected amino acids like methionine, histidine, homocystein, serine, threonine can only be used. This put some restriction for the synthesis of comparatively small and desired peptides whose function could alter due to slight change in the sequence. In order to overcome these shortcomings various research groups started to exploit thioacids in the peptide construction. Because of the distinct nucleophilic property of thioacids, their unique reactivity and selectivity as compared to carboxylic acids, use of thioacids in amide bond formation is gaining momentum.

2A.1.6 Thioacid in origin of life

Reports suggest that thioacids might have played crucial role in the synthesis of polypeptides in prebiotic era. Huber C. *et al.* demonstrated the role of thioacid in construction of life on earth in prebiotic era.²² Through a model experiment with methane thiol, carbon monoxide in presence of nickel and iron sulfide at high temperature and pressure. The activated thioesters formed in the reaction mixtures were trapped with free amines in the form of amides. These results supports the De Duve findings in which he stated, these thioesters formed from carboxylic acid and mercapto compounds serve as an energy source for origin of life.²³

In addition to that, Orgel and colleagues demonstrated the role of thioacid oxidative dimers in the generation of amide bond which is necessary condition for the construction of polypeptides in prebiotic era.²⁴ To demonstrate the amide bond formation by this thioacid oxidative dimers, the reaction of thioacetic acid and other amino thioacids with different amino acids in presence of oxidant potassium ferrocyanide was carried out. In addition, the authors correlated their findings with the prebiotic amide bond formation as it happened in absence of any dehydrating agents.

2A.1.7 Versatile reactivity of thioacid with different functional groups

The versatile reactivity of thioacid and thioester has been extensively explored by various chemists as precursor in the amide bond synthesis. Crich *et al.* in 2007 reported the reaction of thioacid with 2,4 dinitrobenzenesulfonamides in presence of piperidine and cesium carbonate in DMF, resulting in the amide bond formation.²⁵ Danishefsky and co-workers demonstrated the reactivity of thioacids with isonitriles to form amide bond through FCMA (formimidate carboxylate mixed anhydride) active intermediate.²⁶ Reaction of thioacid with isocyanates and isothiocyanates which results in the amide bond formation was introduced by Crich and co-workers in 2009.²⁷ In their strategy Fmoc thioester was treated with piperidine resulting in nucleophilic activation of thioacid which reacts with isocyanates and isothiocyanates resulting in the amide bond formation. Further, Danishefsky and co-workers introduced the amide bond formation by reaction of thioacid with coupling additive HOBt in presence of molecular sieves in DMSO.²⁸ They speculate that HOBt helps in the activation acyl groups in the thioacid mediated coupling reactions. The versatile reactivity of thioacid was then explored by Xian and colleagues by derivatizing thioacids with nitroso compounds to form S-nitrosothioacids.²⁹ This active S-

nitrosoderivative then reacts with amine to form the amide in good yields. Recently Liebeskind and co-workers shown the activation of thioacid with bistrimethylsilylacetamide (BSA) as a silatropic switch to form *O*-silylthionoester which in turn reacts with amine and yields the amide bond.³⁰ Reactions of thioacid with different functional groups are shown Figure 4. In addition Garner and colleagues reported the copper acetate mediated protocol for synthesis of side chain unprotected peptides using thioacids.⁴⁷

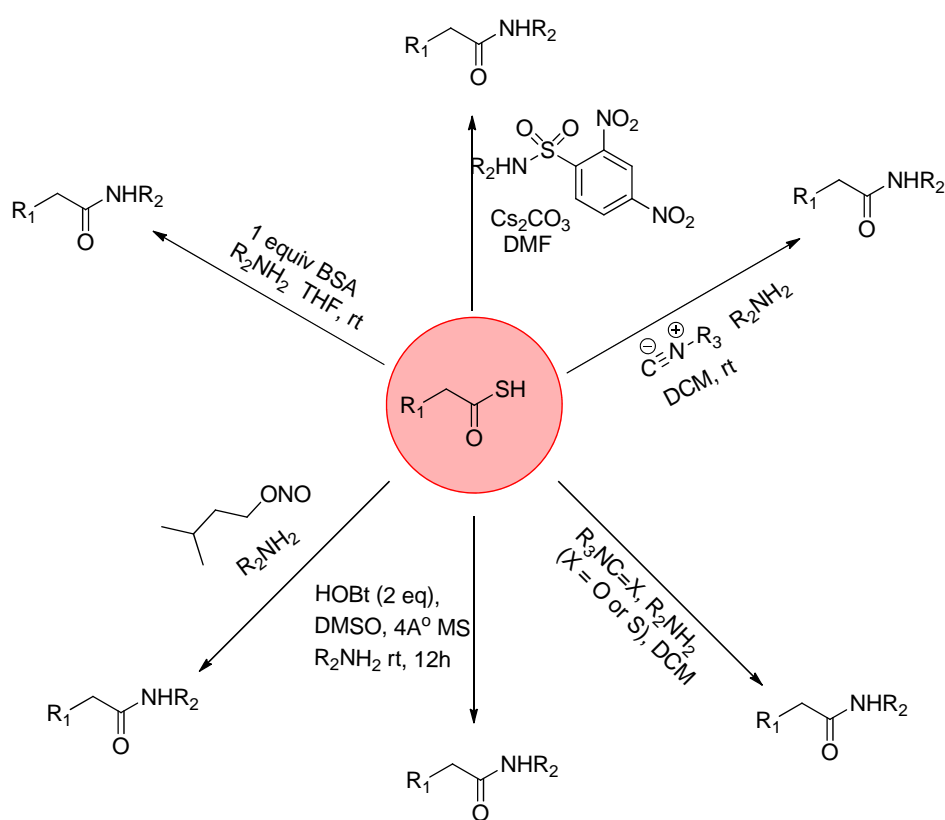
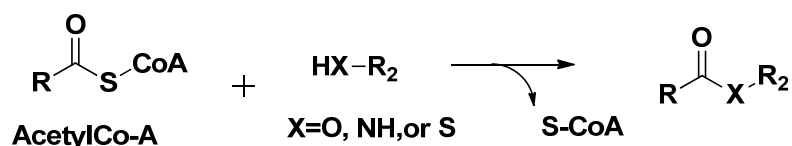


Figure 4: The reactivity of thioacids with various functional groups

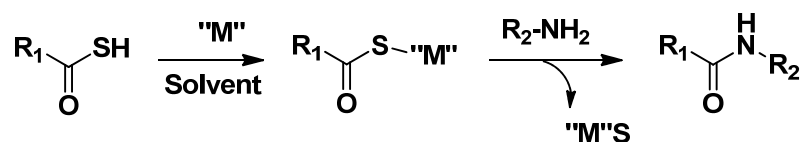
2A.2 Aim and rationale of the present work

Our group has been involved in the synthesis, conformational analysis of biologically relevant foldamers comprising of non ribosomal amino acids and development of mild and facile methods for the synthesis of these non-natural amino acids. During the synthesis of the thiostatines, we encountered migration of acetyl group from thioester to the free amino group of the same amino acid similar to the native chemical ligation.

Similarly, nature utilizes acylCo-A for various *N*-acylation reactions. Inspired by the thioester strategies in the acylation reactions of coenzyme, acetyl-CoA (Scheme 6) and in non-ribosomal peptide synthesis,² as well as our experience in the Chapter 1, we anticipate that if the coenzyme in the thioester or S-alkyl group in the acetyl thioesters in the Chapter 1 is replaced with sulfur loving metal (M) which would readily react with amines to form highly stable metal sulfides (Scheme 7). We hypothesized that peptide can be synthesized by simple reacting thioacids, metals and free amines. In this chapter we investigated the reactivity of metals with thioacids and subsequent peptide/amide synthesis with free amines as well as solvents required for the metal mediated peptide/amide bond synthesis. We realized that, using this method peptides can be synthesized without using standard coupling agents and coupling additives. After the extensive investigation for finding the suitable metals and solvents, the copper (II) was found to be a better metal and methanol was found to be a better solvent to mediate the peptide coupling reactions. Here, we are reporting copper (II) mediated facile and fast peptide synthesis using *N*-protected thioacids and *N*-acylation of amines using commercially available thioacetic acid. The results of these investigations are given under two subsections **2A** (fast peptide synthesis) and **2B** (*N*-acylation of amines).



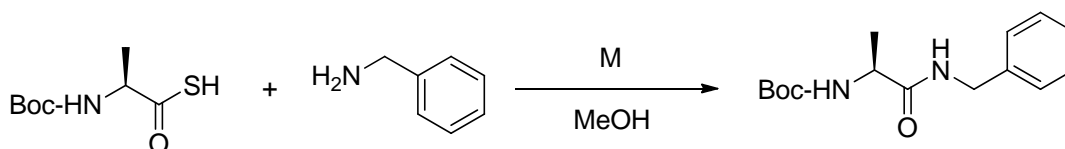
Scheme 6: Acetyl transfer reactions by acetyl coenzyme A through thioesters



Scheme 7: Schematic representation of the metal mediated amide bond formation

2A.3 Results and discussion

The idea of metal mediated amide bond formation solely depends on the nature of metal which could form reactive complex with thioacid, which further reacts with amine to form amide bond. In this regard, we began our search for the suitable metal salts and complexes to mediate the amide bond synthesis using thioacid Boc-Ala-SH and benzylamine in DMF. Various metal salts and complexes including Ag(I), Au(III), Fe(II), Fe(III), Cu(I), Cu(II), Mo(IV) and Zn(II) have been screened (Scheme 8) and we found better yields in Cu(I) and Cu(II) compounds compared to the other metal compounds. In comparison, Cu(II) complexes $\text{CuSO}_4 \cdot 5\text{H}_2\text{O}$ and $\text{Cu}(\text{OAc})_2 \cdot \text{H}_2\text{O}$ gave better yields than Cu(I). These inspiring results of amide bond formation by Cu(II) metal salts led us to continue our work with $\text{CuSO}_4 \cdot 5\text{H}_2\text{O}$ as it is cheap and commonly available in any undergraduate laboratory. The slow reactivity and the longer time duration of $\text{CuSO}_4 \cdot 5\text{H}_2\text{O}$ [also $\text{Cu}(\text{OAc})_2 \cdot \text{H}_2\text{O}$] in the both DMF and DMSO as compared to the standard coupling reagents such as HBTU and HATU, led us to search for a solvent in which both reactant and the metal complex are soluble. So we replaced these polar aprotic solvents with polar protic solvent, methanol. As copper sulfate has better solubility in methanol, we carried out the same coupling reaction in methanol with a suspicion, since methanol has never been used as a good solvent in any acylation reactions. To our surprise the amide bond formation was observed in good yield within 5 min. and no other byproduct was observed other than the insoluble metal sulfide. As metal complex, $\text{CuSO}_4 \cdot 5\text{H}_2\text{O}$ is insoluble in EtOH, EtOAc and THF we did not further pursue the amide bond synthesis in these solvents. The encouraging results of copper sulfate mediated coupling reactions in methanol promoted us to probe the reactivity of other metal salts and complexes towards the amide bond formation in methanol (Scheme 8). The outcome of the study, shows that $\text{CuSO}_4 \cdot 5\text{H}_2\text{O}$ gave better yield (71%) followed by $\text{Cu}(\text{OAc})_2 \cdot \text{H}_2\text{O}$ (57%) and AgOAc gave only 38% in 5 min. Other metal complexes gave low yields with longer time duration (Scheme 8). In their pioneering work, Blake *et al.* reported the Ag(I) mediated fragment coupling reactions of peptide thioacids in 50% aqueous DMF by using AgNO_3 and *N*-hydroxysuccinimide.^{31a, b} The results observed for the Ag(I) mediated coupling reaction in methanol are in accordance with reported results. In order to probe the catalytic concentration of the copper sulfate which mediated this facile and fast amide bond formation, we carried out optimization study of the concentration of copper sulfate from 0 to 100 mol%, results show that reaction with 30 mol% of copper sulfate was comparable

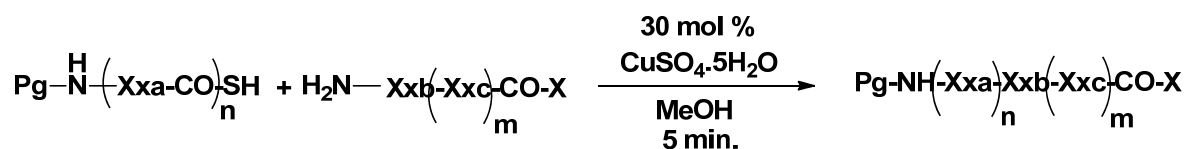


Scheme 8: Amide bond synthesis using thioacids. A comparison of various metals salts and complexes in the acylation reaction is given below. Time is given in minutes.

Entry	M	Time (min)	% Yield
1	Cu(OAc) ₂	5	57
2	CuSO ₄ .5H ₂ O	5	71
3	CuI	30	41
4	ZnCl ₂	30	14
5	AgOAc	5	38
6	FeCl ₂	420	14
7	FeCl ₃	420	14
8	AuCl ₃	30	20

with 100 mol%, however even 10 mol% also mediates the amide bond synthesis with longer time duration (3hrs). In a control reaction, to study whether this amide bond can be formed without metal complex, the reaction of Boc-Ala-SH with benzylamine gives 5% of the product after 24 hrs. We speculate that the oxidative dimerization of thioacids in solution may result in the formation of product.^{32 a,b} We carried out all this copper sulfate mediated coupling reaction with 30 mol% of CuSO₄.5H₂O (Scheme 9).

The pH measurement studies suggest that almost neutral pH (7.76) of the reaction mixture in the amide bond coupling. As this reaction proceeds within 5 min. and during the course of reaction black material was generated as a byproduct. This black material is insoluble in any solvent except concentrated nitric acid. In order to analyze this black material we carried out its elemental analysis which shows the 31.5% of sulfur, which is nearly equivalent to CuS. However, the MALDI-TOF/TOF mass analysis suggests the complex mixture of copper and sulfur. It is also evident from the literature that the copper sulfide may exist in complex of both [Cu(I)- Cu(II)]_nS_x.^{33a, b}



Xxa, Xxb, Xxc: Amino acid

Pg: Boc, Fmoc, Cbz

For Dipeptides: n = 1, m = 0

X: OMe, OEt, Obzl

For Tripeptides: n = 1, m = 1

For Tetrapeptide: n = 2, m = 1

Scheme 9: Synthesis of peptides using 30 mol % of CuSO₄·5H₂O in MeOH

Table 1: Peptides from thioacids mediated by 30 mol% CuSO₄·5H₂O

Entry	Thioacid	Amine	Product	Time (min)	Yield (%)
1	Boc-Ala-SH	NH ₂ -CH ₂ -C ₆ H ₅	Boc-Ala-NHBn	5	71
2	Boc-Leu-SH	NH ₂ -CH ₂ -C ₆ H ₅	Boc-Leu-NHBn	5	69
3	Boc-Ala-SH	NH ₂ -Leu-OMe	Boc-Ala-Leu-OMe	5	68
4	Boc- ^D Ala-SH	NH ₂ -Leu-OMe	Boc- ^D Ala-Leu-OMe	5	62
5	Boc-Ala-SH	NH ₂ -Trp-OMe	Boc-Ala-Trp-OMe	5	67
6	Boc-Val-SH	NH ₂ -Ala-OMe	Boc-Val-Ala-OMe	5	76
7	Boc-Ser(O ^t Bu)SH	NH ₂ -Leu-OMe	Boc-Ser(O ^t Bu)Leu-OMe	5	72
8	Boc-Phe-SH	NH ₂ -Ala-Obzl	Boc-Phe-Ala-OBzl	5	64
9	Boc-Trp-SH	NH ₂ -Val-OMe	Boc-Trp-Val-OMe	5	63
10	Boc-Ser(O ^t Bu)SH	NH ₂ -Trp-OMe	Boc-Ser(O ^t Bu)-Trp-OMe	5	65
11	Fmoc-Aib-SH	NH ₂ -Phe-OMe	Fmoc-Aib-Phe-OMe	5	69
12	Fmoc-Val-SH	NH ₂ -Leu-OMe	Fmoc-Val-Leu-OMe	5	77
13	Fmoc-Ile-SH	NH ₂ -Val-OMe	Fmoc-Ile-Val-OMe	5	70
14	Fmoc-Pro-SH	NH ₂ -Val-OMe	Fmoc-Pro-Val-OMe	5	65
15	Cbz-Leu-SH	NH ₂ -Ala-OMe	Cbz-Leu-Ala-OMe	5	64
16	Cbz-Leu-SH	NH ₂ -Trp-OMe	Cbz-Leu-Trp-OMe	5	60
17	Boc-Ser(O ^t Bu)SH	NH ₂ -Ala-Leu-OMe	Boc-Ser(O ^t Bu)-Ala-Leu-OMe	5	64
18	Boc-Ser(O ^t Bu)SH	NH ₂ -Ala-Val-OMe	Boc-Ser(O ^t Bu)-Ala-Val-OMe	5	61
19	Cbz-Leu-SH	NH ₂ -Val-Val-OMe	Cbz-Leu-Val-Val-OMe	5	65
20	Boc-Ala-Val-SH	NH ₂ -Leu-Leu-OMe	Boc-Ala-Val-Leu-Leu-OMe	5	74
21	Boc-Aib-Ala-SH	NH ₂ -dgL-dgL-OEt	Boc-Aib-Ala-dgL-dgL-OEt	5	69
22	Boc-Val-Leu-SH	NH ₂ -Val-Val-OMe	Boc-Val-Leu-Val-Val-OMe	5	72

2A.3.1 Powder XRD study of the byproduct obtained in the reaction mixture.

Considering the byproduct generated during the reaction is complex mixture of copper and sulfur, we subjected the byproduct for powder XRD analysis. The results from the powder X-ray analysis suggest the formation CuS (covallite) as a byproduct in the amide bond coupling reaction. The powder XRD data of the byproduct along with standard CuS (covellite) shown in Figure 5a and 1b, respectively.^{33a, b}

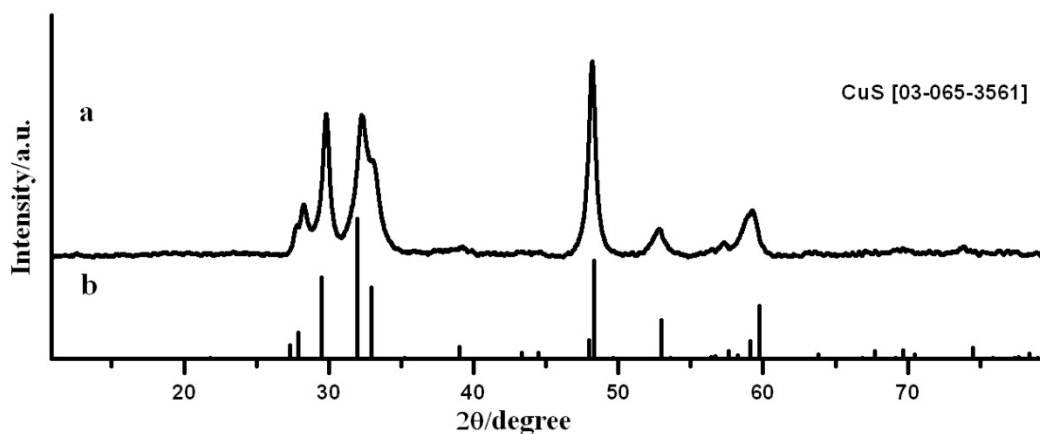


Figure 5: Powder XRD pattern for the byproduct CuS (covellite)

2A.3.2 Racemization studies by using peptides, D3 = Boc-^LAla-Leu-OMe, D4 = Boc-^DAla-Leu-OMe, D3&D4= Boc-(±)Ala-Leu-OMe

As this amide bond formation reaction completes within 5 min. This kind of fast reaction may cause the loss of stereochemical integrity when molecules having chiral centres are involved in the reaction. So in order to understand the racemization during the amide bond synthesis, the two diastereomeric dipeptides **3** and **4** (Table 1) were synthesized using Boc-Ala-SH, and Boc-^DAla-SH along with racemic mixture of Boc-(±)-Ala-SH. The chiral HPLC results of dipeptides **3** and **4** along with racemic mixture suggest the absence of the racemization during the amide bond formation as shown in Figure 6. Additionally, it is also been reported that the presence of Cu(II) complexes reduces the racemization during the peptide couplings.^{34a, b, c}

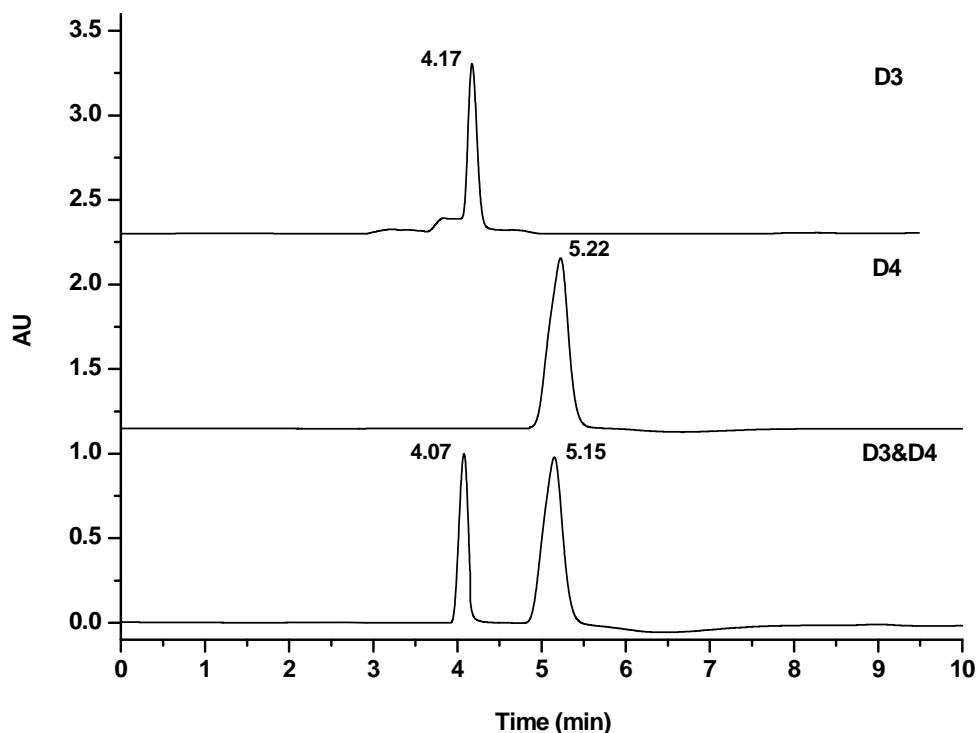


Figure 6: Chiral HPLC of dipeptides **D3**, **D4**: HPLC was performed on Daicel CHIRALPAK-AI column using 20% of isopropanol in n-hexane as a solvent system at isocratic mode with the flow rate of 1mL/min.

Further, the UV absorption measurements of Boc-Ala-SH and H-Leu-OMe with and without copper sulfate in the time course experiments, suggests the complete disappearance of thiol absorption in 1 min., indicating the formation of amide bond within a minute.

Moreover, to realize the compatibility of this protocol to other *N*-terminal protecting groups, a series of *N*-Boc, *N*-Cbz, *N*-Fmoc protected thioacids were synthesized by reported procedure using *N*-hydroxysuccinimide active ester of *N*-protected amino acid and NaSH.³³ Out of all thioacids, we were able to obtain single crystals for Boc-Leu-SH and its X-ray structure is shown in Figure 7 and these various *N*-protected thioacids were subjected for coupling reactions with amines and amino esters in methanol using 30 mol% of copper sulfate. The list of amides and dipeptides (**1-16**) synthesized from this protocol is given in the Table 1. Instructively, no methyl esters or free carboxylic acids of the corresponding thioacids were observed in the acylation reactions.

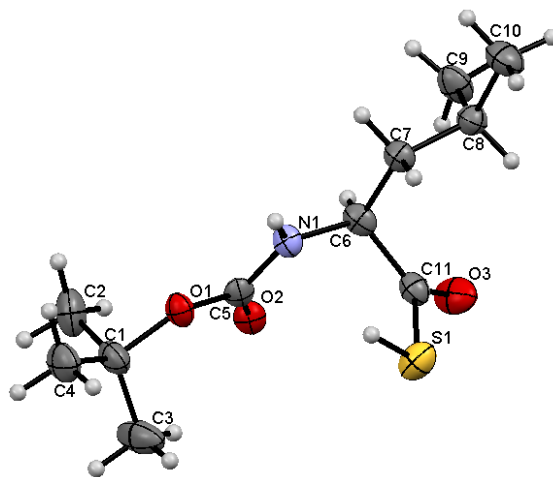


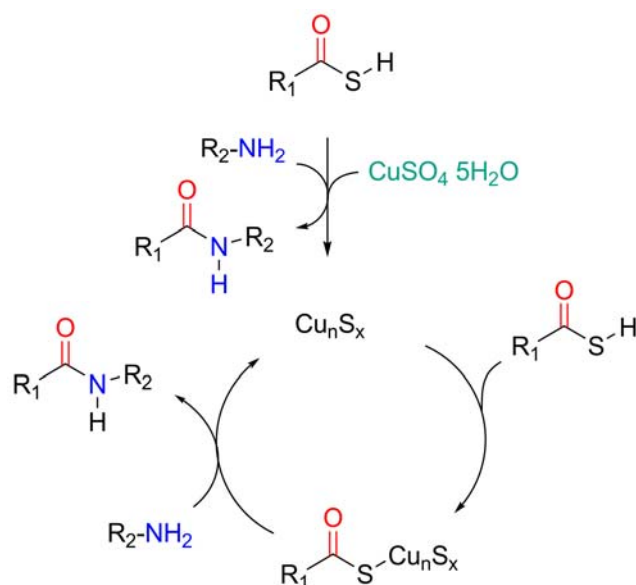
Figure 7: The ORTEP diagram depicting the X-ray structure of Boc-Leu-SH

All dipeptides were isolated in satisfactory yields including sterically hindered amino acids, Val(**6**, **12**), Aib(**11**) and Ile(**13**) in less than 5 min. Though the reaction proceeds with the coupling efficiencies more than 90% (HPLC analysis), the isolated yields after the column purification were given in the Table 1. Inspired by the clean, efficient and fast amide bond coupling reaction, we further extended this strategy to synthesize tri and tetrapeptides. The dipeptide **3** was coupled to the Boc- Ser(OBu^t)-SH, as anticipated the tripeptide **17** was isolated in good yield in less than 5 min. Similarly, other tri peptides **18** and **19** were isolated with satisfactory yields. The tetrapeptides (**20-22**) were synthesized using 2 + 2 convergent strategy. The corresponding dipeptide thioacids were synthesized similar to *N*-protected thioacids and subjected for the coupling reactions with dipeptide amines. Further we applied this protocol for synthesis of peptide comprising of highly β -branched containing amino acid residues. In that regards, peptide **22** with highly β -branched valine residues was isolated in satisfactory yield within 5 min. To ensure the compatibility of the thioacid coupling reaction in the presence of electron deficient unsaturated amides and esters, which are prone for Michael addition reaction,³⁶ the tetrapeptide **21** was synthesized. Instructively, the tetrapeptide was isolated without any side products. All tetrapeptides were isolated with satisfactory yields within 5 minutes and are given in the Table 1. In hindsight, the comparable results of 30 mol% of either copper sulfate or copper acetate with the 100 mol% provoke us to investigate the role of insoluble byproduct CuS in the coupling reactions. To understand whether or not the CuS involved in the amide bond formation, a control reaction with Boc-Ala-SH and benzylamine was carried out in the presence of 30 mol % of CuS. Surprisingly, the formation of amide **1** was observed with the same rate as that of copper sulfate. To verify

its compatibility we further synthesized dipeptides **4**, **6**, and **16**, tripeptide **19** and the tetrapeptide **20** in the Table 1 and found no difference between the insoluble CuS and the soluble CuSO₄. Albeit it is contradicting to our initial assumption of the solubility of the copper sulfate, the serendipity providing insight into the role of metal sulfides as catalysts in the peptide bond formation using thioacids. In contrast to the model experiments on the fixation of the carbon monoxide and the activation of thioacetic acid on metal sulfides under primordial conditions,²² we observed only amide bond formation in the CuS catalyzed reaction.

2A.3.3 Possible mechanism for CuSO₄·5H₂O mediated peptides synthesis

Based on the observations that 30 mol % of CuS can also be acts as catalyst to mediate this fast coupling reaction. We propose the possible mechanism for the amide bond synthesis (Scheme 10). We anticipate that the initial step proceeds with direct involvement of copper complex (CuSO₄·5H₂O or Cu(OAc)₂·H₂O) in the reaction leading to the formation CuS and the amide bond. Subsequently, the *in situ* generated CuS acts as a catalyst to activate the thioacid through coordination. The reaction between the activated intermediate and the free amine leading to the formation of amide bond along with the regeneration of CuS (Scheme 10). Though the LC-MS analysis suggests the presence of mixture of elemental sulfur (S₇, S₁₈ etc.) in the reaction mixture, the detailed mechanism of the liberation of sulfur in the reaction needs to be investigated.



Scheme 10: Proposed mechanism of the CuSO₄·5H₂O mediated and CuS catalyzed amide bond synthesis

2A.4 Conclusions

In conclusion, we have successfully demonstrated, a novel, fast, scalable amide bond synthesis in methanol with a wide range of amides and peptides. The coupling products of sterically hindered amino acids, tri and tetra peptides were isolated in less than few minutes. This protocol provides new tool for the selective coupling of thioacid with amines in presence of other functional groups. While offering specific and fast access to the amides and peptides in methanol, this method also provides new protocol for the synthesis of multi functional copper sulfide. In addition, we also proved that this method is free from racemization. This protocol can be utilized for the synthesis of synthetically challenging membrane peptides and peptides containing sterically hindered amino acids.

Section 2B: Thioacid Mediated Selective and Mild *N*-Acylation of Amines

2B.1 Introduction

After obtaining the impressive results of the metal mediated peptide synthesis in methanol, we sought to explore same protocol for the synthesis of *N*-acetyl amines using commercially available thioacetic acid.

Acylation of amines is a fundamental and most widely used reaction in organic chemistry.³⁷ In addition, *N*-acylation is important reaction in pharmaceutical and agro industry.^{38a,b,c,d} Typically, acetic anhydride or acetyl chloride either in the presence of basic media or acid catalysts have been used for the *N*- acetylation reactions.³⁹ In contrast to the organic synthesis, nature selectively uses *N*-acylation strategy without affecting the other functional groups such as alcohols, phenols, imidazoles, thiols etc. in proteins and other biomolecules.¹ In addition, various *N*-acylated products with alkyl and aryl groups have also been found in many biologically active natural products. Acyl chlorides and acid anhydrides mediated *N*-acylation reactions have been associated with many inherited problems.¹⁷ In addition, many acid chlorides and anhydrides react rapidly with water and alcohols leading to the corresponding acids and esters, respectively. Further, selective acylation of amines in the presences of other functional groups is rather a difficult process. To overcome this high reactivity and poor selectivity problem of acid chlorides and acid anhydrides towards *N*-acylation of amines, several new strategies have been introduced by various groups which includes direct and metal mediated condensation of unactivated

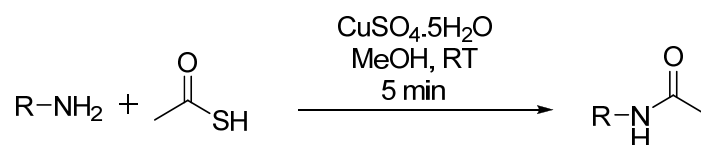
carboxylic acids and amines,^{40a, b, c} acylation through *N*-acyl DBN tetraphenyl borate salts,⁴¹ mercury and ruthenium catalyzed Beckman rearrangements,^{42a, b} copper catalyzed oxidative amidation of benzaldehyde,^{43a,b} triazole and imidazole mediated acyl transfer reactions,^{44a, b, c} and acylations through acylbenzotriazoles.^{45a, b, c} However, most of these reactions either require elevated temperatures or activated carboxylic acids as starting materials. In addition, many of these reactions are not specific to the *N*-acylation of amines.

2B.2 Aim and rationale of the present work

Inspired by the fast peptide synthesis in methanol by amino thioacids and amines in the presence of copper sulfate, we sought to extend this strategy to the *N*-acetylation of amines by using commercially available thioacetic acid and copper sulphate. Here we are reporting the copper sulfate mediated highly selective, mild and rapid *N*-acylation of various aliphatic and aromatic amines using thioacids in methanol at neutral conditions. This method is found to be highly selective to the amines and not sensitive to other functional groups such as phenols, alcohols and thiols. Exciting results of selective and fast *N*-acetylation by thioacid were extended to *N*-benzoylation and fatty acid acylation of amines as both these *N*-acylated products have high importance in chemistry and biology.

2B.3 Results and discussion

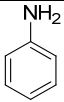
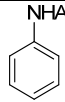
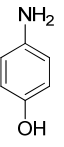
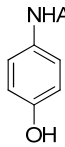
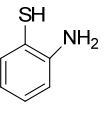
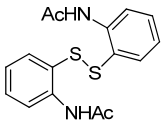
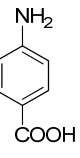
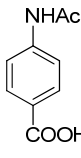
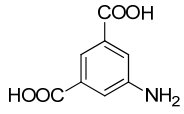
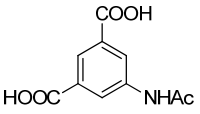
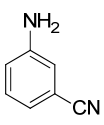
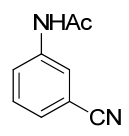
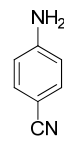
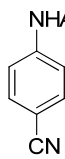
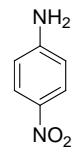
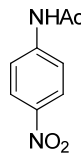
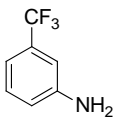
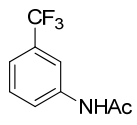
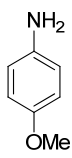
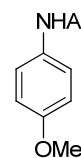
Inspired by encouraging results of thioacid mediated mild and fast peptide synthesis we began our investigation of *N*-acetylation strategy with aniline and thioacetic acid in the presence of 30 mol % of copper sulfate in methanol. The schematic representation of the copper sulfate mediated *N*-acetylation strategy is shown in Scheme 11. Previous studies with *N*-protected amino thioacids suggest that 30 mol % of copper sulfate mediated the coupling reaction with same rate as the 100 mol % of copper sulfate because its insoluble byproduct CuS also mediates the coupling reactions.⁴⁸ In a typical reaction, aniline and thioacetic acid in 1:1 ratio were dissolved in methanol and the solution was treated with 30 mol% (equivalent to the reacting partners) of CuSO₄·5H₂O. Immediate precipitation of CuS as black material indicates the progress of the reaction. Completion of the reaction was confirmed by TLC. The reaction was stirred for another 2 to 3 min, and centrifuged to separate the insoluble CuS



Scheme 11: Copper sulfate mediated selective and fast *N*-acylation of amines using thioacids in methanol.

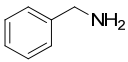
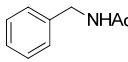


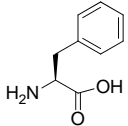
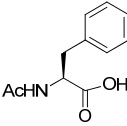
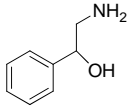
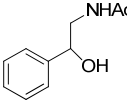
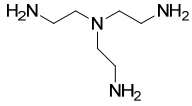
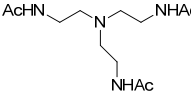
Simple aqueous work-up of the crude product dissolved in ethyl acetate after the evaporation of methanol gave pure sample of *N*-phenylacetamide in 83% yield (Table 2, entry 1a). In a control reaction without copper sulfate no *N*-acetylated product were observed even after stirring the reaction mixture for 5 hrs. The successful strategy of *N*-acetylation of aniline was then applied to the other aromatic and aliphatic amines and results are summarized in the Table 2 and Table 3. In order to understand the selectivity and the reactivity of this protocol, we subjected *p*-amino phenol (Table 2, entry 2b) for *N*-acetylation. Reaction proceeded with the same rate as that of aniline. As anticipated, analysis of the product suggests that this protocol is selective towards *N*-acylation and no *O*-acylation was observed in the reaction mixture even after stirring the reaction for 24 hr. Selective and rapid *N*-acetylation of *p*-amino phenol in methanol is also of significant interest for the preparation of antipyretic drug *p*-paracetamol. In contrast, both *N*- and *O*-acylation products were isolated in the analogous acylation reaction of *p*-aminophenol using acetic anhydride and pyridine. In order to understand whether or not the amino group can undergo specific *N*-acetylation in the presence of free thiol (-SH), we subjected *o*-amino thiophenol (Table 2, entry 3c) for acetylation reaction. In contrast to the intramolecular cyclized heterocyclic product 2-methyl benzothiazole obtained in the acetic anhydride mediated acylations,⁴⁹ we isolated the S-S disulfide dimer of *N*-acetyl *o*-thiophenol in 84% yield and no other products were observed in the reaction. The mass spectral experiments confirm that the starting thiophenol was a monomer and the oxidative disulfide formation occurred in the process of the reaction. In order to explore the functional group tolerance of this rapid *N*-acylation strategy, we further subjected aromatic amines containing mono and dicarboxylic acids (Table 2, 4d and 5e) to realize whether the free carboxylic acids can play any role in the *N*-acetylation. Resultant *N*-acetylation products were isolated in very good yields and confirmed that free carboxylic acids have not played any role in the reaction.

Table 2: *N*-Acetylation of aromatic amines using thioacetic acid

Entry	R-NH ₂	Product	Yield (%)
1a			83
2b			75
3c			84
4d			79
5e			82
6f			76
7g			73
8h			56
9i			88
10j			85

To further understand the electronic effect on the yields of the reaction, we subjected *m*- and *p*-cyano anilines (Table 2, entries 6f and 7g), *p*-nitro aniline (Table 2, entry 8h) and *m*-amino trifluoro toluene (Table 2, entry 9i) for *N*-acetylation. Except the *p*-nitroaniline all other *N*-acetylated products were isolated in moderate to excellent yields. In comparative studies with standard *N*-acetylation reaction of *p*-nitroaniline with acetic anhydride in pyridine, we obtained almost 9% lower yields suggesting that strong electron withdrawing groups may decrease yields compared to the electron donating groups (Table 2, entry 10j).

Table 3: *N*-Acetylation of aliphatic amine using thioacetic acid

Entry	R-NH ₂	Product	Yield (%)
11k			81
12l			76
13m			90
14n			81
15o			84

Further, the encouraging results for *N*-acetylation of aromatic amines inspired us to extend this strategy for *N*-acetylation of aliphatic amines. Several primary and secondary amines were acetylated using this protocol and are listed in Table 3. Results of *N*-acetylation of aliphatic amines (Table 3, entries 11k and 12l), amino acid (Table 3, entry 13m), amino alcohol (Table 3, entry 14n) and tris- amine (Table 3, entry 15o) suggest that reaction was found to be specific to amines and other functional group including alcohols, acids etc were unaffected during the reaction. All *N*-acetylation products of aliphatic amines were isolated in good to excellent yields.

2B.3.1 Benzoylation of aliphatic and aromatic amines using thiobenzoic acid

Similar to the *N*-acetylation, *N*-benzoylation is also a very important reaction in the protection of amino groups in organic synthesis. Typically *N*-benzoylations were performed under classical Schotten-Baumann conditions using benzoyl chloride in the presence of a base.³⁹ In addition several other methodologies were developed for the *N*-benzoylation, using benzoic anhydride³⁹, *N*-benzoyltetrazole^{50a, b}, benzoyl cyanide⁵¹, 2-benzoylthio-1-methylpyridinium chloride,⁵² etc, however most of these protocol are associated with the inherent problems similar to the acetyl chloride and acetic anhydrides. The intriguing results of *N*- acetylations from thioacetic acid encouraged us to carryout *N*-benzoylation under similar reaction conditions. In order to perform the *N*-benzoylation, corresponding thiobenzoic acid was synthesized through the treatment of NaSH with benzoyl chloride and the pure thiobenzoic acid was subjected to the *N*-benzoylation in the presence of 30 mol% CuSO₄.5H₂O in methanol. The list of amines and resultant *N*-benzoylated products are summarized in Table 4. Except the secondary amine (Table 4, entry 18r) all other aromatic and aliphatic amines (Table 4, entry 16p, 17q and 19s) gave excellent yields of *N*-benzoylated products. All benzoylation reactions proceed smoothly and completed within 5 min.

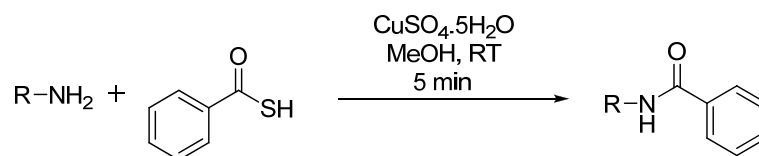


Table 4: *N*-Benzoylation of amine using thiobenzoic acid in methanol

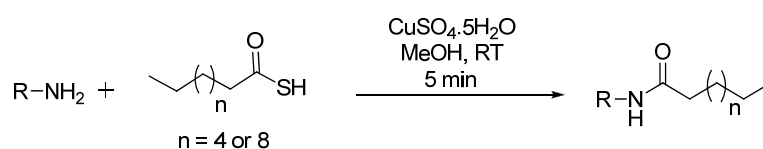
Entry	Amine	Product	Yield (%)
16p			82
17q			88
18r			72
19s			89

2B.3.2 *N*-Acylation of fatty acids using thiooctanoic and thiododecanoic acid

In addition to the *N*-acetylation and *N*-benzoylation, we further sought to explore this thioacid mediated *N*-acylation strategy to the biologically important *N*-acylation of fatty acids. *N*-Acyl fatty acids play a very important role in the anti-microbial activities of lipopeptides.^{53a,b} In order to explore the *N*-acylations, we randomly selected octanoic and dodecanoic acids for the *N*-acylation reactions with aliphatic and aromatic amines. Thiooctanoic and thiododecanoic acids were synthesized from the corresponding fatty acid *N*-hydroxysuccinimide esters and NaSH.⁴² *N*-Acylation of thiofatty acids with various amines also proceeded with complete conversion within 5 min similar to the other thioacids. As a proof of concept, we have used both aromatic (Table 5, entry 21u and 22v)

and aliphatic amines (Table 5, entries 20t and 23w) for the *N*-acylations with thiofatty acids. The list of *N*-acylation of fatty acids with amines is given in the Table 5. All four *N*-acylated products were isolated in good to excellent yields (78-92%).

Table 5: *N*-Acylation of amine using thiofattyacids in methanol



Entry	Amine	Thioacid	Product	Yield (%)
20t				92
21u				89
22v				78
23w				83

2B.4 Conclusion

In conclusion, we have developed a mild, fast, efficient and highly selective method for the synthesis of *N*-acetylation, *N*-benzoylation and *N*-acylation of fatty acids with amines using corresponding thioacids in methanol at room temperature. The reactions were mediated by the 30 mol% of copper sulfate. Compatibility of these reactions was studied with a wide range of aliphatic and aromatic amines with various other functional groups. All *N*-acylation products were isolated in moderate to high yields. This method is found to be highly selective to amines and not sensitive to other functional groups such as phenols, alcohols and thiols. The simple workup, mild reaction conditions, high yields and high selectivity of this reaction may serve as an attractive alternative to the existing protocols.

2.2 Experimental section

General Experimental Details

All amino acids, NHS, DCC were purchased from Aldrich. Di-*tert*-butyl dicarbonate were purchased from Spectrochem. NaSH purchased from Acoris. The solvents DMF, DMSO, MeOH, EtOH were purchased from Merck. MeOH was dried over magnesium turnings and distilled prior to use. Column chromatography was performed on Merck silica gel (100-200 mesh). ¹H NMR spectra were recorded on Jeol 400 MHz and ¹³C NMR on 100 MHz spectrometer using residual solvent as internal standard (CDCl₃ δ_H, 7.24 ppm, δ_C 77.0 ppm). The chemical shifts (δ) were reported in ppm and coupling constant (*J*) in Hz. Mass spectra were obtained from MALDI-TOF/TOF (Applied Biosystem). UV data were performed on Thermo Scientific spectrophotometers. X-Ray data were collected on Bruker APEX (II) DUO.

X-Ray crystal structure analysis

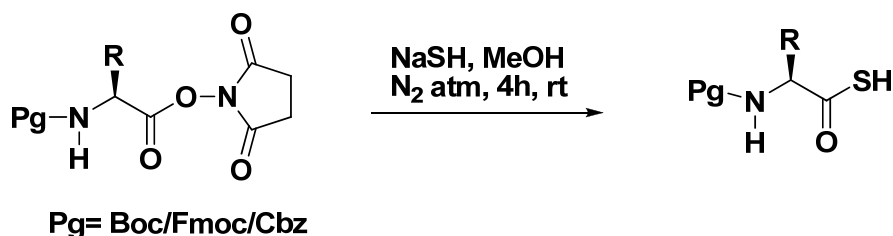
Crystal structure analysis of (Boc-Leu-SH): Crystals of Boc-Leu-SH was grown by on standing gummy Boc-Leu-SH oil. A single crystal (0.27 × 0.24 × 0.22 mm) was mounted in a loop with a small amount of the mother liquor. The X-ray data were collected at 100 K temperature on a Bruker AXS SMART APEX CCD diffractometer using MoK_α radiation (λ = 0.71073 Å), ω-scans (2θ = 56.56°) for a total number of 7001 independent reflections. Space group *P2(1),2(1),2(1)* *a* = 9.439(3), *b* = 16.600(4), *c* = 18.026(4) Å, α = 90.00, β =

90, $\gamma = 90.00$, $V = 2824.3(12) \text{ \AA}^3$ Orthorhombic P , $Z=4$ for chemical formula $C_{22}H_{40}N_2O_6$, with two molecule in asymmetric unit; $\rho_{\text{calcd}} = 1.159 \text{ g cm}^{-3}$, $\mu = 0.233 \text{ mm}^{-1}$, $F(000) = 1064$, $R_{\text{int}} = 0.0610$. The structure was obtained by direct methods using SHELXS-97.^[1] All non-hydrogen atoms were refined anisotropically. The hydrogen atoms were fixed geometrically in the idealized position and refined in the final cycle of refinement as riding over the atoms to which they are bonded. The final R value was 0.0628 ($wR2 = 0.1378$) for 4151 observed reflections ($F_o \geq 4\sigma(|F_o|)$) and 307 variables, $S = 0.934$. The largest difference peak and hole were 0.324 and $-0.283 \text{ e \AA}^{-3}$, respectively.

2.2.1 Synthesis procedure and compound characterization for Section 2A

General procedure for synthesis of *N*-protected amino thioacid

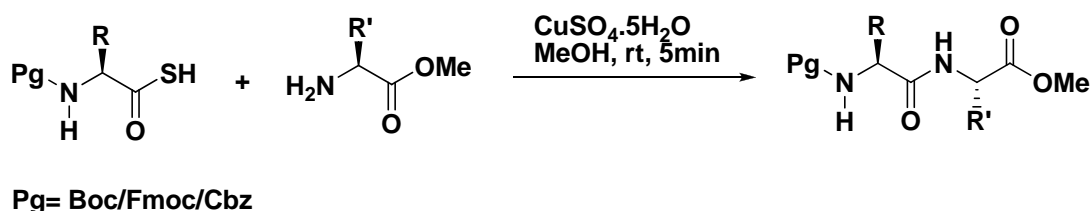
The *N*-protected thioacids was synthesized using the reported procedure.³⁵ Briefly, the NHS ester (2 mmol) of protected amino acid was dissolved in distilled MeOH (50 mL). To this stirring solution NaSH (2 mmol) was added under N_2 atmosphere. This reaction mixture was allowed to stir for another 4h. After completion of reaction (monitored by TLC) the solvent MeOH was evaporated under reduced pressure and the residue was dissolved in water (50 mL). This aqueous solution was acidified to $\text{pH} = 3$ with 5% HCl and extracted with ethyl acetate ($25 \text{ mL} \times 3$). The combined organic layer was then washed with brine and dried over anhydrous Na_2SO_4 and concentrated under reduced pressure to get *N*-protected amino thioacid.



General procedure for $\text{CuSO}_4 \cdot 5\text{H}_2\text{O}$ (or $\text{Cu}(\text{OAc})_2 \cdot 2\text{H}_2\text{O}$) mediated coupling of *N*-protected thioacids and amines.

Isolation of amine ester from $\text{HCl} \cdot \text{NH}_2(\text{R})\text{-OMe}$: Hydrochloride salt of methyl ester of amino acid (2.1 mmol) was dissolved in saturated solution of aq. Na_2CO_3 and extracted with ethyl acetate (30 mL \times 3). The combined organic layer was washed with brine and dried over anhydrous Na_2SO_4 . This organic layer was concentrated to the volume \sim 2 ml under reduced pressure and directly used for the coupling reaction.

The *N*-protected thioacid (2 mmol) was dissolved in distilled methanol (2 mL) either in Falcon tube or in RB flask. To this solution, methyl ester of amino acid (2.1 mmol) was added with stirring. This reaction mixture was then treated with 30 mol% of $\text{CuSO}_4 \cdot 5\text{H}_2\text{O}$ (or $\text{Cu}(\text{OAc})_2 \cdot \text{H}_2\text{O}$). After 5 min, the clean reaction mixture was converted to dark brown color turbid solution indicating the completion of the reaction (also by TLC). The reaction mixture was centrifuged and the residue was further washed with methanol. The combined methanol solution was evaporated under reduced pressure. The residue was then dissolved in ethyl acetate (75 mL) and washed with 10% aq. Na_2CO_3 , 5% aq. HCl and brine, dried over anhydrous Na_2SO_4 and concentrated under reduced pressure. The product was purified by column chromatography using ethyl acetate and pet ether.



General procedure for CuS mediated coupling of *N*-protected thioacid and amine

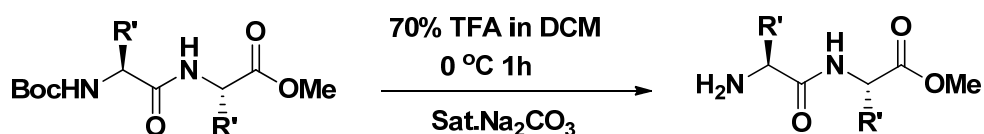
The *N*-protected thioacid (2 mmol) was dissolved in distilled methanol (2 mL) either in Falcon tube or in RB flask. To this solution, methyl ester of amino acid (2.1 mmol) was added with stirring. This reaction mixture was then treated with 30 mol% of CuS . After 5 min TLC shows the complete disappearance of amine protected thioacid and appearance of amide. The reaction mixture was centrifuged and the residue was further washed with methanol. The combined methanol solution was evaporated under reduced pressure. The

residue was then dissolved in ethyl acetate (75 mL) and washed with 10% aq. Na₂CO₃, 5% aq. HCl and brine, dried over anhydrous Na₂SO₄ and concentrated under reduced pressure. The product was purified by column chromatography using ethyl acetate and petroleum ether.



General procedure for synthesis of tri and tetrapeptides

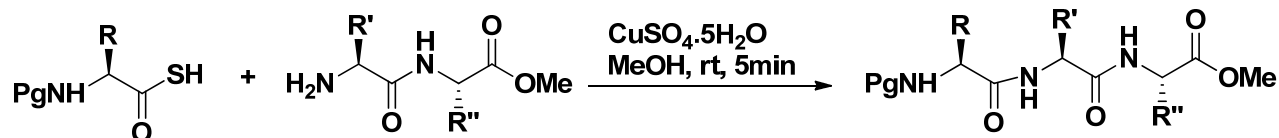
NH₂-X-X-OMe; The dipeptide Boc-X-X-OMe (2.1 mmol) was dissolved in DCM and cooled to 0 °C. To this solution TFA (3 mL) was added slowly. The reaction mixture was allowed to stir for 1hr. After completion of reaction (monitored by TLC) the reaction mixture was evaporated under reduced pressure and residue was dissolved in saturated aq. Na₂CO₃. This aqueous solution was then extracted with ethyl acetate (30 mL × 3). The combined ethyl acetate was washed with brine, dried over anhydrous Na₂SO₄. The organic layer was concentrated under reduced pressure to the volume ~2mL and directly used for the next coupling reaction.



The *N*-protected thioacid or dipeptide thioacid (2 mmol) was dissolved in distilled MeOH. To this solution dipeptide free amine (2.1 mmol, in ~2 mL EtOAc) was added followed by 30 mol% CuSO₄·5H₂O (or CuS catalyst). After 5 min, the clean reaction mixture was converted to dark brown color turbid solution, indicating the completion of the coupling reaction. The reaction mixture was centrifuged and the residue was further washed with methanol. The combined methanol solution was evaporated under

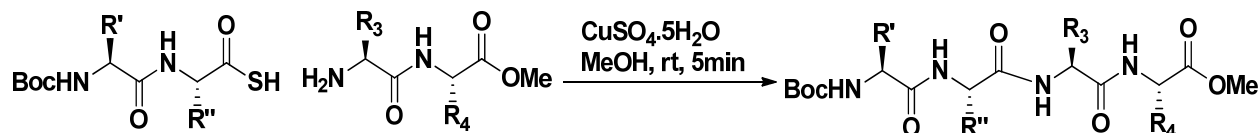
reduced pressure. The residue was then dissolved in ethyl acetate (75 mL) and washed with 10% aq. Na₂CO₃, 5% aq. HCl, brine, dried over anhydrous Na₂SO₄ and concentrated under reduced pressure. The product was further purified by column chromatography using ethyl acetate and petroleum ether.

Tripeptide synthesis



Pg = Boc/Cbz

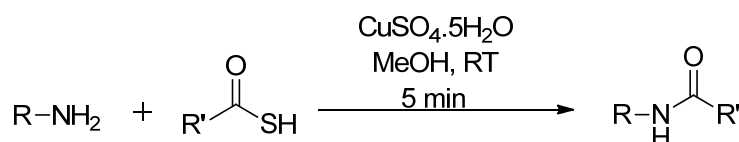
Tetrapeptide synthesis



2.2.2 Synthetic procedure and compound characterization for Section 2B

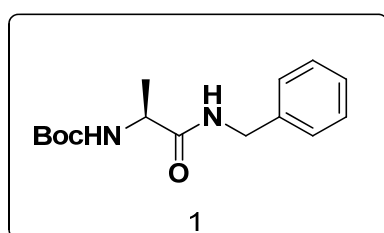
General procedure for *N*-acylation of amines using thioacid and copper sulfate

Thioacid (3 mmol) and free amine (3 mmol) were dissolved in distilled methanol (5 mL) either in Falcon tube or in RB flask. The reaction mixture was then treated with 30 mol% of CuSO₄·5H₂O. After 5 min, the clear reaction mixture was turned into dark brown color turbid solution indicating the completion of the reaction (also by TLC). The reaction mixture was then centrifuged and the residue was further washed with methanol. The combined methanol solution was evaporated under reduced pressure. The residue was then dissolved in ethyl acetate (75 mL) and washed with 10% aq. Na₂CO₃, 5% aq. HCl and brine, dried over anhydrous Na₂SO₄. The organic layer was concentrated under reduced pressure to get *N*-acyl derivatives of amines.

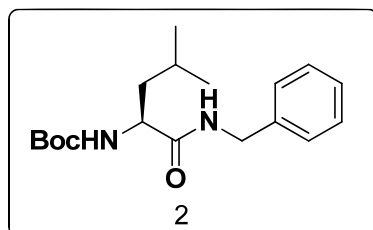


Spectroscopic Data for Dipeptides, Tripeptides

(S)-tert-Butyl (1-(benzylamino)-1-oxopropan-2-yl)carbamate (Boc-Ala-NHBzl) (1); White solid, (0.394 g, 71%) $^1\text{H NMR}$ (400 MHz; CDCl_3): δ 7.320-7.229 (m, 5H, 5 x CH, phenyl), 6.821 (br., 1H, NH, benzylic), 5.201 (br., 1H, NH Boc), 4.412 (br., 2H, $-\text{CH}_2\text{Ph}$), 4.226 (br., 1H αCH , $-\text{NHCHCH}_3$), 1.395 (s, 9H, $\text{C}(\text{CH}_3)_3$ Boc), 1.376-1.357 (d, 3H, $J = 7.6$, $-\text{CHCH}_3$); $^{13}\text{C NMR}$ (100MHz; CDCl_3): 172.78, 155.66, 138.19, 128.71, 127.47, 80.16, 50.20, 43.40, 28.35, 18.50. **MALDI-TOF/TOF** m/z Calcd. for $\text{C}_{15}\text{H}_{22}\text{N}_2\text{O}_3$ (M + Na) is 301.1528 Observed = 301.1804.

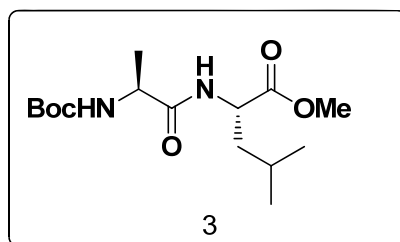


(S)-tert-Butyl (1-(benzylamino)-4-methyl-1-oxopentan-2-yl)carbamate (Boc-Leu-NHBzl) (2); White Solid, (0.441 g, 69%), $^1\text{H NMR}$ (400 MHz; CDCl_3): δ 7.323-7.231 (m, 5H, 5 x CH, phenyl), 6.764 (br., 1H, NH benzylic), 5.066-5.048 (d, 1H, $J = 7.2$, NH Boc), 4.411-4.397 (d, 2H, $J = 5.6$, $-\text{CH}_2\text{Ph}$), 4.163 (br., 1H, αCH , $-\text{NHCHCH}_2-$), 1.716-1.643 (m, 2H, $-\text{CHCH}_2\text{CH}-$), 1.549-1.484 (m, 1H, $-\text{CH}_2\text{CH}(\text{CH}_3)_2$), 1.402 (s, 9H, $-\text{C}(\text{CH}_3)_3$ Boc), 0.943-0.915 (dd, 6H, $J = 6.4$, $\text{CH}(\text{CH}_3)_2$), $^{13}\text{C NMR}$ (100MHz, CDCl_3) 172.55, 155.77, 138.06, 128.56, 127.50, 127.31, 79.97, 53.06, 43.29, 41.11, 28.12, 24.69, 22.89, 21.96. **MALDI TOF/TOF** m/z Calcd. for $\text{C}_{18}\text{H}_{28}\text{N}_2\text{O}_3$ (M + Na) is 343.1998 Observed = 343.2170.

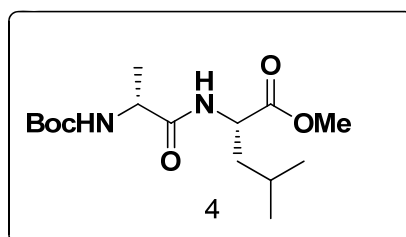


(S)-Methyl 2-((S)-2-((tert-butoxycarbonyl)amino)propanamido)-4-methylpentanoate (Boc-Ala-Leu-OMe) (3); White powder, (0.429 g, 68%) $^1\text{H NMR}$ (400 MHz; CDCl_3): δ 6.602-6.592 (d, 1H, $J = 4$, NH amide), 5.061-5.048 (d, 1H, $J = 5.2$, NH Boc), 4.624-4.589

(m, 1H, α CH -NHCHCH₂, Leu), 4.184-4.167 (m, 1H, δ CH, NHCHCH₃, Ala), 3.719 (s, 3H, OCH₃), 1.656-1.623 (m, 2H, CH₂, -CHCH₂CH(CH₃)₂ Leu), 1.567-1.524 (m, 1H, CH, -CH(CH₃)₂), 1.437 (s, 9H, C(CH₃)₃, Boc), 1.355-1.338 (d, 3H, *J* = 6.8, CHCH₃, Ala), 0.924-0.910 (d, 6H, *J* = 5.6, CH(CH₃)₂ Leu); ¹³C NMR (100 MHz, CDCl₃) 173.29, 172.49, 155.60, 80.146, 52.343, 50.69, 49.92, 41.51, 28.33, 24.78, 22.90, 21.85, 17.97. **MALDI TOF/TOF** m/z Calcd. for C₁₅H₂₈N₂O₅ (M + Na) is 339.1896 Observed = 339.2333

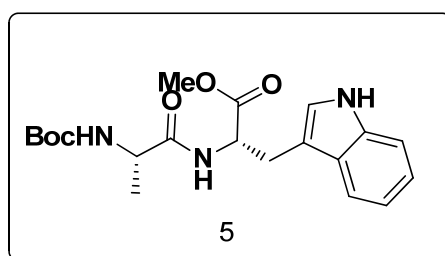


(S)-Methyl 2-((R)-2-((tert-butoxycarbonyl)amino)propanamido)-4-methylpentanoate (Boc-^DAla-Leu-OMe) (4); White powder, (0.391 g, 62%), ¹H NMR (400 MHz; CDCl₃): δ 6.671-6.661 (d, 1H, *J* = 4, NH amide), 5.037-5.031 (d, 1H, *J* = 2.4, NH, Boc), 4.628-4.574 (m, 1H, α CH, -NHCHCH₂-, Leu), 4.225-4.197 (m, 1H, δ CH, NHCHCH₃, Ala), 3.719 (s, 3H, CH₃, OCH₃), 1.664-1.630 (m, 2H, -CHCH₂CH(CH₃)₂), 1.567-1.524 (m, 1H, CH₂CH(CH₃)₂), 1.447 (s, 9H, C(CH₃)₃, Boc), 1.371-1.354 (d, 3H, *J* = 6.8, -CHCH₃, Ala), 0.938-0.916 (dd, 6H, *J* = 6, -CH(CH₃)₂); ¹³C NMR (100 MHz, CDCl₃) 173.40, 172.57, 155.57, 80.24, 52.34, 50.65, 41.47, 28.33, 24.86, 22.91, 21.86, 18.21 **MALDI TOF/TOF** m/z Calcd. for C₁₅H₂₈N₂O₅ (M + Na) is 339.1896 Observed = 339.2218

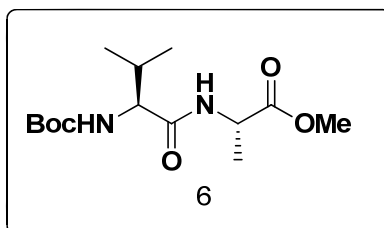


(S)-Methyl 2-((S)-2-((tert-butoxycarbonyl)amino)propanamido)-3-(1H-indol-3-yl)propanoate (Boc-Ala-Trp-OMe) (5); Gummy, (0.521 g, 67%), ¹H NMR (400 MHz; CDCl₃): δ 8.484 (br. 1H, NH indole), 7.524-7.505 (d, 1H, *J* = 7.6, aromatic CH), 7.342-7.322 (d, 1H, *J* = 8, CH aromatic), 7.186-7.149 (t, 1H, *J* = 6.8, CH aromatic), 7.120-7.082 (t, 1H, *J* = 7.2, CH aromatic), 6.995-6.992 (d, 1H, *J* = 1.2, CH aromatic), 6.705-6.686 (d,

1H, $J = 7.6$ NH amide), 5.087-5.072 (d, 1H, $J = 6$, NH Boc), 4.918-4.871 (m, 1H, α CH, Trp), 4.190-4.168 (m, 1H, δ CHCH₃, Ala), 3.652 (s, 3H, -OCH₃), 3.321-3.309 (d, 2H, $J = 4.8$, -CHCH₂- Trp), 1.415 (s, 9H, C(CH₃)₃ Boc), 1.264-1.245 (d, 3H, $J = 7.6$, CHCH₃); ¹³C NMR (100 MHz; CDCl₃): 172.54, 172.22, 171.35, 146, 136.20, 127.64, 123.22, 122.20, 119.60, 118.56, 111.45, 109.65, 80.08, 60.53, 53.04, 52.47, 28.35, 27.63, 21.16, 18.49, 14.28. **MALDI TOF/TOF** m/z Calcd. for (M + Na) is 412.1848 Observed = 412.2072.

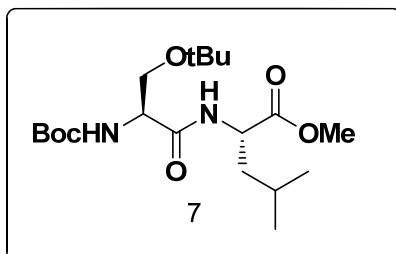


(S)-Methyl 2-((S)-2-((tert-butoxycarbonyl)amino)-3-methylbutanamido)propanoate (Boc-Val-Ala-OMe) (6); White solid, (0.459 g, 76%), ¹H NMR (400 MHz; CDCl₃): δ 6.515-6.499 (d, 1H, $J = 6.4$, NH amide), 5.119-5.098 (d, 1H, $J = 8.4$, NH Boc), 4.620-4.548 (m, 1H, α CH Ala), 3.958-3.922 (m, 1H, δ CH, Val), 3.745 (s, 3H, OCH₃), 2.146-2.098 (m, 1H, CH, -CH(CH₃)₂), 1.444 (s, 9H, C(CH₃)₃ Boc), 1.420-1.403 (d, 3H, $J = 6.8$, -CHCH₃), 0.982-0.916 (dd, 6H, $J = 6.8$, -CH(CH₃)₂); ¹³C NMR (100 MHz, CDCl₃) 173.25, 171.23, 155.91, 79.97, 59.84, 52.54, 48.05, 31.11, 29.77, 28.37, 19.25, 18.38, 17.79. **MALDI TOF/TOF** m/z Calcd. for C₁₄H₂₆N₂O₅ (M + Na) is 325.1739 Observed = 325.2072.

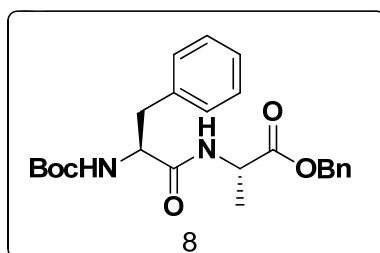


(S)-Methyl 2-((S)-3-(tert-butoxy)-2-((tert-butoxycarbonyl)amino)propanamido)-4-methylpentanoate (Boc-Ser(OtBu)-Leu-OMe) (7); White solid, (0.558 g, 72%), ¹H NMR (400 MHz; CDCl₃): δ 7.205 (br., 1H, NH amide), 5.425 (br., 1H, NH Boc), 4.627-4.620 (m, 1H, α CH NHCHCH₂), 4.180 (br., 1H, δ CH, NHCHCH₂-), 3.806-3.782 & 3.392-3.379 (dd, 2H, $J = 6.8$ CHCH₂O-), 3.717 (s, 3H, -OCH₃), 1.679-1.616 (m, 2H, -

CHCH₂CH(CH₃)₂), 1.560-1.542 (m, 1H, -CH(CH₃)₂), 1.458 (s, 9H, C(CH₃)₃, Boc), 1.206 (s, 9H, C(CH₃)₃ ^tButyl), 0.941-0.921 (dd, 6H, *J* = 4.4, CH(CH₃)₂); ¹³C NMR (100 MHz; CDCl₃): 173.14, 170.57, 155.54, 80.03, 74.14, 61.82, 54.02, 52.26, 50.83, 41.81, 28.37, 27.42, 24.74, 22.93, 21.96. **MALDI TOF/TOF** *m/z* Calcd. for C₁₉H₃₆N₂O₆ (*M* + Na) is 411.2471 Observed = 411.2928.

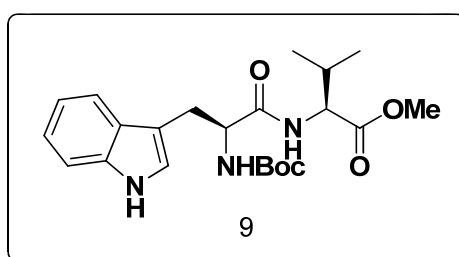


(S)-benzyl 2-((S)-2-((tert-butoxycarbonyl)amino)-3-phenylpropanamido)propanoate (Boc-Phe-Ala-OBn) (8); White solid, (0.545 g, 64%), ¹H NMR (400 MHz; CDCl₃): δ 7.361-7.315 (m, 5H, 5 x CH, Phenyl), 7.275-7.172 (m, 5H, 5 x CH, phenyl), 6.658-6.644 (d, 1H, *J* = 5.6, NH, amide), 5.142 (s, 2H, -CH₂Ph, benzylic), 5.117-5.107 (d, 1H, *J* = 4, NH, Boc), 4.593-4.524 (m, 1H, α CH NHCHCH₃), 4.412-4.398 (br. 1H, δ CH, NHCHCH₂- Phe), 3.050-3.037 (d, 2H, *J* = 5.2, CHCH₂Ph), 1.388 (s, 9H, C(CH₃)₃, Boc), 1.360-1.341 (d, 3H, *J* = 7.6, CHCH₃); ¹³C NMR (100 MHz; CDCl₃): 172.23, 170.84, 155.33, 136.46, 135.20, 129.28, 128.54, 128.38, 126.82, 80.07, 67.03, 55.43, 48.10, 38.32, 28.16, 18.19 **MALDI TOF/TOF** *m/z* Calcd. for C₂₄H₃₀N₂O₅ (*M* + Na) is 449.2052 Observed = 449.2538.

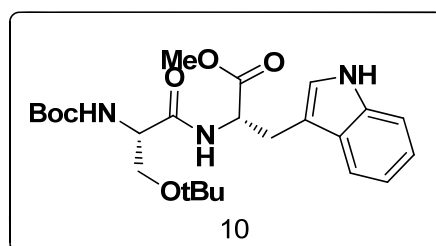


(S)-Methyl 2-((S)-2-((tert-butoxycarbonyl)amino)-3-(1H-indol-3-yl)propanamido)-3-methylbutanoate (Boc-Trp-Val-OMe) (9); White solid, (0.525 g, 63%), ¹H NMR (400 MHz; CDCl₃): δ 8.276 (br., 1H, NH, indole), 7.671-7.656 (d, 1H, *J* = 6, CH aromatic, indole), 7.365-7.348 (d, 1H, *J* = 6.8, CH aromatic, indole), 7.210-7.180 (t, 1H, *J* = 6.4, CH,

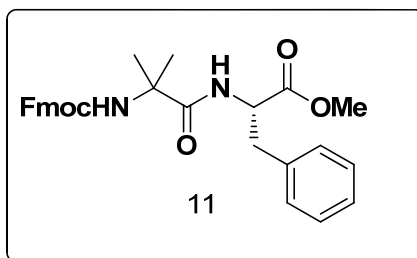
aromatic), 7.141-7.111 (t, 1H, $J = 6.4$, CH aromatic, indole), 7.085 (br., 1H, CH aromatic, indole), 6.338-6.323 (d, 1H, $J = 6$, NH amide), 5.217 (br., 1H, NH, Boc), 4.459 (br., 1H, α CH, NHCHCH-), 4.430-4.403 (q, 1H, $J = 6.8$, δ CH, NHCHCH₂-), 3.636 (s, 3H, OCH₃), 3.307-3.184 (m, 2H, -CHCH₂CH-), 2.070-2.018 (m, 1H, -CHCH(CH₃)₂), 1.443 (s, 9H, C(CH₃)₃), 0.817-0.775 (dd, 6H, $J = 5.6$, CH(CH₃)₂), ¹³C NMR (100 MHz; CDCl₃): 171.84, 171.75, 155.63, 136.32, 127.55, 123.37, 122.23, 119.74, 118.89, 111.25, 110.62, 80.19, 57.34, 55.35, 52.12, 31.29, 28.37, 28.16, 18.79, 17.81. **MALDI-TOF/TOF** m/z Calcd. for C₂₂H₃₁N₃O₅ (M + Na) is 440.2161 Observed = 440.2792.



(S)-Methyl 2-((S)-3-(tert-butoxy)-2-((tert-butoxycarbonyl)amino)propanamido)-3-(1H-indol-3-yl)propanoate (Boc-Ser(O^tBu)-Trp-OMe) (10); Gummy, (0.599 g, 65%), ¹H NMR (400 MHz; CDCl₃): δ 8.331 (br., 1H, NH, indole), 7.569-7.549 (d, 1H, $J = 8$, CH aromatic, indole), 7.354-7.334 (d, 1H, $J = 8$, CH aromatic indole), 7.319 (br., 1H, NH amide), 7.196-7.158 (t, 1H, $J = 7.2$, CH aromatic, indole), 7.134-7.099 (t, 1H, $J = 6.8$, CH aromatic, indole), 7.018-7.015 (d, 1H, $J = 1.2$, CH aromatic, indole), 5.433-5.420 (d, 1H, $J = 5.2$, NH Boc), 4.079-4.933 (m, 1H, α CH, -NHCHCH₂-), 4.187 (br., 1H, δ CH, -NHCHCH₂O-), 3.789-3.776 & 3.389-3.354 (dd, 2H, -CHCH₂O-), 3.330-3.261 (br., 2H, -CHCH₂C-), 3.633 (s, 3H, OCH₃), 1.422 (s, 9H, C(CH₃)₃ Boc), 1.113 (s, 9H, C(CH₃)₃ tButyl); ¹³C NMR (100 MHz, CDCl₃) 172.01, 170.36, 155.57, 136.18, 127.60, 123.01, 122.22, 119.65, 118.72, 111.32, 109.95, 80.02, 74.07, 61.85, 60.51, 54.20, 53.15, 52.31, 28.34, 27.33, 21.15, 14.28. **MALDI TOF/TOF** m/z Calcd. for C₂₄H₃₅N₃O₆ (M + Na) is 484.2424 Observed = 484.2915.

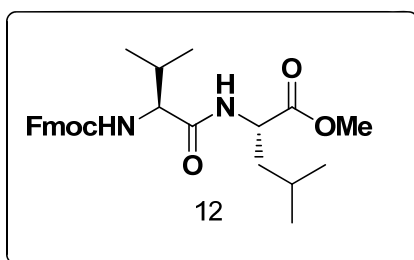


(S)-Methyl 2-(2-((((9H-fluoren-9-yl)methoxy)carbonyl)amino)-2-methylpropanamido)-3-phenylpropanoate (Fmoc-Aib-Phe-OMe) (11); White solid (0.67 g, 69%), $^1\text{H NMR}$ (400 MHz; CDCl_3): δ 7.768-7.748(d, 2H, $J = 8$, 2 x CH, Fmoc), 7.588-7.561 (dd, 2H, $J = 7.6$, 2 x CH, Fmoc), 7.411-7.375 (t, 2H, $J = 7.2$, 2 x CH, Fmoc), 7.322-7.28 (t, 2H, $J = 7.2$, 2 x CH, Fmoc), 7.224-7.164 (m, 3H, 3 x CH, Phenyl), 7.085-7.068 (d, 2H, $J = 6.8$, 2 x CH, Phenyl), 6.686-6.677 (d, 1H, $J = 3.6$, NH, amide), 5.439 (br. 1H, NH, Aib), 4.848(br. 1H, CH, $-\text{CHCH}_2-$, Fmoc), 4.399-4.339 (m, 2H, $-\text{CHCH}_2$, Fmoc), 4.189-4.156 (t, 1H, $J = 6.4$, αCH , $-\text{NHCHCH}_2$, Phe), 3.683 (s, 3H, OCH_3), 3.126-3.091 (m, 2H, $-\text{CHCH}_2\text{Ph}$), 1.465 (s, 6H, 2 x CH_3 , $\text{C}(\text{CH}_3)_2$, Aib); $^{13}\text{C NMR}$ (100 MHz, CDCl_3) 173.82, 171.79, 154.84, 143.70, 141.19, 135.70, 129.17, 128.39, 126.98, 124.93, 119.89, 66.56, 60.31, 56.68, 52.21, 47.02, 37.66, 30.83, 25.35, 20.95, 14.10. **MALDI-TOF/TOF** m/z Calcd. For $\text{C}_{29}\text{H}_{30}\text{N}_2\text{O}_5$ ($\text{M} + \text{Na}$) is 509.2052 Observed = 509.2054.

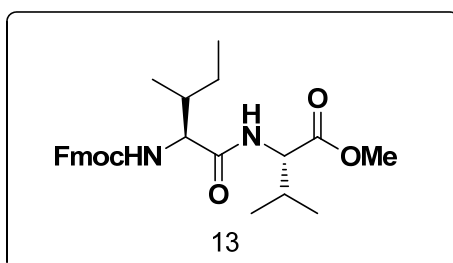


(S)-Methyl 2-((S)-2-((((9H-fluoren-9-yl)methoxy)carbonyl)amino)-3-methylbutanamido)-4-methylpentanoate (Fmoc-Val-Leu-OMe) (12); White solid, (0.717 g, 77%), $^1\text{H NMR}$ (400 MHz; CDCl_3): δ 7.775-7.761 (d, 2H, $J = 5.6$, 2 x CH, Fmoc), 7.606-7.592 (d, 2H, $J = 5.6$, 2 x CH, Fmoc), 7.415-7.388 (t, 2H, $J = 4.8$, 2 x CH, Fmoc), 7.329-7.299 (t, 2H, $J = 6.4$, 2 x CH, Fmoc), 6.366-6.352 (d, 1H, $J = 5.6$, NH amide), 5.510-5.493 (d, 1H, $J = 6.8$, NH, Fmoc), 4.654-4.610 (m, 1H, αCH , NHCHCH_2-), 4.458-4.423 & 4.373- 4.338 (br. 2H, $-\text{CH}_2\text{CH}-$ Fmoc), 4.241-4.213 (t, , 1H, $J = 5.6$, $-\text{CH}_2\text{CH}-$ Fmoc), 4.080-4.050 (t, 1H, $J = 6$, δCH , $-\text{NHCHCH}-$), 3.730 (s, 3H, OCH_3), 2.146-2.108 (m, 1H, $-\text{CHCH}(\text{CH}_3)_2$), 1.673-1.648 (m, 2H, $-\text{CHCH}_2\text{CH}$), 1.566-1.533 (m, 1H, $-\text{CH}_2\text{CH}(\text{CH}_3)_2$), 1.0-0.964 (dd, 6H, $J = 5.2$, $\text{CH}(\text{CH}_3)_2$), 0.922-0.911 (d, 6H, $J = 4.4$, $\text{CH}(\text{CH}_3)_2$ Leu) $^{13}\text{C NMR}$ (100 MHz; CDCl_3): 173.25, 171.31, 156.49, 143.92, 141.35, 127.80, 127.16, 125.16, 120.04, 67.20, 60.25, 52.36, 50.84, 47.20, 41.36, 31.52, 24.89,

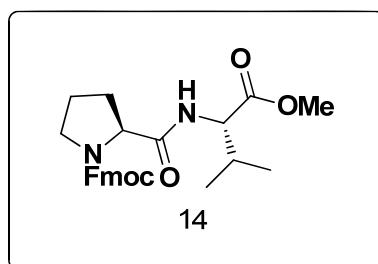
22.81, 21.95, 18.07 **MALDI-TOF/TOF** m/z Calcd. for $C_{27}H_{34}N_2O_5$ 489.2365 (M + Na) is Observed = 489.3064.



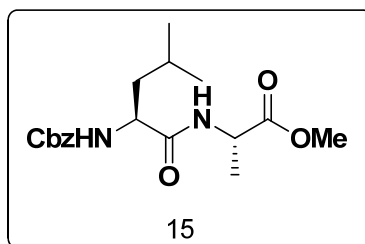
(S)-Methyl 2-(((2S,3R)-2-(((9H-fluoren-9-yl)methoxy)carbonyl)amino)-3-methylpentanamido)-3-methylbutanoate (Fmoc-Ile-Val-OMe) (13); White solid, (0.652 g, 70%) $^1\text{H NMR}$ (400 MHz; CDCl_3): δ 7.772-7.752 (d, 2H, $J = 8$, 2 x CH, Fmoc), 7.602-7.588 (d, 2H, $J = 5.6$, 2 x CH, Fmoc), 7.415-7.379 (t, 2H, $J = 7.2$, 2 x CH, Fmoc), 7.323-7.286 (t, 2H, $J = 7.6$, 2 x CH, Fmoc), 6.571-6.551 (d, 1H, $J = 8$, NH amide), 5.578-5.557 (d, 1H, $J = 8.4$, NH Fmoc), 4.575-4.540 (dd, 1H, $J = 5.2$, $-\text{CH}_2\text{CHCH}-$, Fmoc), 4.457-4.412 & 4.380-4.335 (m, 2H, $-\text{OCH}_2\text{CH}-$, Fmoc), 4.238-4.202 (t, 1H, $J = 7.2$, αCH , $-\text{NHCHCH}-$), 4.155-4.116 (m, 1H, δCH , $-\text{NHCHCH}-$ Ile), 3.718 (s, 3H, OCH_3), 2.207-2.127 (m, 1H, $-\text{CHCH}(\text{CH}_3)_2$ Val), 1.871-1.855 (m, 1H, CH, $-\text{CHCHCH}_3$ Ile), 1.594-1.535 & 1.213-1.138 (m, 2H, $-\text{CHCH}_2\text{CH}_3$ Ile), 0.958-0.882 (m, 12H, $\text{CH}(\text{CH}_3)_2$ Val & $\text{CH}(\text{CH}_3)_2$ Leu); $^{13}\text{C NMR}$ (100 MHz, CDCl_3) 172.04, 171.37, 156.25, 143.79, 141.20, 127.63, 126.99, 125.03, 119.88, 67.00, 59.54, 57.07, 52.08, 47.05, 37.47, 31.04, 24.78, 18.86, 17.74, 15.28, 11.27. **MALDI-TOF/TOF** m/z Calcd. for $C_{27}H_{34}N_2O_5$ (M + Na) is 489.2365 Observed = 489.2964.



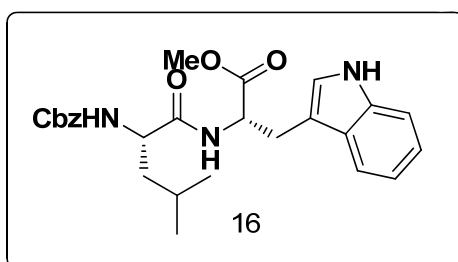
(S)-(9H-Fluoren-9-yl)methyl 2-(((S)-1-methoxy-3-methyl-1-oxobutan-2-yl)carbamoyl)pyrrolidine-1-carboxylate (Fmoc-Pro-Val-OMe) (14); White solid, (0.585 g, 65%), $^1\text{H NMR}$ (400 MHz; CDCl_3): δ 7.784-7.766 (d, 2H, $J = 7.2$, 2 x CH, Fmoc), 7.596-7.543 (d, 2H, 2 x CH, Fmoc), 7.427-7.391 (t, 2H, $J = 6.8$, 2 x CH, Fmoc), 7.335-7.301 (t, 2H, $J = 7.2$, 2 x CH, Fmoc), 7.212-7.193 (d, 1H, $J = 7.6$, NH amide), 6.523-6.506 (d, 1H, $J = 6.8$, NH Fmoc), 4.482-4.438 (m, 3H, $-\text{CH}_2\text{CHCH}-$ & $-\text{OCH}_2\text{CHCH}-$, Fmoc), 4.421-4.391 (m, 1H, $\text{CH}_2\text{CHN}-$ pro), 4.291-4.257 (t, 1H, $J = 6.4$, αCH , $-\text{NHCHCH}-$), 3.726 (s, 3H, OCH_3), 3.593-3.554 (t, 2H, $J = 8.4$, $-\text{NCH}_2\text{CH}_2-$, Pro), 2.380-2.365 (br., 1H, $-\text{CHCH}(\text{CH}_3)_2$), 1.957-1.926 (br., 4H, $-\text{CH}_2\text{CH}_2\text{CH}_2\text{CH}_2-$), 0.916-0.899 (d, 6H, $J = 6.8$, $\text{CH}(\text{CH}_3)_2$); $^{13}\text{C NMR}$ (100 MHz, CDCl_3) 172.26, 171.55, 156.21, 143.98, 141.35, 127.82, 127.15, 125.14, 120.07, 67.86, 60.41, 57.41, 52.17, 47.24, 34.19, 31.20, 29.78, 28.11, 25.69, 24.80, 19.11, 17.77. **MALDI TOF/TOF** m/z Calcd. for $\text{C}_{26}\text{H}_{30}\text{N}_2\text{O}_5$ ($\text{M} + \text{Na}$) is 473.2052 Observed = 473.2640.



(S)-Methyl 2-(((S)-2-(((benzyloxy)carbonyl)amino)-4-methylpentanamido)propanoate (Cbz-Leu-Ala-OMe) (15); White solid, (0.448 g, 64%), $^1\text{H NMR}$ (400 MHz; CDCl_3): δ 7.360-7.346 (m, 5H, 5 x CH, phenyl), 6.631-6.617 (d, 1H, $J = 5.6$, NH, amide), 5.314-5.293 (d, 1H, $J = 8.4$, NH, Cbz), 5.107 (s, 2H, $-\text{CH}_2\text{Ph}$), 4.596-4.544 (m, 1H, αCH , NHCHCH_3 Ala), 4.260-4.205 (m, 1H, δCH , $-\text{NHCHCH}_2$, Leu), 3.748 (s, 3H, OCH_3), 1.732-1.609 (m, 2H, $-\text{CHCH}_2\text{CH}-$, Leu), 1.559-1.489 (m, 1H, $-\text{CH}_2\text{CH}(\text{CH}_3)_2$), 1.398-1.381 (d, 3H, $J = 6.8$, $-\text{CHCH}_3$), 0.949-0.933 (d, 6H, $J = 6.4$, $-\text{CH}(\text{CH}_3)_2$); $^{13}\text{C NMR}$ (100 MHz; CDCl_3): 173.13, 171.76, 156.15, 136.12, 128.49, 128.15, 128.01, 67.01, 53.33, 52.46, 47.97, 41.53, 24.56, 22.87, 21.93, 18.17. **MALDI TOF/TOF** m/z Calcd. for $\text{C}_{18}\text{H}_{26}\text{N}_2\text{O}_5$ ($\text{M} + \text{Na}$) is 373.1739 Observed = 373.2563.

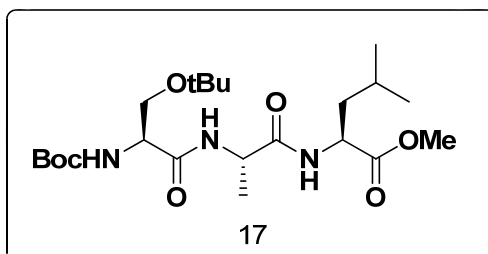


(S)-Methyl 2-(((benzyloxy)carbonyl)amino)-4-methylpentanamido)-3-(1H-indol-3-yl)propanoate (Cbz-Leu-Trp-OMe) (16); White solid, (0.558 g, 60%), $^1\text{H NMR}$ (400 MHz, CDCl_3) δ 8.166 (br. 1H, NH, indole), 7.519-7.499 (d, 1H, $J = 8$, CH, aromatic, indole), 7.338-7.303 (m, 5H, 5 x CH, Phenyl), 7.186-7.073 (m, 2H, 2 x CH aromatic, indole), 6.945 (br., 1H, CH, indole), 6.729-6.711 (d, 1H, $J = 7.2$, NH amide), 5.261-5.240 (d, 1H, $J = 8.4$, NH, Cbz), 5.063-4.984 (m, 2H, $-\text{CH}_2\text{Ph}$), 4.953-4.906 (m, 1H, αCH , $-\text{NHCHCH}_2$), 4.313-4.280 (m, 1H, δCH , $-\text{NHCHCH}_2$ - Leu), 3.665 (s, 3H, OCH_3), 3.301-3.295 (d, 2H, $J = 2.4$, $-\text{CHCH}_2$ -C-), 1.643-1.588 (m, 2H, $-\text{CHCH}_2\text{CH}(\text{CH}_3)_2$), 1.483-1.460 (m, 1H, $-\text{CH}_2\text{CH}(\text{CH}_3)_2$), 0.893-0.887 (d, 6H, $J = 6$, $-\text{CH}(\text{CH}_3)_2$); $^{13}\text{C NMR}$ (100 MHz, CDCl_3) 172.01, 156.08, 135.97, 128.49, 128.00, 127.39, 123.23, 122.07, 119.50, 118.39, 111.26, 109.33, 66.90, 53.38, 52.77, 52.38, 41.50, 27.43, 24.56, 22.88, 21.80. **MALDI TOF/TOF** m/z Calcd. for $\text{C}_{26}\text{H}_{31}\text{N}_3\text{O}_5$ ($\text{M} + \text{Na}$) is 488.2161 Observed = 488.3227.

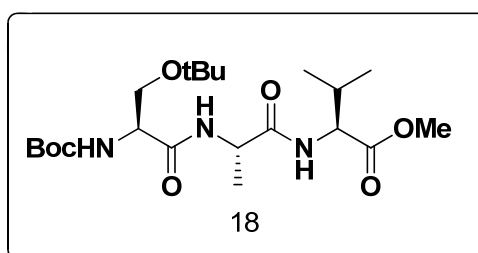


(6S,9S,12S)-Methyl 6-(tert-butoxymethyl)-12-isobutyl-2,2,9-trimethyl-4,7,10-trioxo-3-oxa-5,8,11-triazatridecan-13-oate (Boc-Ser(O^tBu)-Ala-Leu-OMe) (17); White solid (0.587 g, 64%), $^1\text{H NMR}$ (400 MHz; CDCl_3): δ 7.162-7.144 (d, 1H, $J = 7.2$, NH amide, Leu), 6.716-6.697 (d, 1H, $J = 7.6$, NH amide, Ala), 5.433-5.420 (d, 1H, $J = 5.2$, NH Boc), 4.604-4.476 (m, 2H, $-\text{CHCH}_2\text{O}-$), 4.163 (br., 1H, αCH , $-\text{NHCHCH}-$, Leu), 3.796-3.766 (m, 1H, δCH , $-\text{NHCHCH}_3$), 3.722 (s, 3H, OCH_3), 3.405-3.365 (dd, 1H, $J = 7.2$, $-\text{NHCHCH}_2\text{O}-$), 1.661-1.596 (m, 2H, $-\text{CHCH}_2\text{CH}(\text{CH}_3)_2$), 1.567-1.524 (m, 1H, $-\text{CH}_2\text{CH}(\text{CH}_3)_2$), 1.450

(s, 9H, C(CH₃)₃ Boc), 1.389-1.372 (d, 3H, *J* = 6.8, -CHCH₃), 1.183 (s, 9H, -C(CH₃)₃, tButyl), 0.925-0.901 (dd, 6H, *J* = 6, -CH(CH₃)₂). **MALDI TOF/TOF** *m/z* Calcd. for C₂₂H₄₁N₃O₇ (M + Na) is 482.2842 Observed = 482.3709.

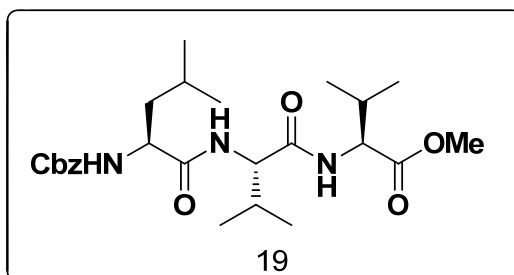


(6*S*,9*S*,12*S*)-Methyl 6-(*tert*-butoxymethyl)-12-isopropyl-2,2,9-trimethyl-4,7,10-trioxo-3-oxa-5,8,11-triazatridecan-13-oate (Boc-Ser(O^tBu)-Ala-Val-OMe) (18); White powder (0.542 g, 61%), ¹H NMR (400 MHz, CDCl₃) δ 7.199-7.186 (d, 1H, *J* = 5.2, NH amide Val), 6.703-6.681 (d, 1H, *J* = 8.8, NH amide, Ala), 5.445-5.434 (d, 1H, *J* = 4.4 NH Boc), 4.545-4.474 (m, 2H, -CHCH₂O-), 4.187 (br., 1H, αCH, -NHCHCH-, Val), 3.814-3.783 (m, 1H, δCH, -NHCHCH₃), 3.741 (s, 3H, OCH₃), 3.428-3.362 (m, 1H, -NHCHCH₂O-, Ser), 2.198-2.129 (m, 1H, -CHCH(CH₃)₂), 1.453 (s, 9H, -C(CH₃)₃ Boc), 1.396-1.378 (d, 3H, *J* = 7.2, -CHCH₃), 1.192 (s, 9H, C(CH₃)₃, ^tButyl); **MALDI TOF/TOF** *m/z* Calcd for C₂₁H₃₉N₃O₇ (M + Na) is 468.2686 Observed = 468.3583.



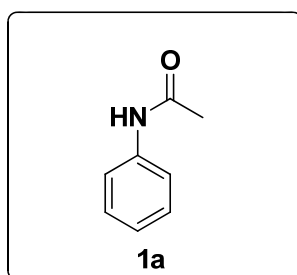
(*S*)-Benzyl 2-(((*S*)-1-(((*S*)-1-methoxy-3-methyl-1-oxobutan-2-yl)amino)-3-methyl-1-oxobutan-2-yl)carbamoyl)-4-methylpentanoate (Cbz-Leu-Val-Val-OMe) (19); White solid (0.620 g, 65%), ¹H NMR (400 MHz; CDCl₃): δ 7.328-7.283 (m, 5H, 5 x CH, Phenyl), 7.192-7.170 (d, 1H, *J* = 8.8, NH amide, Val), 7.016-6.994 (d, 1H, *J* = 8.8, NH amide, Val), 5.848-5.827 (d, 1H, *J* = 8.4, NH Cbz), 5.095-5.076 (d, 2H, *J* = 7.6, CH₂Ph), 4.571-4.537 (m, 1H, αCH, -NHCHCH- Val), 4.457-4.415 (m, 1H, δCH, -NHCHCH- Val), 4.354-4.319 (m, 1H, CH, -NHCHCH₂- Leu), 3.709 (s, 3H, OCH₃), 2.197-2.137 (m, 1H -

CHCH(CH₃)₂), 2.080-2.029 (m, 1H, CH(CH₃)₂), 1.646-1.510 (m, 3H, -CHCH₂CH(CH₃)₂), 0.922-0.850 (m, 18H, -CH(CH₃)₂ x 3 Val, Val, Leu). **MALDI TOF/TOF** *m/z* Calcd. for C₂₅H₃₉N₃O₆ (M + Na) is 500.2737 Observed = 500.3626.

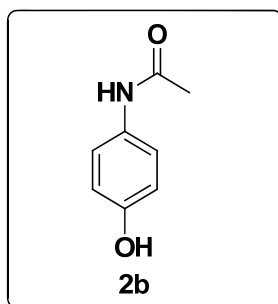


Spectroscopic Data for the compounds from Section 2B

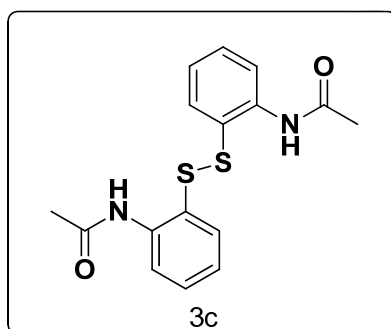
N-phenylacetamide (N-Acyl Aniline) (1a); White powder (0.336 g, 83 %); mp = 112-115 °C; UV (λ_{max}) = 241 nm; IR ν (cm⁻¹) 3293, 1661, 1603, 1550, 1493, 1468, 1435, 1319, 1260, 755, 696; ¹H NMR (400 MHz; CDCl₃): δ 7.70 (br. 1H, NH), 7.52-7.49 (d, 2H, *J* = 8.2, CH x 2, phenyl), 7.32-7.29 (t, 2H, *J* = 7.3, CH x 2, phenyl), 7.12-7.08 (t, 1H, *J* = 7.36, CH x 1, Phenyl), ¹³C NMR (100 MHz; CDCl₃): δ 168.6, 137.8, 128.9, 124.2, 119.9, 24.4 **HRMS (ESI)** *m/z* calcd. for C₈H₁₀NO [M + H]⁺ = 136.0762, observed [M+H]⁺ = 136.0766.



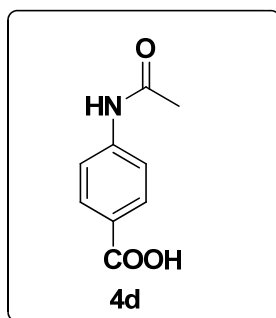
N-(4-Hydroxyphenyl)acetamide (N-Acyl Amino Phenol)(2b); White powder (0.339 g, 75%); mp = 168-171 °C; UV (λ_{max}) = 248 nm; IR ν (cm⁻¹) 3326, 3161, 1655, 1610, 1565, 1506, 1442, 1372, 1259, 1243, 1226, 837, 808, 713, 518 ; ¹H NMR (400 MHz; DMSO-*d*₆): δ 9.64 (br. 1H, -OH, Ph-OH), 9.13 (s, 1H, NH), 7.34-7.32 (d, 2H, *J* = 8.68, CH x 2, Phenyl), 6.67-6.65 (d, 2H, *J* = 8.72, CH x 2, Phenyl), 1.97 (s, 3H, CH₃, COCH₃), ¹³C NMR (100 MHz; DMSO-*d*₆): δ 167.5, 153.1, 131.0, 120.8, 115.6, 23.7; **HRMS (ESI)** *m/z* calcd. for C₈H₁₀NO₂ [M + H]⁺ = 152.0712, observed [M+H]⁺ = 152.0713.



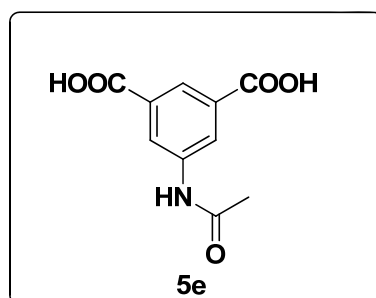
***N,N'*-(Disulfanediyldis(2,1-phenylene))diacetamide (*N*-Acyl 2-Amino Thiophenol) (**3c**);** colourless oil (0.420 g, 84 %); UV (λ_{max}) = 266 nm; IR ν (cm^{-1}) 3063, 2924, 2853, 1698, 1568, 1433, 1306, 1241, 760, 729, 643; $^1\text{H NMR}$ (400 MHz; CDCl_3): δ 7.94-7.92 (d, 2H, $J = 8.24$, CH x 2, Phenyl), 7.78-7.76 (d, 2H, $J = 7.32$, CH x 2, Phenyl), 7.43-7.38 (m, 2H, CH x 2, Phenyl), $^{13}\text{C NMR}$ (100 MHz; CDCl_3): δ 166.7, 153.1, 135.4, 125.7, 124.5, 122.1, 121.1, 19.8; **HRMS (ESI)** m/z calcd. for $\text{C}_{16}\text{H}_{17}\text{N}_2\text{O}_2\text{S}_2$ $[\text{M} + \text{H}]^+ = 333.0731$, observed $[\text{M} + \text{H}]^+ = 333.0737$.



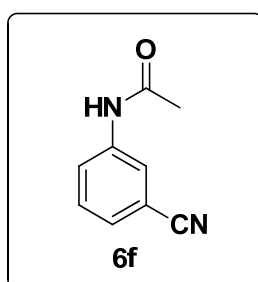
4-Acetamidobenzoic acid (*N*-Acyl 4-Aminobenzoic acid) (4d**);** White powder (0.424 g, 79%); mp = $>320^\circ\text{C}$; UV (λ_{max}) = 266 nm; IR ν (cm^{-1}) 3305, 2924, 1671, 1522, 1426, 1314, 1296, 1264, 768, 701, 546; $^1\text{H NMR}$ (400 MHz; $\text{DMSO-}d_6$): δ 12.66 (br. 1H, OH, -COOH), 10.23 (br., 1H, NH), 7.88-7.86 (d, 2H, $J = 8.72$, CH x 2, Phenyl), 7.69-7.67 (d, 2H, $J = 8.72$, CH x 2, Phenyl), 2.07 (s, 3H, CH_3 , -COCH₃); $^{13}\text{C NMR}$ (100 MHz; $\text{DMSO-}d_6$): δ 168.8, 166.9, 143.3, 130.3, 124.8, 118.1, 24.1; **HRMS (ESI)** m/z calcd. for $\text{C}_9\text{H}_{10}\text{NO}_3$ $[\text{M} + \text{H}]^+ = 180.0661$, observed $[\text{M} + \text{H}]^+ = 180.0663$.



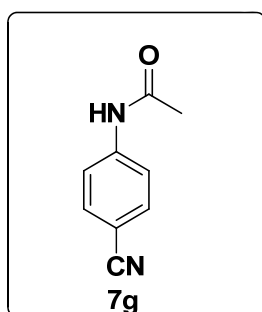
5-Acetamidobenzoic acid (5e); White powder (0.548 g, 82%), mp = 230-232°C; UV (λ_{max}) = 218 nm; IR ν (cm^{-1}) 3741, 3589, 2929, 2315, 1794, 1677, 1547, 1215, 749, 669; $^1\text{H NMR}$ (400 MHz; DMSO- d_6): δ 13.99 (br. 2H, 2 \times -COOH), 10.31 (s, 1H, NH), 8.41-8.41 (d, 2H, J = 1.36, 2 \times CH), 8.14-8.13 (t, 1H, J = 1.36, CH), 2.07 (s, 3H, -COCH₃); $^{13}\text{C NMR}$ (100 MHz; DMSO- d_6): δ 168.8, 166.5, 139.9, 131.6, 124.3, 123.3, 24.0; **HRMS (ESI)** m/z calcd. for C₁₀H₁₀NO₅ [M + H]⁺ = 224.0559, observed = 224.0555.



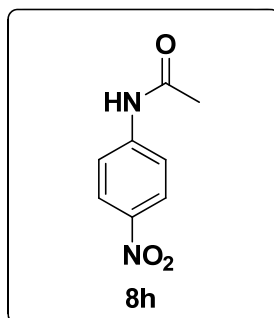
***N*-(3-Cyanophenyl)acetamide (N-Acyl 3 Amino benzonitrile) (6f)**; White powder (0.364 g, 76%); mp = 130-132 °C; UV (λ_{max}) = 221 nm & 248 nm; IR ν (cm^{-1}) 3269, 2226, 1667, 1605, 1586, 1557, 1326, 1294, 1262, 1021, 895, 794, 680, 531; $^1\text{H NMR}$ (400 MHz; DMSO- d_6): δ 10.27 (br., 1H, NH), 8.07 (br. 1H, CH, Phenyl), 7.77-7.74 (m, 1H, CH, Phenyl), 7.53-7.47 (m, 2H, CH \times 2, Phenyl), 2.07 (s, 3H, CH₃, -COCH₃); $^{13}\text{C NMR}$ (100 MHz; DMSO- d_6): δ 168.9, 140.0, 130.2, 126.5, 123.4, 121.5, 118.7, 111.4, 24.0; **HRMS (ESI)** m/z calcd. for C₉H₉N₂O [M + H]⁺ = 161.0715, observed [M+H]⁺ = 161.0720.



***N*-(4-Cyanophenyl)acetamide (*N*- Acyl Benzonitrile) (7g)**; White powder (0.350 g, 73%); mp = 201-204 °C; UV (λ_{\max}) = 217nm & 251 nm; IR ν (cm^{-1}) 3259, 3303, 2221, 1665, 1594, 1541, 1507, 1404, 1361, 1322, 1265, 1175, 836, 546; $^1\text{H NMR}$ (400 MHz; DMSO- d_6): δ 10.36 (br., 1H, NH), 7.74 (br., 4H, CH x 4, Phenyl), 2.08 (s, 3H, CH₃, -COCH₃); $^{13}\text{C NMR}$ (100 MHz; DMSO- d_6): δ 169.1, 143.4, 133.2, 119.0, 118.8, 104.6, 24.1; **HRMS (ESI)** m/z calcd. for C₉H₉N₂O [M + H]⁺ =161.0715 , observed [M+H]⁺=161.0722.

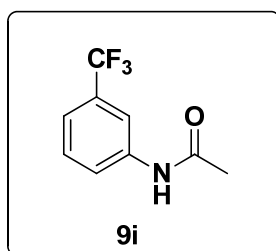


***N*-(4-Nitrophenyl) acetamide (8h)**; Yellowish solid (0.302 g, 56 %); mp = 145-147 °C ; UV (λ_{\max}) = 370 nm; $^1\text{H NMR}$ (400 MHz; CDCl₃): δ 10.56 (br., 1H, NH), 8.22-8.20 (d, 2H, $J = 8$, 2 \times CH), 7.83-7.81 (d, 2H, $J = 8$, 2 \times CH), 2.08 (s, 3H, COCH₃); $^{13}\text{C NMR}$ (100 MHz; CDCl₃): δ 169.4, 145.5, 142.0, 125.0, 118.5, 24.3; **HRMS (ESI)** m/z calcd. for C₈H₉N₂O₃ [M + H]⁺ = 181.0613, observed = 181.0614.

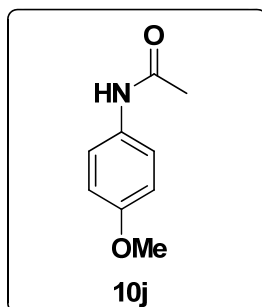


***N*-(3-(Trifluoromethyl)phenyl) acetamide (9i)**; White powder (0.535 g, 88%); mp = 109-111°C; UV (λ_{\max}) = 220 nm; IR ν (cm^{-1}) 3306, 3282, 1661, 1607, 1554, 1446, 1327, 1284, 1212, 1175, 1114, 1068, 1019, 895, 792, 696, 667; $^1\text{H NMR}$ (400 MHz; CDCl₃): δ 7.79 (br. 1H, NH), 7.73-7.72 (d, 1H, $J = 7.8$, CH), 7.67 (br. 1H, CH), 7.44-7.34 (m, 2H, 2 \times CH), 2.20 (s, 3H, -COCH₃); $^{13}\text{C NMR}$ (100 MHz; CDCl₃): δ 168.6, 138.3, 129.5, 125.1,

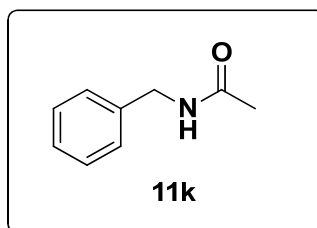
122.8, 120.8, 118.8, 116.4, 24.5; **HRMS (ESI)** m/z calcd. for $C_9H_9F_3NO$ $[M + H]^+ = 204.0636$, observed = 204.0642.



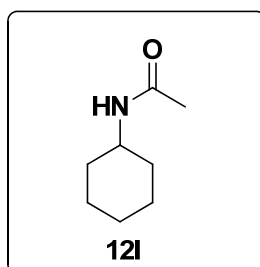
4-Methoxyaniline (N-Acyl Anisidine) (10j); White powder (0.420 g, 85%); mp = 128-130 °C; UV (λ_{max}) = 248 nm; IR ν (cm^{-1}) 3243, 1647, 1606, 1560, 1512, 1465, 1455, 1410, 1368, 1303, 1285, 1246, 1031, 838; 1H NMR (400 MHz; $CDCl_3$): δ 7.40-7.37 (d, 3H, $J = 9.16$, CH x 2 & NH), 6.85-6.83 (d, 2H, $J = 9.16$, CH x 2, Phenyl), 3.78 (s, 3H, CH_3 , -OCH₃), 2.14 (s, 3H, CH_3 , -COCH₃), ^{13}C NMR (100 MHz; $CDCl_3$): δ 168.3, 156.3, 130.9, 121.9, 114.0, 55.4, 24.2; **HRMS (ESI)** m/z calcd. for $C_9H_{12}NO_2$ $[M + H]^+ = 166.0868$, observed $[M+H]^+ = 166.0872$.



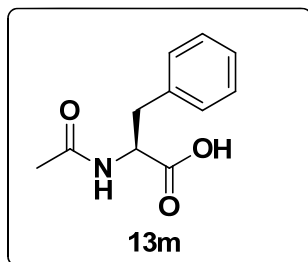
N-Benzylacetamide (N-Acyl Benzylamine) (11k); White powder (0.362 g, 81%); mp = 62-64 °C; UV (λ_{max}) = 213 nm; IR ν (cm^{-1}) 3294, 1647, 1545, 1499, 1374, 1357, 1282, 1067, 1032, 751, 741, 696, 606, 503; 1H NMR (400 MHz; $CDCl_3$): δ 7.33-7.24 (m, 5H, CH x 5, Phenyl), 6.21 (br., 1H, NH), 4.38-4.36 (d, 2H, $J = 5.5$, CH₂, -CH₂-Ph), 1.97 (s, 3H, CH_3 , -COCH₃), ^{13}C NMR (100 MHz; $CDCl_3$): δ 170.0, 138.1, 128.5, 127.7, 127.3, 43.5, 23.0 **HRMS (ESI)** m/z calcd. For $C_9H_{12}NO$ $[M + H]^+ = 150.0919$, observed $[M+H]^+ = 150.0910$.



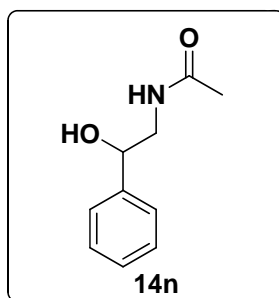
N-Cyclohexylacetamide (N-Acyl Cyclohexylamine) (12l); White powder (0.321 g, 76%); mp = 109-111°C; IR ν (cm⁻¹) 3290, 2932, 2851, 1639, 1557, 1443, 1373, 1314, 1154, 1116, 980, 892, 736, 606, 550; ¹H NMR (400 MHz; CDCl₃): δ 5.68 (br., 1H, NH), 3.76-3.66 (m, 1H, CH, -CH₂CH(NH)CH₂-), 1.92 (s, 3H, CH₃, -COCH₃), 1.89-1.86 (dd, 2H, *J* = 3.2, CH x 2, -CHCHCH-), 1.70- 1.55 (m, 3H, -CHCHCH- CH x 3), 1.37-1.28 (m, 2H, CH₂, -CH₂CH₂CH₂-), 1.17-1.04 (m, 3H, CH x 3, -CHCHCH-); ¹³C NMR (100 MHz; CDCl₃): δ 169.1, 48.1, 33.0, 25.4, 24.8, 23.0; **HRMS (ESI)** *m/z* calcd. for C₈H₁₆NO [M + H]⁺ = 142.1232, observed [M+H]⁺ = 142.1232.



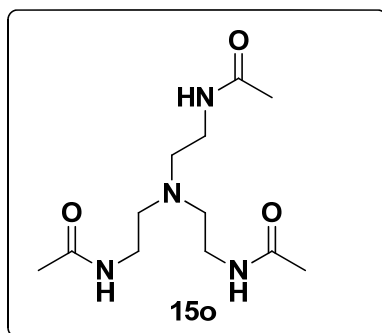
2-Acetamido-3-phenylpropanoic acid (N-Acyl Phenylalanine) (13m); White powder (0.558 g, 90%); mp = 170-174 °C; UV (λ_{\max}) = 206 nm; IR ν (cm⁻¹) 3329, 1697, 1624, 1555, 1438, 1276, 1243, 1117, 707; ¹H NMR (400 MHz; DMSO-*d*₆): δ 12.66 (br., 1H, -OH, -COOH), 8.19-8.17 (d, 1H, *J* = 8.24, NH), 7.29-7.18 (m, 5H, CH x 5, Phenyl), 4.42-4.36 (m, 1H, CH, -NHCHCH₂-), 3.05-3.01 & 2.85-2.79 (dd & dd 2H, *J* = 5.04 & *J* = 9.6, -CHCH₂Ph), 1.77 (s, 3H, CH₃ -COCH₃); ¹³C NMR (100 MHz; DMSO-*d*₆): δ 173.1, 169.2, 137.7, 129.0, 128.1, 126.3, 53.4, 36.7, 22.3; **HRMS (ESI)** *m/z* calcd. For C₁₁H₁₄NO₃ [M + H]⁺ = 208.0974, observed [M+H]⁺ = 208.0969.



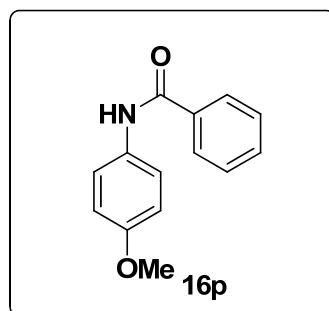
***N*-(2-Hydroxy-2-phenylethyl)acetamide (*N*-Acyl Phenylglycine) (14n)**; Colourless oil (0.434 g, 81%); UV (λ_{max}) = 202 nm; IR ν (cm^{-1}) 3280, 2929, 1646, 1547, 1373, 1295, 1215, 1073, 1041, 754, 668; $^1\text{H NMR}$ (400 MHz; DMSO- d_6): δ 8.24-8.22 (d, 1H, J = 8.24, 1H, NH), 7.30-7.19 (m, 5H, CH x 5, Phenyl), 4.86-4.79 (m, 2H, -CH-OH), 3.54-3.51 (t, 2H, J = 5.9, CH_2 , - CH_2NHCO -), 1.86 (s, 3H, CH_3 , - COCH_3), $^{13}\text{C NMR}$ (100 MHz; DMSO- d_6): δ 168.8, 141.4, 128.0, 126.9, 126.7, 64.7, 54.9, 22.7; **HRMS (ESI)** m/z calcd. for $\text{C}_{10}\text{H}_{14}\text{NO}_2$ $[\text{M} + \text{H}]^+ = 180.1025$, observed $[\text{M} + \text{H}]^+ = 180.1024$.



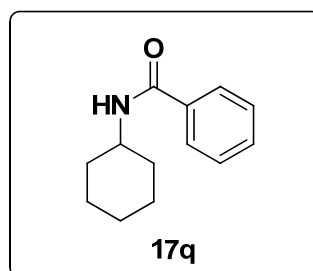
***N,N',N''*-(nitrilotris(ethane-2,1-diyl))triacetamide(15o)**; Yellowish oil (0.473 g, 84%); IR ν (cm^{-1}) 3282, 1633, 1546, 1435, 1371, 1291, 1169, 749; $^1\text{H NMR}$ (400 MHz; DMSO- d_6): δ 7.79-7.76 (t, 3H, J = 5.04, NH x 3), 3.07-3.02 (q, 6H, J = 6.4, CH_2 , - $\text{CH}_2\text{CH}_2\text{NH}$ -), 2.45-2.42 (t, 6H, J = 6.4, CH_2 , - $\text{NCH}_2\text{CH}_2\text{NH}$ -), 1.80 (s, 9H, CH_3 x 3, - COCH_3 x 3); $^{13}\text{C NMR}$ (100 MHz; DMSO- d_6): δ 169.7, 53.5, 37.1, 22.7; **HRMS (ESI)** m/z calcd. For $\text{C}_{12}\text{H}_{25}\text{N}_4\text{O}_3$ $[\text{M} + \text{H}]^+ = 273.1927$, observed $[\text{M} + \text{H}]^+ = 273.1930$.



***N*-(4-Methoxyphenyl)benzamide (*N*-Benzoyl Anisidine) (16p)**; White powder (0.681 g, 82%); mp = > 320 °C; UV (λ_{max}) = 223 nm & 277 nm; IR ν (cm^{-1}) 3330, 1646, 1529, 1514, 1414, 1270, 1249, 1032, 825, 716; $^1\text{H NMR}$ (400 MHz; CDCl_3): δ 7.87-7.85 (d, 3H, $J = 7.36$, CH x 2, Phenyl), 7.55-7.45 (m, 5H, CH x 5, Phenyl), 6.91-6.89 (d, 2H, $J = 8.68$, CH x 2, Phenyl), 3.81 (s, 3H, $-\text{COCH}_3$); $^{13}\text{C NMR}$ (100 MHz; CDCl_3): δ 160.3, 156.5, 134.9, 131.6, 130.9, 128.7, 126.9, 122.1, 114.1, 55.4; **HRMS (ESI)** m/z calcd. for $\text{C}_{14}\text{H}_{14}\text{NO}_2$ $[\text{M} + \text{H}]^+ = 228.1025$, observed = 228.1048.

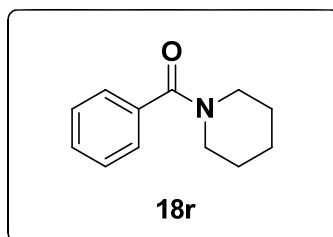


***N*-Cyclohexylbenzamide (*N*-Benzoyl Cyclohexylamine) (17q)**; White powder (0.535 g, 88%); mp = 151-153 °C; UV (λ_{max}) = 224 nm; IR ν (cm^{-1}) 3238, 2928, 2851, 1638, 1626, 1577, 1560, 1453, 1330, 1089, 700; $^1\text{H NMR}$ (400 MHz; CDCl_3): δ 7.76-7.74 (m, 2H, CH x 2, Phenyl), 7.50-7.40 (m, 3H, CH x 3, Phenyl), 6.01-6.00 (d, 1H, $J = 4.56$, NH), 4.03-3.93 (m, 1H, $\text{CH}_2\text{CH}(\text{NH})\text{CH}_2$), 2.05-2.01 (dd, 2H, $J = 3.68$, $-\text{CH}_2\text{CH}_2\text{CH}-$), 1.78-1.63 (m, 4H, $-\text{CH}_2\text{CHCH}_2-$), 1.48-1.37 (m, 2H, $\text{CH}_2\text{CH}_2\text{CH}_2$), 1.29-1.18 (m, 3H, $\text{CH}_2\text{CH}_2\text{CH}_2$); $^{13}\text{C NMR}$ (100 MHz; CDCl_3): δ 166.6, 135.0, 131.2, 128.4, 126.7, 48.6, 33.2, 25.5, 24.8; **HRMS (ESI)** m/z calcd. For $\text{C}_{13}\text{H}_{18}\text{NO}$ $[\text{M} + \text{H}]^+ = 204.1388$, observed = 204.1393.

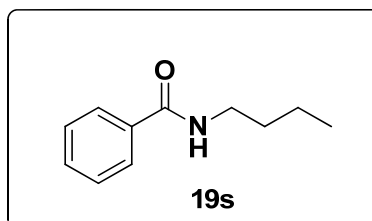


Phenyl(piperidin-1-yl) methanone (18r); Colourless oil (0.408 g, 72%); UV (λ_{max}) = 224 nm; IR ν (cm^{-1}) 2929, 2856, 1736, 1632, 1442, 1371, 1277, 1237, 1043, 913, 775, 729; $^1\text{H NMR}$ (400 MHz; CDCl_3): δ 7.98-7.96 (d, 2H, $J = 7.32$, $2 \times \text{CH}$), 7.46-7.43 (t, 1H, $J = 5.9$, CH), 7.34-7.30 (t, 2H, $J = 7.8$, $2 \times \text{CH}$), 3.6 (br., 2H, CH_2), 3.2 (br., 2H, CH_2), 1.81-1.78 (d, 1H, $J = 12$, CH), 1.39 (br., 2H, CH_2), 1.25-0.97 (m, 3H, $3 \times \text{CH}$); $^{13}\text{C NMR}$ (100

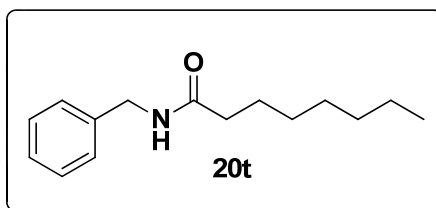
MHz; CDCl₃): δ 170.4, 136.1, 133.2, 129.9, 129.3, 128.3, 126.7, 49.2, 48.7, 26.4, 25.4, 24.7, 24.4; **HRMS (ESI)** m/z calcd. for C₁₂H₁₆NO [M + H]⁺ = 190.1232, observed = 190.1229.



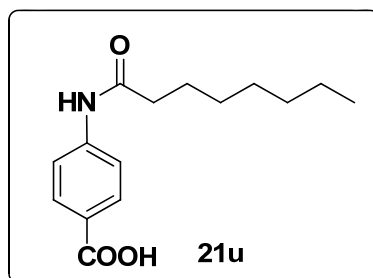
N-Butylbenzamide (N-Benzoyl n-Butylamine) (19s); colourless oil (0.472 g, 89%); UV (λ_{\max}) = 224 nm; IR ν (cm⁻¹) 3317, 2959, 2930, 2867, 1639, 1542, 1489, 1460, 1306, 701; **¹H NMR** (400 MHz; CDCl₃): δ 7.77-7.74 (d, 2H, J = 8.72, CH x 2, Phenyl), 7.50-7.39 (m, 3H, CH x 3, Phenyl), 6.27 (br. 1H, NH), 3.47-3.42 (q, 2H, J = 6, -CH₂CH₂NH-), 1.63-1.55 (q, 2H, J = 7.32, -CH₂CH₂CH₂-), 1.45-1.36 (q, 2H, J = 7.32, CH₃CH₂CH₂-), 0.97-0.93 (t, 3H, J = 7.24, CH₃CH₂-); **¹³C NMR** (100 MHz; DMSO-*d*₆): δ 167.5, 134.7, 131.2, 128.4, 126.7, 39.7, 31.6, 20.1, 13.7; **HRMS (ESI)** m/z calcd. for C₁₁H₁₆NO [M + H]⁺ = 178.1232, observed [M+H]⁺ = 178.1236.



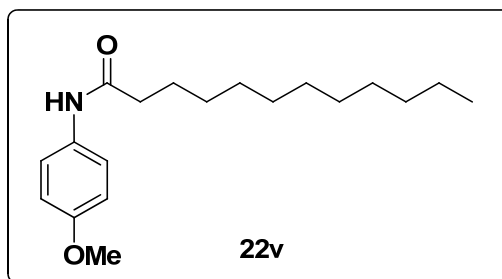
N-benzylloctanamide (20t); White powder (0.643 g, 92%); mp = 70-72 °C; UV (λ_{\max}) = 213 nm; IR ν (cm⁻¹) 3291, 2921, 2854, 1632, 1553, 1444, 732, 692; **¹H NMR** (400 MHz; CDCl₃): δ 7.35-7.26 (m, 5H, CH x 5, Phenyl), 5.83 (br., 1H, NH), 4.44-4.43 (d, 2H, J = 5.96, -CHCH₂Ph), 2.22-2.19 (t, 2H, J = 7.76, -COCH₂CH₂-), 1.69-1.61 (q, 2H, J = 7.8, -COCH₂CH₂CH₂-), 1.30-1.27 (m, 8H, CH₂ x 8), 0.89-0.86 (t, 3H, J = 6.84, CH₃CH₂CH₂-); **¹³C NMR** (100 MHz; CDCl₃): δ 173.0, 138.3, 128.6, 127.7, 127.4, 43.5, 36.7, 31.6, 29.2, 28.9, 25.7, 22.5, 14.0; **HRMS (ESI)** m/z calcd. for C₁₅H₂₄NO [M + H]⁺ = 234.1858, observed = 234.1861.



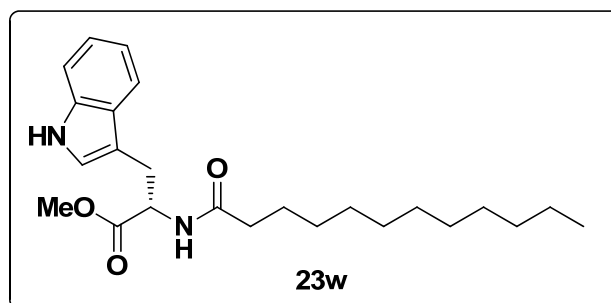
4-Octanamidobenzoic acid (21u); White powder (0.702 g, 89%); mp = 176-178 °C; UV (λ_{max}) = 214 nm; IR ν (cm^{-1}) 3319, 2924, 2855, 1666, 1607, 1591, 1519, 1509, 1427, 1404, 1322, 1300, 1250, 1181, 769; $^1\text{H NMR}$ (400 MHz; DMSO- d_6): δ 12.62 (br., 1H, -OH, -COOH), 10.17 (s, 1H, NH), 7.87-7.85 (d, 2H, J = 8.68, CH x 2, Phenyl), 7.71-7.68 (d, 2H, J = 9.16, CH x 2, Phenyl), 2.34-2.30 (t, 2H, J = 7.8, -COCH₂CH₂-), 1.59-1.56 (t, 2H, J = 6.88, -COCH₂CH₂CH₂-), 1.27-1.23 (m, 8H, CH₂ x 4), 0.86-0.82 (t, 3H, J = 6.88, CH₃CH₂CH₂-); $^{13}\text{C NMR}$ (100 MHz; DMSO- d_6): δ 171.8, 166.9, 143.4, 130.3, 124.8, 118.2, 36.5, 31.2, 28.5, 25.0, 22.1, 13.9; HRMS (ESI) m/z calcd. For C₁₅H₂₂NO₃ [M + H]⁺ = 264.1600, observed = 264.1604.



N-(4-methoxyphenyl)dodecanamide (22v); White powder (0.713 g, 78 %); mp = 90-92 °C; UV (λ_{max}) = 249 nm; IR ν (cm^{-1}) 3238, 2928, 2851, 1626, 1638, 1577, 1560, 1453, 1330, 1082, 700; $^1\text{H NMR}$ (400 MHz; CDCl₃): δ 7.42-7.39 (d, 2H, J = 9.16, CH x 2, Phenyl), 6.85-6.83 (d, 2H, J = 16, CH x 2, Phenyl), 3.78 (s, 3H, CH₃, -OCH₃), 2.35-2.30 (m, 2H, -COCH₂CH₂-), 1.74-1.67 (m, 2H, -COCH₂CH₂CH₂-), 1.25 (br., 16H, CH₂ x 8), 0.89-0.86 (t, 3H, J = 6.44, CH₃CH₂CH₂-); $^{13}\text{C NMR}$ (100 MHz; CDCl₃): δ 171.4, 156.2, 131.0, 121.7, 114.0, 55.4, 37.6, 33.9, 31.8, 29.5, 29.3, 25.7, 22.6, 14.0; HRMS (ESI) m/z calcd. for C₁₉H₃₂NO₂ [M + H]⁺ = 306.2433, observed = 306.2431.



(S)-Methyl 2-dodecanamido-3-(1H-indol-3-yl)propanoate (23w); Colourless oil (0.996 g, 83%); UV (λ_{max}) = 221nm; IR ν (cm^{-1}) 3305, 2924, 2852, 1737, 1652, 1517, 1458, 1370, 1236, 1100, 1044, 912, 733; $^1\text{H NMR}$ (400 MHz; CDCl_3): δ 8.30 (br. 1H, NH), 7.54-7.52 (d, 1H, $J = 7.8$, CH), 7.37-7.35 (d, 1H, $J = 8.2$, CH), 7.21-7.17 (t, 1H, $J = 6.88$, CH), 7.13-7.09 (t, 1H, $J = 7.3$, CH), 6.97-6.97 (d, 1H, $J = 1.8$, CH), 6.02-6.00 (d, 1H, $J = 7.8$, NH), 6.99-6.95 (m, 1H, CH α Trp), 3.69 (s, 3H, $-\text{OCH}_3$, Trp), 3.33-3.31 (m, 2H, CH_2 , Trp), 2.16-2.12 (t, 2H, $J = 7.8$, $-\text{CH}_2-\text{CH}_2\text{CO}-$), 1.58-1.54 (t, 2H, $J = 6.8$, CH_2), 1.24 (br, 16H, 8 x CH_2), 0.90-0.86 (t, 3H, $J = 6.4$, $\text{CH}_3-\text{CH}_2-\text{CH}_2-$); $^{13}\text{C NMR}$ (100 MHz; CDCl_3): δ 172.8, 172.5, 122.6, 122.1, 119.8, 118.5, 111.2, 110.0, 52.8, 52.3, 36.5, 31.8, 29.6, 29.5, 29.4, 29.2, 29.1, 27.6, 25.4, 22.6, 14.1; **HRMS (ESI)** m/z calcd. For $\text{C}_{24}\text{H}_{37}\text{N}_2\text{O}_3$ $[\text{M} + \text{H}]^+ = 401.2804$, observed = 401.2795.



2.3 Reference

1. Nelson, D. L.; Cox, M. M. "*Lehninger Principles of Biochemistry*" 3rd ed. Worth Publishing: New York, **2000**.
2. a) Fischbach, M. A.; Walsh, C. T. *Chem Rev.* **2006**, *106*, 3468; b) Sieber, S. A.; Marahiel, M. A. *Chem. Rev.* **2005**, *105*, 715.
3. Curtius, T. *J. Prakt. Chemie* **1882**, *26*, 145.
4. Fisher, E.; Fourneau, E. *Ber. Dtsch.chem.Ges.* **1901**, *34*, 2868.
5. Curtius, T. *J. Prakt. Chemie* **1904**, *70*, 57.
6. Fisher, E. *Ber. Dtsch chem. Ges.* **1905**, *38*, 605.
7. a) Carpino, L. A. *J. Am. Chem. Soc.* **1957**, *79*, 4427; b) McKay, F. C.; Albertson, N. F. *J. Am. Chem. Soc.* **1957**, *79*, 4686.
8. Sheehan, J. C., Hess, G. P. *J. Am. Chem. Soc.* **1955**, *77*, 1067.
9. a) El-Faham, A.; Albericio, A. *Chem. Rev.* **2011**, *111*, 6557; b) Valeur, E.; Bradley, M. *Chem. Soc. Rev.* **2009**, *38*, 606; c) Lloyd-Williams, P.; Albericio, F.; Giralt, E. *Chemical Approaches to the Synthesis of Peptides and Proteins*, CRC, Boca Raton, **1997**; d) Allen, C. L.; Williams, J. M. J. *Chem. Soc. Rev.*, **2011**, *40*, 3405.
10. Merrifield, R. B. *J. Am. Chem. Soc.* **1963**, *85*, 2149.
11. a) Kemp, D. S.; Leung, S. L.; Kerkman, D. J. *Tetrahedron lett.* **1981**, *22*, 181; b) Kemp, D. S.; Kerkman, D. J. *Tetrahedron lett.* **1981**, *22*, 185.
12. Wieland, T.; Bokelmann, E.; Bauer, L.; Lang, H. U.; Lau, H. *Justus Liebigs Ann. Chem* *583*, 129.
13. Kemp, D. S.; Galakatos, N. G.; Bowen, B.; Tan, K. *J. Org. Chem.* **1986**, *51*, 1829.
14. Schnolzer, M.; Kent, S. B. H. *Science* **1992**, *256*, 221.
15. Dawson, P. E.; Churchill, M. J.; Ghadiri, M. R.; Kent, S. B. H., *J. Am. Chem. Soc.* **1997**, *119*, 4325.
16. Tam, J. P.; Yu, Q. *Biopolymers*, **1998**, *46*, 319.
17. a) Quaderer, R.; Sewing, A.; Hilvert, D. *Helv. Chim. Acta.* **2001**, *84*, 1197; b) Quaderer, R.; Hilver, D. *Chem. Comm.* **2002**, *12*, 2620.
18. a) Gieselman, M. D.; Xie, L.; van der Donk, W. A. *Org. Lett.* **2001**, *3*, 1331; b) Gieselman, M. D.; Zhu, Y.; Zhou, H.; Galoni, D.; van der Donk, W. A. *ChemBioChem*, **2002**, *3*, 709.
19. Canne, L. E.; Bark, S. J.; Kent, S. B. H. *J. Am. Chem. Soc.* **1996**, *118*, 5891.

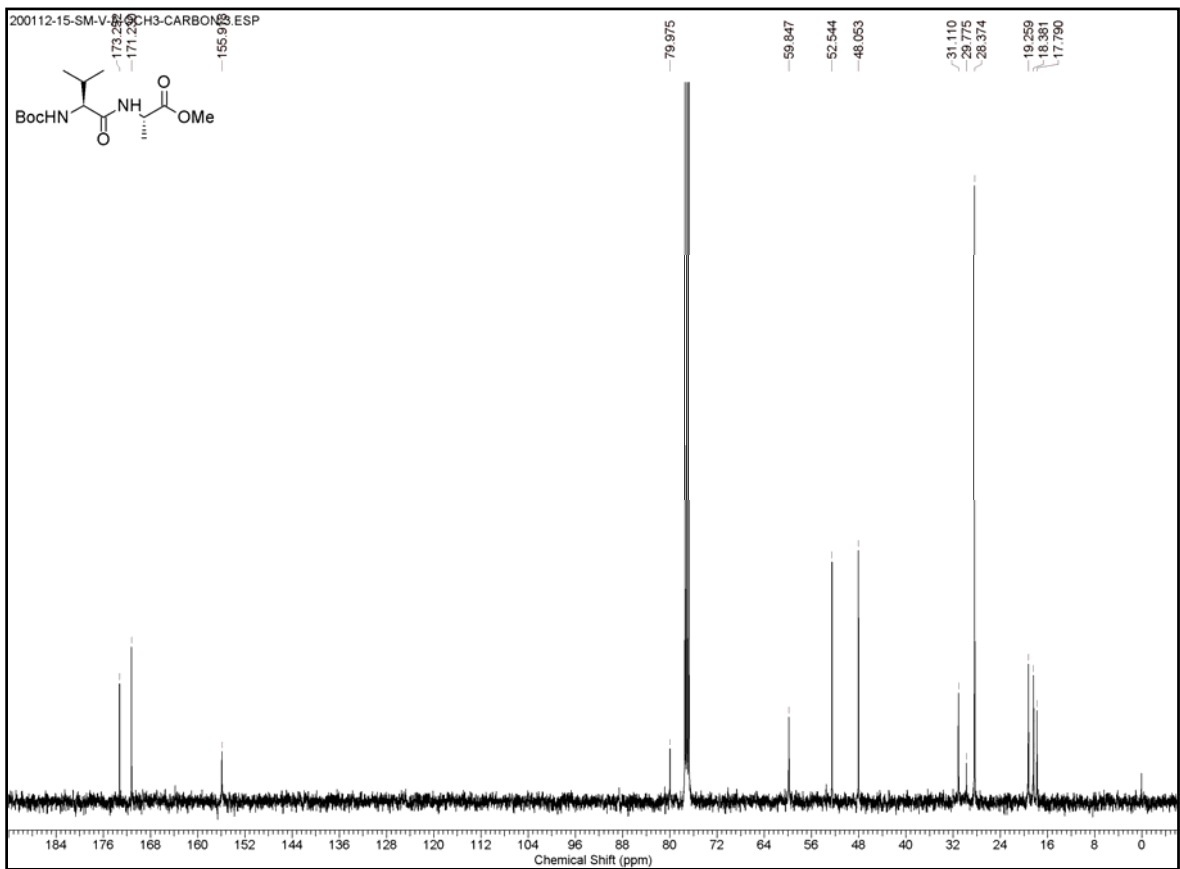
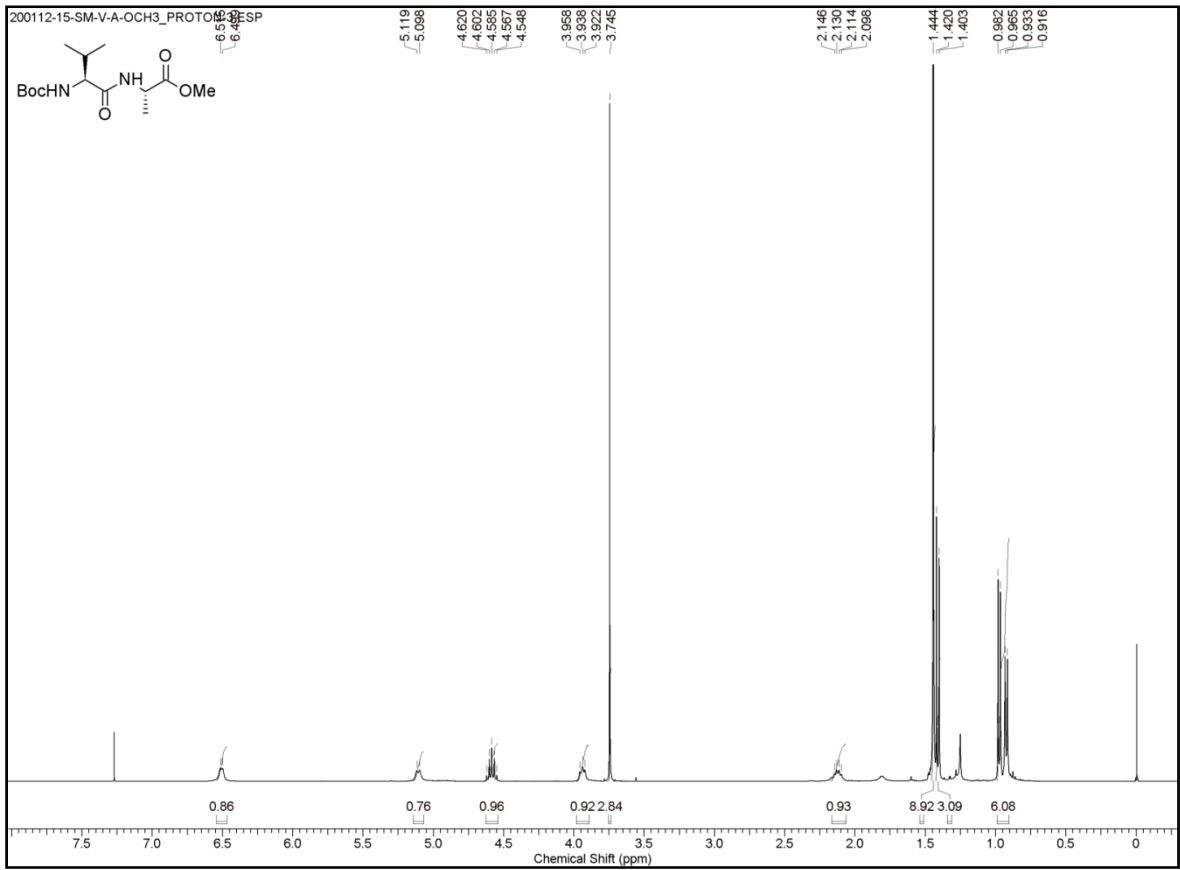
20. a) Nilsson, B. L.; Kiessling, L. L.; Raines, R. T. *Org. Lett.* **2000**, *2*, 1939; b) Nilsson, B. L.; Kiessling, L. L.; Raines, R. T. *Org. Lett.* **2001**, *3*, 9; c) Nilsson, B. L.; Hondal, R. J.; Soellener, M. B.; Raines, R. T. *J. Am. Chem. Soc.* **2003**, *125*, 5268.
21. a) Saxon, E.; Bertozzi, C. R. *Science*, **2000**, *287*, 2007; b) Saxon, E.; Armstrong, J. I.; Bertozzi, C. R. *Org. Lett.*, **2000**, *2*, 2141.
22. Huber, C.; Wachtershauser, G. *Science*, **1997**, *276*, 245.
23. C. de Duve. *Blueprint for cell* (Neil Patterson Burlington, NC, 1991)
24. Leu, R.; Orgel, L. E. *Nature* **1997**, *389*, 52.
25. Crich, D.; Sana, K.; Guo, S. *Org. Lett.* **2007**, *9*, 4423.
26. Rao, Y.; Li, X.; Danishefsky, S. J. *J. Am. Chem. Soc.* **2009**, *131*, 12924.
27. Crich, D.; Sasaki, K. *Org. Lett.* **2009**, *11*, 3514.
28. a) Wang, P.; Li, X.; Zhu, J.; Chen, J.; Yuan, Y.; Wu, X.; Danishefsky, S. J. *J. Am. Chem. Soc.* **2011**, *133*, 1597; b) Wang, P.; Danishefsky, S. J.; *J. Am. Chem. Soc.* **2010**, *132*, 17045.
29. Pan, J.; Devarie-Baez, N. O.; Xian, M. *Org. Lett.* **2011**, *13*, 1092.
30. Wu, W.; Zhang, Z.; Liebeskind, L. S. *J. Am. Chem. Soc.* **2011**, *133*, 14256.
31. a) Blake, J. J. *Int. J. Pept. Prot. Res.* **1981**, *17*, 273; b) Blake, J.; Li, C. H. *Proc. Natl. Acad. Sci. U.S.A.* **1981**, *78*, 4055.
32. a) Wang, P.; Danishefsky, S. J. *J. Am. Chem. Soc.*, **2010**, *132*, 17045; b) Maurel, M.-C.; Orgel, L. E. *Orig Life Evol Biosph.* **2000**, *30*, 423.
33. a) Greenwood, N. N.; Earnshaw, A. *Chemistry of Elements*, 2nd Ed., Elsevier, **2005**; b) Zhao, Y.; Pan, H.; Lou, Y.; Qiu, X.; Zhu, J.; Burda, C. *J. Am. Chem. Soc.* **2009**, *131*, 4253.
34. a) Ryadnov, M. G.; Klimenko, L. V.; Mitin, Y. V.; *J. Pept. Res.* **1999**, *53*, 322; b) Thieriet, N.; Guibé, F.; Albericio, F. *Org. Lett.* **2000**, *2*, 1815; c) Coste, J.; Le-Nguyen, D.; Castro, B. *Tetrahedron Lett.* **1990**, *31*, 205.
35. Goldstein, A. S.; Gelb, M. H. *Tetrahedron Lett.*, **2000**, *41*, 2797.
36. a) Tsogoeva, S. B. *Eur. J. Org. Chem.* **2007**, 1701; b) Perlmutter, P.; *Conjugate Addition Reactions in Organic Synthesis*; Pergamon: Oxford, **1992**
37. a) Larock, R. C. *Comprehensive Organic Transformations*, 2nd ed.; VCH: Weinheim, **1989**; b) Greene, T. W.; Wuts, P. G. M. *Protective Groups in Organic synthesis*, 3rd ed., John Wiley & Sons, Inc., New York, **1999**, 150.

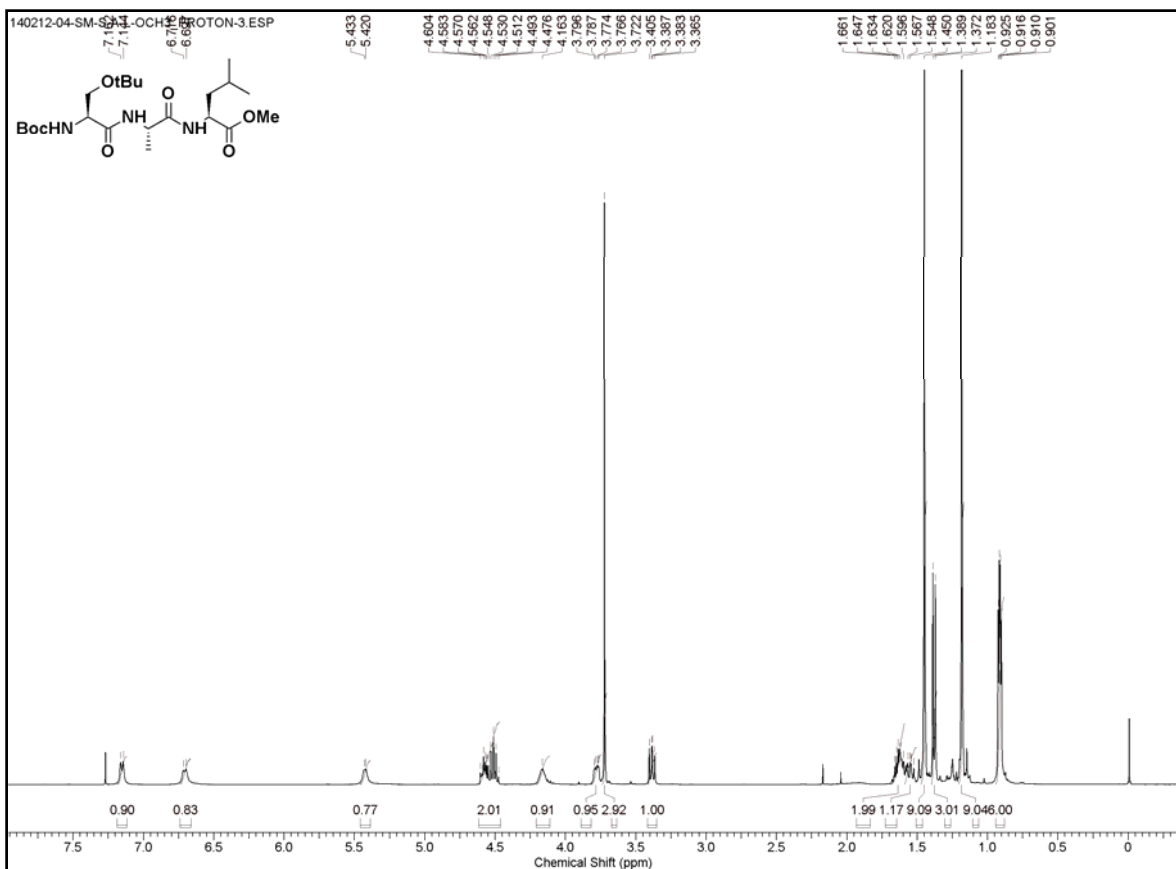
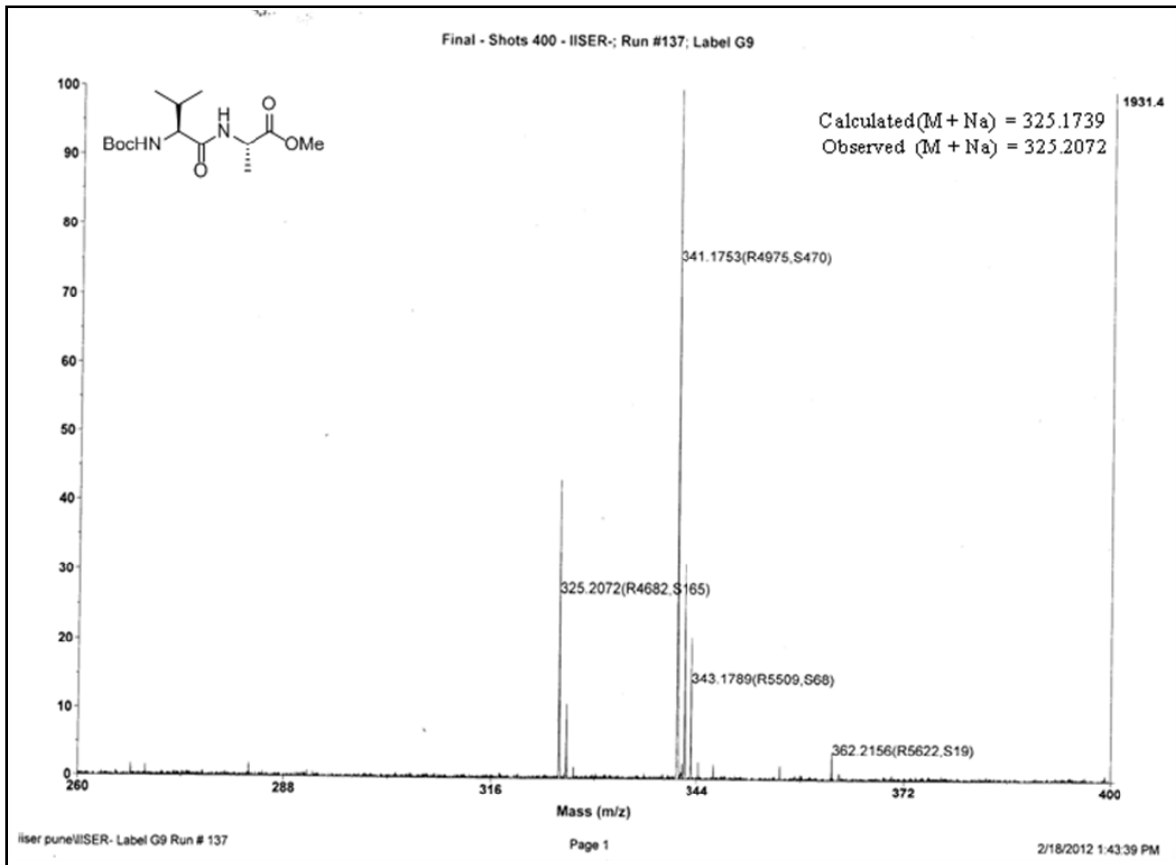
38. a) Humphrey, J. M.; Chamberlin, A. R. *Chem. Rev.* **1997**, *97*, 2243; b) Scozzafava, A.; Owa, T.; Mastrolorenzo, A.; Supuran, C. T. *Curr. Med. Chem.* **2003**, *10*, 925; c) Carey, J. S.; Laffan, D.; Thomson, C.; Williams, M. T. *Org. Biomol. Chem.* **2006**, *4*, 2337; d) Abbate, F.; Supuran, C. T.; Scozzafava, A.; Orioli, P.; Stubbs, M. T.; Klebe, G. *J. Med. Chem.* **2002**, *45*, 3583.
39. a) Vogel, A. *Practical Organic Chemistry*; Langman Scientific & Technical and Wiley: New York, **1989**; pp 708. b) March, J. *Advanced Organic Chemistry*, 4th ed.; John Wiley & Sons: New York, **1992**; pp 416. c) Baker, R. H.; Bordwell, F. G. *Organic Syntheses*; Wiley: New York, **1955**; Collect. Vol. III, p 141.
40. a) Allen, C. L.; Williams, J. M. J. *Chem. Soc. Rev.*, **2011**, *40*, 3405; b) Cossy, J.; Palegrosdemange, C. *Tetrahedron Lett.*, **1989**, *30*, 2771; c) Spivey, A. C.; Arseniyadis, S. *Angew. Chem., Int. Ed.* **2004**, *43*, 5436.
41. Taylor, J. E.; Jones, M. D.; Williams, J. M. J.; Bull, S.D. *J. Org. Chem.* **2012**, *77*, 2808.
42. a) Owston, N. A.; Parker, A. J.; Williams, J. M. J. *Org. Lett.* **2007**, *9*, 3599; b) Ramalingan, C.; Park, Y. -T. *J. Org. Chem.* **2007**, *72*, 4536.
43. a) Yoo, W.-J.; Li, C.-J. *J. Am. Chem. Soc.* **2006**, *128*, 13064; b) Ekoue-Kovi, K.; Wolf, C. *Chem.-Eur. J.* **2008**, *14*, 6302; and references therein
44. a) Yang, X.; Birman, V. B. *Org. Lett.* **2009**, *11*, 1499; b) Miller, S. J. *Acc. Chem. Res.* **2004**, *37*, 601; c) Ishihara, K.; Kosugi, Y.; Akakura, M. *J. Am. Chem. Soc.* **2004**, *126*, 12212.
45. a) Katritzky, A. R.; He, H. -Y.; Suzuki, K. *J. Org. Chem.* **2000**, *65*, 8210; b) Katritzky, A. R.; Suzuki, K.; Wang, Z. Synlett, **2005**, 1656; c) Katritzky, A. R.; Rogovoy, B. V.; Kirichenko, N.; Vvedensky, V. *Bioorg. Med. Chem. Lett.* **2002**, *12*, 1809.
46. a) Shangguan, N.; Katukojvala, S.; Greenberg, R.; Williams, L. J. *J. Am. Chem. Soc.* **2003**, *125*, 7754; b) Crich, D.; Sharma, I. *Angew. Chem., Int. Ed.* **2009**, *48*, 2355.
47. Dyer, F. B.; Park, C. M.; Joseph, R.; Garner, P. *J. Am. Chem. Soc.* **2011**, *133*, 20033; d) Joseph, R.; Dyer, F. B.; Garner, P. *Org. Lett.* **2013**, *15*, 732.
48. Mali, S. M.; Jadhav, S.V.; Gopi, H. N. *Chem. Commun.* **2012**, *48*, 7085.
49. Naik, S.; Bhattacharjya, G.; Talukdar, B.; Patel, B. K. *Eur. J. Org. Chem.* **2004**, 1254.

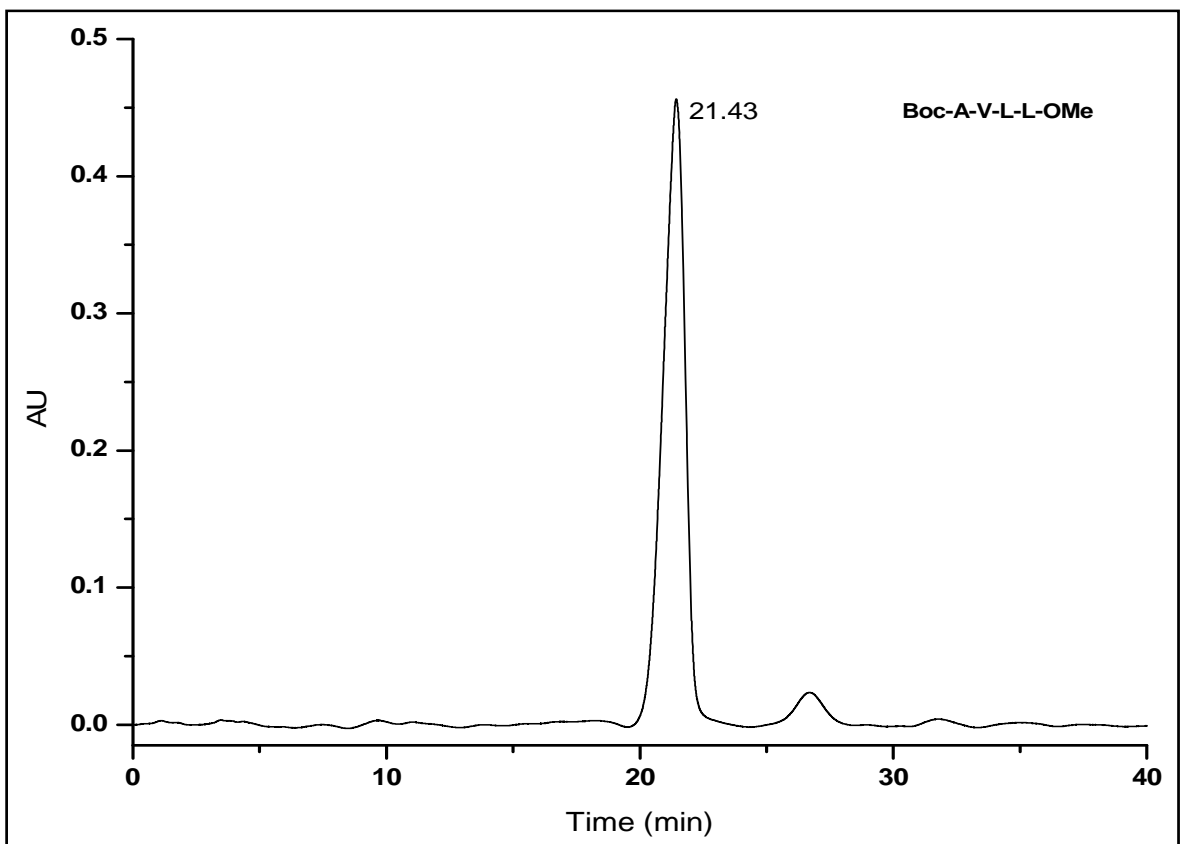
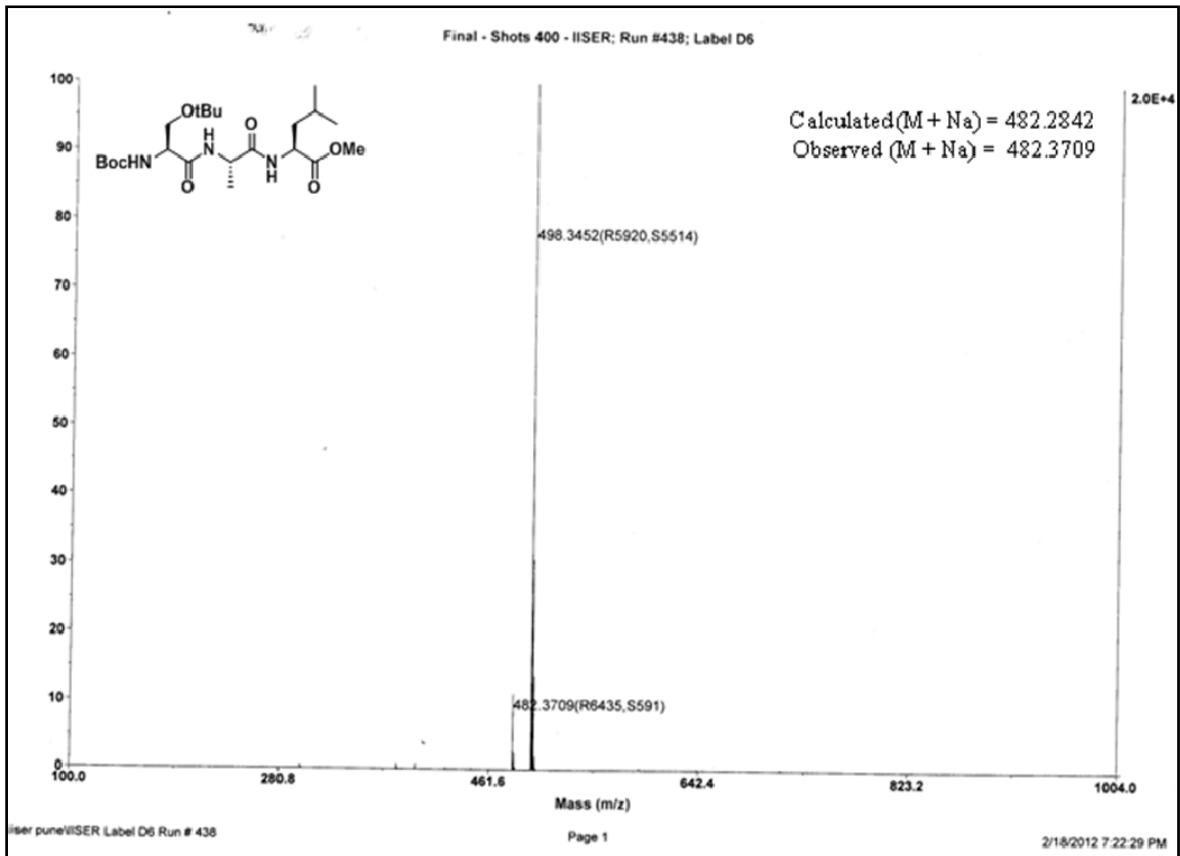
50. a) Bhat, B.; Sanghvi, Y. S. *Tetrahedron Lett.* **1997**, 38, 8811; b) Stawinski, J.; Hozumi, T; Narang, S. A. *J. Chem. Soc. Chem. Commun.* **1976** 243.
51. Carey, F. A.; Hodgson, K. O. *Carbohydr. Res.* **1970**, 12, 463.
52. Yamada, M.; Watabe, Y.; Sakakibara, T.; Sudoh, R. *J. Chem. Soc. Chem. Commun.* **1979**, 179.
53. a) Lavery, G.; McLaughlin, M.; Shaw, C.; Gorman, S. P.; Gilmore, F. B. *Chem Biol Drug Des.* **2010**, 75, 563; b) Powell, A.; Borg, M.; Amir-Heidari, B.; Neary, J. M.; Thirlway, J.; Wilkinson, B.; Smith, C. P.; Micklefield, J. *J. Am. Chem. Soc.* **2007**, 129, 15182.

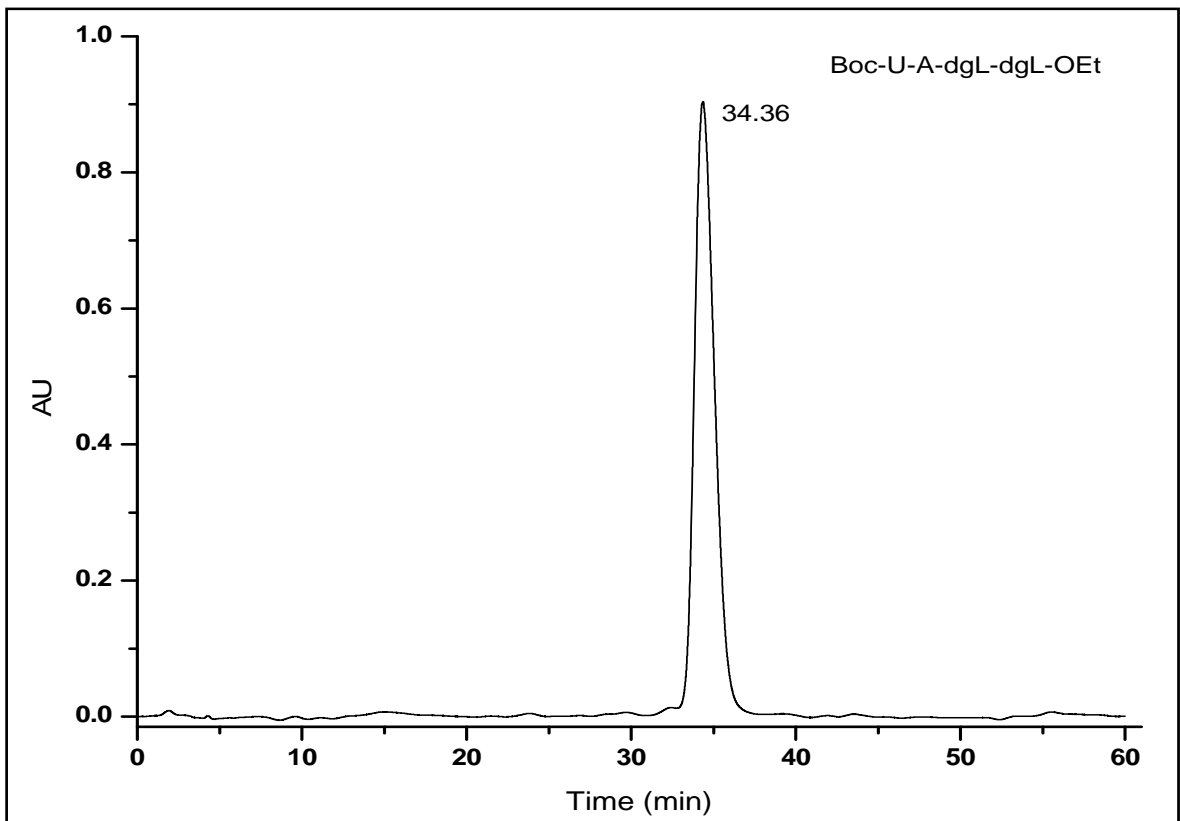
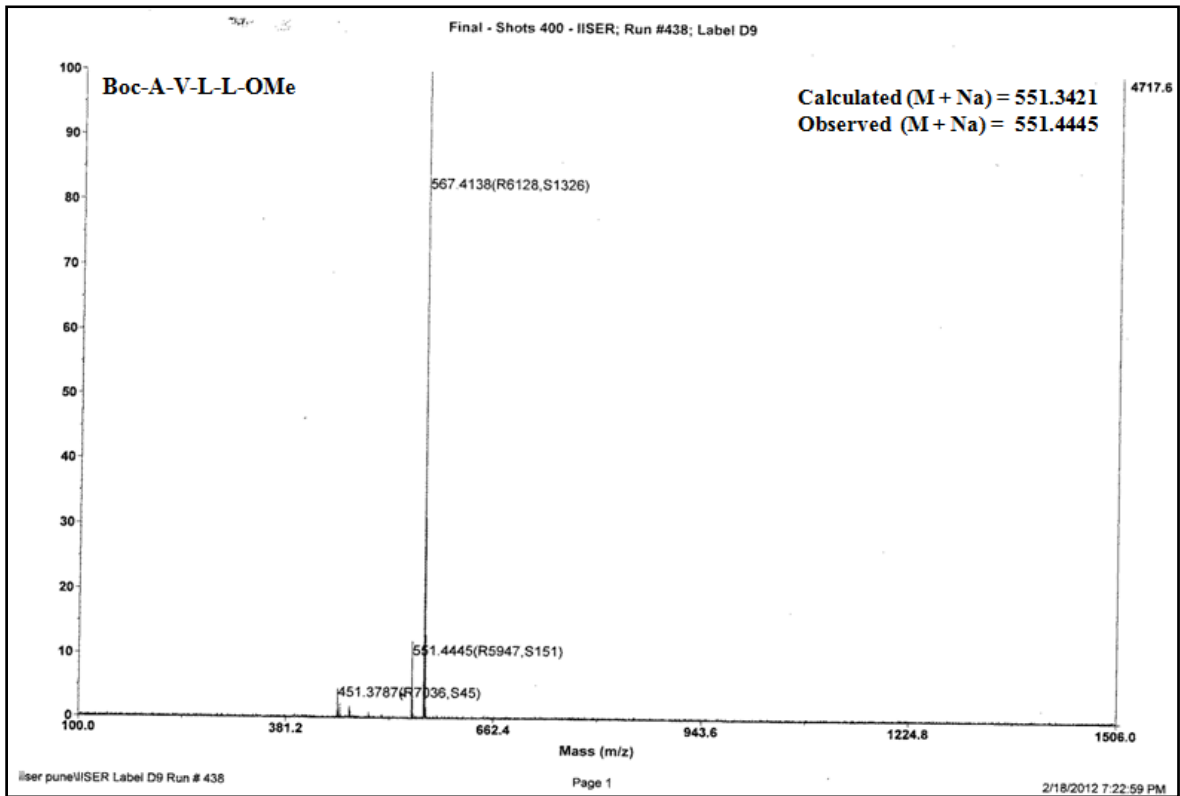
2.4 Appendix I: Representative Characterization Data of Synthesized Compounds

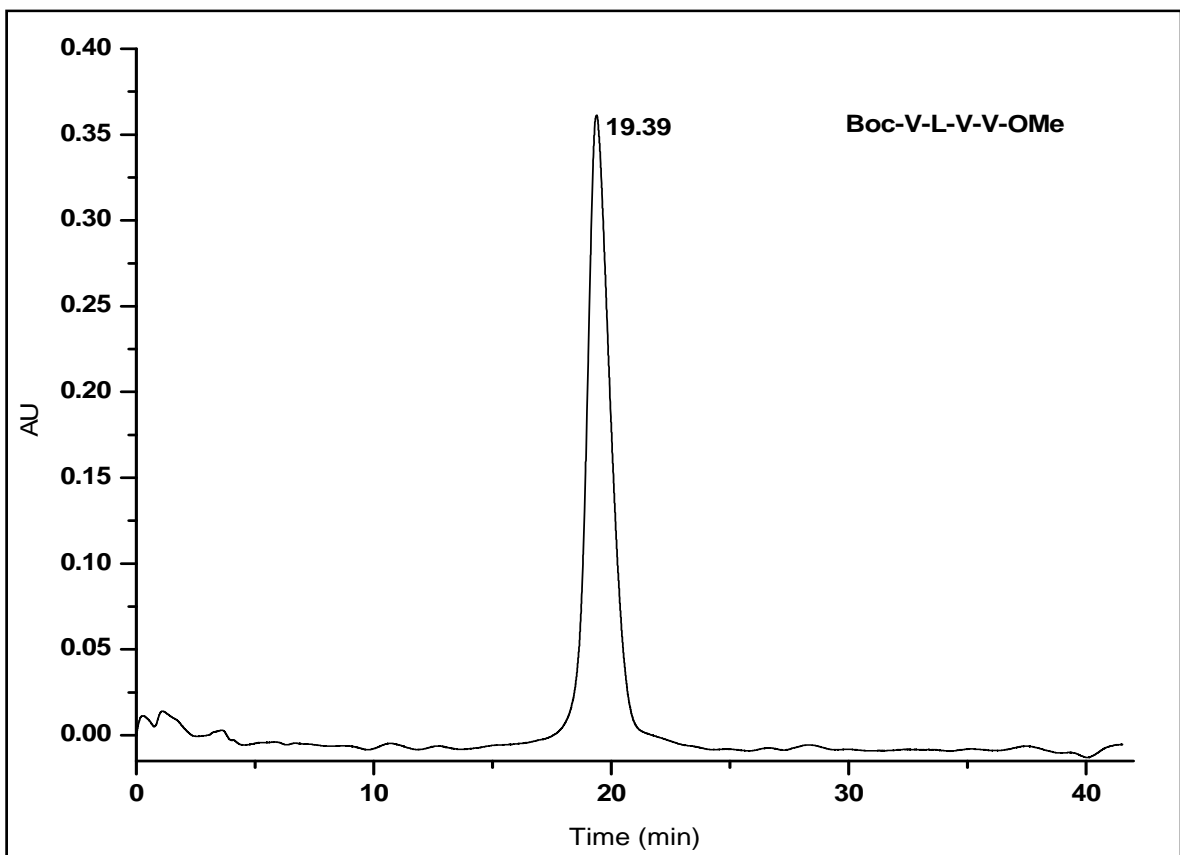
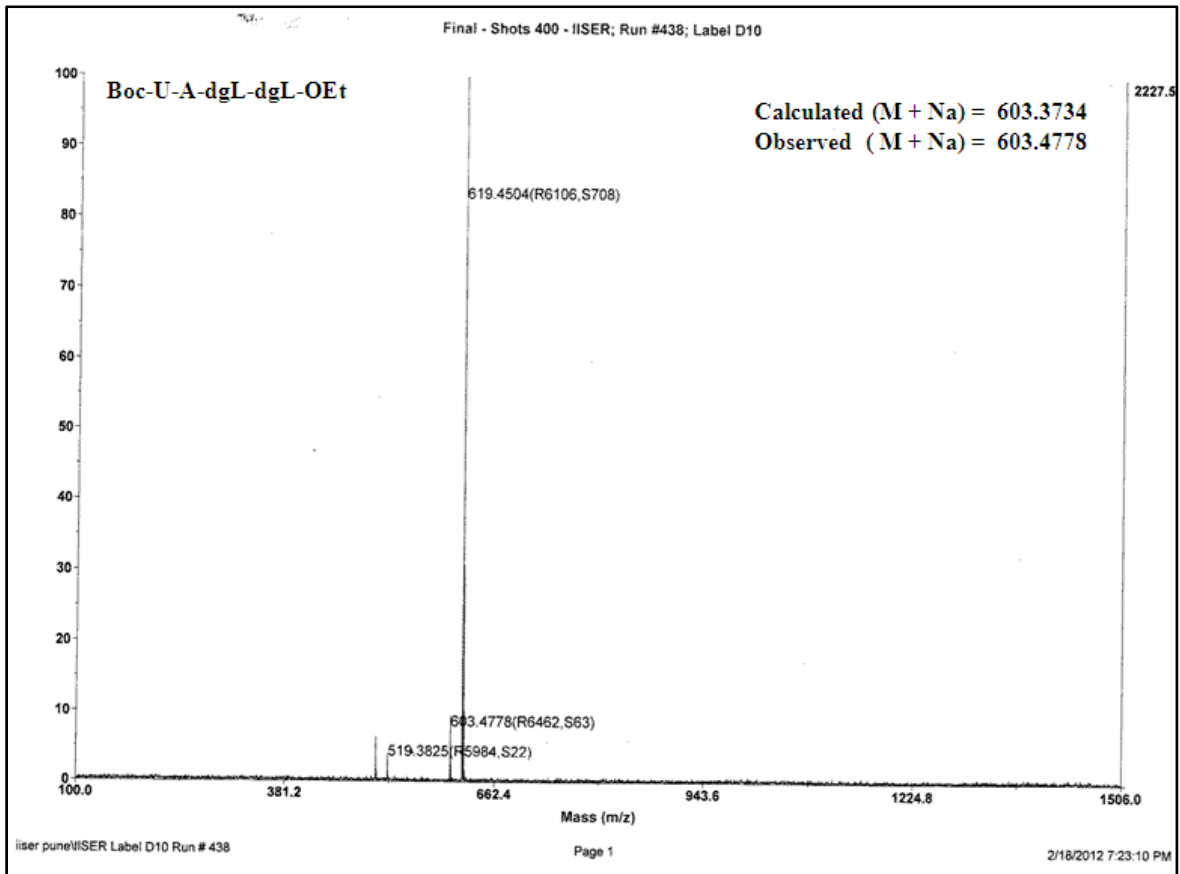
Designation	Description	Page
Boc-Val-Ala-OMe (6)	¹ H NMR (400 MHz)	161
Boc-Val-Ala-OMe (6)	¹³ C NMR (400 MHz)	161
Boc-Val-Ala-OMe (6)	Mass Spectrum	162
Boc-Ser(O ^t Bu)-Ala-Leu-OMe (17)	¹ H NMR (400 MHz)	162
Boc-Ser(O ^t Bu)-Ala-Leu-OMe (17)	Mass Spectrum	163
Boc-Ala-Val-Leu-Leu-OMe (20)	HPLC Profile	163
Boc-Ala-Val-Leu-Leu-OMe (20)	Mass Spectrum	164
Boc-Aib-Ala-dgL-dgL-OEt (21)	HPLC Profile	164
Boc-Aib-Ala-dgL-dgL-OEt (21)	Mass Spectrum	165
Boc-Val-Leu-Val-Val-OMe (22)	HPLC Profile	165
Boc-Val-Leu-Val-Val-OMe (22)	Mass Spectrum	166
<i>N</i> -Acyl Aniline (1a)	¹ H NMR (400 MHz)	166
<i>N</i> -Acyl Aniline (1a)	¹³ C NMR (400 MHz)	167

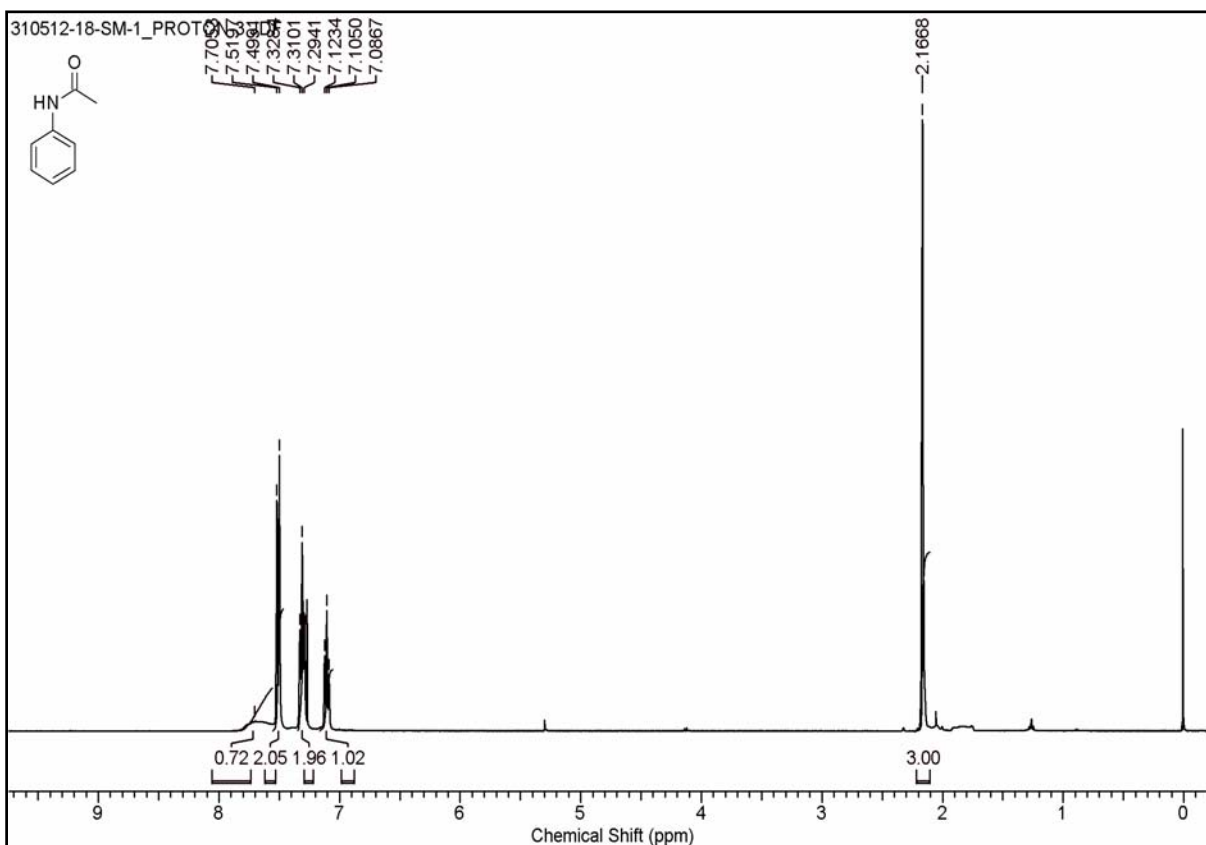
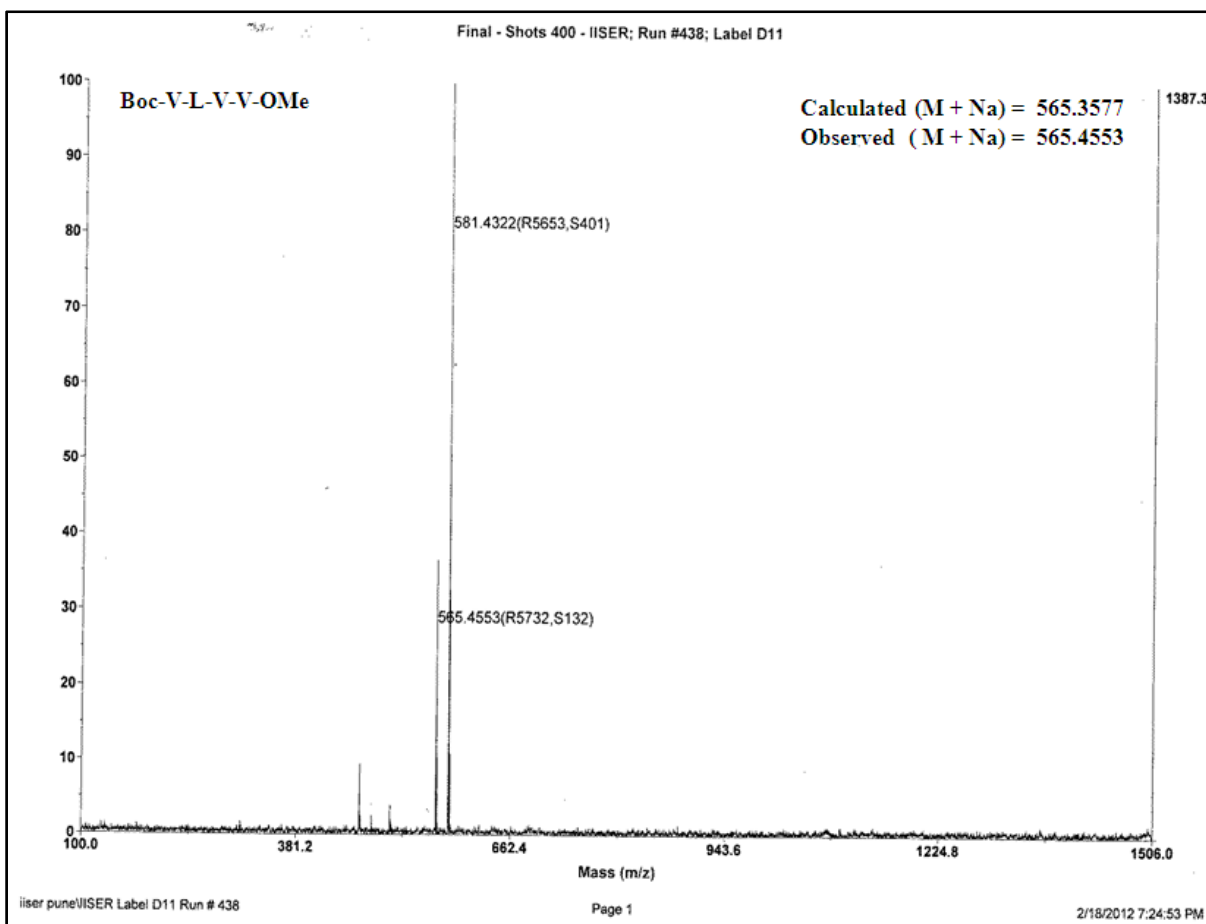


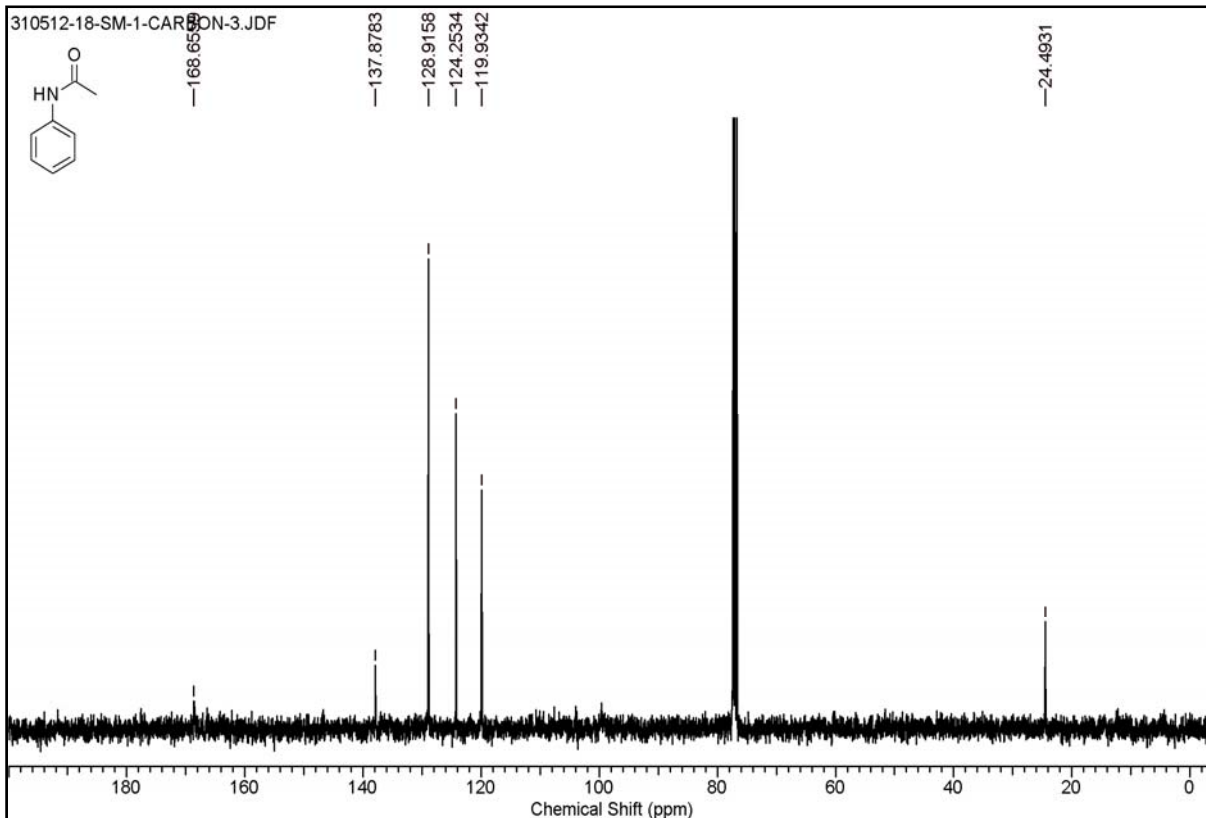












Chapter 3

**Synthesis of *N*-protected amino thioacids
and their utilization in thioacid oxidative
dimers and peptide synthesis**

3.1 Introduction

Sulfur in the form of thiols, disulfides and thioacids play a significant role in biology.¹ The distinct properties of thiol containing precursors have been utilized in mediating various biological processes, for example protein thioacids are used as sulphide donors in biosynthesis of thiamin, thioquinolobactin, vitamin B1, and cysteine.² The formation of covalent disulfide (R-S-S-R) bonds through the oxidation of thiols (R-SH) is a most unique property of sulfur and these disulfide bonds are ubiquitous in nature. Wieland and co-workers in their pioneering work demonstrated the potential of α -amino thioacids as acylating agents in the peptide synthesis as well as thioester strategy in the chemical ligation.³ Inspired by these early finding and versatile reactivity of thioacids recently various groups explored the reactivity of thioacids with different functional groups. Reactivity of thioacids with azide in the construction of amide has been reported.⁴ Similarly reactivity of thioacids with isonitriles,⁵ sulphonamides,⁶ nitroso derivatives,⁷ isocyanates,⁸ dinitrofluorobenzene,⁹ aziridines^{10,11} and thiocarbamates¹² has been recently demonstrated in the amide bond formation. In addition, reactivity of thioacids with metal has been explored in the peptide synthesis.¹³⁻¹⁶ Danishefsky and colleagues reported activation of thioacid for the synthesis of peptide and glycopeptides using additives HOBt.^{17,18} Further, to prove the concept that the thioacids are the possible precursors in the synthesis of polypeptides in primordial conditions, Orgel and colleagues demonstrated the *N*-acylation and polypeptide synthesis using thioacetic acid and α -amino thioacids, respectively, in the presence of oxidizing agents.^{19,20} Further Huber C. *et al.* also demonstrated the role of thioesters in construction of polypeptides in prebiotic era.²¹ These finding by Orgel and colleagues as well as by the Huber *et al.* signifies the thioacid and thioesters might have played vital role in the construction of life in the primordial conditions.

3.1.1 Reported protocols for the synthesis of *N*-protected amino thioacids

The versatile reactivity of thioacids has been extensively explored by various research groups in the construction of amide bonds. Goldstein and colleagues reported the synthesis of *N*-protected amino thioacids by treating *N*-hydroxysuccinimide active esters of protected amino acid with NaSH in methanol.²² In another protocol Suresh babu and co-workers have utilized the sodium sulfide in the presence of coupling reagent EDC for the synthesis of amino thioacids.²³ Crich and co-worker have demonstrated synthesis of the

Fm-thioester [(9H-fluoren-9-yl)methanethiol] as precursor for the amino thioacids.²⁴ Danishefsky and colleagues showed the utility of Lawesson's reagent for the transformation of carboxylic acids to corresponding thioacids.²⁵ Recently Rademann *et al.* have reported the synthesis of peptide thioacid by using solid phase chemistry.²⁶ Melnyk and co-workers documented the thioacids synthesis using Bis(2-sulfanylethyl) amides.²⁷ The schematic representation of various protocols utilized for the thioacids synthesis is shown in Figure 1.

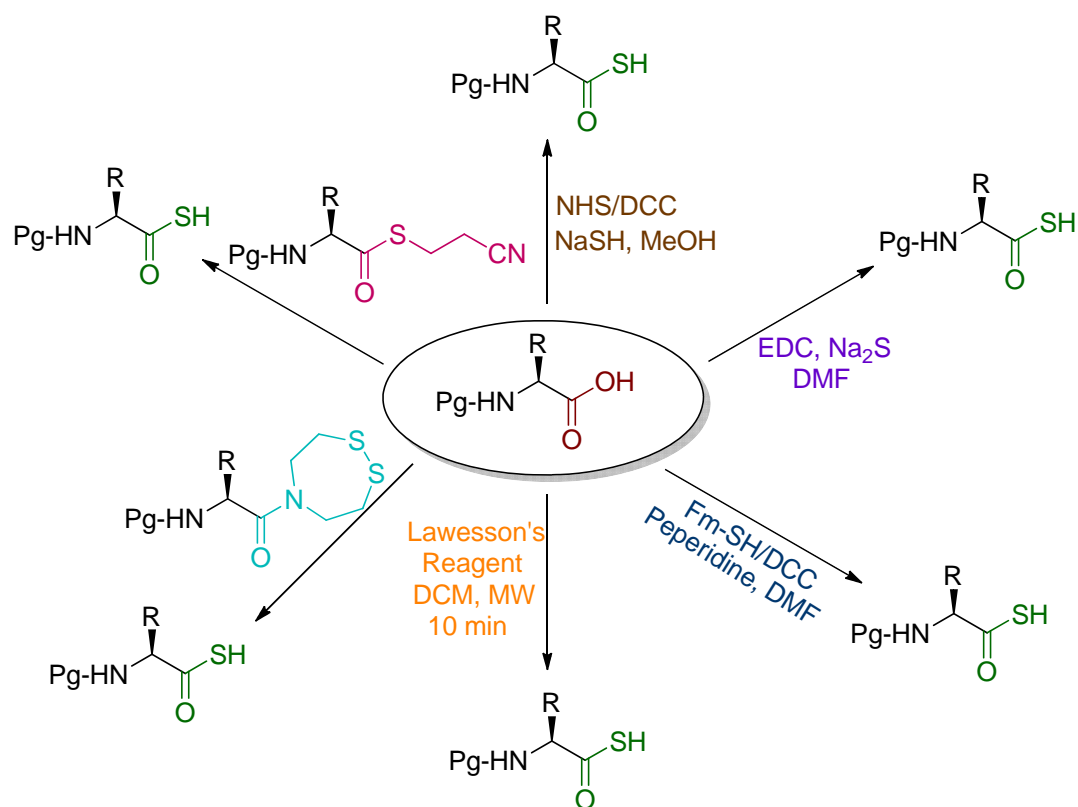


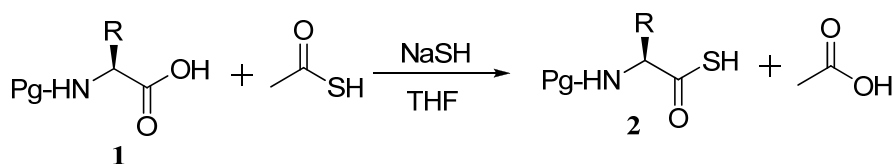
Figure 1: Various protocols documented in the literature for the synthesis of *N*-protected amino thioacids and peptide thioacids.

Most of these protocols involve the activation of carboxylic acid followed by the nucleophilic substitution with sulphur reagents such as NaSH, Na₂S, H₂S, Fm-SH [(9H-fluoren-9-yl)methanethiol] etc. For the activation of free carboxylic acids, various strategies including carbodiimides, active esters, acid chlorides etc., have been utilized. All these activated carboxylic acid derivatives have been practiced directly in the synthesis of peptides/amides. The major concern in the thioacid-mediated peptide coupling reactions is the synthesis of *N*-protected amino thioacids from the corresponding activated carboxylic acids of *N*-protected amino acids. Because the activated carboxylic acids can also serve as

acylating agents, it requires an additional step in the thioacid-mediated peptide synthesis. Further the protocols reported for the synthesis of *N*-protected amino thioacids by using Lawesson's reagent and 2-cyanoethyl thioesters are associated with the problem of epimerization.^{25, 26}

3.2 Aim and rationale of the present work

Based on the versatile reactivity of sulfur as well as thioacids and our own experience in the *N*-protected thioacids mediated peptide synthesis in the chapter 2, we anticipated that *N*-protected amino thioacids can be synthesized by simply treating the *N*-protected amino acids with thioacetic acid and NaSH without activating the carboxylic acids. We hypothesized that in the presence of NaSH, the thioacetic acid can be converted to reactive thioacetic acid persulfide, which will further react with free carboxylic acid to give *in situ* activated carboxylic acid and this intermediate subsequently reacted with NaSH leads to the formation of *N*-protected amino thioacids. The schematic representation is shown in Scheme 1.

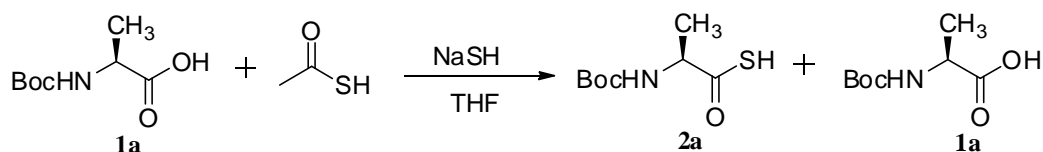


Scheme 1: Thioacetic acid and NaSH mediated synthesis of *N*-protected α -amino thioacids directly from the corresponding *N*-protected α -amino acids.

3.3 Results and discussion

We sought to utilize the versatile reactivity of sulfur, disulfides, persulfides and thioacids for the synthesis of *N*-protected amino thioacids, and its subsequent utilization in peptide synthesis in the presence or absence of metals. To realize our hypothesis, the *N*-Boc-Ala (**1a**) was treated with thioacetic acid and NaSH in THF. The reaction mixture was subjected to the mass spectral analysis after stirring for about 36 h in open air at room temperature. Instructively, the mass spectral results shown in Figure 2 suggested the partial conversion of *N*-Boc-Ala (**1a**) to corresponding *N*-Boc-Ala-SH (**2a**). The schematic representation of the reaction is shown in Scheme 2. Though the results were quite encouraging, we found it difficult to separate the pure *N*-Boc-Ala-SH from the reaction

mixture as it is contaminated with unreacted Boc-Ala. We anticipate that thioacids can be selectively separated from the reaction mixture through the oxidative dimerization.



Scheme 2: Schematic representation for synthesis of Boc-Ala-SH from the thioacetic acid and NaSH

In this regard, the excess thioacetic acid was removed from the reaction mixture through the evaporation under reduced pressure. The crude reaction mixture containing both **1a** and **2a**, after the aqueous workup, was subjected to the iodine mediated oxidation reaction²⁸ in THF and water in the ratio of 4:1 (Scheme 3).

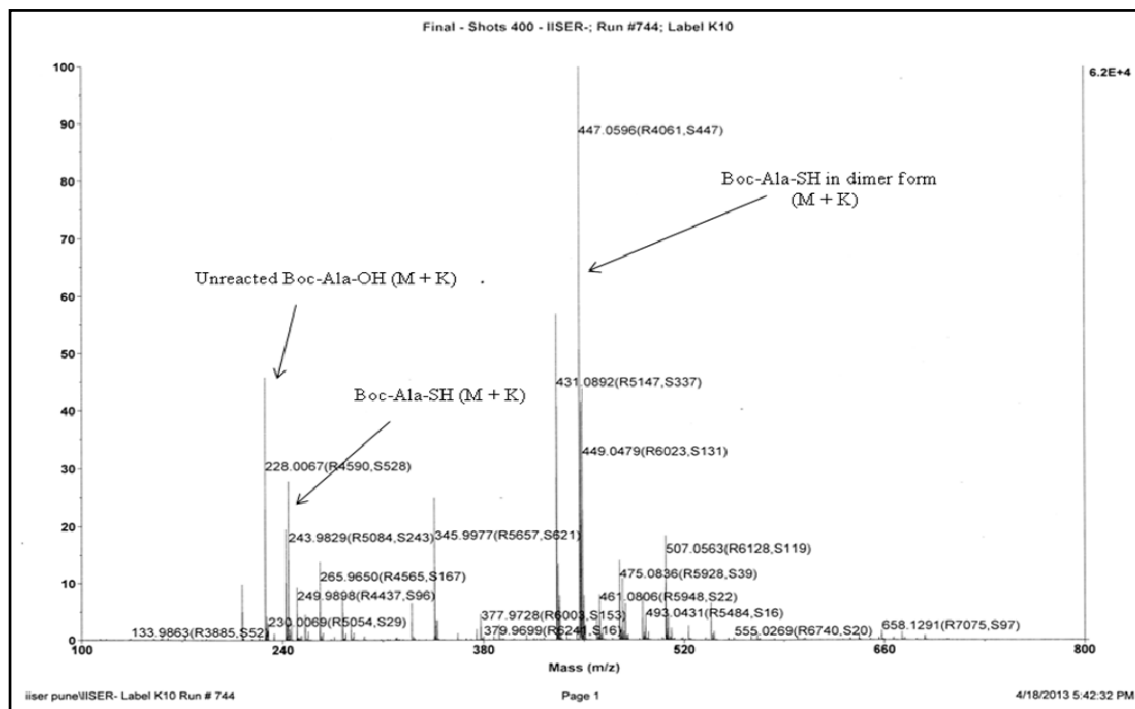
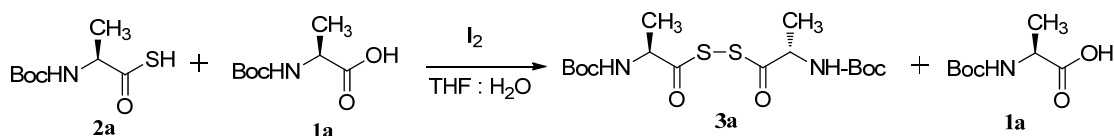


Figure 2: Mass spectrum for reaction mixture of *N*-Boc-Ala-SH (**2a**) synthesized from thioacetic acid and NaSH.

The pure Boc-Ala thioacid dimer (**3a**) was isolated after the aqueous work-up and column purification with 40% yield. Further to understand necessity of thioacetic acid and NaSH in the conversion of *N*-protected amino acids to the corresponding thioacids, we performed two control reactions, one without thioacetic acid and the other without NaSH.



Scheme 3: Schematic representation of oxidative dimerization of *N*-Boc-Ala-SH

Furthermore, the mass spectral analysis reveals that there is no conversion to *N*-protected amino thioacids in both the control reactions, suggesting the requirement of thioacetic acid and NaSH for the formation of *N*-protected amino thioacids. In order to understand the role of solvents in the conversion of carboxylic acids to corresponding thioacids, we carried out the same experiment in DCM, EtOAc, MeOH, DMF and THF, however, we found better yields of thioacids in THF compared to other solvents.

With these encouraging results, we subjected various other Boc-amino acids (Table 1) including the sterically hindered Boc-Aib (α -amino isobutyric acid) to the synthesis of corresponding thioacids mediated by the thioacetic acid and NaSH and subsequent oxidative dimerization. The list of *N*-Boc-amino thioacid oxidative dimers synthesized using the above protocol is given in Table 1. All *N*-Boc-thioacid oxidative dimers (**3a-e**) were isolated after the column purification in 25 to 40% overall yield. The compatibility of the reaction with Fmoc-protected amino acids was studied using Fmoc-Leu.

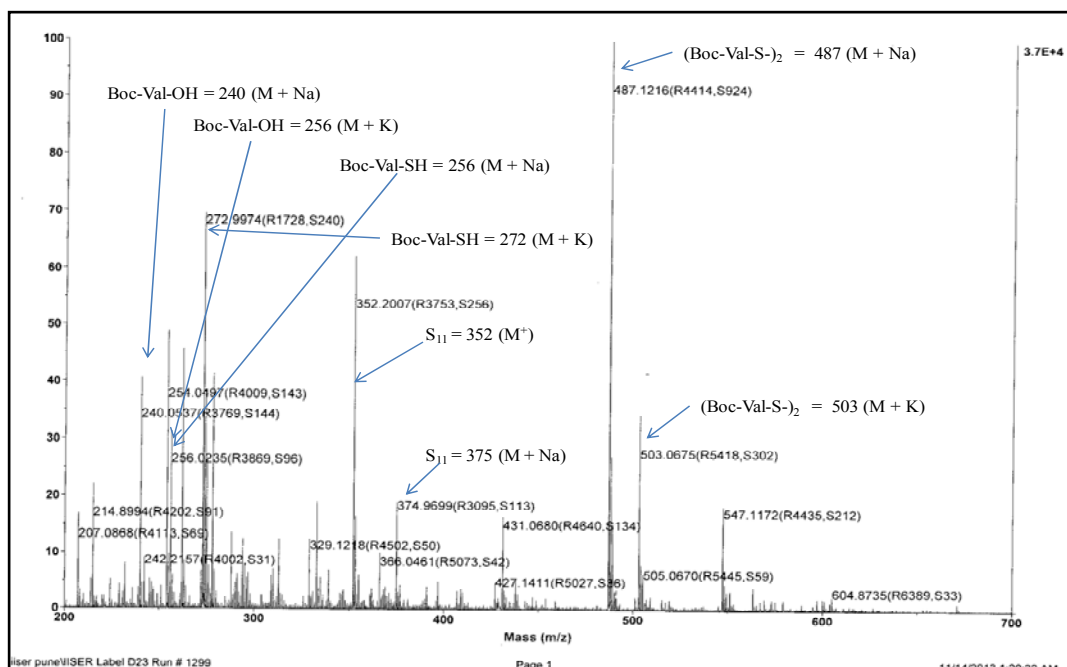


Figure 3: Mass spectrum for reaction mixture of thioacid dimer of *N*-Boc-Val after treatment with 10% Na₂CO₃ solution

The thioacid oxidative dimer of Fmoc-Leu (**3f**) was isolated in similar yields as that of Boc-amino acids. Results suggest that this method is compatible for both *N*-Fmoc- and *N*-Boc- protecting groups. We anticipate that the lower yields of the oxidative dimers is probably due to the dissociation/hydrolysis of thioacid disulfides during the aqueous work-up and column chromatography. To validate our assumption, the solution of pure thioacid dimer **3d** in THF was treated with 10% Na₂CO₃ solution, the TLC and mass spectral analysis suggests that dissociation of thioacid dimer into corresponding *N*-protected amino acids and thioacids, indicating the instability of thioacid oxidative dimers in the aqueous solution and corresponding mass spectral details are shown in Figure 3.

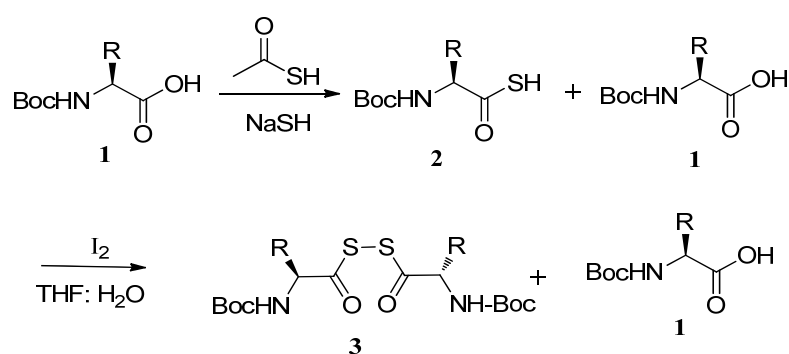


Table 1: Synthesis of *N*-protected amino thioacid oxidative dimers starting from the corresponding amino acids

	Boc-AA	Boc-AA-SH	Boc-AA-S-S-AA-Boc	Yield
	(1)	(2)	(3)	(%)
a	Boc-Ala	Boc-Ala-SH	Boc-Ala-S-S-Ala-Boc	40
b	Boc-Leu	Boc-Lue-SH	Boc-Leu-S-S-Leu-Boc	35
c	Boc-Phe	Boc-Phe-SH	Boc-Phe-S-S-Phe-Boc	31
d	Boc-Val	Boc-Val-SH	Boc-Val-S-S-Val-Boc	33
e	Boc-Aib	Boc-Aib-SH	Boc-Aib-S-S-Aib-Boc	25
f	Fmoc-Leu	Fmoc-Leu-SH	Fmoc-Leu-S-S-Leu-Fmoc	26

3.3.1 Crystal structure of thioacid oxidative dimers of *N*-Boc-Ala and *N*-Boc-Aib

However, out of all the thioacid oxidative dimers in the Table 1, we were able to get the rod shaped single crystals for **3a** and **3e** by the slow evaporation for ethyl acetate/n-hexane and their X-ray structures are shown in Figure 4. Analysis of the crystal structures reveals that the disulfides adopted *gauche* conformation ($g \sim \pm 60^\circ$) with a S-S bond distance of 2.03 Å.

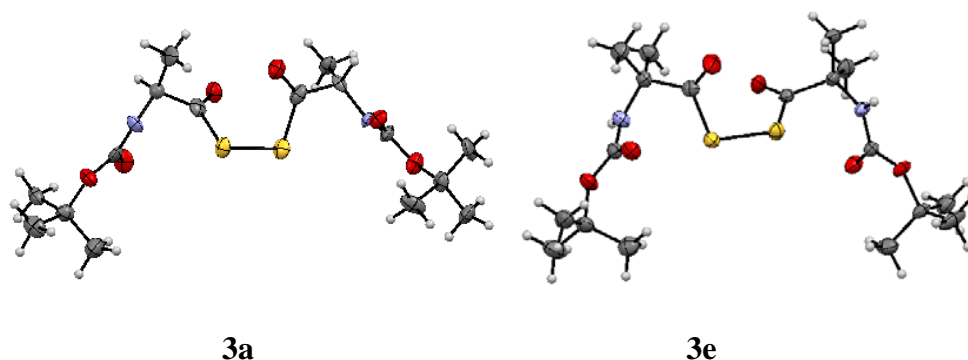
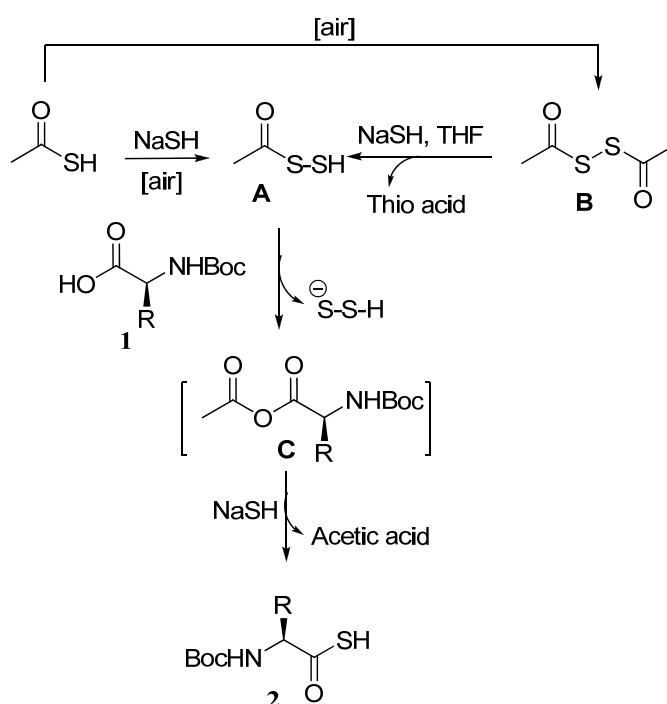


Figure 4: X-ray structures **3a** [(Boc-Ala-S)₂] and **3e** [(Boc-Aib-S)₂]

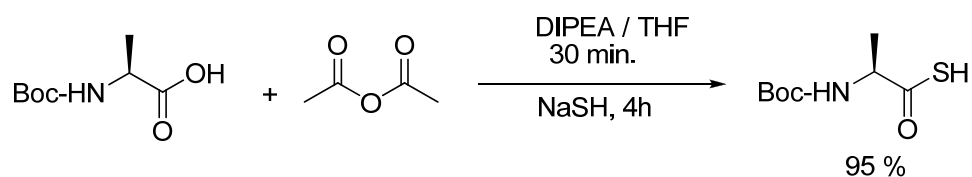
3.3.2 Possible mechanism of the synthesis of *N*-protected amino thioacids from thioacetic acid and NaSH

The remarkable results of the thioacetic acid and NaSH mediated conversion of a variety of *N*-protected amino acids to the corresponding amino thioacids enable us to propose the possible mechanism of the reaction. The schematic representation is shown in Scheme 4. Both Orgel^{19, 20} and Danishefsky^{17, 18} in their pioneering work proposed that diacyl disulfide and thioacid persulfide are the probable intermediates in the thioacid mediated amide bond synthesis. We speculate that the treatment of NaSH with the thioacetic acid may lead to the formation of activated thioacetic acid persulfide **A**. The persulfide formation may be facilitated by the open air oxidation as the reactions were performed in the open flasks and hydrated NaSH. The reaction between **A** and the *N*-Boc-amino acid (**1**) leads to the formation of a mixed anhydride, **C**. The *in situ* generated reactive mixed anhydride (**C**) further reacted with NaSH to give thioacid **2**. In addition, persulfide **A** can also be expected from the reaction between oxidative dimer (**B**) and

NaSH. To confirm whether the mixed anhydride **C** will undergo thionation reaction, we synthesized the mixed anhydride by reacting Boc-Ala with acetic anhydride in the presence of DIPEA (Scheme 5). The *in situ* generated mixed anhydride was further treated with NaSH. After the aqueous work-up, the Boc-Ala-SH was isolated in 95% yield, supporting the mixed anhydride **C** is a probable intermediate in the formation of *N*-protected amino thioacids. In a control reaction under inert argon atmosphere, we observed drastic decrease in the yield of *N*-protected thioacid (**2a**), indicating the requirement of open air for the formation of **A**.



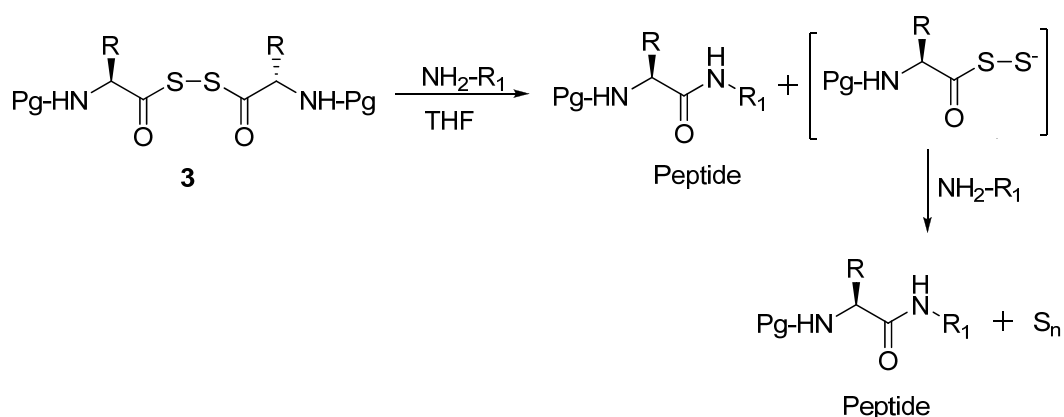
Scheme 4: Mechanism for the synthesis of α -amino thioacid from α -amino acids mediated by thioacetic acid and NaSH.



Scheme 5: Synthesis of thioacids from *in situ* generated mixed anhydrides

3.3.3 Utilization of thioacid oxidative dimers in peptide synthesis

In order to understand whether these *N*-protected thioacid oxidative dimers can undergo coupling reactions with free amino acid esters and peptides, we subjected them for the coupling reactions with various amino esters in THF. The schematic representation of the peptide synthesis is shown in Scheme 6. Results reveal that all thioacid oxidative dimers undergo coupling reactions with amines and peptides without any additives. The coupling reactions were found to be rapid and the products were isolated within 30 min. The list of peptides synthesized using *N*-protected diacyl disulfides is given in the Table 2. Further, these coupling reactions also suggest that thioacid persulfide, a reactive intermediate after the first coupling reaction, can undergo a coupling reaction with free amines as postulated by the Danishefsky and colleagues.^{17, 18} As both the acyl groups in the diacyl disulfides are involved in the acylation reactions it requires two equivalents of free amine to complete the reaction. The dipeptides **P1** and **P2** were synthesized by reacting **3a** with methyl esters of valine and tryptophan, respectively.



Scheme 6: Synthesis of peptides from diacyl disulfides

The tripeptides **P3** and **P4** were synthesized from **3b** by reacting with benzyl and methyl esters of the dipeptides Phe-Ala and Trp-Val, respectively. Further, **3c** was coupled with methyl esters of L-Val, D-Val and Ala to give dipeptides **P5**, **P6** and **P7**, respectively. Similarly, tripeptide **P8** was isolated from the reaction between **3d** and the methyl ester of dipeptide Ala-Trp. To ensure whether the sterically hindered thioacid dimers can undergo peptide coupling reactions, we subjected *N*-Boc-Aib thioacid dimer

(**3e**) to the coupling reaction with the methyl ester of valine as well as the methyl ester of Trp to give dipeptides **P9** and **P10**, respectively.

Table 2: Peptides synthesized from diacyl disulfides

No	3	NH ₂ -R1	Peptides	Yield (%)
P1	3a	H-Val-OMe	Boc-Ala-Val-OMe	75
P2	3a	H-Trp-OMe	Boc-Ala-Trp-OMe	86
P3	3b	H-Phe-Ala-OBn	Boc-Leu-Phe-Ala-OBn	84
P4	3b	H-Trp-Val-OMe	Boc-Leu-Trp-Val-OMe	70
P5	3c	H-Val-OMe	Boc-Phe- ^L Val-OMe	74
P6	3c	H-D-Val-OMe	Boc-Phe- ^D Val-OMe	76
P7	3c	H-Ala-OMe	Boc-Phe-Ala-OMe	81
P8	3d	H-Ala-Trp-OMe	Boc-Val-Ala-Trp-OMe	73
P9	3e	H-Val-OMe	Boc-Aib-Val-OMe	65
P10	3e	H-Trp-OMe	Boc-Aib-Trp-OMe	74
P11	3f	H-Ala-Leu-OMe	Fmoc-Leu-Ala-Leu-OMe	84

Peptide **P11** was synthesized from the reaction between **3f** and the free dipeptide Ala-Leu methyl ester. All peptides (**P1- P11**) were isolated in moderate to good yields and are given in the Table 2. The only byproduct that we observed in the coupling reaction is **S_n** (poly sulfur, n = 1, 2, 3, etc). Overall, these findings signify that peptides can be synthesized without using coupling reagents, additives and the activated carboxylic acids of *N*-protected amino acids.

3.3.4 Racemization study of peptides, **P5** = Boc-Phe-^LVal-OMe, **P6** = Boc-Phe-^DVal-OMe and **P5 & P6** = Boc-Phe-(±)Val-OMe.

To understand whether this protocol of peptide synthesis is free from the racemization, we couple **3c** with the methyl ester of racemic mixture of (±) Val and subjected to chiral HPLC analysis along with diastereomeric dipeptides **P5** and **P6**. The HPLC profiles of these peptides are shown in Figure 5. Single peaks were observed for peptides **P5** and **P6** at t_R 12.15 and 13.23 min. respectively, whereas the diastereomeric mixture obtained after the coupling of **3c** with (±) Val methyl ester showed two peaks at t_R 12.20 and 13.28 min., corresponding to the individual **P5** and **P6**, respectively. Analysis suggests that no racemization during the synthesis of these dipeptides and it was further supported by the ¹H NMR.

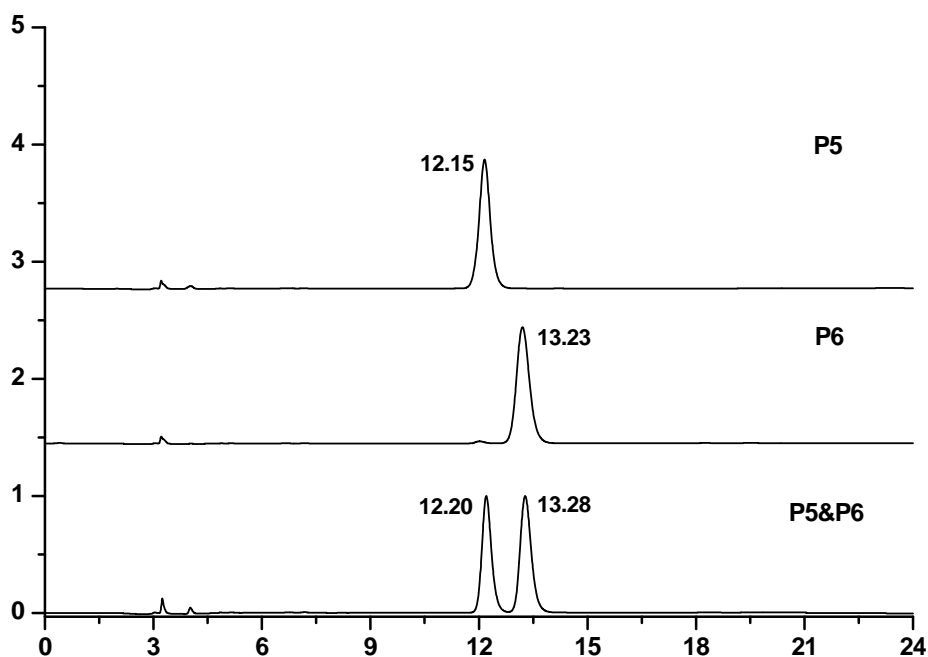
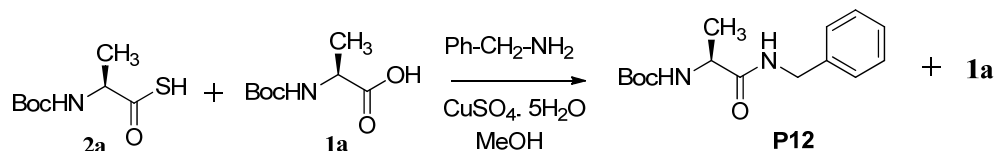


Figure 5: Chiral HPLC profile for the peptide **P5** and **P6**

3.3.5 Utilization of *N*-protected amino thioacids in peptide synthesis

Although the coupling reactions of thioacid oxidative dimers were found to be mild, clean and required no additional coupling agents, base or additives, however, the major issue remains the dissociation of thioacid dimers during the aqueous work-up. We hypothesized that instead of the isolation of thioacid oxidative dimers, we can selectively couple the *N*-protected amino thioacids from the reaction mixture (Scheme 1) containing carboxylic acids with free amines the presence of 30 mol% copper sulphate (CuSO₄·5H₂O)

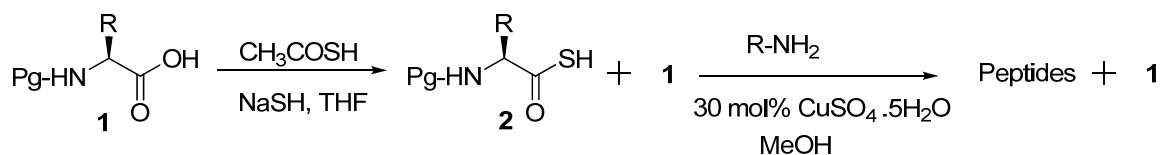
as described in the Chapter 2. To validate, we subjected the crude mixture containing unreacted **1a** and thioacid **2a** for the coupling reaction with benzylamine in the presence of 30 mol% copper sulphate in methanol as reported earlier (Scheme 7).^{15, 16}



Scheme 7: Selective amide bond formation from the crude reaction mixture containing unreacted Boc-Ala and Boc-Ala-SH

The *N*-acylated product **P12** was isolated in 78% yield. The unreacted *N*-protected amino acid was removed through aqueous work-up. Motivated by this result, we extend the same methodology for the synthesis of peptides. Using this methodology, peptides **P1**, **P2**, **P5** and **P7** were synthesized and isolated in good yields. Along with these peptides, we also synthesized dipeptides **P13** and **P14** and isolated in good yields after the column purification (Table 3).

Table 3: List of the thioacids and peptides synthesized by using NaSH and thioacetic acid

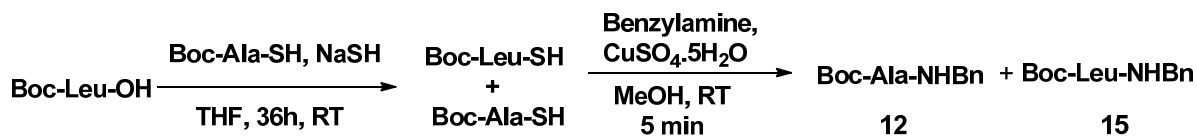


Entry	Thioacid	Amine	Peptide	Yield (%)
1	Boc-Ala-SH	H ₂ N-Val-OMe	P1	67
2	Boc-Ala-SH	H ₂ N-Trp-OMe	P2	63
3	Boc-Phe-SH	H ₂ N-Val-OMe	P5	65
4	Boc-Phe-SH	H ₂ N-Ala-OMe	P7	69
5	Boc-Ser(O ^t Bu)-SH	H ₂ N-Trp-OMe	Boc-Ser(O ^t Bu)-Trp-OMe (P13)	65
6	Cbz-Leu-SH	H ₂ N-Ala-OMe	Cbz-Leu-Ala-OMe (P14)	60

In comparison of thioacid dimers versus copper sulphate mediated thioacid peptide coupling reactions, better yields were observed in the case of thioacid dimer mediated coupling reactions. Overall, these results indicate peptides can be synthesized through selective coupling of *N*-protected thioacids in the presence *N*-protected carboxylic acids.

3.3.6 Amino thioacids mediated synthesis of other *N*-protected amino thioacids and its subsequent utilization in peptide synthesis

We further investigated whether *N*-protected amino thioacids can also serve as starting material to synthesize the thioacids of other *N*-protected amino acids. To examine the hypothesis, we treated Boc-Leu with Boc-Ala-SH and NaSH in THF. The crude products isolated after aqueous work-up were subjected to the reaction with benzyl amine and copper sulphate in methanol.



Scheme 8: Boc-Ala-SH and NaSH mediated synthesis of Boc-Leu-SH and subsequent amide bond formation.

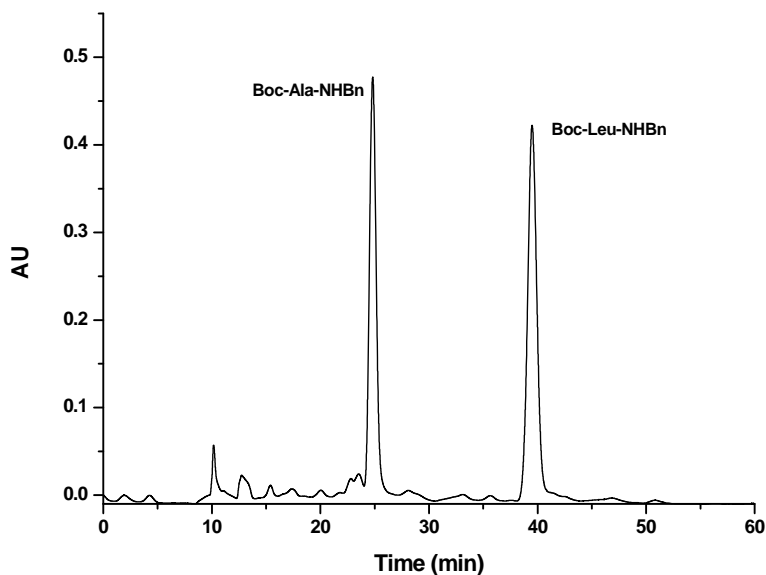
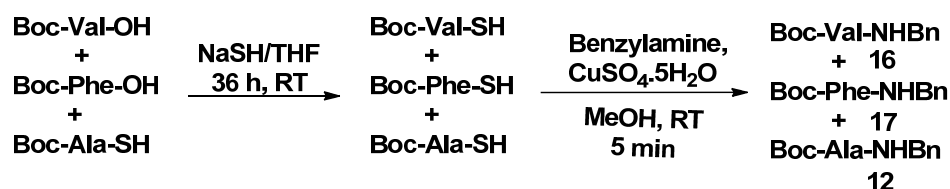


Figure 6: HPLC profile of amide **12** and **15** synthesized from the Boc-Ala-SH mediated Boc-Leu-SH.

Reverse phase HPLC and mass spectral analysis indeed suggests that the formation acylated products **12** and **15** in almost 1:1 ratio. The schematic representation of the reaction is shown in Scheme 8. These results suggest that almost 50% of Boc-Ala-SH was transformed to Boc-Ala as well as 50% Boc-Leu was transformed into Boc-Leu-SH.

Further, in order to understand whether it is possible to convert more than one amino acid in the reaction mixture to corresponding thioacids, we subjected Boc-Val and Boc-Phe along with Boc-Ala-SH in presence of NaSH in THF. The reaction mixture was stirred for another 36 h in open air, the crude thioacid products were isolated after aqueous work-up and subjected for the amide bond formation reaction with benzyl amine by using copper sulphate in methanol. The products were characterized by reverse phase HPLC and mass spectral analysis. The schematic representation is shown in Scheme 9.



Scheme 9: Boc-Ala-SH and NaSH mediated synthesis of Boc-Val-SH and Boc-Phe-SH and subsequent amide bond formation.

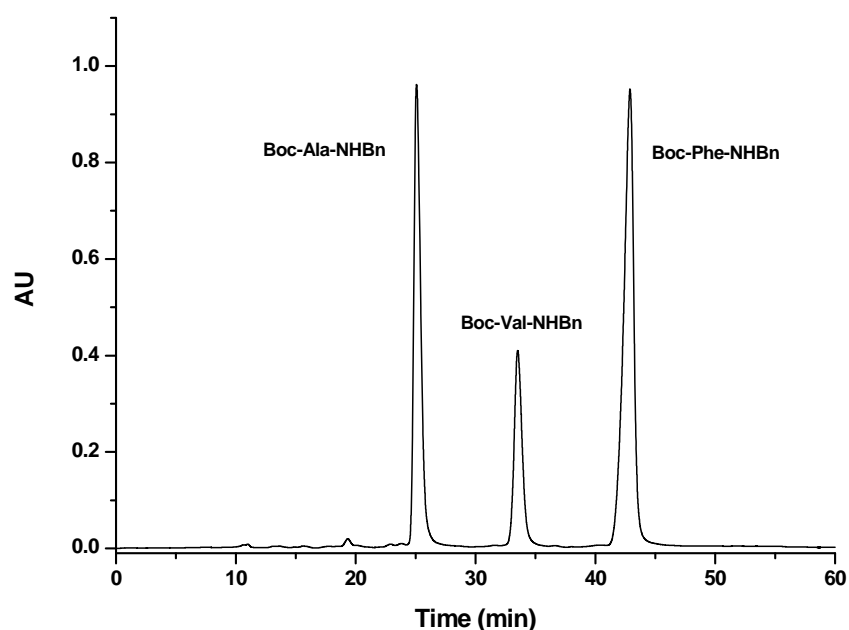
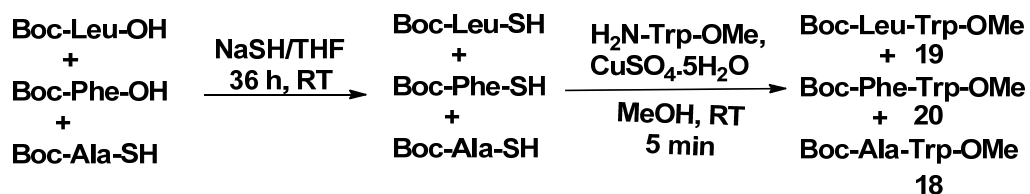


Figure 7: HPLC profile of amide **12**, **16** and **17** synthesized from the Boc-Ala-SH mediated Boc-Val-SH and Boc-Phe-SH

Inspired by this amide bond formation, we utilized this protocol for the synthesis of dipeptides. We carried out the synthesis of *N*-protected amino thioacids by similar protocol and subsequent treatment of these thioacids with methyl ester of tryptophane in presence of copper sulphate yields the dipeptides is shown in Scheme 10.



Scheme 10: Boc-Ala-SH and NaSH mediated synthesis of Boc-Leu-SH and Boc-Phe-SH and subsequent dipeptide formation.

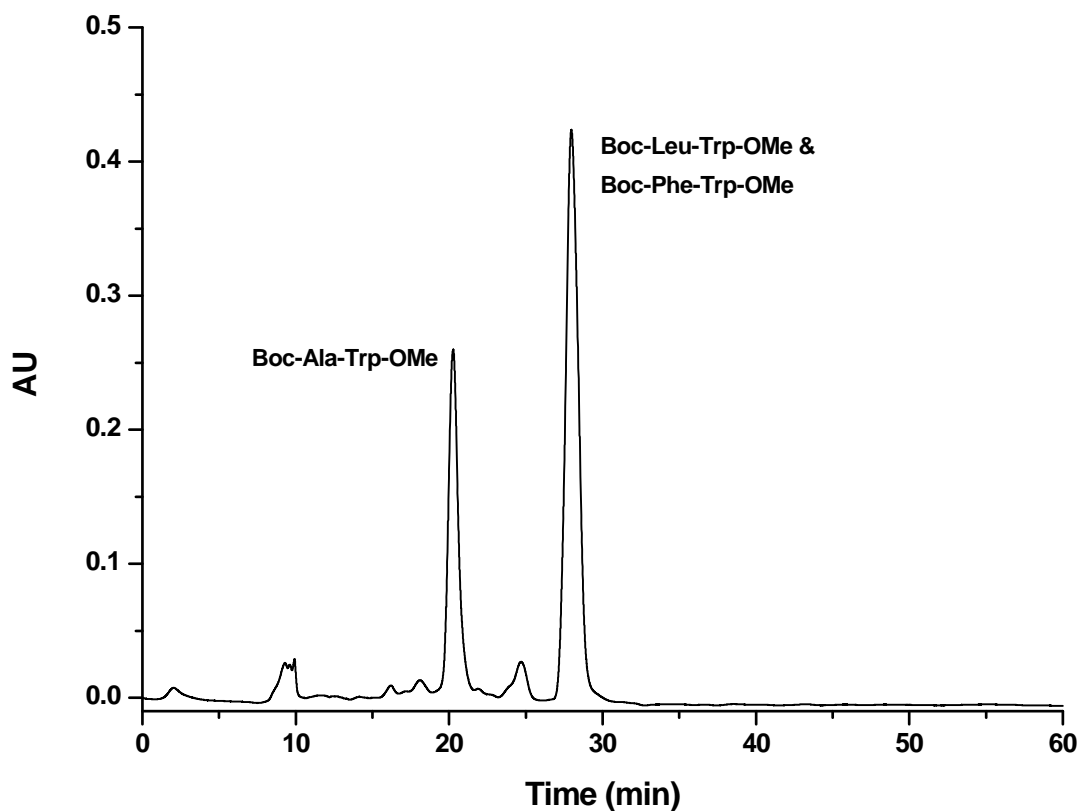
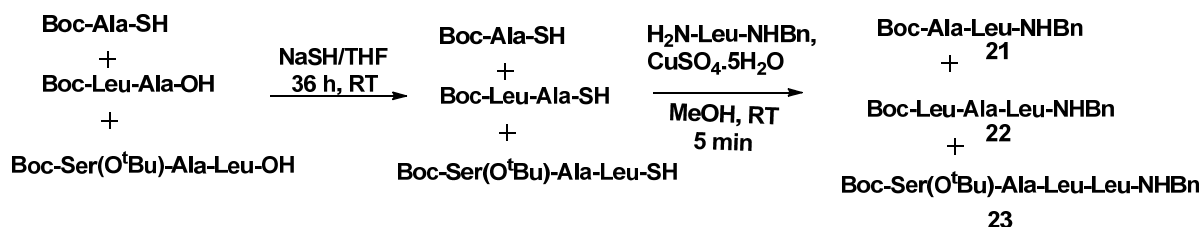


Figure 8: HPLC profile of amide **18**, **19** and **20** synthesized from the Boc-Ala-SH mediated Boc-Val-SH and Boc-Phe-SH

To understand whether this strategy can be further extended to the di and tripeptide acids, the Boc-Ala-SH was treated with Boc-Leu-Ala-OH and Boc-Ser(OBu^t)-Ala-Leu-

OH in the presence of NaSH in THF in a single pot. The crude product was again treated with Leucine benzylamide (H-Leu-CONHBn) and 30 mol% of copper sulphate in methanol. The schematic presentation of the reaction is shown in Scheme 11.



Scheme 11: Boc-Ala-SH and NaSH mediated synthesis of Boc-Leu-Ala-SH and Boc-Ser(O^tBu)-Ala-Leu-SH and subsequent peptide formation.

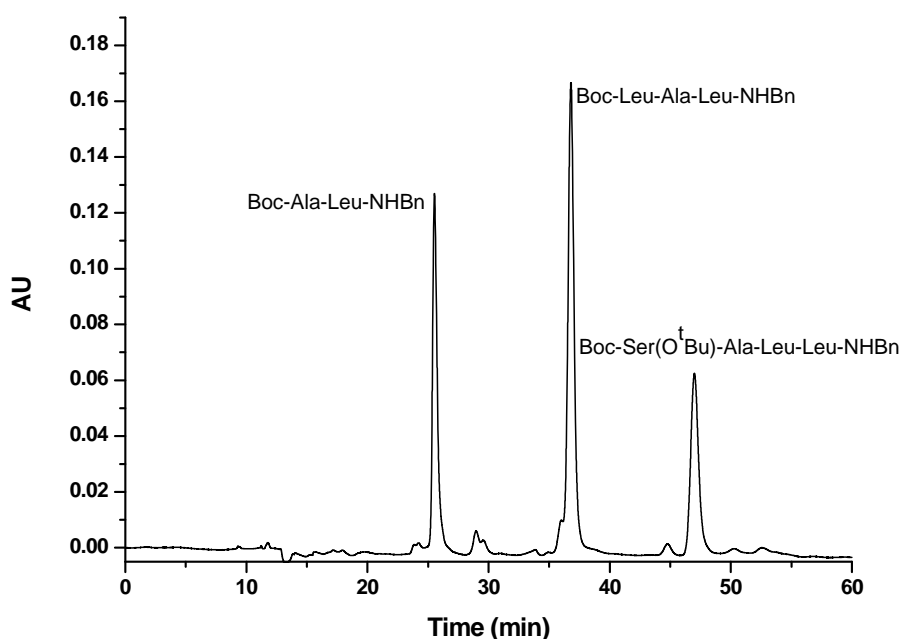
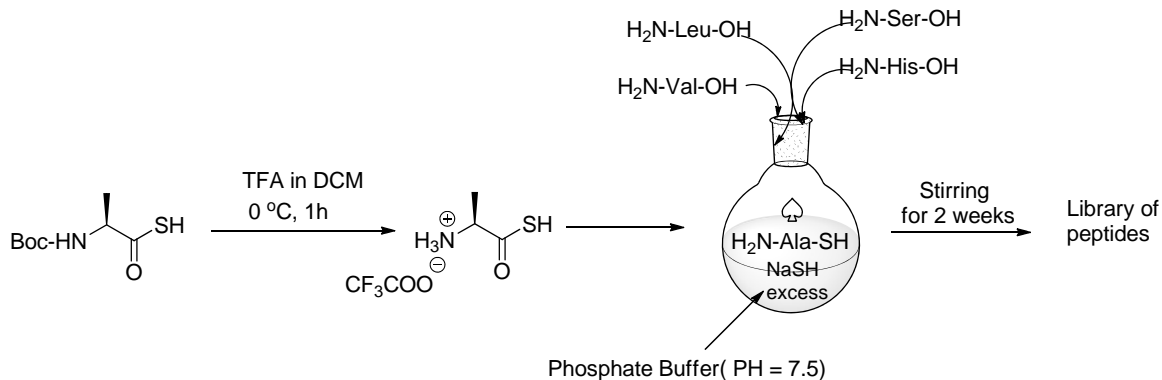


Figure 9: HPLC profile of peptides **21**, **22** and **23**.

The di, tri and tetra peptides (**21-23**) were isolated after aqueous work-up and subjected for reverse phase HPLC and mass spectral analysis. The HPLC profile of these peptides is shown in Figure 9 and mass spectral analysis is shown in the experimental section. As the reactions were performed in small scale to show the proof of the concept, these peptides were not further characterized.

3.3.7 Amino thioacid mediated polypeptide library synthesis in aqueous condition

The intriguing results of *N*-protected amino thioacids as a precursor for the synthesis of other *N*-protected amino thioacids motivated us to explore the reactivity of unprotected amino thioacids in polypeptide synthesis. As earlier reports by Orgel *et al.* and Huber and colleagues on the involvement of thioacids and thioesters in polypeptide synthesis in primordial condition led us to investigate reactivity of amino thioacids in the polypeptide synthesis at near physiological conditions. We anticipate that, with the proper physiological conditions and utilizing this distinct reactivity of amino thioacids, it is possible to synthesize the polypeptide libraries. In that regard, the trifluoroacetic acid salt of Ala thioacid was dissolved in phosphate buffer with pH~7.5 and treated with excess NaSH. The pH of the reaction mixture was maintained at ~7.5-8 by adding HCl. This solution was treated with the free amino acids Leu, Val, Ser and His. The schematic representation is shown in Scheme 12.



Scheme 12: Schematic representation for amino thioacid mediated polypeptide library synthesis

After stirring the reaction mixture for two weeks, we performed mass analysis of the reaction mixture. Analysis reveals the formation of various peptide sequences and we could able to trace out possible hexa and tetrapeptides, however, it is difficult to predict the sequence of the peptides. We speculate that there might be a large number of probable peptide sequences within the reaction mixture. The mass spectrum of the reaction mixture indicating the formation of tetra and hexapeptides is shown in Figure 10. The possible amino acid residues observed in peptide sequences and their corresponding mass are

shown in Figure 11. These results of amino thioacid mediated peptide synthesis in aqueous media support the Orgel and Huber findings regarding the vital role of thioacids and thioesters in the origin of life.

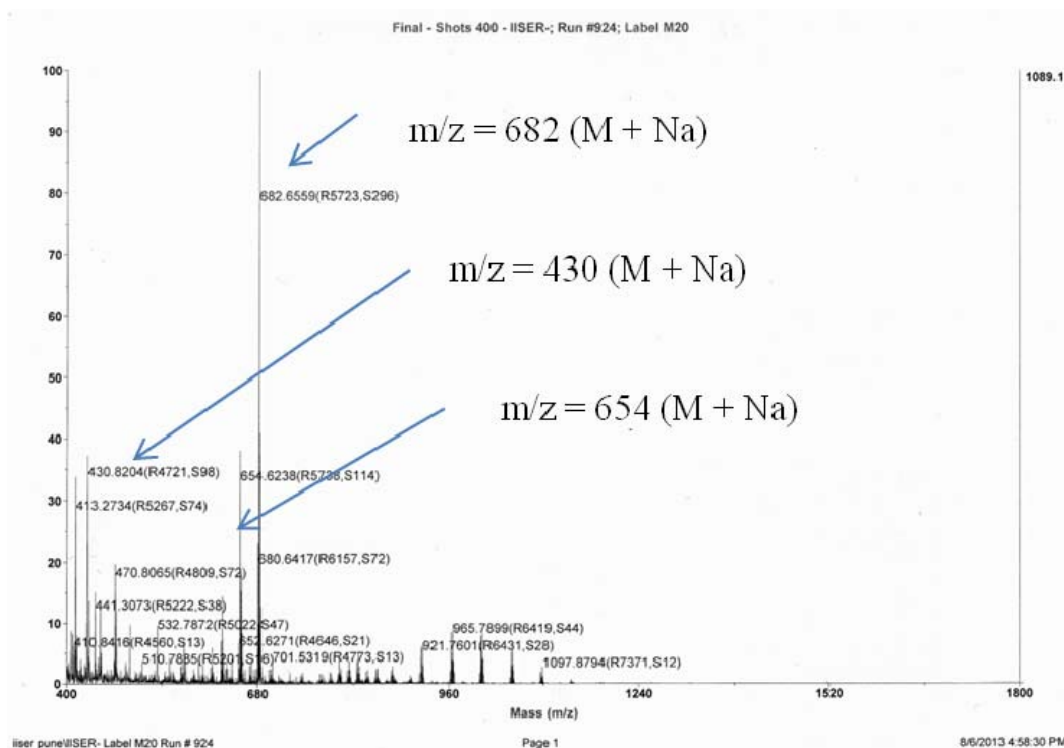


Figure 10: Mass spectrum for the crude reaction mixture of amino thioacid mediated polypeptide library synthesis.

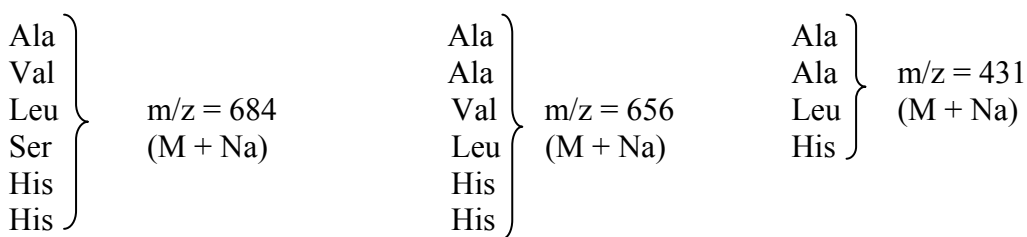


Figure 11: Possible amino acid residues in the observed peptide sequences and their corresponding mass.

3.4 Conclusions

In conclusion, we have demonstrated the potential utility of thioacetic acid and NaSH in the synthesis of *N*-Boc-protected amino thioacids. In addition, the novel *N*-protected amino thioacid oxidative dimers were isolated and studied their conformations in single crystals. Though yields of these diacyl disulfides are low, however, their coupling reactions were found to be very neat, fast and high yielding. We are presently investigating to improve the yields of thioacid oxidative dimers and their utility in the solid phase peptide synthesis. The results presented here suggest that peptides can be synthesized without using activated carboxylic acids of amino acids or standard coupling reagents. In addition, *N*-protected amino thioacid mediated synthesis of other amino thioacids and peptide thioacids and their coupling reaction with free amines is highly surprising and provides an alternative opportunity to synthesize library of peptides in single pot without coupling agents. The results obtained from this work also support the role of thioacids in polypeptide synthesis in prebiotic conditions.^{19, 21} Overall, the chemistry reported here may open new opportunities to rethink the amide bond formation in chemistry and biology.²⁹

3.5 Experimental

General Information.

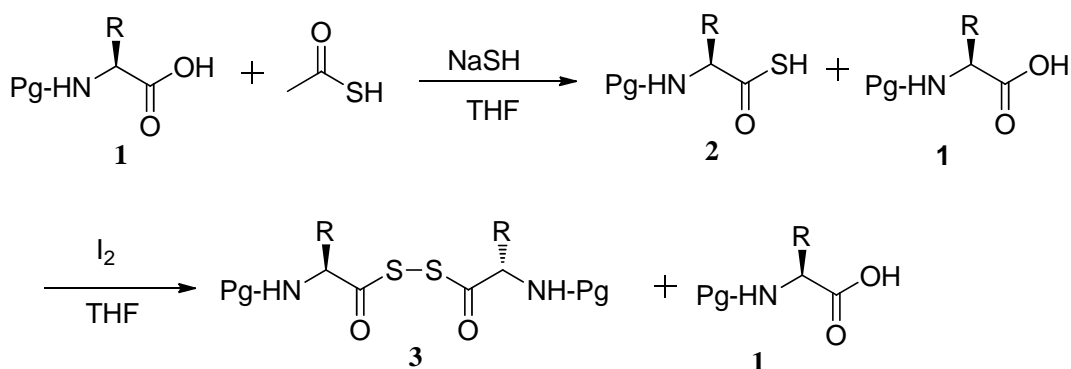
All amino acids, thioacetic acid, *N*-hydroxysuccinimide, Di-*tert*-butyl dicarbonate, CuSO₄·5H₂O, NaSH and THF were used as commercially available. Column chromatography was performed on silica gel (100-200 mesh). ¹H and ¹³C NMR were recorded on a 400 MHz instrument (100 MHz for ¹³C) using the residual solvent signals as an internal reference. The chemical shifts (δ) are reported in ppm and coupling constants (*J*) are given in Hz. IR spectra were recorded on FT-IR spectrophotometer using KBr pellet. High-resolution mass spectra were obtained from ESI-TOF MS spectrometer.

General procedure for the synthesis of *N*-protected amino thioacid oxidative dimers:

In a 50 mL RB flask *N*-protected amino acid (10 mmol) was dissolved in 15 mL of dry THF. This solution was then treated with NaSH (20 mmol) and thioacetic acid (10 mmol) at room temperature. After stirring the reaction mixture for about 36 h, the solvent was evaporated under reduced pressure. The residue was diluted with water (50 mL) and acidified with 5 % HCl (pH ~ 2). This aqueous solution was extracted with ethyl acetate (30 mL × 3). The combined organic layer was washed with brine, dried over anhydrous

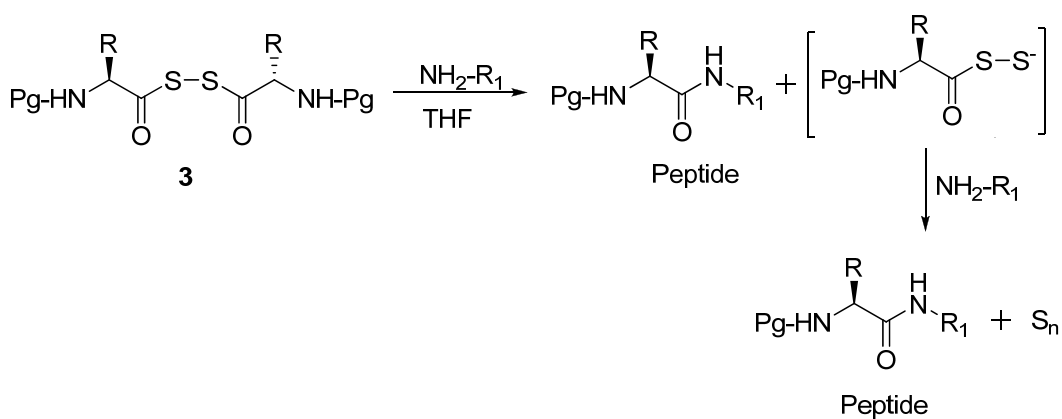
Na₂SO₄ and evaporated under reduced pressure to give *N*-protected amino thioacid which was used for oxidative dimerization without further purification.

The *N*-protected amino thioacid obtained from the above procedure was dissolved in THF: H₂O (4:1, 20 mL: 5 mL) solvent mixture at room temperature. To this solution, iodine (10 mmol) was added. The reaction mixture was stirred for about 12 h. The solvent was evaporated under reduced pressure. The residue was diluted with water (40 mL) and extracted with ethyl acetate (30 mL × 3). The combined organic layer was washed with 10 % aq. Na₂CO₃, brine and dried over anhydrous Na₂SO₄. The combined organic layer was evaporated under reduced pressure to give *N*-protected amino thioacid dimer. The pure thioacid oxidative dimer was obtained after the silica gel column purification using ethyl acetate and petroleum ether.



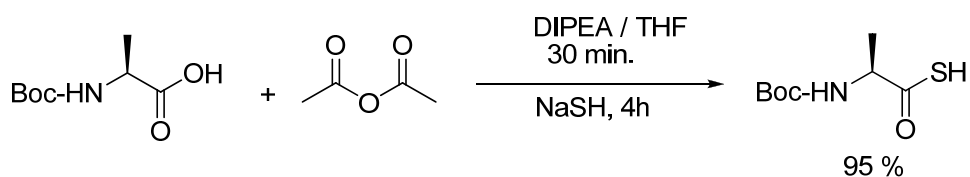
General procedure for the synthesis of peptides using *N*-protected amino thioacid oxidative dimers

The *N*-protected amino thioacid oxidative dimer (0.5 mmol) was dissolved in dry THF at room temperature. To this solution, methyl ester of amino acid or *N*-terminal free peptide (1.5 mmol in ~2 mL ethyl acetate) was added. The reaction mixture was stirred for about 30 min. After completion of the reaction (as monitored by TLC), the reaction mixture was diluted with ethyl acetate (50 mL) and washed with 5 % aq. HCl, 10 % Na₂CO₃ and brine. The organic layer was dried over anhydrous Na₂SO₄ and concentrated under reduced pressure to give crude peptide which was purified by column chromatography using ethyl acetate and petroleum ether.



Synthesis of Boc-Ala-SH by using Boc-Ala-OH, NaSH and acetic anhydride.

In 50 ml RB flask, Boc-Ala-OH (0.945 g, 0.5 mmol) was dissolved in 7 mL of dry THF. To this solution, diisopropylethylamine (1 mmol) was added. This reaction mixture was then cooled to 0 °C prior to addition of acetic anhydride (0.510 g, 0.5 mmol) and stirred for another 30 min. The reaction mixture was treated NaSH (0.308 g, 0.55 mmol) and stirred for another 4h. After completion of reaction (indicated by mass spectra), the solvent THF was evaporated and residue was treated with water (25 mL) and acidified with 5 % HCl to make pH ~ 2. This aqueous layer was then extracted with ethyl acetate (20 mL × 3) washed with brine, dried over anhydrous Na₂SO₄ and evaporated under reduced pressure to get Boc-Ala-SH in 95 % (0.974 g).

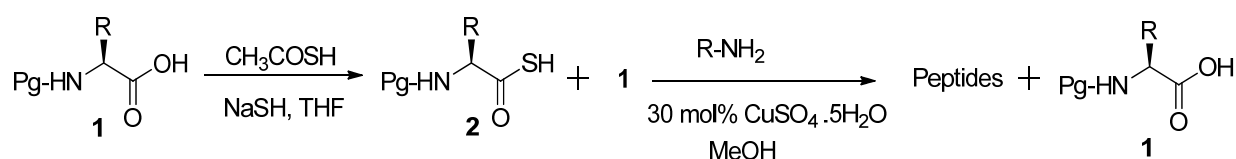


General procedure for the synthesis of di/tripeptides by using *N*-protected amino thioacids and copper sulphate.

Isolation of Amine Ester from HCl.NH₂(R)-OMe: Hydrochloride salt of methyl ester of amino acid or trifluoroacetic acid salt of dipeptide methyl ester (12 mmol) was dissolved in saturated solution of aq. Na₂CO₃ and extracted with ethyl acetate (40 mL x 3). The

combined organic layer was washed with brine and dried over anhydrous Na_2SO_4 . This organic layer was concentrated to the volume ~ 4 mL under reduced pressure and used directly for the coupling reaction.

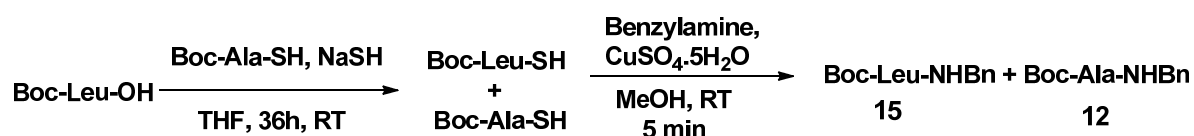
The *N*-protected amino thioacid (10 mmol) obtained by above procedure was dissolved in distilled methanol (10 mL). To this solution, methyl ester of amino acid or *N*-terminal free peptide (12 mmol) was added with stirring. This reaction mixture was treated with 30 mol% of $\text{CuSO}_4 \cdot 5\text{H}_2\text{O}$. After 5 min, the clean reaction mixture was converted to dark brown color turbid solution indicating the completion of the reaction (also monitored by TLC). The reaction mixture was centrifuged and the residue was further washed with methanol. The combined methanol solution was evaporated under reduced pressure. The residue was then dissolved in ethyl acetate (80 mL) and washed with 10% aq. Na_2CO_3 , 5% aq. HCl and brine, dried over anhydrous Na_2SO_4 and concentrated under reduced pressure. The product was purified by column chromatography using ethyl acetate and petroleum ether.



Procedure for synthesis of *N*-Boc-Leu-SH from *N*-Boc-Leu-OH mediated by *N*-Boc-Ala-SH and NaSH and its subsequent amide formation

In 50 ml RB flask, Boc-Leu-OH (1.5 mmol) was dissolved in dry THF (7 ml). To this solution Boc-Ala-SH (1.5 mmol) and NaSH (3 mmol) was added at room temperature. This reaction mixture was stirred for another 36 h in open air condition. Followed by evaporation of solvent under reduced pressure. The residue was diluted with water (20 ml) and acidified with 5 % HCl to make $\text{pH} \sim 2$. This aqueous layer was extracted with ethyl acetate ($25\text{mL} \times 3$) washed with brine, dried over anhydrous Na_2SO_4 . Organic layer was concentrated under reduced pressure to give Boc-Leu-SH thioacid along with some unreacted Boc-Ala-SH and Boc-Leu-OH. This crude product was utilized without purification for peptide synthesis.

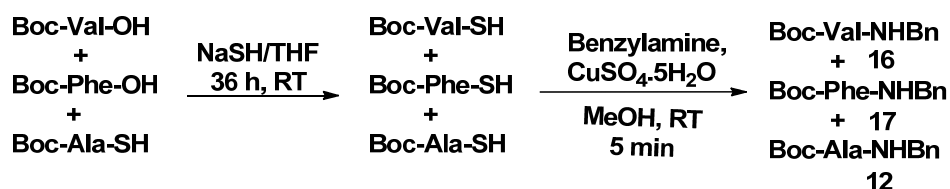
The crude mixture of Boc-Leu-SH and Boc-Ala-SH was dissolved in methanol (5 mL). To this solution benzylamine (3.5 mmol) and CuSO₄·5H₂O (30 mol%) was added at room temperature. The reaction mixture was stirred for further 5 min which results in conversion of clear solution in dark brown color turbid solution indicating formation of peptides. The reaction mixture was centrifuged and the residue was further washed with methanol. The combined methanol solution was evaporated under reduced pressure. The residue was then dissolved in ethyl acetate (80 mL) and washed with 10% aq. Na₂CO₃, 5% aq. HCl and brine, dried over anhydrous Na₂SO₄ and concentrated under reduced pressure. Resulted amides were analyzed by MALDI TOF/TOF mass spectroscopy and reverse phase HPLC.



Procedure for synthesis of *N*-Boc-Val-SH and *N*-Boc-Phe-SH from *N*-Boc-Val-OH and *N*-Boc-Phe-OH mediated by *N*-Boc-Ala-SH and NaSH and its utilization in amide formation

Similar procedure was followed as mentioned above for the synthesis of *N*-Boc-Val-SH and *N*-Boc-Phe-SH starting from *N*-Boc-Val-OH (1.5 mmol) and *N*-Boc-Phe-OH (1.5 mmol) along with *N*-Boc-Ala-SH (3 mmol) and NaSH (6 mmol).

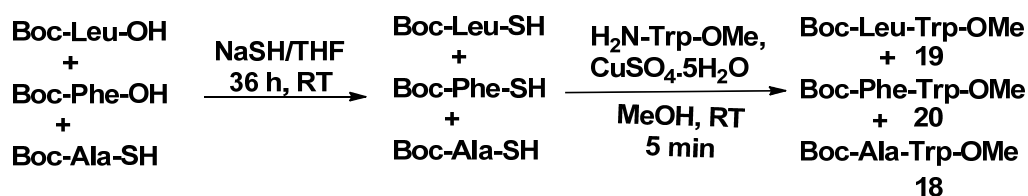
The thioacids obtained was treated with benzylamine (5 mmol) in the presence of copper sulphate in methanol. The corresponding amides was isolated and characterized by the similar procedure as mentioned above.



Procedure for synthesis of *N*-Boc-Leu-SH and *N*-Boc-Phe-SH from *N*-Boc-Leu-OH and *N*-Boc-Phe-OH mediated by *N*-Boc-Ala-SH and NaSH and its utilization in peptide formation

Similar procedure was followed as mentioned above for the synthesis of *N*-Boc-Leu-SH and *N*-Boc-Phe-SH starting from *N*-Boc-Leu-OH (1.5 mmol) and *N*-Boc-Phe-OH (1.5 mmol) along with *N*-Boc-Ala-SH (3 mmol) and NaSH (6 mmol).

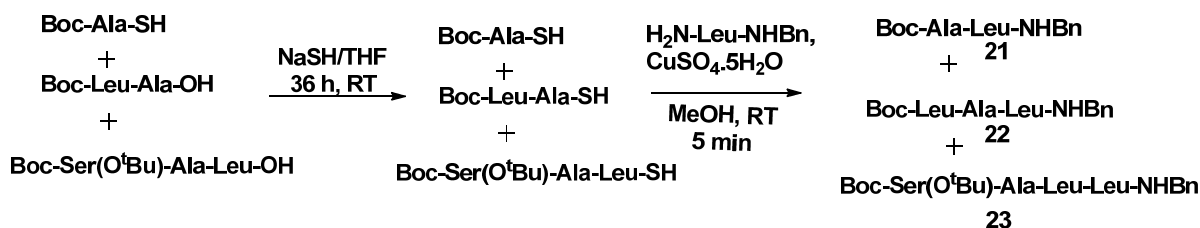
The thioacids obtained was treated with free amine methyl ester of tryptophan (5 mmol) in the presence of copper sulphate in methanol. The corresponding dipeptides was isolated and characterized by the similar procedure as mentioned above.



Procedure for synthesis of *N*-Boc-Leu-Ala-SH and *N*-Boc-Ser(O^tBu)-Ala-Leu-SH from *N*-Boc-Leu-Ala-OH and *N*-Boc-Ser(O^tBu)-Ala-Leu-OH mediated by *N*-Boc-Ala-SH and NaSH and its utilization in amide formation

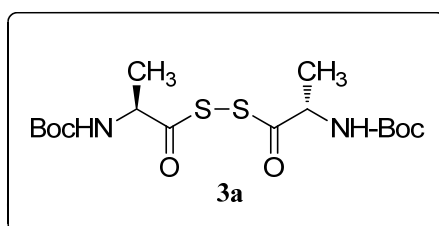
Similar procedure was followed as mentioned above for the synthesis of *N*-Boc-Leu-Ala-SH and *N*-Boc-Ser(O^tBu)-Ala-Leu-SH starting from *N*-Boc-Leu-Ala-OH (1.5 mmol) and *N*-Boc-Ser(O^tBu)-Ala-Leu-OH (1.5 mmol) along with *N*-Boc-Ala-SH (3 mmol) and NaSH (6 mmol).

The thioacids obtained was treated with free amine leucine benzylamide (5 mmol) in the presence of copper sulphate in methanol. The corresponding peptide amides was isolated and characterized by the similar procedure as mentioned above.

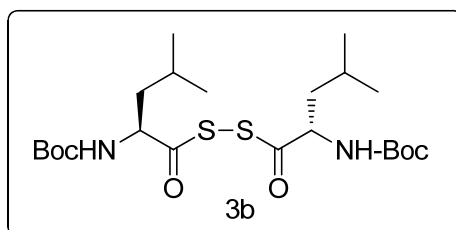


Spectroscopic data for the products

(R)-2-((Tert-butoxycarbonyl)amino)Propanoic dithioperoxyanhydride [(Boc-Ala-S)₂] (3a); White powder (0.82 g, 40%), mp = 123-125 °C; $[\alpha]_D^{25} +20$ (*c* 0.1, MeOH); UV (λ_{\max}) = 231 nm; IR ν (cm⁻¹) 3379, 2972, 1705, 1507, 1367, 1271, 1241, 1164, 1048, 1031, 965, 912; ¹H NMR (400 MHz; CDCl₃); δ 5.07 (d, *J* = 8 Hz, 2H), 4.54 (t, *J* = 6 Hz, 2H), 1.48 (s, 18H), 1.45 (d, *J* = 8 Hz, 6H), ¹³C NMR (100 MHz, CDCl₃); 199.6, 154.8, 80.9, 56.3, 28.2, 18.7; HRMS (ESI) *m/z* calcd. for C₁₆H₂₈N₂NaO₆S₂ [M + Na]⁺ = 431.1286, observed [M+Na]⁺ = 431.1287.

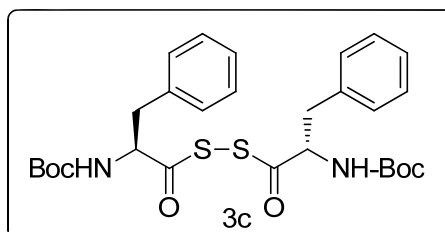


(R)-2-((Tert-butoxycarbonyl)amino)-4-Methylpentanoic dithioperoxyanhydride [(Boc-Leu-S)₂] (3b); White powder (0.87 g, 35%), mp = 106-108 °C; $[\alpha]_D^{25} +2$ (*c* 0.1, MeOH); UV (λ_{\max}) = 231 nm; IR ν (cm⁻¹) 3395, 2973, 1719, 1701, 1495, 1393, 1366, 1235, 1162, 1052, 870; ¹H NMR (400 MHz; CDCl₃); δ 4.97 (d, *J* = 8, 2H), 4.51 (br., 2H), 1.74 (t, *J* = 6 Hz, 4H), 1.60-1.57 (m, 2H), 1.47 (s, 18H), 0.96 (dd, *J* = 8 Hz, 12H); ¹³C NMR (100 MHz, CDCl₃); 196.7, 155.0, 80.8, 59.2, 41.0, 28.2, 24.6, 22.9, 21.4; HRMS (ESI) *m/z* calcd. for C₂₂H₄₀N₂NaO₆S₂ [M + Na]⁺ = 515.2225, observed [M+Na]⁺ = 515.2228.

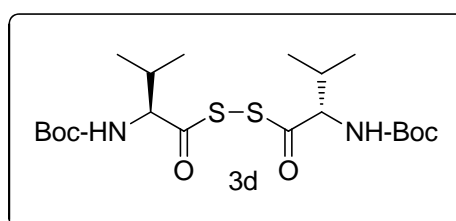


(S)-2-((Tert-butoxycarbonyl)amino)-3-Phenylpropanoic dithioperoxyanhydride [(Boc-Phe-S)₂] (3c); White powder (0.868 g, 31 %) mp = 137-139 °C; $[\alpha]_D^{25} -14$ (*c* 0.1, MeOH); UV (λ_{\max}) = 209 nm and 252 nm; IR ν (cm⁻¹) 3337, 2972, 2928, 1733, 1502,

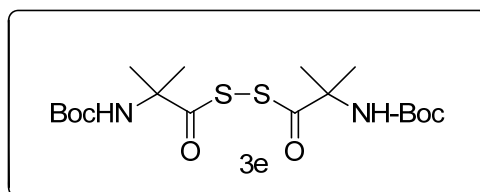
1449, 1368, 1224, 1163, 1053, 849, 750, 701; ^1H NMR (400 MHz; CDCl_3): δ 7.37-7.23 (m, 10H), 5.01 (br., 2H), 4.81 (br., 2H), 3.27-3.14 (m, 4H), 1.44 (s, 18H); ^{13}C NMR (100 MHz; CDCl_3): δ 196.1, 154.9, 135.0, 129.3, 128.8, 127.3, 80.9, 81.0, 61.0, 37.8, 28.1 HRMS (ESI) m/z calcd. for $\text{C}_{28}\text{H}_{36}\text{N}_2\text{NaO}_6\text{S}_2$ $[\text{M} + \text{Na}]^+ = 583.1912$, observed $[\text{M} + \text{Na}]^+ = 583.1919$.



(R)-2-((Tert-butoxycarbonyl)amino)-3-Methylbutanoic dithioperoxyanhydride [(Boc-Val-S) $_2$] (3d); White powder (0.8 g, 33%), mp = 127-129 °C; $[\alpha]_{\text{D}}^{25} +18$ (c 0.1, MeOH); UV (λ_{max}) = 231 nm; IR ν (cm^{-1}) 3383, 2961, 1721, 1705, 1504, 1368, 1250, 1167, 1057, 1019; ^1H NMR (400 MHz; CDCl_3): δ 5.09 (d, $J = 8$ Hz, 2H), 4.42 (q, $J = 4$ Hz, 2H), 2.38-2.34 (m, 2H), 1.48 (s, 18H), 1.0 (dd, $J = 8$ Hz, 12H); ^{13}C NMR (100 MHz, CDCl_3); 195.9, 155.3, 80.8, 65.3, 31, 28.2, 19.1, 16.8; HRMS (ESI) m/z calcd. for $\text{C}_{20}\text{H}_{36}\text{N}_2\text{NaO}_6\text{S}_2$ $[\text{M} + \text{Na}]^+ = 487.1912$, observed $[\text{M} + \text{Na}]^+ = 487.1925$.

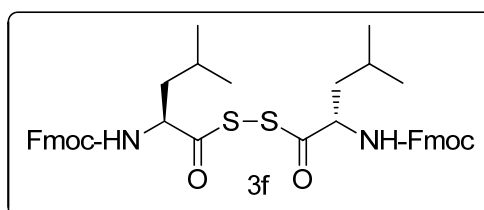


2-((Tert-butoxycarbonyl)amino)-2-Methylpropanoic dithioperoxyanhydride [(Boc-Aib-S) $_2$] (3e); White powder (0.54 g, 25%), mp = 167-169 °C; UV (λ_{max}) = 231 nm; IR ν (cm^{-1}) 3368, 2980, 2929, 1712, 1507, 1386, 1366, 1274, 1253, 1159, 970, 878, 828; ^1H NMR (400 MHz; CDCl_3): δ 5.09 (br., 2H), 1.55 (s, 12H), 1.46 (s, 18H); ^{13}C NMR (100 MHz, CDCl_3); 198.3, 153.9, 80.6, 62.5, 28.2, 25.5; HRMS (ESI) m/z calcd. for $\text{C}_{18}\text{H}_{32}\text{N}_2\text{NaO}_6\text{S}_2$ $[\text{M} + \text{Na}]^+ = 459.1599$, observed $[\text{M} + \text{Na}]^+ = 459.1592$.

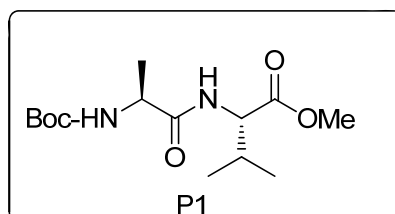


2-(((9H-Fluoren-9-yl)methoxy)carbonyl)amino)-4-methylpentanoic

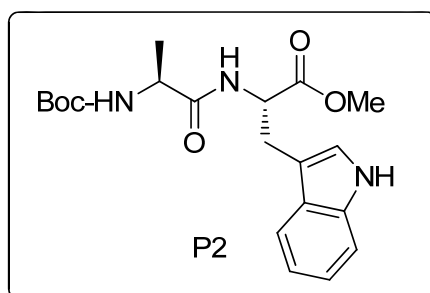
dithioperoxyanhydride [(Fmoc-Leu-S-)₂] (3f); White powder (0.95 g, 26%), mp = 154-156 °C; $[\alpha]_D^{25}$ -14 (*c* 0.1, MeOH); UV (λ_{\max}) = 212 nm, 265 nm, 289 nm, 300 nm; IR ν (cm^{-1}) = 3387, 2956, 2922, 2861, 1703, 1522, 1447, 1381, 1323, 1246, 1122, 1045, 738, 547; ^1H NMR (200 MHz, CDCl_3) δ 7.77 (d, J = 8 Hz, 4H), 7.62 (t, J = 6 Hz, 4H), 7.44-7.31 (m, 8H), 5.21 (d, J = 8 Hz, 1H), 5.05 (d, J = 8 Hz, 1H), 4.67-4.42 (m, 6H), 4.25 (t, J = 6 Hz, 2H), 0.93 (dd, J = 6 Hz & 6 Hz, 12H); ^{13}C NMR (100 MHz, CDCl_3) 196.1, 155.6, 143.6, 141.3, 127.7, 127.1, 124.9, 120.0, 67.1, 60.4, 59.7, 59.4, 47.2, 41.0, 24.6, 23.0, 21.3; HRMS (ESI) m/z calculated for $\text{C}_{42}\text{H}_{44}\text{N}_2\text{O}_6\text{S}_2$ $[\text{M} + \text{Na}]^+ = 759.2538$, observed $[\text{M} + \text{Na}]^+ = 759.2536$.



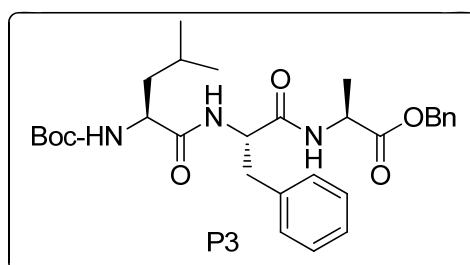
Boc-Ala-Val-OMe (P1); White powder (0.226g, 75 %); $[\alpha]_D^{25}$ -44 (*c* 0.1, MeOH); ^1H NMR (400 MHz; CDCl_3); δ 6.76 (d, J = 4, 1H), 5.09 (d, J = 8 Hz, 1H), 4.51 (dd, J = 8 Hz, 1H), 4.18 (br., 1H), 3.72 (s, 3H), 2.20-2.21 (m, 1H), 1.43 (s, 9H), 1.34 (d, J = 8 Hz, 3H), 0.90 (dd, J = 4 Hz, J = 8 Hz, 6H); ^{13}C NMR (100 MHz, CDCl_3); δ 172.5, 172.2, 155.5, 80.0, 56.9, 52.0, 49.9, 31.1, 28.1, 18.8, 17.6; MALDI TOF/TOF m/z Calcd. for $\text{C}_{14}\text{H}_{26}\text{N}_2\text{NaO}_5$ ($\text{M} + \text{Na}$) is 325.1739 Observed = 325.1589.



Boc-Ala-Trp-OMe (P2); White powder (0.334 g, 86%); $[\alpha]_D^{25}$ -12 (*c* 0.1, MeOH); ^1H NMR (400 MHz; CDCl_3); δ 8.35 (d, $J = 8$ Hz, 1H), 7.52 (d, $J = 8$ Hz, 1H), 7.35 (d, $J = 8$ Hz, 1H), 7.18 (t, $J = 8$ Hz, 1H), 7.11 (t, $J = 8$ Hz, 1H), 7.01 (br., 1H), 6.63 (d, $J = 8$ Hz, 1H), 5.01 (br., 1H), 4.92-4.87 (m, 1H), 4.16-4.14 (m, 1H), 3.66 (s, 3H), 3.32 (d, $J = 8$ Hz, 2H), 1.41 (s, 9H), 1.29 (d, $J = 8$ Hz, 3H); ^{13}C NMR (100 MHz, CDCl_3); 172.3, 172.0, 136.0, 127.5, 123.0, 122.1, 119.5, 118.4, 111.2, 109.6, 80.0, 52.9, 52.3, 28.2, 27.5, 18.3; MALDI TOF/TOF m/z Calcd. for $\text{C}_{20}\text{H}_{27}\text{N}_3\text{NaO}_5$ ($M + \text{Na}$) is 412.1848 Observed = 412.1998.

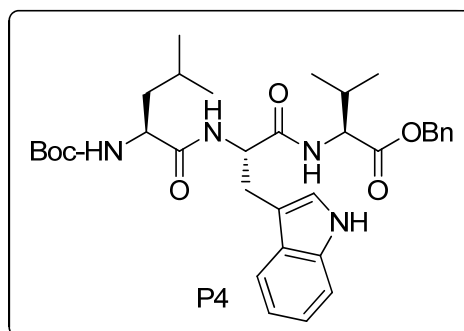


Boc-Leu-Phe-Ala-OBn (P3); White powder (0.452 g, 84%); $[\alpha]_D^{25}$ -36 (*c* 0.1, MeOH); ^1H NMR (400 MHz; CDCl_3); δ 7.38-7.32 (m, 5H), 7.25-7.17 (m, 5H), 6.71-6.69 & 6.67-6.65 (d, $J = 8$ Hz, 1H) & (d, $J = 8$ Hz, 1H), 5.15 (s, 2H), 4.83 (d, $J = 8$ Hz, 1H), 4.69 (q, $J = 8$ Hz, $J = 4$ Hz, 1H), 4.56-4.49 (m, $J = 8$ Hz, 1H), 4.05 (br., 1H), 3.14-3.02 (m, 2H), 1.62-1.55 (m, 2H), 1.4 (s, 9H), 1.34 (d, $J = 8$ Hz, 3H), 0.90 (t, $J = 8$ Hz, 6H); ^{13}C NMR (100 MHz, CDCl_3); 172.3, 172.0, 170.1, 155.6, 136.3, 135.3, 129.2, 128.5, 128.3, 128.1, 126.9, 80.2, 67.0, 53.8, 48.2, 40.9, 37.8, 29.6, 28.2, 24.6, 22.9, 21.7, 17.9; MALDI TOF/TOF m/z Calcd. for $\text{C}_{30}\text{H}_{41}\text{N}_3\text{NaO}_6$ ($M + \text{Na}$) is 562.2893 Observed = 562.3182.

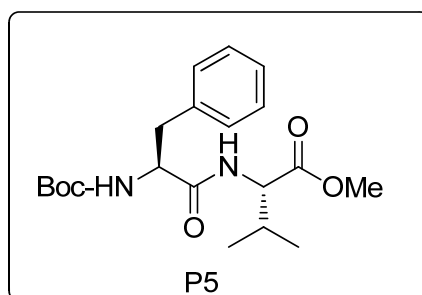


Boc-Leu-Trp-Val-OMe (P4);³⁴ White powder (0.371 g, 70%); $[\alpha]_D^{25}$ -28 (*c* 0.1, MeOH); ^1H NMR (400 MHz; CDCl_3); δ 8.23 (br., 1H), 7.71 (d, $J = 8$ Hz, 1H), 7.35 (d, $J = 8$ Hz,

1H), 7.20-7.11 (m, 3H), 6.88 (d, $J = 8$ Hz, 1H), 6.34 (d, $J = 8$ Hz, 1H), 4.83 (d, $J = 8$ Hz, 1H), 4.76 (br., 1H), 4.13 (q, $J = 4$ Hz, 1H), 4.13 (q, $J = 8$ Hz, 1H), 3.63 (s, 3H), 3.33 (dd, $J = 8$ Hz, $J = 4$ Hz, 1H), 3.15 (dd, $J = 8$ Hz, $J = 4$ Hz, 1H), 2.03-1.97 (m, 1H), 1.63 (t, $J = 6$ Hz, 2H), 1.39 (s, 9H), 0.91 (d, $J = 4$ Hz, 6H), 0.77 (dd, $J = 8$ Hz, $J = 8$ Hz, 6H); ^{13}C NMR (100 MHz, CDCl_3); 171.9, 171.7, 171.2, 156.0, 136.0, 127.4, 123.3, 122.0, 119.4, 118.3, 111.3, 109.3, 80.2, 52.6, 52.3, 51.4, 30.4, 28.2, 27.4, 24.5, 22.8, 17.3; MALDI TOF/TOF m/z Calcd .for $\text{C}_{28}\text{H}_{42}\text{N}_4\text{NaO}_6$ ($\text{M} + \text{Na}$) is 553.3002 Observed = 553.3280.

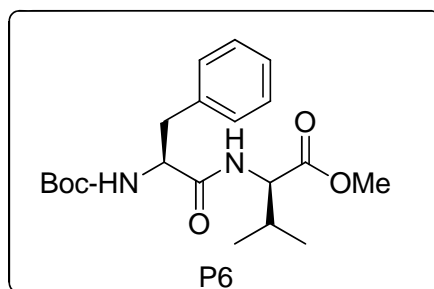


Boc-Phe-Val-OMe (P5),³⁵ White powder (0.279 g, 74%); $[\alpha]_{\text{D}}^{25}$ -18 (c 0.1, MeOH); ^1H NMR (400 MHz; CDCl_3): δ 7.35-7.26 (m, 5H), 6.45 (d, $J = 8$ Hz, 1H), 5.10 (br., 1H), 4.51 (q, $J = 4$ Hz, 1H), 4.4 (br., 1H), 3.74 (s, 3H), 3.12 (d, $J = 8$ Hz, 2H), 2.18-2.12 (m, 1H), 1.46 (s, 9H), 0.90 (dd, $J = 4$ Hz, $J = 8$ Hz, 6H); ^{13}C NMR (100 MHz; CDCl_3): δ 171.7, 171.1, 155.3, 136.5, 129.2, 128.5, 126.8, 80.1, 57.1, 55.7, 52.0, 37.9, 31.2, 28.1, 18.7, 17.6; MALDI TOF/TOF m/z calcd for $\text{C}_{20}\text{H}_{30}\text{N}_2\text{O}_5$ ($\text{M} + \text{Na}$) = 401.2052 Observed ($\text{M} + \text{Na}$) = 401.2318.

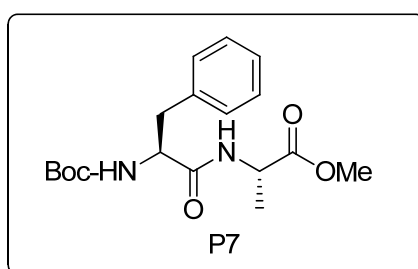


Boc-Phe-^DVal-OMe (P6); White powder (0.287 g, 76%); $[\alpha]_{\text{D}}^{25}$ +6 (c 0.1, MeOH); ^1H NMR (400 MHz; CDCl_3): δ 7.35-7.25 (m, 5H), 6.45 (d, $J = 4$ Hz, 1H), 5.06 (br., 1H),

4.51 (br., 1H), 4.45 (br., 1H), 3.75 (s, 3H), 3.12 (d, $J = 8$ Hz, 2H), 2.13-2.06 (m., 1H), 1.46 (s, 9H), 0.83 (dd, $J = 8$ Hz, $J = 8$ Hz, 6H); ^{13}C NMR (100 MHz; CDCl_3): δ 171.9, 171.1, 155.3, 136.5, 129.2, 128.7, 126.9, 80.2, 57.0, 55.8, 52.1, 38.2, 31.0, 28.2, 18.7, 17.5; MALDI TOF/TOF m/z calcd for $\text{C}_{20}\text{H}_{30}\text{N}_2\text{O}_5$ ($\text{M} + \text{Na}$) = 401.2052 Observed ($\text{M} + \text{Na}$) = 401.2291.

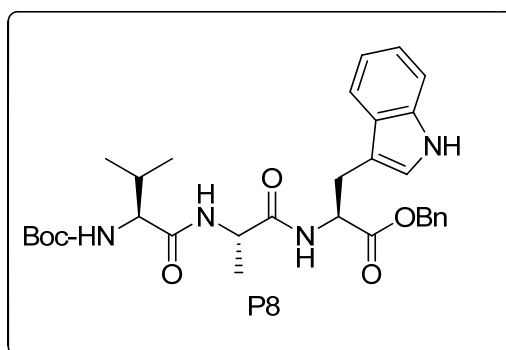


Boc-Phe-Ala-OMe (P7); White powder (0.283 g, 81%); $[\alpha]_{\text{D}}^{25}$ -22 (c 0.1, MeOH); ^1H NMR (400 MHz; CDCl_3): δ 7.32-7.20 (m, 5H), 6.47 (d, $J = 4$ Hz, 1H), 5.03 (d, $J = 8$ Hz, 1H), 4.56-4.49 (m, 1H), 4.38-4.37 (m, 1H), 3.72 (s, 3H), 3.08 (t, $J = 6$ Hz, 2H), 1.41 (s, 9H), 1.35 (d, $J = 8$ Hz, 3H) ^{13}C NMR (100 MHz; CDCl_3): δ 172.8, 170.7, 155.3, 136.4, 129.3, 128.6, 126.9, 80.2, 55.5, 52.4, 48.0, 38.3, 28.2, 18.3; MALDI TOF/TOF m/z calcd. for $\text{C}_{18}\text{H}_{26}\text{N}_2\text{O}_5$ ($\text{M} + \text{Na}$) = 373.1739 Observed ($\text{M} + \text{Na}$) = 373.1906.

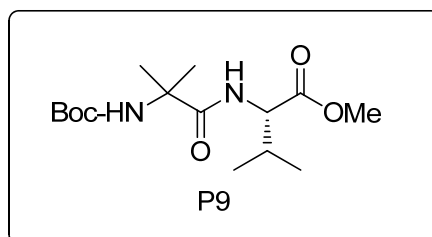


Boc-Val-Ala-Trp-OMe (P8); White powder (0.356 g, 73%); $[\alpha]_{\text{D}}^{25}$ -34 (c 0.1, MeOH); ^1H NMR (400 MHz; CDCl_3): δ 8.56 (br., 1H), 7.48 (d, $J = 8$ Hz, 1H), 7.33 (d, $J = 8$ Hz, 1H), 7.16 (t, $J = 8$ Hz, 1H), 7.09 (t, $J = 8$ Hz, 1H), 7.00 (br., 1H), 6.78 (d, $J = 8$ Hz, 1H), 6.69 (d, $J = 8$ Hz, 1H), 5.12 (d, $J = 8$ Hz, 1H), 4.90-4.85 (m, 1H), 4.53-4.45 (m, 1H), 3.94 (t, $J = 8$ Hz, 1H), 3.67 (s, 3H), 3.30 (d, $J = 8$ Hz, 2H), 2.06-2.00 (m, 1H), 1.45 (s, 9H), 1.32 (d, $J = 8$ Hz, 3H), 0.86 (dd, $J = 8$ Hz, $J = 16$ Hz, 6H); ^{13}C NMR (100 MHz, CDCl_3): 171.9, 171.8, 171.5, 136.0, 127.4, 123.3, 122.0, 119.4, 118.3, 111.3, 109.3, 80.2, 59.8, 52.8, 52.4,

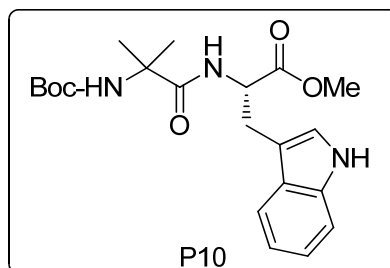
48.6, 30.7, 29.6, 28.7, 19.1, 17.2; MALDI TOF/TOF m/z Calcd. for $C_{25}H_{36}N_4NaO_6$ ($M + Na$) is 511.2532 Observed = 511.2528.



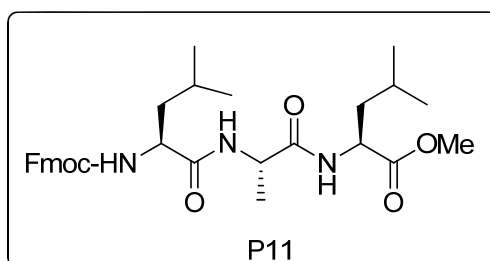
Boc-Aib-Val-OMe (P9); White powder (0.205 g, 65%); $[\alpha]_D^{25}$ -6 (c 0.1, MeOH); 1H NMR (400 MHz; $CDCl_3$); δ 7.02 (br., 1H), 4.94 (br., 1H), 4.52 (q, $J = 4$ Hz, 1H), 3.71 (s, 3H), 2.19-2.13 (m, 1H), 1.51 & 1.47 (s, 6H), 1.43 (s, 9H), 0.92 (dd, $J = 8$ Hz, $J = 4$ Hz, 6H); ^{13}C NMR (100 MHz, $CDCl_3$); 174.4, 172.4, 154.5, 80.1, 57.0, 56.8, 52.0, 31.1, 28.3, 28.2, 26.0, 18.9, 17.5; MALDI TOF/TOF m/z Calcd. for $C_{15}H_{28}N_2NaO_5$ ($M + Na$) is 339.1896 Observed = 339.1841.



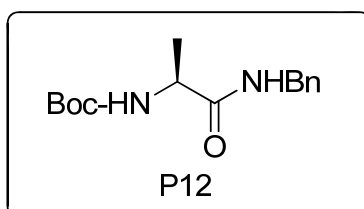
Boc-Aib-Trp-OMe (P10); White powder (0.298 g, 74%); $[\alpha]_D^{25}$ +2 (c 0.1, MeOH); 1H NMR (400 MHz; $CDCl_3$); δ 8.43 (br., 1H), 7.54 (d, $J = 8$ Hz, 1H), 7.34 (d, $J = 4$ Hz, 1H), 7.18-7.03 (m, 3H), 6.89 (br., 1H), 5.02 (d, $J = 4$ Hz, 1H), 4.91-4.85 (m, 1H), 3.63 (s, 3H), 3.36-3.25 (m, 2H), 1.43 & 1.39 (s, 6H) & (s, 9H); ^{13}C NMR (100 MHz, $CDCl_3$); 174.4, 172.4, 154.5, 136.0, 127.4, 122.9, 121.9, 119.3, 118.4, 111.2, 109.7, 79.9, 56.6, 53.0, 52.2, 28.1, 27.6, 24.4; MALDI TOF/TOF m/z Calcd. for $C_{21}H_{29}N_3NaO_5$ ($M + Na$) is 426.2005 Observed = 426.1302.



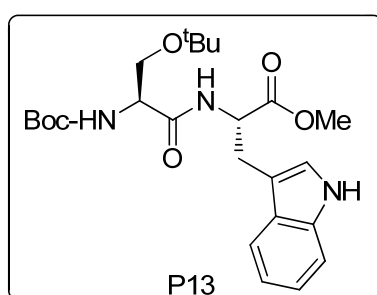
Fmoc-Leu-Ala-Leu-OMe (P11); White powder (0.460 g, 84%); $[\alpha]_D^{25}$ -50 (*c* 0.1, MeOH); $^1\text{H NMR}$ (400 MHz, CDCl_3) δ 7.76 (d, $J = 8\text{Hz}$, 2H), 7.58 (d, $J = 8\text{Hz}$, 2H), 7.39 (t, $J = 6\text{Hz}$, 2H), 7.30 (t, $J = 8\text{Hz}$, 2H), 6.77 (d, $J = 16\text{Hz}$, 2H), 7.30 (t, $J = 8\text{Hz}$, 2H), 6.77 (d, $J = 16\text{Hz}$, 2H), 5.43 (d, $J = 8\text{Hz}$, 1H), 4.56 (br., 2H), 4.47-4.34 (m, 2H), 4.20 (t, $J = 6\text{ Hz}$, 2H), 3.71 (s, 3H), 1.62-1.54 (m, 6H), 1.37 (d, $J = 8\text{ Hz}$, 3H), 0.92 (t, $J = 6\text{Hz}$, 12H); $^{13}\text{C NMR}$ (100 MHz, CDCl_3) 173.1, 172.2, 171.7, 156.2, 143.7, 141.3, 127.7, 127.0, 125.0, 120.0, 67.0, 54.0, 52.3, 50.8, 48.7, 47.1, 41.7, 42.3, 29.7, 24.7, 24.6, 23.0, 21.8, 18.0; MALDI TOF/TOF m/z calculated for $\text{C}_{31}\text{H}_{41}\text{N}_3\text{NaO}_6$ $[\text{M} + \text{Na}] = 574.2893$ observed = 574.3691.



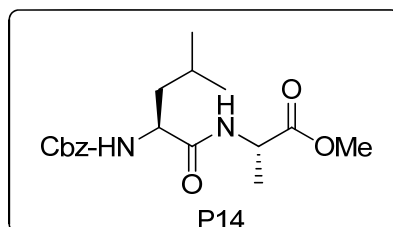
Boc-Ala-NHBn (P12);¹⁹ White solid, (1.5 g, 78%) $^1\text{HNMR}$ (400 MHz; CDCl_3): δ 7.32-7.22 (m, 5H), 6.821 (br., 1H), 5.201 (br., 1H), 4.412 (br., 2H), 4.226 (br., 1H), 1.395 (s, 9H), 1.376-1.357 (d, 3H, $J = 7.6\text{ Hz}$); $^{13}\text{CNMR}$ (100 MHz; CDCl_3): 172.7, 155.6, 138.1, 128.7, 127.4, 80.1, 50.2, 43.4, 28.3, 18.5; MALDI TOF/TOF m/z Calculated for $\text{C}_{15}\text{H}_{22}\text{N}_2\text{O}_3$ (M + Na) is 301.1528 Observed = 301.1804.



Boc-Ser(OtBu)-Trp-OMe (P13); Gummy, (1.94 g, 65%), ^1H NMR (400 MHz; CDCl_3): δ 8.331 (br., 1H), 7.55 (d, $J = 8$ Hz, 1H), 7.34 (d, $J = 8$ Hz, 1H), 7.31 (br., 1H), 7.17 (t, $J = 7.2$ Hz, 1H), 7.11 (t, $J = 6.8$ Hz, 1H), 7.01 (d, $J = 1$ Hz, 1H), 5.42 (d, $J = 5.2$ Hz, 1H), 4.5 (m, 1H), 4.18 (br., 1H), 3.75 & 3.37 (dd, 2H), 3.30 (br., 2H), 3.63 (s, 3H), 1.42 (s, 9H), 1.11 (s, 9H); ^{13}C NMR (100 MHz, CDCl_3) 172.0, 170.3, 155.5, 136.1, 127.6, 123.0, 122.2, 119.6, 118.7, 111.3, 109.9, 80.0, 74.0, 61.8, 60.5, 54.2, 53.1, 52.3, 28.3, 27.3, 21.1, 14.3. MALDI TOF/TOF m/z Calcd. for $\text{C}_{24}\text{H}_{35}\text{N}_3\text{O}_6$ ($\text{M} + \text{Na}$) = 484.2424 Observed = 484.2915.



Cbz-Leu-Ala-OMe (P14);³⁶ White powder, (1.26 g, 60%), ^1H NMR (400 MHz; CDCl_3): δ 7.35 (m, 5H), 6.62 (d, $J = 5.6$ Hz, 1H), 5.30 (d, $J = 8.4$ Hz, 1H), 5.10 (s, 2H), 4.59-4.54 (m, 1H), 4.26-4.20 (m, 1H), 3.74 (s, 3H), 1.73-1.60 (m, 2H), 1.55-1.48 (m, 1H), 1.39 (d, $J = 6.8$ Hz, 3H), 0.94 (d, $J = 6.4$ Hz, 6H); ^{13}C NMR (100 MHz; CDCl_3): 173.1, 171.7, 156.1, 136.1, 128.5, 128.1, 128.0, 67.0, 53.3, 52.5, 48.0, 41.5, 24.6, 22.9, 22.0, 18.2. MALDI TOF/TOF m/z Calcd. for $\text{C}_{18}\text{H}_{26}\text{N}_2\text{O}_5$ ($\text{M} + \text{Na}$) = 373.1739 Observed = 373.2563.



Crystal Structure Analysis of (Boc-Ala-S-)₂ (3a): Crystals of (Boc-Ala-CO-S-)₂ were grown by slow evaporation of ethyl acetate/n-hexane (40/60). A single crystal (0.12 × 0.07 × 0.04 mm) was mounted in a loop with a small amount of the mother liquor. The X-ray data were collected at 100 K temperature using MoK_α radiation ($\lambda = 0.71073 \text{ \AA}$), ω -scans ($2\theta = 56.56^\circ$) for a total number of 3080 independent reflections. Space group $P2(1),2(1),2(1)$ $a = 10.322(3)$, $b = 11.312(4)$, $c = 18.663(6) \text{ \AA}$, $\alpha = 90.00$, $\beta = 90$, $\gamma = 90.00$, $V = 2179.1(12) \text{ \AA}^3$ Orthorhombic P , $Z=4$ for chemical formula $C_{16}H_{28}N_2O_6S_2$, with one molecule in asymmetric unit; $\rho_{\text{calcd}} = 1.245 \text{ g cm}^{-3}$, $\mu = 0.275 \text{ mm}^{-1}$, $F(000) = 872$, $R_{\text{int}} = 0.1890$. All non-hydrogen atoms were refined anisotropically. The hydrogen atoms were fixed geometrically in the idealized position and refined in the final cycle of refinement as riding over the atoms to which they are bonded. The final R value was 0.0684 ($wR2 = 0.1170$) for 3080 observed reflections ($F_0 \geq 4\sigma(|F_0|)$) and 243 variables, $S = 0.943$. The largest difference peak and hole were 0.284 and -0.341 e \AA^3 , respectively.

Crystal Structure Analysis of (Boc-Aib-S-)₂ (3e) : Crystals of (Boc-Aib-CO-S-)₂ were grown by slow evaporation of ethyl acetate/n-hexane (40/60). A single crystal (0.1 × 0.06 × 0.03 mm) was mounted in a loop with a small amount of the mother liquor. The X-ray data were collected at 100 K temperature using MoK_α radiation ($\lambda = 0.71073 \text{ \AA}$), ω -scans ($2\theta = 56.56^\circ$) for a total number of 6601 independent reflections. Space group $Pca2(1)$, $a = 23.375(11)$, $b = 9.575(4)$, $c = 10.580(5) \text{ \AA}$, $\alpha = 90.00$, $\beta = 90$, $\gamma = 90.00$, $V = 2368.1(19) \text{ \AA}^3$ Orthorhombic P , $Z=4$ for chemical formula $C_{18}H_{32}N_2O_6S_2$, with one molecule in asymmetric unit; $\rho_{\text{calcd}} = 1.225 \text{ g cm}^{-3}$, $\mu = 0.258 \text{ mm}^{-1}$, $F(000) = 936$, $R_{\text{int}} = 0.0806$. All non-hydrogen atoms were refined anisotropically. The hydrogen atoms were fixed geometrically in the idealized position and refined in the final cycle of refinement as riding over the atoms to which they are bonded. The final R value was 0.0386 ($wR2 = 0.0680$) for 6601 observed reflections ($F_0 \geq 4\sigma(|F_0|)$) and 263 variables, $S = 0.766$. The largest difference peak and hole were 0.205 and -0.249 e \AA^3 , respectively.

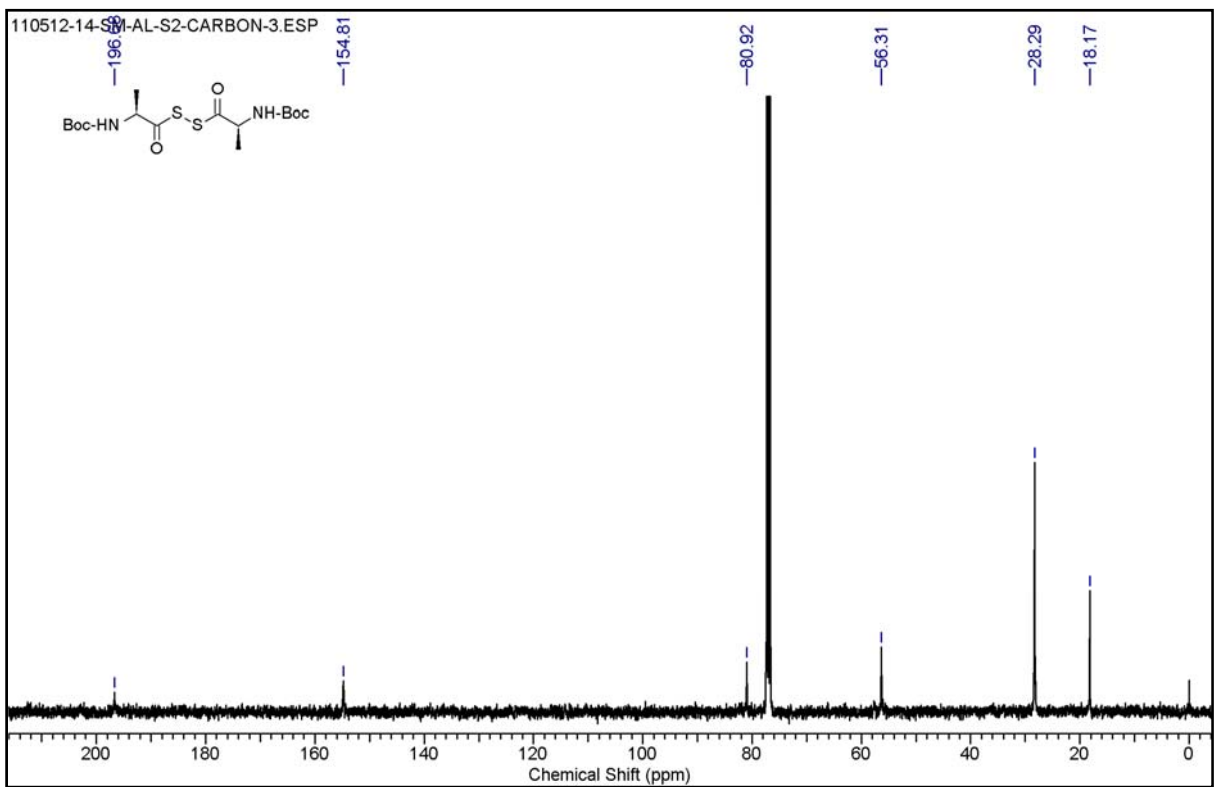
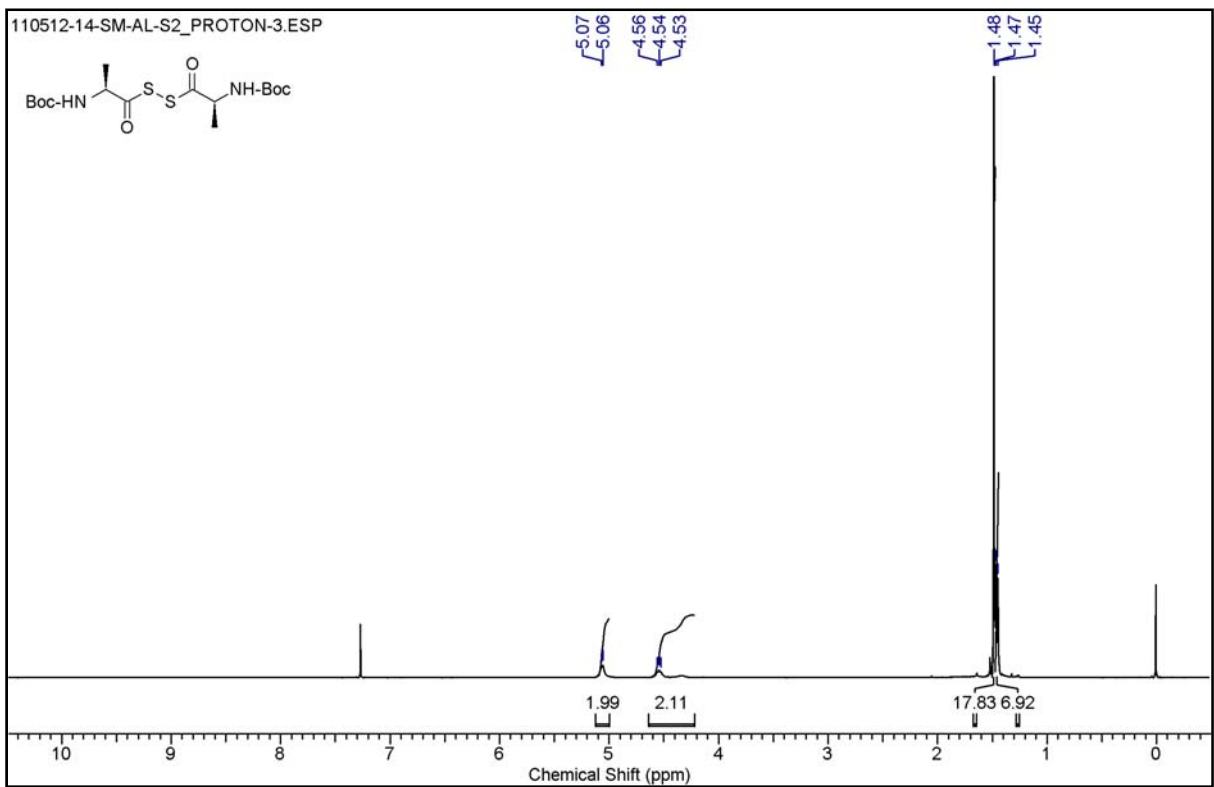
3.6 References

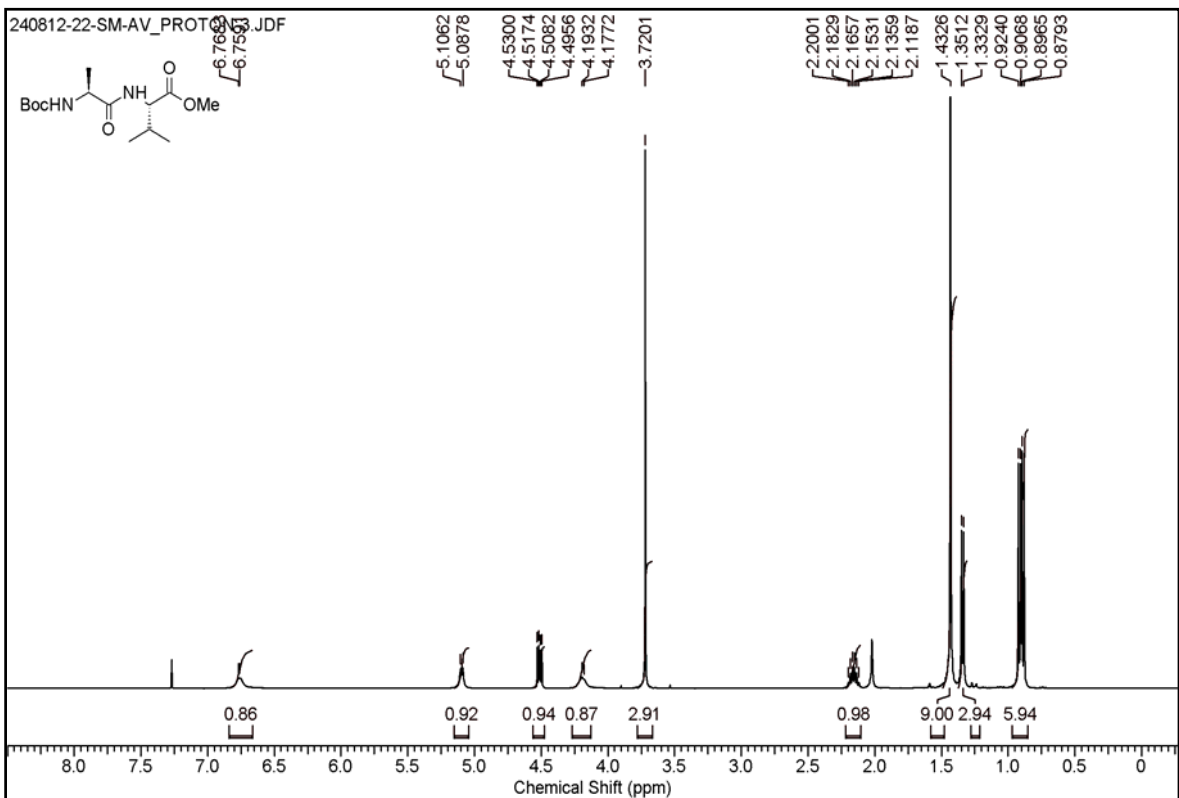
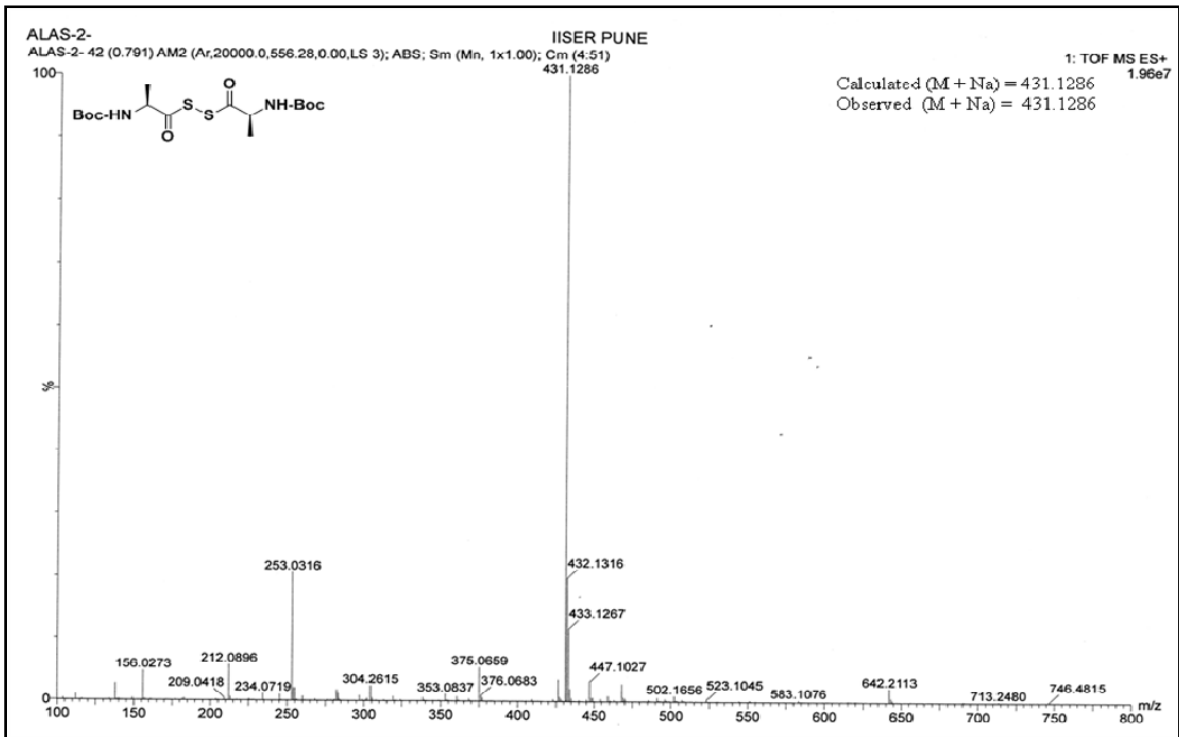
1. a) Santiveri, C. M.; Leon, E.; Rico, M.; Jimenez, M. A. *Chem.–Eur. J.* **2008**, *14*, 488; b) Bulet, P.; Stocklin, R.; Menin, L. *Immunol. Rev.* **2004**, *198*, 169; c) Andreu, D.; Rivas, L. *Biopolymers* **1998**, *47*, 415; d) McDonald, N. Q.; Hendrickson, W. A. *Cell* **1993**, 421; e) Willey, J. M.; van der Donk, W. A. *Annu. Rev. Microbiol.* **2007**, *61*, 477; f) Davidson, B. S. *Chem. Rev.* **1993**, *93*, 1771; g) Wipf, P. In *Alkaloids: Chemical and Biological Perspectives*, Pelletier, S. W., Ed.; Pergamon: New York, **1998**, 187; h) Houssen, W. E.; Jaspars, M. *ChemBioChem* **2010**, *11*, 1803.
2. a) Krishnamoorthy, K.; Begley, T. P. *J. Am. Chem. Soc.* **2011**, *133*, 379; b) Krishnamoorthy, K.; Begley, T. P. *J. Am. Chem. Soc.* **2010**, *132*, 11608; c) Jurgenson, C. T.; Burns, K. E.; Begley, T. P.; Ealick, S. E. *Biochemistry* **2008**, *47*, 10354.
3. Wieland, T. in *The Roots of Modern Biochemistry: Fritz Lipmann's Squiggle and its Consequences* (eds Kleinkauf, H., von Dohren, H. & Lothar, J.) 213 (de Gruyter, Berlin, 1988).
4. a) Rosen, T.; Lico, I. M.; Chu, D. T. W. *J. Org. Chem.* **1988**, *53*, 1580; b) Shangguan, N.; Katukojvala, S.; Greenberg, R.; Williams, L. J. *J. Am. Chem. Soc.* **2003**, *125*, 7754; c) Barlett, K. N.; Kolakowski, R. V.; Katukojvala, S.; Williams, L. J. *Org. Lett.* **2006**, *8*, 823; d) Zhang, X.; Li, F.; Lu, X. –W.; Liu, C. –F. *Bioconjugate. Chem.* **2009**, *20*, 197.
5. Rao, Y.; Li, X.; Danishefsky, S. J. *J. Am. Chem. Soc.* **2009**, *131*, 12924.
6. Crich, D.; Sana, K.; Guo, S. *Org. Lett.* **2007**, *9*, 4423.
7. Pan, J.; Devarie-Baez, N. O.; Xian, M. *Org. Lett.* **2011**, *13*, 1092.
8. Crich, D.; Sasaki, K. *Org. Lett.* **2009**, *11*, 3514.
9. Crich, D.; Sharma, I. *Angew. Chem. Int. Engl. Ed. Engl.* **2009**, *48*, 2355.
10. Assem, N.; Natarajan, A.; Yudin, A. K. *J. Am. Chem. Soc.* **2010**, *132*, 10986.
11. Dyer, F. B.; Park, C. M.; Joseph, R.; Garner, P. *J. Am. Chem. Soc.* **2011**, *133*, 20033.
12. Chen, W.; Shao, J.; Hu, M.; Yu, W.; Giulianotti, M. A.; Houghten, R. A.; Yu, Y. *Chem. Sci.* **2013**, *4*, 970.
13. Blake, J. *Int. J. Pept. Protein Res.* **1981**, *17*, 273.
14. Blake, J.; Li, C. H. *Proc. Natl. Acad. Sci. U.S.A.* **1981**, *78*, 4055.

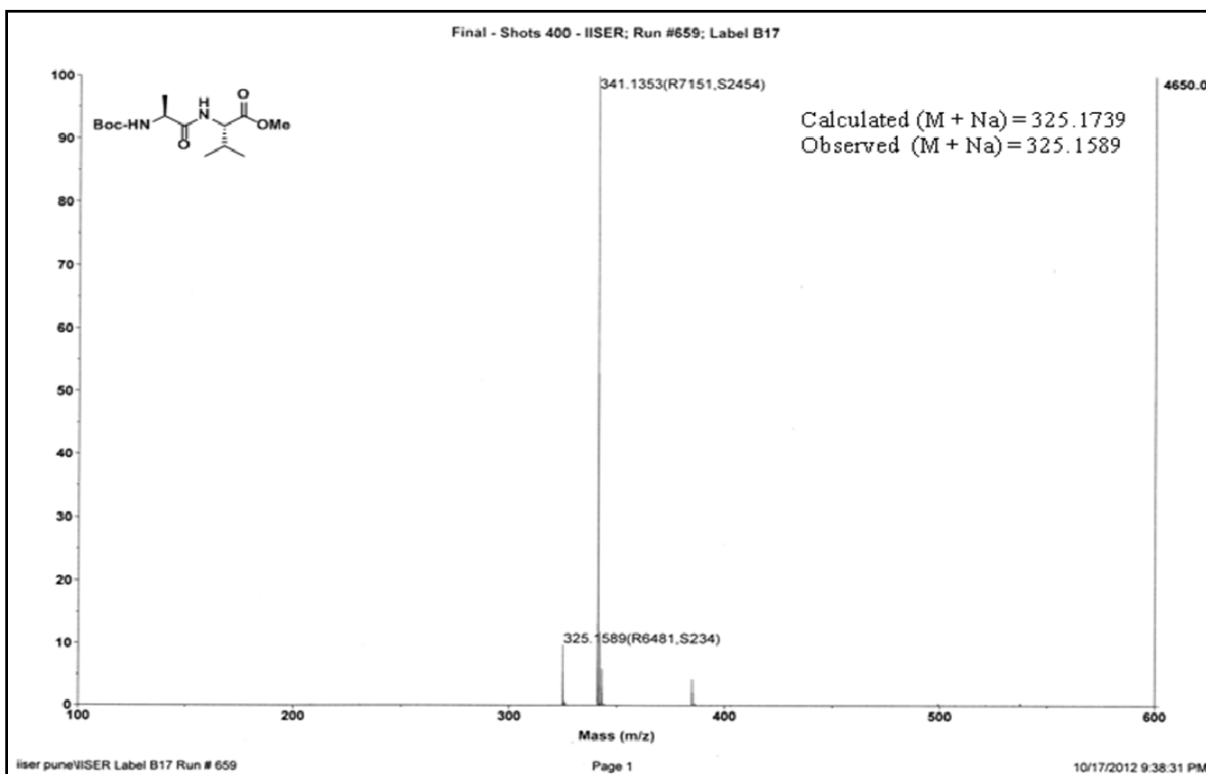
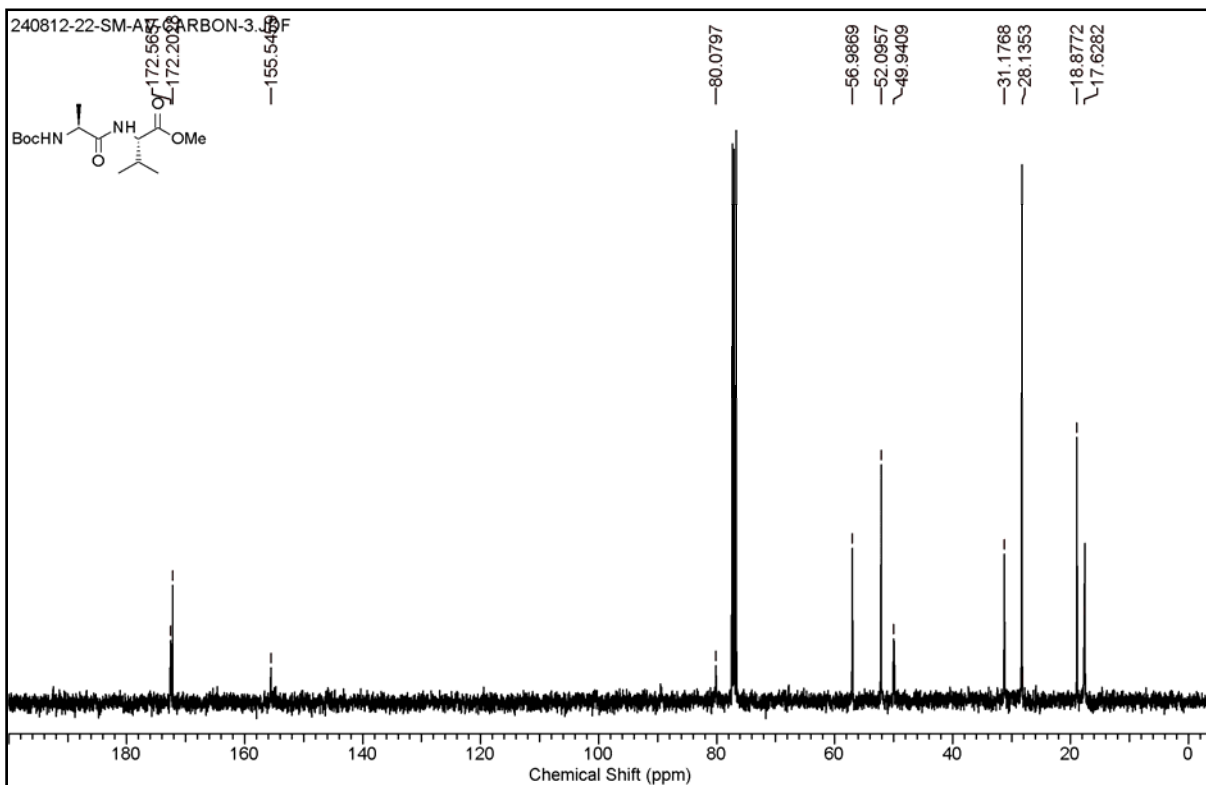
15. Mali, S. M.; Jadhav, S. V.; Gopi, H. N. *Chem. Commun.* **2012**, 48, 7085.
16. Mali, S. M.; Bhaisare, R. D.; Gopi, H. N. *J. Org. Chem.* **2013**, 78, 5550.
17. Wang, P.; Li, X.; Zhu, J.; Chen, J.; Yuan, Y.; Wu, X.; Danishefsky, S. J. *J. Am. Chem. Soc.* **2011**, 133, 1597.
18. Wang, P.; Danishefsky, S. J. *J. Am. Chem. Soc.* **2010**, 132, 17045.
19. Liu, L.; Orgel, L. E. *Nature* **1997**, 389, 52.
20. Maurel, M. -C.; Orgel, L. E. *Orig. Life Evol. Biosph.* **2000**, 30, 423.
21. Huber, C.; Wachtershauser, G. *Science*, **1997**, 276, 245.
22. Goldstein, A. S.; Gelb, M. H. *Tetrahedron Lett.*, **2000**, 41, 2797.
23. Vishwanatha, T. M.; Samarasimhareddy, M.; Sureshbabu, V.V. *Synlett*, **2012**, 23, 89.
24. Crich, D.; Sana, K.; Guo, S. *Org. Lett.* **2007**, 9, 4423.
25. Rao, Y.; Li, X.; Nagorny, P.; Hayashida, J.; Danishefsky, S. J. *Tetrahedron Lett.* **2009**, 50, 6684.
26. Raz, R.; Rademann, J. *Org. Lett.* **2012**, 14, 5038.
27. Pira, S. L.; Boll, E.; Melnyk, O. *Org. Lett.* **2013**, 15, 5346.
28. Kamber, B.; Hartmann, A.; Eisler, K.; Riniker, B.; Rink, H.; Seiber, P.; Rittel, W.; *Helv. Chim. Acta* **1980**, 63, 899
29. Pattabiraman, V. R.; Bode, J. W. *Nature* **2011**, 480, 471

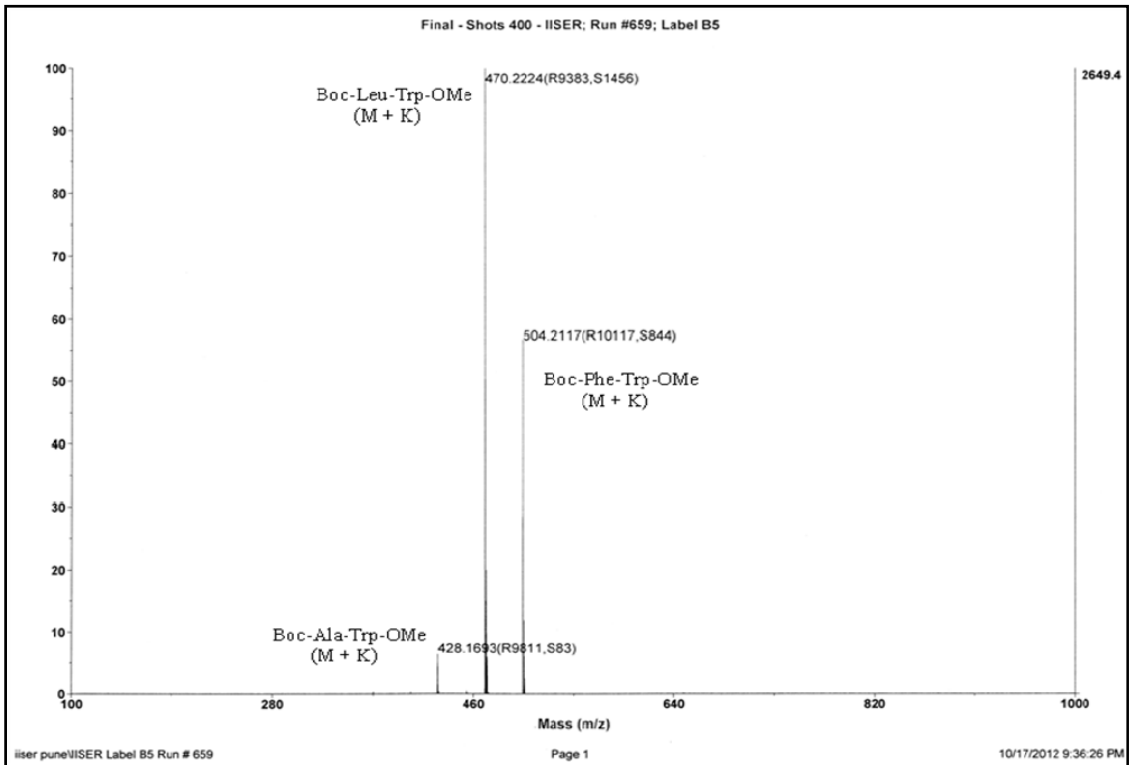
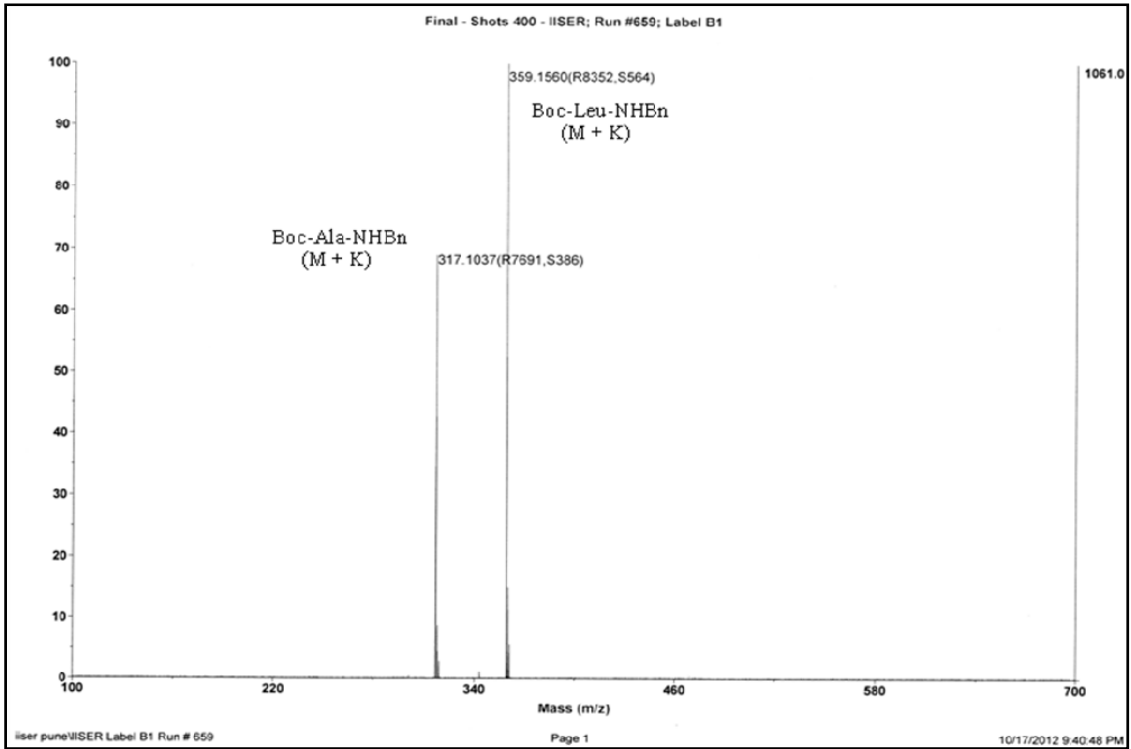
3.7 Appendix I: Representative Characterization Data of Synthesized Compounds

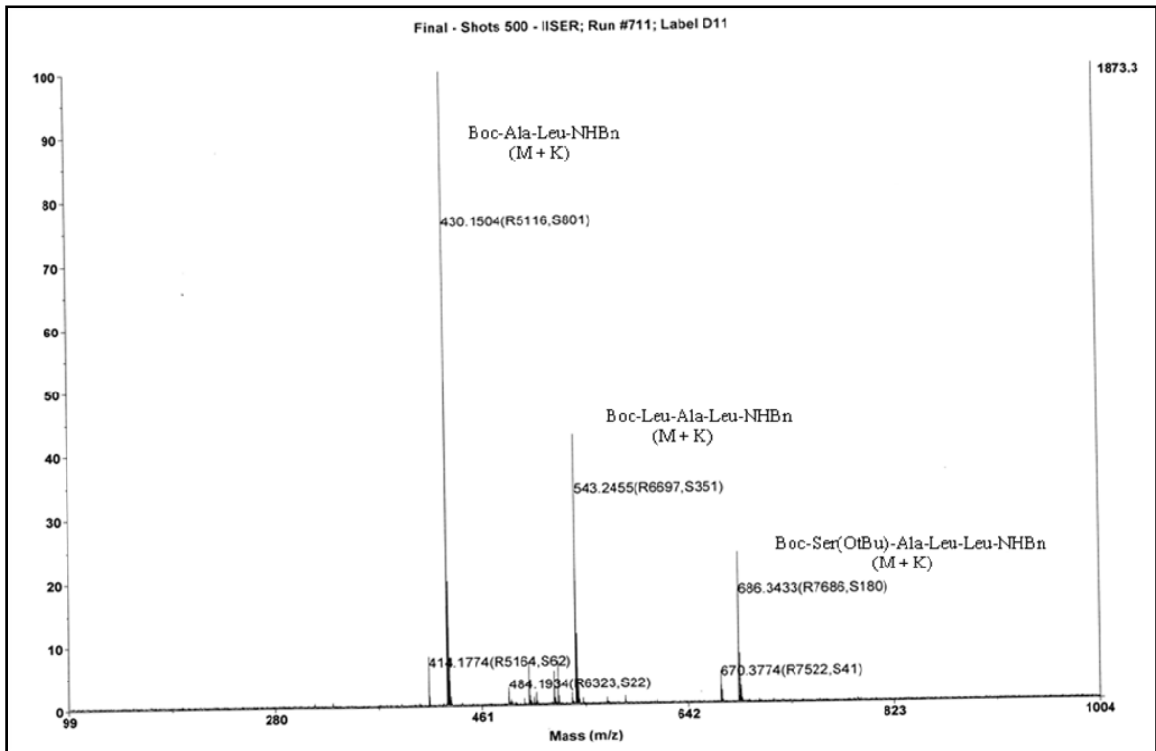
Designation	Description	Page
(Boc-Ala-S-) ₂ (3a)	¹ H NMR (400 MHz)	206
(Boc-Ala-S-) ₂ (3a)	¹³ C NMR (400 MHz)	206
(Boc-Ala-S-) ₂ (3a)	HRMS Spectrum	207
Boc-Ala-Val-OMe (P1)	¹ H NMR (400 MHz)	207
Boc-Ala-Val-OMe (P1)	¹³ C NMR (400 MHz)	208
Boc-Ala-Val-OMe (P1)	Mass Spectrum	208
Peptides (12, 15)	Mass Spectrum	209
Peptides (18, 19, 20)	Mass Spectrum	209
Peptides (21, 22, 23)	Mass Spectrum	210











Chapter 4

Utilization of thiazole δ -amino acids in design of cyclic peptide self assemblies

4.1 Introduction

The wide range of azole heterocycle based bioactive peptides have been isolated from marine source.¹ They show potent biological activities including antibiotic, immunosuppressant, cytotoxicity.² The biological activities of these peptides are the result of their metal binding properties and conformational constraints due to heterocycles.³ In addition, cyclic nature of these azole based natural products signifies their therapeutic application over the linear peptides. Several thiazoline, oxazoline, thiazoles and oxazole containing natural products isolated from marine source are from the family of *Lissoclinum*. Some of the representative examples of these cyclic peptides are shown in Figure 1. The high importance of these heterocyclic azole based peptides in the therapeutic application led various synthetic chemist to construct these cyclic peptides with various size and side chain functionalities.⁴ The ring size, side chain orientation and the conformation of these heterocyclic natural products governs their metal binding properties. In addition, by effective utilization of ring size and side chain orientation these heterocyclic peptides serve as scaffold for the construction of larger and protein like supramolecular structures, design of functional molecules and molecular shapes.⁵ Extensive studies of these cyclic peptides revealed the factors including self assembly, non covalent interaction, orientation of side chains plays a major role in their biological activity.

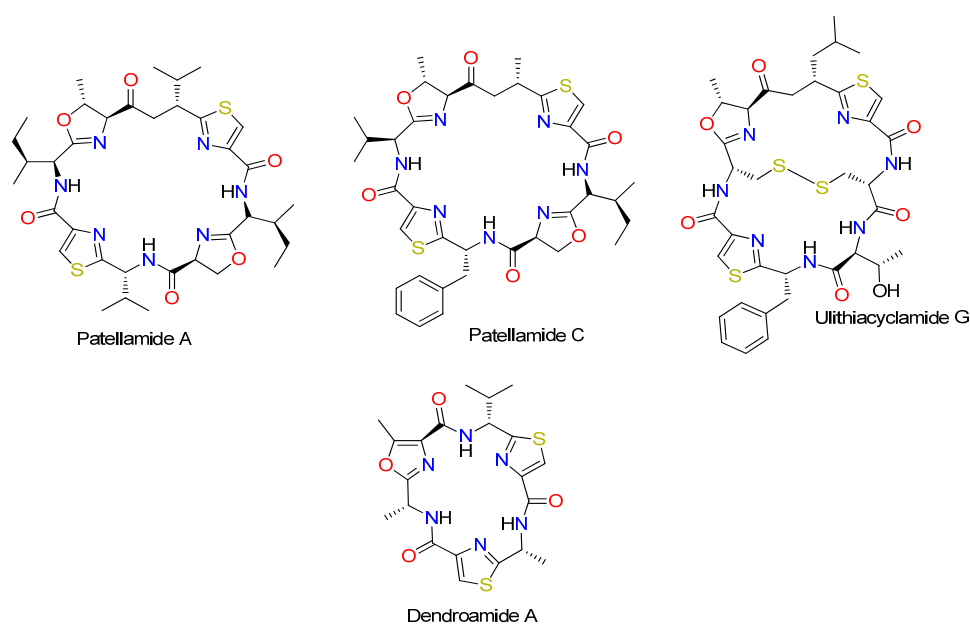
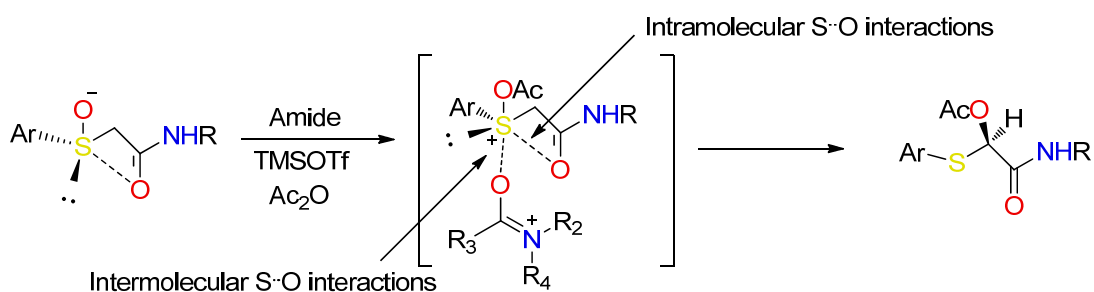


Figure 1: Representative examples for azole based heterocyclic natural products from *Lissoclinum* family.

The influence of solvents on the rates of chemical reactions and chemical equilibria has been extensively investigated and has become a central discipline of the physical organic chemistry. In addition, biomacromolecular self assemblies including protein folding, various protein-protein interactions, organization of amphiphiles into micelles are governed by solvent and their non covalent interactions.⁶ The solvent mediated self assemblies of biomacromolecules are responsible for the different biological processes. β – amyloid peptides are the examples of such self assemblies governed by the solvent water and their non covalent interactions.⁷ The peptide self assemblies which result from such non covalent interactions are used as a tool to construct the various well ordered nanostructures including peptide nanofibrils, nanotubes, nanospheres.^{8,9} These uniquely ordered self assembled structures of biomolecules have wide applications in medicine as antimicrobial agents, regeneration of bones and enamel, cartilage, wound-healing, cardiovascular therapies to molecular electronics.¹⁰ The selection of an appropriate solvent or solvent mixture is also of paramount importance in the physical processes such as recrystallization, chromatographic separations, phase-transfer catalytic reactions, etc. The behavior of solvent with various solutes solely depends upon the kind of non covalent interactions associated with them. Stronger the non-covalent interactions greater will be the strength of such solvent –solute interaction. Hydrogen bonding is one of the most commonly observed and studied non covalent interaction. It is an important non covalent interaction which directs the morphology and the function of biomolecules. Apart from the hydrogen bonding other non covalent interactions include ionic interactions, $\pi \cdots \pi$ interactions, dipole-dipole, lone pair $\cdots \pi$ and other non-covalent interactions.^{11,12} These interactions are well recognized in the field of supramolecular chemistry and are the basis of any self assembled structure. In addition to these non covalent interactions, recently chalcogen-chalcogen¹³ interactions have also been utilized in the construction of sulfur, selenium, tellurium¹⁴ containing self assemblies. Utilization of these chalcogen-chalcogen interactions in various well ordered self assemblies including columnar structures, nanotubes, nanorods have been reported in literature. These self assemblies mediated by chalcogen interactions have been utilized in the molecular recognitions, synthesis of channel like structure for inclusion of host molecules.^{14a, 14f, 14i}

4.1.1 Chalcogen-Chalcogen interactions in mediating the organic transformations

In addition to the macromolecular self assemblies, the chalcogen-chalcogen interactions have played significant role in the stereoselective organic transformations and catalyzing the organic reactions. Nagao and co-workers has demonstrated the role of non-bonded S \cdots O interaction in asymmetric Pummerer reaction (Scheme 1).^{13f} Recently Singh and colleagues explored the utility of chalcogen-chalcogen interactions governing the glutathione peroxidase like activity of organochalcogens derived from benzyl alcohol.^{13l} Further Gonzalez *et al.* have shown the significance of S \cdots O interaction in controlling the stereoisomerization of β -Hydroxy- α -sulfenyl- γ -butyrolactones through the X-ray crystallography.^{13m}



Scheme 1: Schematic representation of asymmetric Pummerer reaction mediated by S \cdots O (chalcogen-chalcogen) interactions

4.1.2 Chalcogen-Chalcogen interactions in biological system

Apart from the role of chalcogen-chalcogen interactions in governing the self assemblies *in vitro* they have played a vital role in the enzyme activity and stabilization of folded protein structures. Markham and colleagues showed the role of S \cdots O interaction in stabilizing protein-ligand complex for catalytic activity of S-Adenosyl methionine synthetase by using mutant S-Adenosyl methionine synthetase. Figure 2 represents the S \cdots O interaction between the ligand and enzyme.¹⁵ Similarly, S \cdots O interaction mediated enzyme inhibitory activity of antitumor agent Tiazofurin have been demonstrated by the Goldstein and co-workers.¹⁶ Theoretical studies of various drugs- enzyme and drug-DNA interactions shown the chalcogen-chalcogen interactions are also major factor governing the bioactivity of these drug candidates. Tomoda *et al.* applied the MP2 theoretical calculation on a model system using dimethyl disulfide and various carbonyl compounds for S \cdots O (chalcogen-chalcogen) interactions in the design of protein engineering and

molecular scaffold.¹⁷ In another interesting theoretical study by Greer and colleagues reported the importance of through space S··O interactions of antitumor, antibiotic drug Leinamycin in DNA cleavage.¹⁸

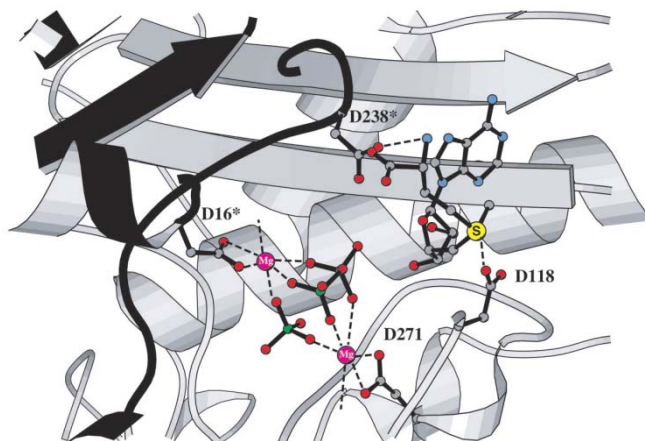


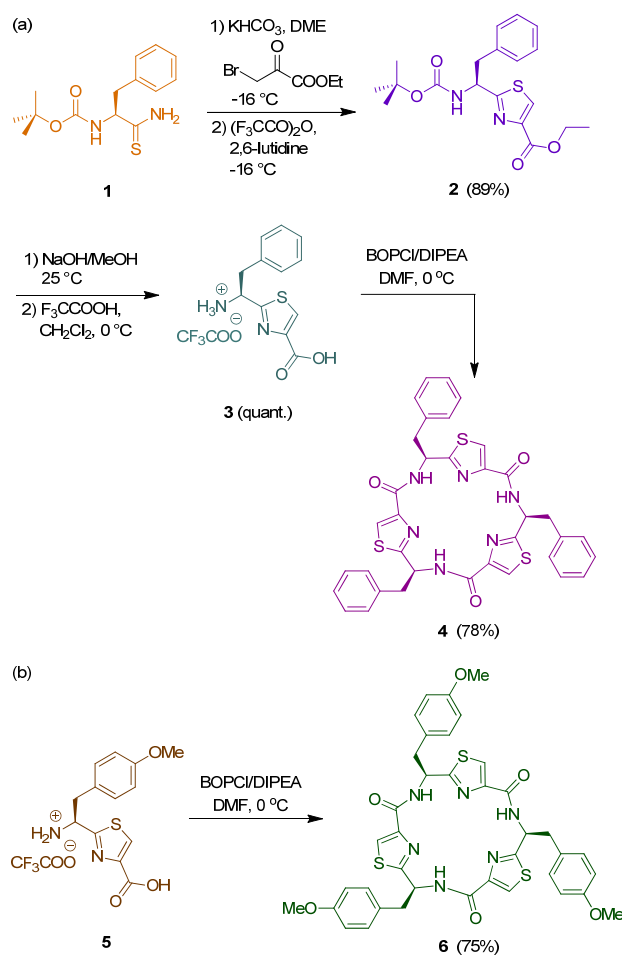
Figure 2: S··O interactions observed in the protein-ligand complex of enzyme AdoMet synthetase

4.2 Aim and rationale of the present work

As we have been working on the design, synthesis, conformational analysis and biological activities of hybrid peptides comprising of non ribosomal amino acids as well as thioacid mediated peptide synthesis, we sought to investigate the involvement of the sulfur in the supramolecular assembly of thiazole heterocyclic amino acid containing peptides and peptide antibiotics and their behavior in various organic solvents. These heterocyclic amino acids containing cyclic peptides have shown their potential as bioactive peptides, metal transporter in biological system and as a template for mimicking the proteins loops, protein secondary structures. These heterocyclic amino acids have been used to induce the turn in various bioactive peptides. The heterocycles such as thiazoline, oxazoline, thiazole and oxazole have been frequently found in many bioactive natural product cyclic peptides. Inspired by the intriguing properties of these heterocyclic amino acids containing cyclic peptides, we investigated the role of thiazole sulfur in the self-assembling properties of these peptides in various organic solvents. Instructively, all these self assemblies are mediated by unique S··O (chalcogen-chalcogen) interactions. Further the theoretical calculation with a model system containing thiazole and acetyl-*N*-methylamide were carried out using MP2/6-311G++(3df,3dp) level of theory. Theoretical calculation showed the average gain of energy of about 16 kJ/mol in comparison with separated species.

4.3 Result and discussion

As a part of our ongoing research to study heterocyclic amino acid containing cyclic peptide antibiotics and to understand their molecular architectures and polymorphisms, we started our research with synthesis of the thiazole containing ω amino acid. The synthesis of phenylalanine thiazole ω amino acid was carried out by reported procedure⁵. In key step the Boc-Phenylalanine thioamide **1** was treated with ethyl bromopyruvate and trifluoroacetic anhydride in 2, 6 lutidine to assemble the thiazole ring **2**. The macrocyclization of phenylalanine thiazole **3** was achieved by BOP-Cl after the hydrolysis and Boc deprotection of ethyl ester of phenylalanine thiazole **2** as shown in Scheme 2a.



Scheme 2: Synthesis of thiazole-containing cyclic tripeptides **4** and **6**, respectively

This BOP-Cl mediated macrocyclization offered the cyclic tripeptide phenylalanine thiazole in 78% after column purification along with the traces of cyclic tetra and penta

peptides. Similar procedure was used to yield 75% of cyclic tyrosine thiazole tripeptide starting from trifluoro acetic acid salt of tyrosine thiazole amino acid. The ^1H and ^{13}C NMR analysis of these cyclic tripeptides has unequivocally indicated the C_3 -symmetric nature of the molecules.

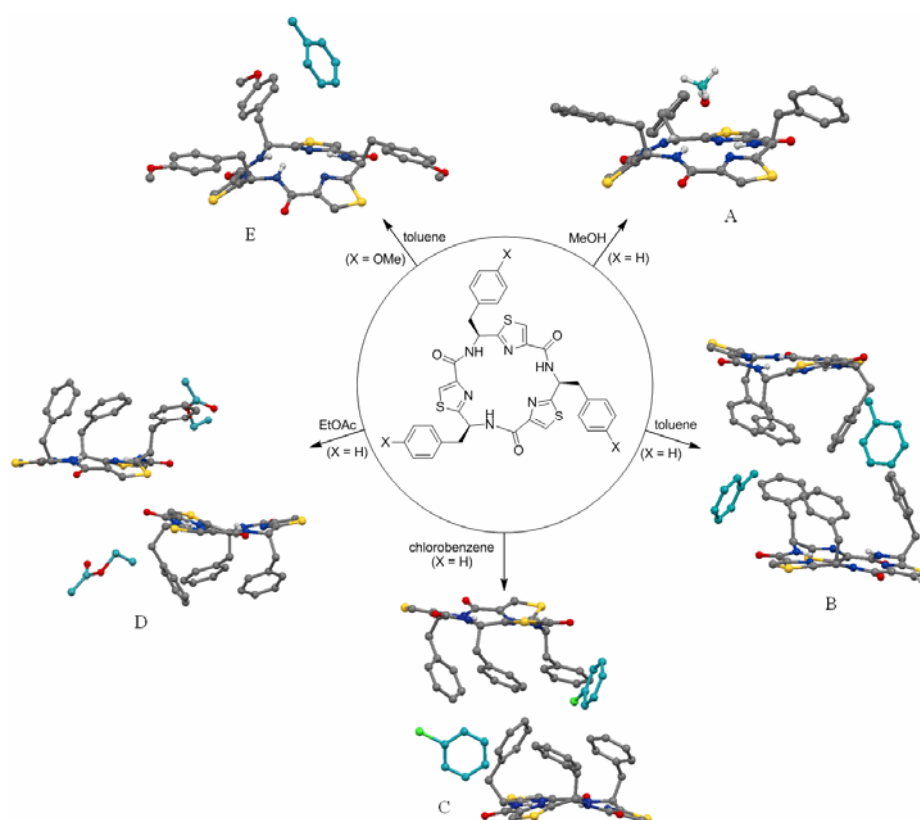


Figure 3: The crystal structures of thiazole cyclic tripeptides **4** and **6**: A) **4** from methanol, crystal system monoclinic, space group $P2_1$; B) **4** from toluene, crystal system triclinic, space group $P1$; C) **4** from chlorobenzene, crystal system triclinic, space group $P1$, D) **4** from ethyl acetate, crystal system trigonal, space group $P3_2$; E) **6** from toluene, crystal system orthorhombic, space group $P2_12_12_1$

4.3.1 Crystal structure and self assembly analysis of the structure obtained from methanol

The ring size of the macrocycles and orientation of side chains plays a significant role in governing the bioactivity and morphology of the self assemblies. To understand the behavior of side chains of these macrocyclic structures, we tried to crystallize the cyclic tripeptide of phenylalanine thiazole **4** in various solvents. The crystals obtained from the

slow evaporation of methanol give the molecular structure as shown in Figure 3A. The comparative study of crystal structure obtained from methanol with planner cyclic model peptides shows that cyclic peptide backbone appeared little distorted from the planarity with RMS value 0.417. The overlay of the planar model and crystal structure is shown in Figure 4. As anticipated all benzyl groups of the cyclic peptide are projecting at one face of the molecule. Interestingly, the solvent methanol is trapped in the center above the cyclic ring backbone of the tripeptide by forming a weak hydrogen bond (2.693 Å) with the proton of an amide moiety.

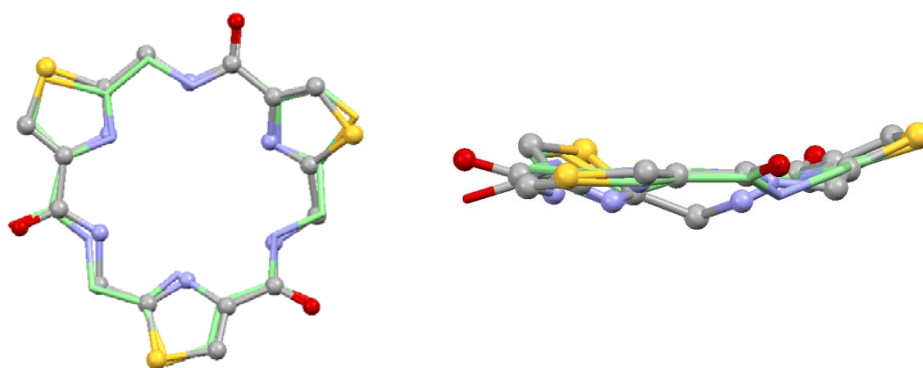


Figure 4: Superposition of a planar model of thiazole cyclic tripeptide backbone (green color with capped stick model) over the crystal structure of the tripeptide grown in solution of methanol (A).

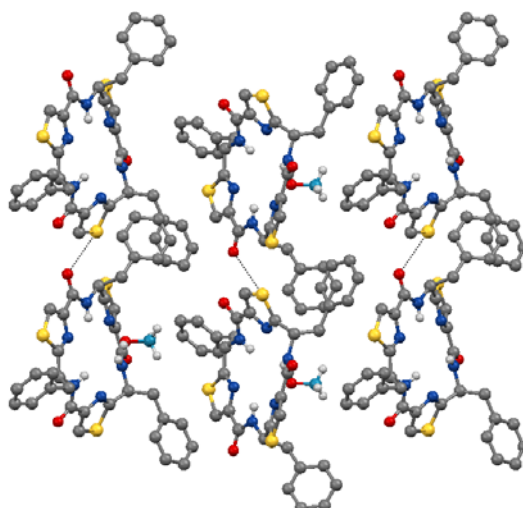


Figure 5: Self assembly of the cyclic tripeptide 4 from methanol

Table 1: S...O interactions observed in the crystal structures of thiazole cyclic tripeptides

Crystals from	S...O	<i>d</i> [Å]	S...O=C [°]	Crystals from	S...O	<i>d</i> [Å]	S...O=C [°]
4 (MeOH)	S1...O2	3.039	133	4 (EtOAc)	S5...O8	3.305	140
4 (PhMe)	S1...O2	3.049	146	4 (PhCl)	S1...O2	3.303	141
	S2...O3	3.219	143		S2...O3	3.249	141
	S3...O1	3.213	143		S3...O1	3.074	146
	S4...O5	3.312	141		S4...O4	3.132	142
	S5...O6	3.055	145		S5...O6	3.064	148
	S6...O4	3.130	143		S6...O5	3.275	141
4 (EtOAc)	S2...O3	3.171	144	<i>O</i> -methyl tyrosine cyclic tripeptide			
	S3...O1	3.236	141				
	S4...O7	3.189	143	6 (toluene)	S2...O6	3.140	149

All *trans* amide NHs are pointing inside the ring. Inspection of the hydrogen bond parameters reveals that there is no intramolecular hydrogen bond observed between the NH units or with the nitrogen of the thiazole ring.¹¹ Examination of the crystal packing reveals that the cyclic peptide adapted a well-organized supramolecular architecture in the crystal (Figure 5). A network of S...O interactions with a distance of 3.03 Å (the sum of the van der Waals radii of sulfur and oxygen is 3.32 Å) and S...H interactions determines the self-assembly. The most important intermolecular S...O distances are compiled in Table 1. In addition, also other interactions such as C-H... π , C-H...O, π ... π and S... π interactions support the supramolecular assembly. Details with respect to these distances are provided in the Table 2.

The serendipity of S...O mediated supramolecular assembly of the tripeptide **4** led us to grow the crystals in toluene, chlorobenzene and ethyl acetate to further understand the molecular behavior and polymorphisms.

Table 2: Other non-covalent interactions observed in the self assembly of cyclic peptide from the crystals obtained in MeOH solution

	Interactions	D-H---A Dist[Å]	D-H---A [°]	Type of Interaction
1	14C-H---S1	2.929	118	C-H---S
2	26C-H---S1	2.891	139	C-H---S
3	1C-H---C29	2.882	173	C-H--- π
4	14C-H---C=O(36)	2.707	173	C-H--- π
5	8C-H---C30	2.899	113	C-H--- π
6	31C-H---C22	2.877	131	C-H--- π
7	6C-H---O1	2.374	144	C-H---O
8	31C-H---O2	2.696	167	C-H---O
9	C5---C22	3.384	---	π --- π
10	N-H---O-H(MeOH)	2.693	120	N-H---O
11	O3---H-O(MeOH)	1.992	163	C=O---H-O

4.3.2 The crystal and self assembly analysis of the structure obtained from toluene

The crystals of cyclic peptide obtained from the solution in toluene revealed a structure as shown in Figure 3B. Surprisingly, the cyclic peptide adapted overall a different type of crystal packing compared to the crystals grown in methanol. The asymmetric unit contains two molecules of the cyclic tripeptide associated with two molecules of toluene. In contrast to the structure in methanol, the tripeptide **4** adapted a closed structure exposing the cyclic backbone for other non-covalent interactions. Two molecules of **4** are connected

via toluene through CH $\cdots\pi$ and C-H \cdots O interactions. The corresponding side view is depicted in Figure 6. The careful examination of the crystal structure reveals that the supramolecular architecture is stabilized by the six C-H \cdots O and the six S \cdots O interactions in the horizontal direction (Figure 7). The distances of C-H \cdots O=C interactions lie within the limits of the standard C-H \cdots O distances (2-3 Å),¹² whereas the C-H \cdots O angles were found to be in the range of 108-120°. The carbonyl oxygen is involving in bifurcated C-H \cdots O and S \cdots O interactions. The distances of six different S \cdots O interactions from the top and the bottom plane are in the range of 3.06-3.31 Å (Table 1).

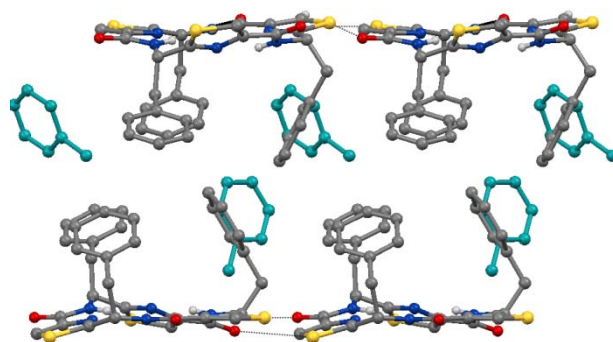


Figure 6. Self assembly of the cyclic tripeptide peptide from toluene

Table 3: C-H \cdots O interactions along the horizontal planes of cyclic peptide from the crystals obtained in toluene solution

	Interactions	D-H \cdots A Dist[Å]	D-H \cdots A[°]	Type of interaction
1	10C-H \cdots O2	2.435	115	C-H \cdots O
2	22C-H \cdots O3	2.497	116	C-H \cdots O
3	34C-H \cdots O1	2.461	116	C-H \cdots O
4	46C-H \cdots O5	2.473	120	C-H \cdots O
5	58C-H \cdots O6	2.575	108	C-H \cdots O
6	70C-H \cdots O4	2.465	116	C-H \cdots O

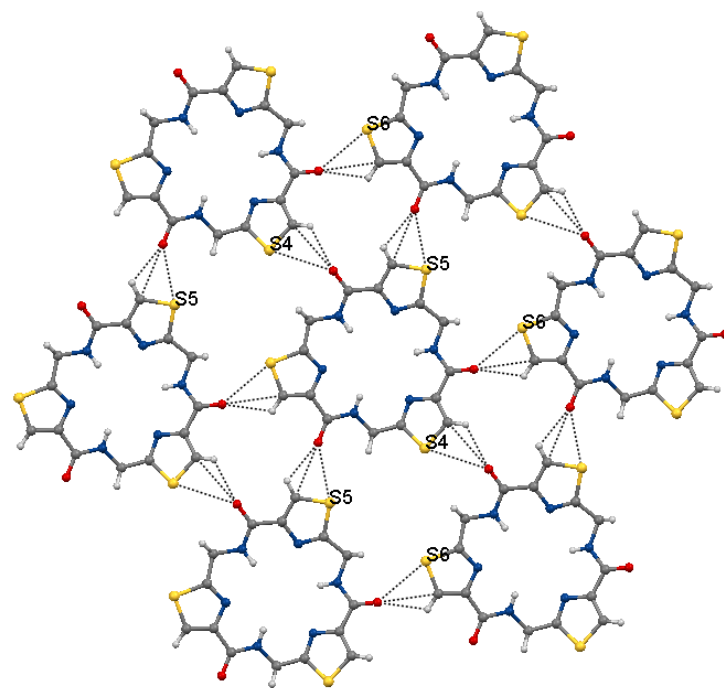


Figure 7: Top view of **3B** showing a network of S...O interactions in the horizontal direction

Table 4: Vertical non-covalent interactions between the two planes of the cyclic peptides in the crystals obtained in toluene solution

	Interactions	D-H...A Dist[Å]	D-H...A[°]	Type of interaction
1	13C-H...C=O(48C)	2.779/2.708	132	C-H... π
2	(24C)O=C...C=O (60C)	3.314	---	π ... π (b/w C...C of carbonyl)
3	34C-H...C70	2.754	130	C-H... π (Thz...Thz)
4	O3...C=O(72C)	3.095	105	Electrostatic /dipole

Table 5: Other non-covalent interactions observed in the self assembly of cyclic peptide in the crystals obtained in toluene solution

	Interactions	D-H---A Dist[Å]	D-H---A[°]	Type of interaction
1	C15---C20	3.371		π --- π (Phe---Phe)
2	75C-H---C64	2.803	155	C-H--- π (Tol---Phe)
3	76C-H---C81	2.879	130	C-H--- π (Tol---Tol)
4	56C---H-C40	2.857	143	C-H--- π (Phe---Phe)
5	70CH3---O2	2.662	141	C-H---O (C=O---Tol)
6	78C-H---O2	2.623	165	C-H---O (C=O---Tol)
7	83C-H---C47	2.883	147	C-H--- π (Tol---Thz)
8	C-H---O1	2.620	153	C-H---O1 (Tol---OC)

4.3.3 Crystal and self assembly analysis of the structure obtained from chlorobenzene

Similarly, the crystals grown from a solution of chlorobenzene show an isomorphous structure (Figure 3C) and it closely resembles to the structure in toluene. Furthermore, the crystal packing is stabilized by six C-H...O and six S...O interactions in the horizontal planes (top and bottom) and the two tripeptides are interconnected by chlorobenzene molecules similar to toluene. The supramolecular self assembly of cyclic peptide crystal obtained from chlorobenzene is shown in Figure 8.

The distances and bond angles of S...O interactions are given in the Table 1 and the parameters of the other interactions which support this self assembly are tabulated in the Table 6. In addition to the other non-covalent interactions, the involvement of chlorine in supporting the molecular architecture is also observed in the structure obtained from chlorobenzene. The Cl(1) is involved in a bifurcated hydrogen bonding with C(6)-H and

C(50)-H with distances of 2.82 and 2.89 Å and C-H...Cl(1) angles of 152° and 149°, respectively. Interestingly, Cl(2) is involved in a lone pair... π interaction with another molecule of chlorobenzene, but not in hydrogen bonding.

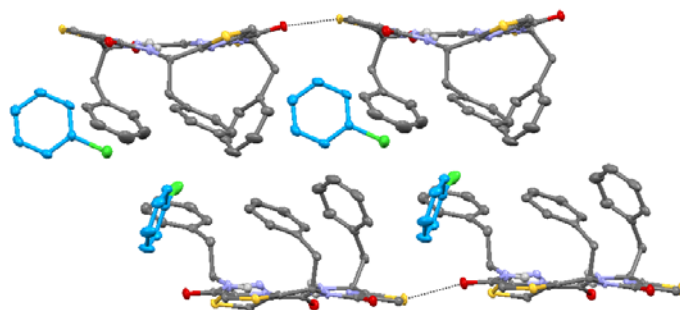


Figure 8. Self assembly of the cyclic tripeptide from chlorobenzene

Table 6: Other non-covalent interactions observed in the crystal structure of cyclic peptide from the crystals obtained in chlorobenzene solution

	Interactions	D-H...A Dist[Å]	D-H...A[°]	Type of interaction
1	26C-H...S1	2.976	130	S...H
2	17C-H...Phe	3.260	157	C-H... π
3	31CH...Phe	3.371	129	C-H... π
4	80CH...Phe	2.621	162	C-H... π
5	6C-H...Cl1	2.815	152	C-H...Cl
6	50CH...Cl1	2.893	149	C-H...Cl
7	Cl2...Cl-Phe	3.751	151	Cl...Ar
8	82C-H...Thz	3.084	158	C-H... π
9	84C-H...O6	2.666	129	C-H...O

4.3.4 Crystal and self assembly analysis of the structure obtained from ethyl acetate

The distinct morphology of cyclic tripeptide obtained from the polar protic and non polar solvent led us to grow the crystals from the polar aprotic solvent ethyl acetate to understand the orientation of side chains and their self organization behaviour. The crystals of the peptide obtained from ethyl acetate revealed the structure shown in Figure 3D. In contrast to the structure obtained from the crystals grown in toluene, the peptide adapted a different packing. The structure obtained from the ethyl acetate adapted the open structure with side chains exposing in outward direction. Interestingly, the phenyl side chains are directly involved in the C-H... π interaction with phenyl groups of another cyclic peptide in the crystal packing. In contrast to the structures from toluene and chlorobenzene four S...O interactions (Table 1) along with C-H...O interactions are observed in the horizontal assemblies of both the planes shown in Figure 9. Instructively, an average C=O...S bond angle of about 143° is observed in all crystal structures.

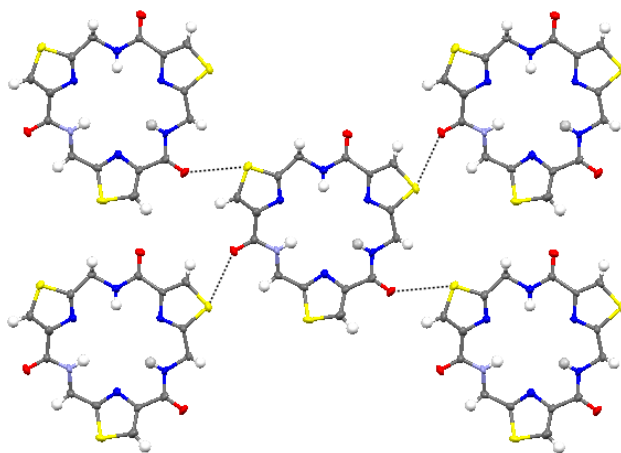


Figure 9: Top view of B showing a network of S...O interactions in the horizontal direction

Table 7: Other non-covalent interactions observed in the self assembly of cyclic peptide from the crystals obtained in EtOAc solution

	Interactions	D-H---A[Å]	D-H---A [°]	Type of interaction
1	48C-H---O9(EtOAc)	2.642	136	C-H---O
2	37C-H---45C(EtOAc---Phe)	2.852	---	C-H--- π
3	30C-H---C47 (Phe)	2.890	135	C-H--- π
4	14C-H---S3	2.947	131	C-H---S

Table 8: C-H---O interactions along the horizontal planes of the cyclic peptide from the crystals obtained in ethyl acetate solution

	interactions	Dist[Å]	D-H---A[Å]	C=O---H[°]	Type of interaction
1	34C-H---O1	2.454	120	163	C-H---O
2	22C-H---O3	2.521	114	160	C-H---O
3	10C-H---O2	2.513	123	172	C-H---O
4	62C-H---O8	2.469	119	174	C-H---O
5	50C-H---O7	2.380	120	168	C-H---O
6	74C-H---O6	2.412	122	165	C-H---O

4.3.5 Crystal structure and self assembly analysis of the peptide structure 6 obtained from ethyl acetate

To further understand the influence of non-polar solvents in the crystallization of tripeptides with the polar head groups, crystals of the tyrosine-derived cyclic tripeptide **6** were grown from a solution of toluene yielding the solid state structure shown in

Figure 3E. Instructively, the peptide adapted a molecular assembly similar to that of **4** obtained from a solution of methanol (Figure 3A). The self-assembly of the peptide in crystal packing is mediated by only one S...O interaction with a distance of 3.14 Å and an S...O=C bond angle of 149°(Figure 10). However, in contrast to the peptide crystals grown in methanol, the interaction of solvent toluene with thiazole ring is observed in the tripeptide **6**.

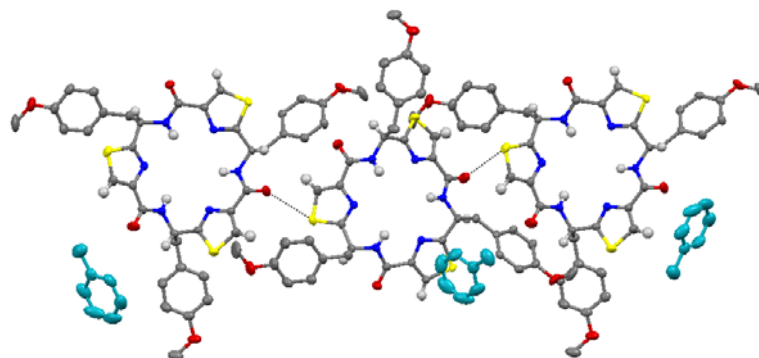


Figure 10. Self assembly of the tyrosine cyclic tripeptide **6** from ethyl acetate

Table 9: Vertical non-covalent interactions between the two planes of the cyclic peptides in the crystals obtained from EtOAc solution.

	Interactions	D-H...A[Å]	C=O...H[°]	Type of interaction
1	O8...C=O (36)	3.171	100	Electrostatic
2	74C-H...C34(Thz)	2.783	126	C-H... π
3	53C-H...C=O(12)	2.767	144	C-H... π
4	24C=O...C=O(64)	3.343	----	π ... π
5	S3...C50	3.434	---	Lone pair... π

Table 10: Non-covalent Interactions observed in the crystal structure of O-methyl tyrosine thiazole cyclic tripeptide

	Interactions	D-H...A Dist [Å]	D-H...A[°]	Type of interaction
1	11C-H---Ar	2.577	137	C-H--- π
2	5NH---O1	2.664	151	N-H---O
3	9C-H---N4	2.664	160	C-H---N
4	44C-H---O6	2.695	146	C-H---O
5	24C-H---O6	2.362	119	C-H---O
6	12C---34C	3.399	---	π --- π
7	46C-H---S1	2.933	149	C-H---S
8	38C---O5	3.182	----	Electrostatic
9	41CH---Ar	3.435	147	C-H--- π
10	Tol---Thz	3.661	---	π --- π
11	41C-H---O4	2.705	124	C-H---O
12	5C-H---O4	2.665	123	C-H---O
13	46C-H---O4	2.609	138	C-H---O
14	35C-H---O2	2.475	140	C-H---O
15	15C-H---Ar	3.229	140	C-H--- π

Table 11: C-H...O interactions along the horizontal planes of cyclic peptide from the crystals obtained in ethyl acetate solution

	Interactions	D-H...A Dist[Å]	D-H...A[°]	Type of interaction
1	46C-H...O4	2.479	116	C-H...O
2	70C-H...O6	2.618	108	C-H...O
3	58C-H...O5	2.478	113	C-H...O
4	34C-H...O1	2.425	115	C-H...O
5	10C-H...O2	2.505	118	C-H...O
6	22C-H...O3	2.837	119	C-H...O

The analysis of the crystal structures from different solvents suggests the striking influence of the solvent in architecting divergent supramolecular assemblies. The cyclic peptides may adopt different molecular conformations based on the polarity of the molecule and the solvent. However, all these divergent supramolecular assemblies are predominantly mediated by S...O interactions. The role of non-bonded intramolecular S...O interactions in organic reactions has been well recognized;^{13f,i-m} however, very little is known about intermolecular S...O interactions.

4.3.6 Theoretical Studies of S...O interactions using MP2/6-311G++(3df,3dp) level of theory

To get deeper insights into the supramolecular assemblies in the solid state and the respective S...O interactions, theoretical calculations were performed. The most striking structural motif is the close contact between a peptidic carbonyl on the one hand side and the sulfur and the hydrogen of the thiazole ring on the other (as depicted in Figure 7). Therefore, two model systems **7** and **8** consisting of thiazole and acetyl-*N*-methylamide

were investigated (Figure 9) by means of the MP2/6-311G++(3df,3dp) level of theory.^{19,20} Previous studies revealed that such a level of theory provides a very efficient way for estimating coupled cluster interaction energies whereas the B3LYP method leads to quite good geometries, but is incapable of recovering correct interactions energies.^{13e,h} For the model systems shown in Figure 11 all the geometrical parameters were optimized with Gaussian03²¹ using the counterpoise procedure to obtain a BSSE-corrected supramolecular assembly. Energies were corrected for zero-point and the corresponding geometries were characterized as minima by subsequent frequency calculation. Our investigations revealed several minima, a global one with a skewed arrangement being 20.4 kJ/mol more stable than the separate monomers (see experimental section) and the two local ones showing a very similar geometry as observed in the solid-state architecture. The local ones in which the two molecules are almost located in one plane are about 16.0 kJ/mol (**7**) and 16.6 kJ/mol (**8**) more stable than separated thiazole and acetyl-*N*-methylamide.

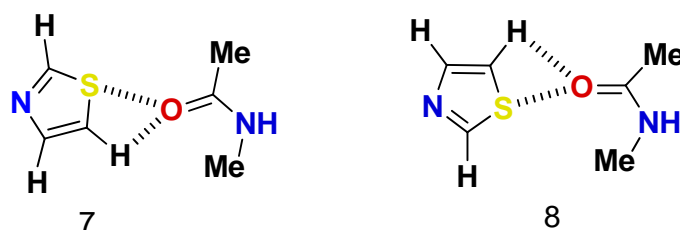


Figure 11: Simplified predominant motifs **7** and **8** in the solid-state structure of the cyclic thiazoles resulting in interaction energy of 16.0 kJ/mol (**7**) and 16.6 kJ/mol (**8**), respectively

We assume that most of the interaction energy is attributed to dispersion forces; corresponding natural bond orbital (NBO) analyses²² having been performed on the dimer's optimized geometry did not result in a clear-cut charge transfer from one functionality to another.

4.4 Conclusions

In summary, phenylalanine- and tyrosine-derived thiazole-containing cyclic tripeptides **4** and **6** were synthesized by BOP-Cl/DIPEA-mediated trimerisation of the corresponding amino acids. X-ray investigations performed with crystals obtained from various solvents (methanol, toluene, chlorobenzene and ethyl acetate) revealed strongly divergent supramolecular assemblies in the solid state. All of them are predominantly mediated by non-bonded intermolecular S...O interactions of a thiazole and a carbonyl unit arranged in a co-planar fashion. Theoretical calculations at the MP2 level of theory using appropriate model systems have shown that a significant energy gain of about 16 kJ/mol is associated with such an arrangement. Thus, interactions with thiazole as the crucial structural element might also play an important role for the biological activity of thiazole-containing cyclic peptide antibiotics and may offer new opportunities for the construction of novel supramolecular assemblies and materials.

4.5 Experimental Section

General Methods. Phenylalanine, tyrosine, DCC, Lawesson's reagent, ethyl bromopyruvate, trifluoroacetic anhydride, trifluoroacetic acid, *N*-hydroxy succinimide, 2,6-lutidine, BOP-Cl, DME, and DIPEA were used as commercially available. THF was dried over sodium and distilled prior to use. Column chromatography was performed on silica gel (100-200 mesh). ¹H and ¹³C NMR were recorded on a 400 MHz instrument (100 MHz for ¹³C) using the residual solvent signals as an internal reference. The chemical shifts (δ) are reported in ppm and coupling constants (*J*) are given in Hz. IR spectra were recorded on FT-IR spectrophotometer using KBr pellet. High-resolution mass spectra were obtained from ESI-TOF MS spectrometer.

X-Ray Crystallography: Single crystal X-ray data sets were collected on a Bruker APEX DUO CCD diffractometer using Mo K α radiation ($\lambda = 0.71073 \text{ \AA}$) at desired temperature by using Oxford Instrument Cryojet-HT controller. The collected data were reduced by using program SAINT²³. Empirical absorption correction was carried out by using program SADABS²⁴. The crystal system was determined by Laue symmetry and space group were assigned on the basis of systematic absences by using XPREP. All the structures were obtained by direct methods using SHELXS-97.²⁵ Hydrogen atoms were fixed geometrically and refined isotropically. ORTEP were used for structure visualization

and making the molecular representation. Packing diagrams were generated by using Mercury.

1. X-Ray Structure Analyses.

X-ray structure analysis of phenylalanine thiazole cyclic tripeptide 4 crystallized from methanol. Crystals of the cyclic thiazole-containing tripeptide **4** were grown by slow evaporation from a solution of methanol. A single crystal (0.60 × 0.42 × 0.35 mm) was mounted on a glass fiber. The X-ray data were collected at a temperature of 200 K using Mo K_α radiation ($\lambda = 0.71073 \text{ \AA}$), ω -scans ($2\theta = 56.56^\circ$) for a total of 6169 independent reflections. Space group $P2_1$, $a = 8.4345(7)$, $b = 18.6369(15)$, $c = 11.8554(9) \text{ \AA}$, $\beta = 109.105(3)^\circ$, $V = 1760.9(2) \text{ \AA}^3$, monoclinic, $Z = 2$ for $C_{36}H_{30}N_3O_3S_3 \times CH_3OH$ with one molecule in the asymmetric unit; $\rho_{\text{calcd}} = 1.295 \text{ gcm}^{-3}$, $\mu = 0.254 \text{ mm}^{-1}$, $R_{\text{int}} = 0.0160$. The structure was obtained by direct methods using SHELXS-97.¹⁵ The final R value was 0.030 ($wR2 = 0.0540$) for 5860 observed reflections ($F_0 \geq 4\sigma(|F_0|)$) and 453 variables, $S_{\text{Gof}} = 1.870$. The largest difference peak and hole were 0.223 and -0.228 e\AA^{-3} , respectively.

X-ray structure analysis of phenylalanine thiazole cyclic tripeptide 4 crystallized from toluene. Crystals of the cyclic thiazole-containing tripeptide **4** were grown by slow evaporation from a solution of toluene. A single crystal (0.45 × 0.40 × 0.37 mm) was mounted on loop with a small amount of paraffin oil. The X-ray data were collected at a temperature of 100 K using Mo K_α radiation ($\lambda = 0.71073 \text{ \AA}$), ω -scans ($2\theta = 56.56^\circ$) for a total of 15268 independent reflections. Space group $P1$, $a = 12.3387(16)$, $b = 12.3708(16)$, $c = 15.603(2) \text{ \AA}$, $\alpha = 74.361(2)$, $\beta = 85.392(3)$, $\gamma = 60.480(2)$, $V = 1991.8(4) \text{ \AA}^3$, triclinic, $Z = 1$ for $C_{72}H_{60}N_{12}O_6S_6 \times 2 C_7H_8$ with two molecules in asymmetric unit; $\rho_{\text{calcd}} = 1.235 \text{ gcm}^{-3}$, $\mu = 0.228 \text{ mm}^{-1}$, $R_{\text{int}} = 0.0341$. The structure was obtained by direct methods using SHELXS-97.¹⁵ The final R value was 0.0467 ($wR2 = 0.1020$) for 12708 observed reflections ($F_0 \geq 4\sigma(|F_0|)$) and 993 variables, $S_{\text{Gof}} = 1.014$. The largest difference peak and hole were 0.345 and -0.298 e\AA^{-3} , respectively.

X-ray structure analysis of phenylalanine thiazole cyclic tripeptide 4 crystallized from chlorobenzene. Crystals of the cyclic thiazole-containing tripeptide **4** were grown by slow evaporation from a solution of chlorobenzene. A single crystal (0.75 × 0.65 × 0.60 mm) was mounted on a glass fiber. The X-ray data were collected at a temperature of 200 K using Mo K_α radiation ($\lambda = 0.71073 \text{ \AA}$), ω -scans ($2\theta = 56.56^\circ$), for a total of 14106

independent reflections. Space group $P1$, $a = 12.3346(12)$, $b = 12.4280(13)$, $c = 15.3231(16)$ Å, $\alpha = 76.445(2)$, $\beta = 85.581(2)$, $\gamma = 60.330(2)$, $V = 1982.0(4)$ Å³, triclinic, $Z = 1$ for $C_{72}H_{60}N_{12}O_6S_6 \times 2 C_6H_5Cl$ with two molecules in the asymmetric unit; $\rho_{\text{calcd}} = 1.346$ gcm⁻³, $\mu = 0.302$ mm⁻¹, $R_{\text{int}} = 0.0518$. The structure was obtained by direct methods using SHELXS-97.¹⁵ The final R value was 0.0398 ($wR2 = 0.1059$) for 13964 observed reflections ($F_0 \geq 4\sigma(|F_0|)$) and 991 variables, $S_{\text{Gof}} = 1.022$. The largest difference peak and hole were 0.639 and -0.572 eÅ³, respectively.

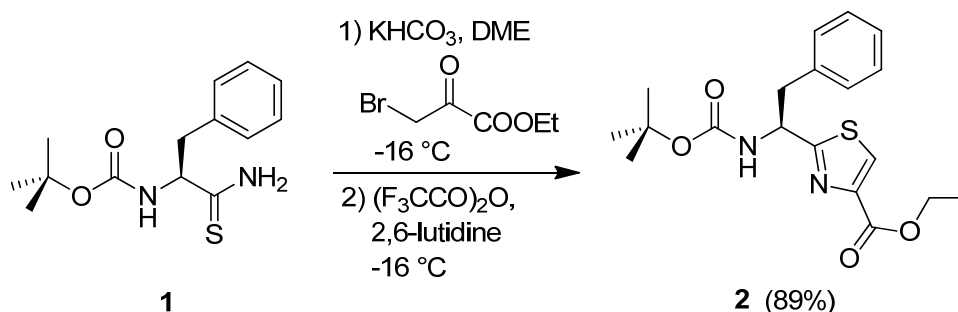
X-ray structure analysis of phenylalanine thiazole cyclic tripeptide 4 crystallized from ethyl acetate. Crystals of the cyclic thiazole-containing tripeptide (**4**) were grown by slow evaporation from a solution of ethyl acetate. A single crystal ($0.54 \times 0.40 \times 0.34$ mm) was mounted on a glass fiber. The X-ray data were collected at a temperature of 200 K using Mo K_{α} radiation ($\lambda = 0.71073$ Å), ω -scans ($2\theta = 56.56^\circ$), for a total of 12443 independent reflections. Space group $P3_2$, $a = 12.4150(12)$, $b = 12.4150(12)$, $c = 44.499(5)$ Å, $\alpha = \beta = 90^\circ$, $\gamma = 120^\circ$, $V = 5939.8(10)$ Å³, trigonal, $Z = 3$ for $C_{72}H_{60}N_{12}O_6S_6 \times 2 C_4H_8O_2$ with two molecules in the asymmetric unit; $\rho_{\text{calcd}} = 1.243$ gcm⁻³, $\mu = 0.236$ mm⁻¹, $R_{\text{int}} = 0.0586$. The structure was obtained by direct methods using SHELXS-97.¹⁵ The final R value was 0.0641 ($wR2 = 0.1495$) for 9881 observed reflections ($F_0 \geq 4\sigma(|F_0|)$) and 977 variables, $S = 1.081$. The largest difference peak and hole were 0.316 and -0.436 eÅ³, respectively.

X-ray structure analysis of O-methyl tyrosine thiazole cyclic tripeptide (6) crystallized from toluene. Crystals of the cyclic thiazole-containing tripeptide **6** were grown by slow evaporation from a solution of toluene. A single crystal ($0.45 \times 0.34 \times 0.32$ mm) was mounted on a glass fiber. The X-ray data were collected at a temperature of 100 K using Mo K_{α} radiation ($\lambda = 0.71073$ Å), ω -scans ($2\theta = 56.56^\circ$) for a total of 10310 independent reflections. Space group $P2_12_12_1$, $a = 10.477(3)$, $b = 18.005(5)$, $c = 22.648(6)$ Å, $\alpha = \beta = \gamma = 90^\circ$, $V = 4272(2)$ Å³, orthorhombic, $Z = 4$ for $C_{39}H_{36}N_6O_6S_3 \times C_7H_8$ with one

molecule in the asymmetric unit, $\rho_{\text{calcd}} = 1.357$ gcm⁻³, $\mu = 0.231$ mm⁻¹, $R_{\text{int}} = 0.0206$. The structure was obtained by direct methods using SHELXS-97.¹⁵ The final R value was 0.0330 ($wR2 = 0.0876$) for 9498 observed reflections ($F_0 \geq 4\sigma(|F_0|)$) and 554 variables, $S_{\text{Gof}} = 1.070$. The largest difference peak and hole were 0.229 and -0.277 eÅ³, respectively.

Procedure for the synthesis of ethyl ester of Boc-Phenylalanine thiazole (2)

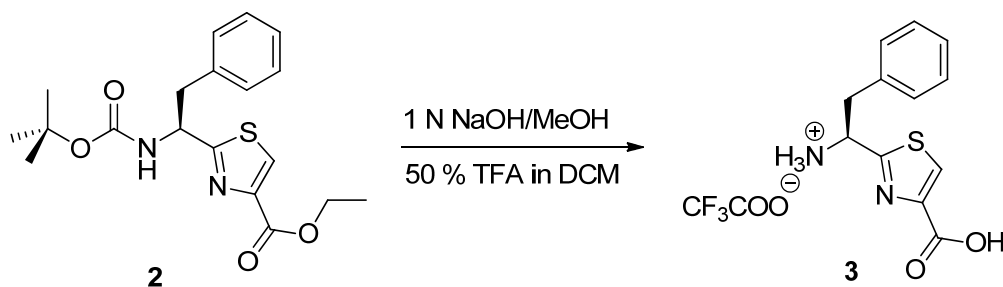
4.38 g (15.6 mmol) of Boc-phenylalanine thioamide **1** in DME (80 mL) was cooled to $-16\text{ }^{\circ}\text{C}$. To this solution 12.50 g (124 mmol) of solid KHCO_3 was added under nitrogen atmosphere. The reaction mixture was stirred for another 20 min prior to the addition of 9.73 g (49.9 mmol) of ethyl bromopyruvate. The reaction mixture was stirred at the same temperature for about 30 min and then at room temperature for another 30 min. The reaction mixture was cooled to $-16\text{ }^{\circ}\text{C}$, then the solution of trifluoroacetic anhydride (8.7 mL, 63 mmol) and 2,6-lutidine (15 mL, 129 mmol) in DME (25 mL) was added in a dropwise manner. The reaction mixture was allowed to reach room temperature and stirred for another 12 h. After the completion of the reaction, volatiles were evaporated under reduced pressure. The reaction mixture was diluted with water and extracted with chloroform ($3 \times 50\text{ mL}$). The combined organic layer was washed with brine and dried over anhydrous Na_2SO_4 . The organic layer was concentrated under reduced pressure and purified by silica gel column chromatography using 20% EtOAc/petroleum ether to afford Ethyl Ester of Boc-Phenylalanine Thiazole **2** as a yellowish solid.



Procedure for the synthesis of Phenylalanine thiazole (3)

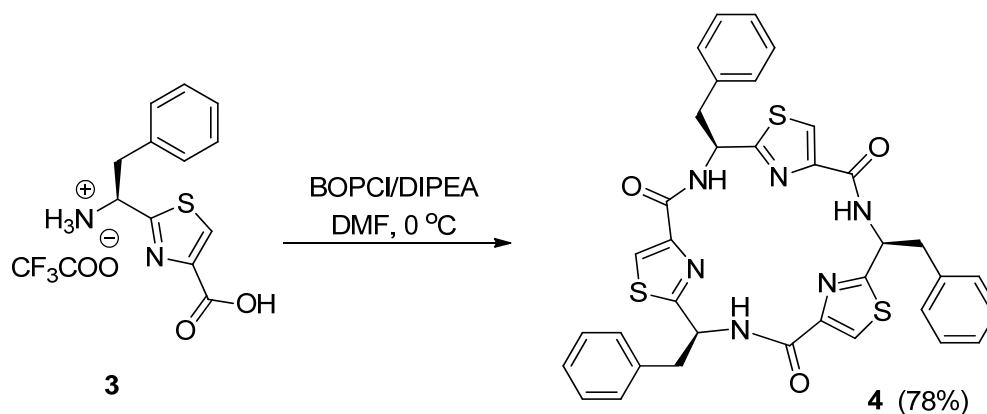
2.0 g (5.3 mmol) of Boc-protected phenylalanine thiazole **2** was dissolved in methanol (7 mL). To this stirred solution, NaOH (1 N, 12 mL) was added dropwise. The reaction mixture was stirred for another 1.5 h. After completion of the reaction, the methanol was evaporated and the aqueous layer was acidified with 5% of aqueous hydrochloric acid. The

aqueous layer was extracted with EtOAc (3 × 30 mL). The organic layer was washed with brine, dried over Na₂SO₄ and concentrated under reduced pressure. The gummy free carboxylic acid was dissolved in dichloromethane (10 mL). To this solution, trifluoroacetic acid (10 mL) was added at 0 °C and stirred for about 1.5 h. After completion of the reaction, the volatiles were removed under reduced pressure and the product (free amino acid) was precipitated using diethyl ether to yield 1.8 g (94%). The free amino acid was directly used in the next step without purification.



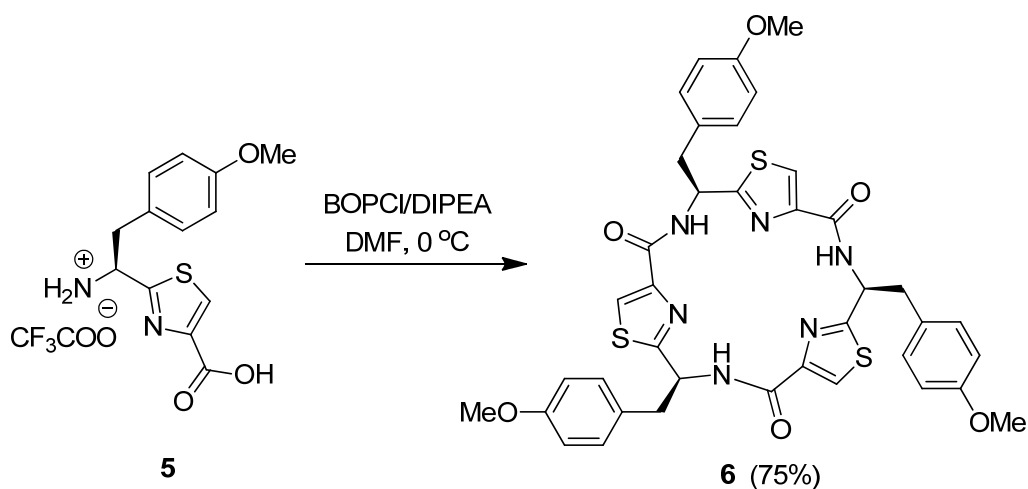
Procedure for the cyclization of phenylalanine thiazole **3** to afford cyclic tripeptide **4**

1.80 g (5.0 mmol) of amino acid trifluoroacetate **3** and 3.34 g (7.5 mmol) of BOPCl were dissolved in DMF (140 mL) and cooled to 0 °C. To this solution 5.48 g (42.4 mmol) of DIPEA was added and the reaction mixture was stirred for further 12 h. After completion of the reaction, the solvent was evaporated under reduced pressure and diluted with EtOAc (150 mL). The organic layer was washed with 5% HCl (2 × 50 mL), saturated NaHCO₃ solution (3 × 50 mL), brine (50 mL) and dried over anhydrous Na₂SO₄. The organic layer was then concentrated under reduced pressure. The product was purified by silica gel column chromatography using 60 % EtOAc /petroleum ether as solvent system to afford 0.926 g (78%) of the pure cyclic tripeptide **4** as a colorless solid.



Procedure for the cyclization of **5** to afford cyclic tripeptide **6**

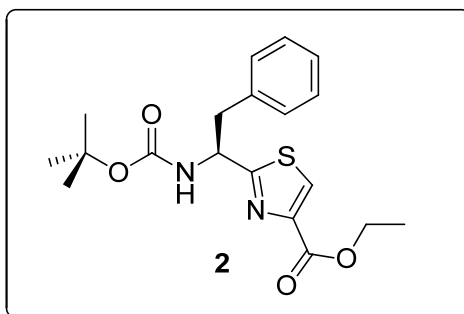
The same protocol as described above was used for the synthesis of the tyrosine-containing cyclic tripeptide **6**. 1.96 g (5.0 mmol) of amino acid trifluoroacetate **5** afforded 1.0 g (75%) of **6** as a white solid.



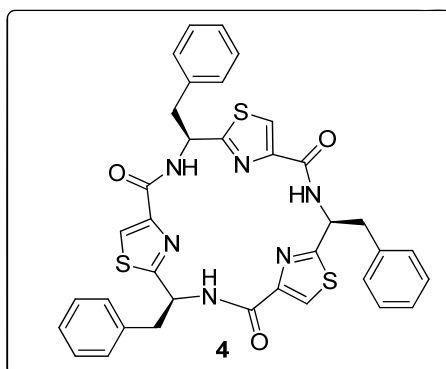
Spectroscopic data for the synthesized compounds

(*S*)-Ethyl 2-(1-((*tert*-butoxycarbonyl)amino)-2-phenylethyl)thiazole-4-carboxylate (**Boc-PheThz-OEt**) (**2**); yellowish solid (5.2 g, 89%), mp = 82-84 °C; UV (λ_{max}) = 235 nm; $[\alpha]_{\text{D}}^{20} + 9.32$ (c = 1, MeOH); IR ν (cm^{-1}) 3352, 2979, 1729, 1693, 1514, 1368, 1251, 1212, 1169, 1093, 1022, 854, 744; $^1\text{H NMR}$ (400 MHz, CDCl_3) δ 8.04 (s, 1H, CH (thiazole)), 7.28-7.22 (dd, 3H, J = 8.3 Hz, 3 \times CH (phenyl)), 7.11-7.09 (d, 2H, J = 6.4 Hz, 2 \times CH (phenyl)), 5.30 (br., 2H, 1 \times NH, Boc, 1 \times CH δ), 4.46-4.40 (q, 2H, J = 6.9 Hz,

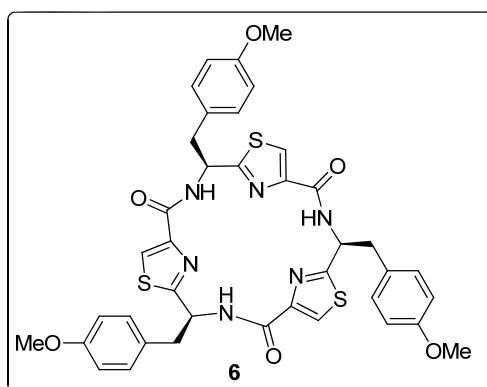
OCH₂CH₃), 3.36-3.30 (t, 2H, CHCH₂Ph), 1.43 (s, 9H, C(CH₃)₃) 1.40-1.34 (t, 3H, *J* = 7.3 Hz, OCH₂CH₃); ¹³C NMR (100 MHz, CDCl₃) δ 173.0, 161.3, 154.9, 147.2, 136.1, 129.3, 128.5, 127.1, 80.2, 61.4, 53.8, 41.5, 28.2, 14.3; HRMS (ESI) *m/z* calcd. for C₁₉H₂₄N₂NaO₄S [M + Na]⁺ 399.1354, observed 399.1346.



Phenylalanine thiazole cyclic tripeptide (4); colorless solid, mp = 131-133 °C; UV (λ_{\max}) = 230 nm; $[\alpha]_D^{20} + 15.63$ (*c* = 1, MeOH); IR ν (cm⁻¹) 3393, 2926, 1668, 1538, 1486, 1277, 1123, 1068, 995, 804, 745, 705; ¹H NMR (400 MHz, CDCl₃) δ 8.65-8.63 (d, 3H, *J* = 8.0 Hz, 3 × NH), 8.02 (s, 3H, CH, thiazole), 7.34-7.29, 7.15-7.13 (m, 15H, 15 × CH (Phenyl)), 5.76-5.71 (m, 3H, 3 × NHCHCH₂), 3.59- 3.54 (dd, 3H, *J* = 4.6 Hz, CHCH₂Ph), 3.13-3.07 (dd, 3H, *J* = 3.6 Hz, CHCH₂Ph); ¹³C NMR (100 MHz, CDCl₃) δ 168.2, 159.4, 148.5, 135.8, 129.7, 128.6, 127.2, 123.9, 52.7, 44.0, 26.8; HRMS (ESI) *m/z* calcd. for C₃₆H₃₀N₆NaO₃S₃ [M + Na]⁺ 713.1439; observed 713.1434.

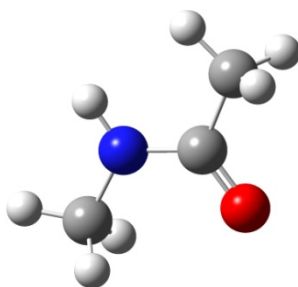


Tyrosine thiazole cyclic tripeptide (6); white solid (1 g, 75%); mp = 115-117 °C; UV (λ_{max}) = 228 nm, 251 nm; $[\alpha]_{\text{D}}^{20} + 18.42$ (c = 1, MeOH); IR ν (cm⁻¹) 3401, 2924, 1665, 1540, 1511, 1383, 1247, 1178, 1107, 1033, 821, 756; ¹H NMR (400 MHz, CDCl₃) δ 8.65-8.63 (d, 3H, *J* = 8.0 Hz, NH, amide), 8.02 (s, 3H, CH(thiazole)), 7.06-7.04 (d, *J* = 8.8 Hz, 6H, 6 × CH(phenyl)), 6.86-6.83 (d, *J* = 8.8 Hz, 6H, 6 × CH(phenyl)), 5.70-5.65 (m, 3H, 3 × CH, NHCH₂), 3.80 (s, 9H, 3 × OCH₃), 3.53-3.48 (dd, 3H, *J* = 4.4 Hz, CHCH₂), 3.06-3.00 (dd, 3H, *J* = 4.4 Hz, -CHCH₂-); ¹³C NMR (125 MHz, CDCl₃) δ 168.4, 159.5, 158.8, 148.6, 130.7, 127.8, 123.9, 113.9, 55.2, 52.9, 43.1; HRMS (ESI) *m/z* calcd. for C₃₉H₃₆N₆NaO₆S₃ [M + Na]⁺ 803.1756 observed 803.1754.



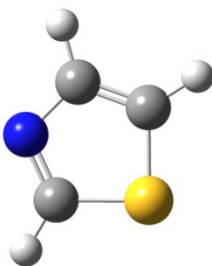
Gaussian Archive Entries

N-Methylacetamide



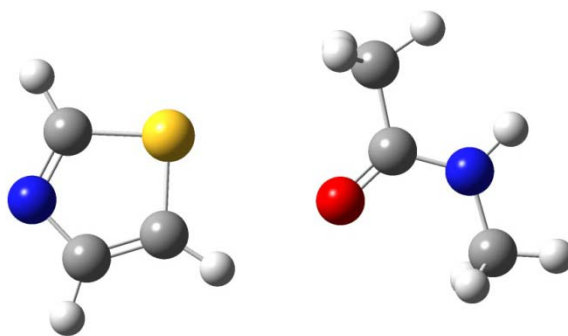
```
1\1\GINC-WERZ01\FOpt\RMP2-FC\6-311++G(3df,3pd)\C3H7N1O1\TSCHNEI\22-Jul-2011\0\# opt freq mp2/6-311++g(3df,3pd)\CI_nmethylacetamid_mp2x\0,1\O,0.0131981205,-0.1169987717,0.0071785189\N,0.000852302,0.0002964966,2.258888535\H,0.5358279133,0.1250452352,3.0981765616\C,-1.4292745376,-0.2123543175,2.3364645328\C,2.1205585422,0.260716973,1.0901881127\C,0.6282388819,0.0316733138,1.0543260396\H,2.3452839086,1.1584373873,0.5196017882\H,2.516824366,0.3669354518,2.0973989685\H,-1.9614500539,0.5692590582,1.7984889424\H,-1.6981515027,-1.1688648119,1.8933123231\H,-1.7291361067,-0.2008633476,3.379894717\H,2.6096937561,-0.5761864314,0.5980986424\Version=AM64L-G03RevC.02\State=1-A\HF=-247.0989375\MP2=-248.0566111\RMSD=6.049e-09\RMSF=4.750e-06\Thermal=0.\Dipole=0.3660707,0.1322788,1.4481585\PG=C01 [X(C3H7N1O1)]\
```

Thiazole



```
1\1\GINC-WERZ01\FOpt\RMP2-FC\6-311++G(3df,3pd)\C3H3N1S1\TSCHNEI\22-Jul-2011\0\# opt freq mp2/6-311++g(3df,3pd)\CI_thiazole_mp2x\0,1\S,0.,0.,0.\N,0.,0.,2.56102248\C,0.7965715533,0.,1.5138769541\C,-1.5009888288,0.,0.7951594848\H,-2.4320623678,0.0001131835,0.2539215152\C,-1.3007850353,0.,2.1564919292\H,-2.0889234165,0.0000923103,2.8938971204\H,1.8734668237,-0.0002487463,1.5792743656\Version=AM64L-G03RevC.02\State=1-A\HF=-567.3765084\MP2=-568.2310087\RMSD=4.911e-09\RMSF=3.911e-06\Thermal=0.\Dipole=-0.2690089,-0.0000072,-0.6719753\PG=C01 [X(C3H3N1S1)]\
```

Local Minimum Model System A



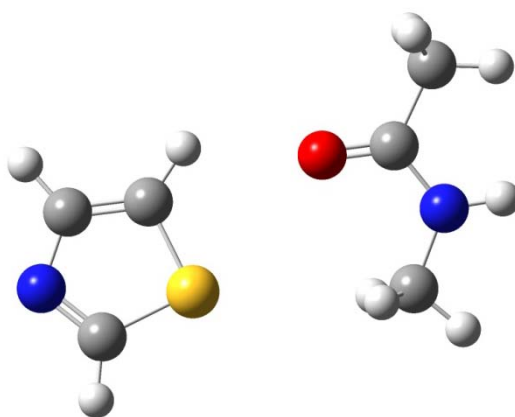
```
1\1\GINC-WERZ01\FOpt\RMP2-FC\6-311++G(3df,3pd)\C6H10N2O1S1\TSCHNEI\12-J
an-2012\0\# opt=modredundant mp2/6-311++g(3df,3pd) int=ultrafine\CI_thiazole_nmeth
ylacetamid_mp2opt4.com\0,1\C,-0.0016863104,-0.003069043,0.00018027\C,-0.0003545
458,0.0082632022,2.409033447\S,1.2047034795,0.0074454048,1.1959975438\H,0.26539
87481,-0.00456669,-1.0421511485\H,0.2549779996,0.0137226254,3.4576205724\C,-1.23
88431875,-0.0041094713,0.601157783\N,-1.2413392379,0.0016582616,1.9653772911\H,
-2.1783291822,-0.0096396186,0.0692205736\O,2.590951515,0.0165308394,-1.61086423
3\C,3.8150050973,-0.0659363508,-1.5961013306\H,5.6623099818,-0.3702316314,-0.479
4206353\H,4.3879916929,0.5398577748,0.3546835537\N,4.5445351076,0.0426410942,-
2.7319798811\C,4.5895302126,-0.2883021195,-0.3209422005\H,4.223885401,-1.196246
6203,0.1525627648\H,5.5440774753,-0.0310492488,-2.6835079456\C,3.8956420825,0.2
630332432,-4.0082038628\H,3.2145588277,-0.5540733774,-4.235997526\H,4.655743749
4,0.3253483553,-4.7807004027\H,3.3221938574,1.1872233061,-3.9893431792\Version=
AM64L-G03RevC.02\State=1-A\HF=-814.478299\MP2=-816.2961198\RMSD=7.080e-09
\RMSF=4.126e-05\Thermal=0.\Dipole=2.317886,-0.0349549,-1.187341\PG=C01 [X(C6H
10N2O1S1)]\
```

Counterpoise: corrected energy = -816.294533929322

Counterpoise: BSSE energy = 0.001585855423

```
1\1\GINC-WERZ01\SP\RMP2-FC\6-311++G(3df,3pd)\C6H10N2O1S1\TSCHNEI\02-Ma
r-2012\0\# mp2/6-311++g(3df,3pd) counterpoise=2\CI_thiazole_nmethyacetamid_count
erpoise\0,1\C,0,-1.642657,-1.001265,0.082445\C,0,-3.255409,0.778303,-0.104306\S,0,-1.
54814,0.686705,-0.08276\H,0,-0.746078,-1.592909,0.144849\H,0,-3.768325,1.722993,-0.
200413\C,0,-2.963718,-1.38313,0.109115\N,0,-3.879494,-0.377408,0.004181\H,0,-3.3048
27,-2.40287,0.206048\O,0,1.3615,-0.462386,0.03481\C,0,2.259716,0.373305,0.047196\H,
0,2.880788,2.459554,0.165281\H,0,1.38249,2.14163,-0.730212\N,0,3.563061,0.011207,-0.
019137\C,0,1.978805,1.852902,0.132331\H,0,1.383624,2.041815,1.022465\H,0,4.272086
,0.721107,-0.005352\C,0,3.937936,-1.385119,-0.109276\H,0,3.579073,-1.933265,0.75916
\H,0,5.020195,-1.454092,-0.157715\H,0,3.506218,-1.838725,-0.998763\Version=AM64L
-G03RevC.02\State=1-A\HF=-247.0987732\MP2=-248.0565763\RMSD=3.912e-
09\Thermal=0.\PG=C01 [X(C6H10N2O1S1)]\
```

Local Minimum Model System B



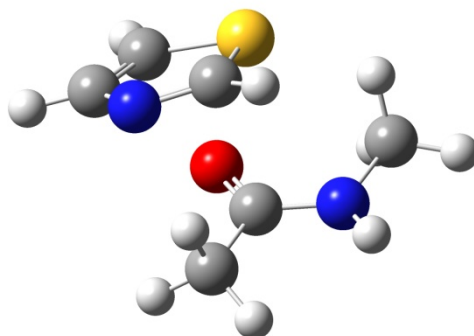
```
1\1\GINC-WERZ01\FOpt\RMP2-FC\6-311++G(3df,3pd)\C6H10N2O1S1\TSCHNEI\25-J
an-2012\0\# opt=modredundant mp2/6-311++g(3df,3pd)\CI_thiazole_nmethylacetamid_s
witch_opt\0,1\C,0.0096587541,0.0185378164,0.0392499352\C,-0.0758392447,0.144247
8062,2.4439298959\S,1.1653814577,-0.0437468688,1.2828652236\H,0.3124749867,-0.06
27083839,-0.9903623804\H,0.1404786314,0.1727735641,3.5008631006\C,-1.241422825
6,0.1777419137,0.5883521084\N,-1.2928306676,0.248911335,1.9496862022\H,-2.15595
82211,0.2473718278,0.0188150799\O,2.5709099446,-0.3986908356,-1.5408154987\C,3.
6628712777,-0.6606308812,-2.035283442\C,3.893054811,-0.6530630866,-3.5259896535
\H,4.9138697975,-0.9028362545,-3.8051007369\H,3.2110815838,-1.3653207545,-3.9840
11358\H,3.6475093862,0.3348869543,-3.907804619\N,4.7297275177,-0.9750983736,-1.2
630679008\H,5.6104926017,-1.1782873503,-1.6988356038\C,4.6103588284,-1.00725914
69,0.1804866476\H,5.5626712216,-1.311922579,0.6036323336\H,4.3397336579,-0.0259
851947,0.5652686386\H,3.8375963116,-1.7114039994,0.4815032083\\Version=AM64L-
G03RevC.02\State=1-A\HF=-814.4783317\MP2=-816.296503\RMSD=9.189e-09\RMSF=
1.942e-05\Thermal=0.\Dipole=2.3418482,-0.5086144,-0.9412455\PG=C01 [X(C6H10N2
O1S1)]\
```

Counterpoise: corrected energy = -816.294850372975

Counterpoise: BSSE energy = 0.001652638336

```
1\1\GINC-WERZ01\SP\RMP2-FC\6-311++G(3df,3pd)\C6H10N2O1S1\TSCHNEI\02-Ma
r-2012\0\# mp2/6-311++g(3df,3pd) counterpoise=2\CI_thiazole_nmethylacetamid_switc
h_counterpoise\0,1\C,0,1.619168,-1.004534,-0.046087\C,0,3.140506,0.860504,0.066885\
S,0,1.441635,0.675964,0.128727\H,0,0.753972,-1.64435,-0.067833\H,0,3.605175,1.83171
4,0.14137\C,0,2.956262,-1.313472,-0.139895\N,0,3.819885,-0.259394,-0.076541\H,0,3.3
47206,-2.312984,-0.257091\O,0,-1.40463,-0.726902,0.055194\C,0,-2.600358,-0.454444,0.
016551\C,0,-3.66921,-1.517632,0.065871\H,0,-4.678598,-1.115317,0.025479\H,0,-3.5194
98,-2.196403,-0.770214\H,0,-3.546072,-2.088089,0.983224\N,0,-3.029339,0.826571,-0.07
4902\H,0,-4.014535,1.015697,-0.098255\C,0,-2.079709,1.919597,-0.126186\H,0,-2.62517
8,2.852348,-0.232066\H,0,-1.48075,1.950682,0.781821\H,0,-1.40463,1.796139,-0.970354
\\Version=AM64L-G03RevC.02\State=1-A\HF=-247.0987544\MP2=-
248.0565752\RMSD=3.921e-09\Thermal=0.\PG=C01 [X(C6H10N2O1S1)]\
```

Global Minimum



```
1\1\GINC-WERZ01\FOpt\RMP2-FC\6-311++G(3df,3pd)\C6H10N2O1S1\TSCHNEI\14-S
ep-2011\0\# opt freq mp2/6-311++g(3df,3pd)\CI_thiazole_nmethylacetamid_mp2opt2\0,
1\C,0.2430232442,-0.247909081,-0.5123663439\C,1.0405175259,1.3117199504,1.14565
62224\S,0.8699232946,1.3293771093,-0.5577509958\H,-0.0082253628,-0.7798981935,-1
.4141369193\H,1.4263572202,2.1654802662,1.6810717918\C,0.2007440941,-0.6852665
997,0.7919629406\N,0.6537867757,0.1957335966,1.7291072489\H,-0.1501673482,-1.65
83160327,1.1003403844\O,2.4984665064,-1.2335216614,-2.3982678042\C,3.316589074
3,-0.7198174938,-1.6437930301\H,4.6114126627,-0.9871001731,0.0796137438\H,2.8787
676924,-0.8640242785,0.4280949249\N,3.9927010142,0.40683153,-1.9906651636\C,3.6
17838691,-1.2613195405,-0.2692805694\H,3.5196450582,-2.3422663779,-0.2871048855
\H,4.577095525,0.8496384199,-1.3045266395\C,3.6739491338,1.1069070582,-3.216053
0326\H,3.6995082395,0.411421425,-4.0504421874\H,4.4086496926,1.8902767537,-3.37
68816108\H,2.6777241714,1.5487365669,-3.1727656173\\Version=AM64L-G03RevC.02
\State=1-A\HF=-814.4717978\MP2=-816.2987762\RMSD=1.989e-09\RMSF=5.387e-
06\Thermal=0.\Dipole=0.8804934,0.9305858,-0.1619916\PG=C01 [X(C6H10N2O1S1)]\
```

Counterpoise: corrected energy = -816.295369173592

Counterpoise: BSSE energy = 0.003580558643

```
1\1\GINC-WERZ01\SP\RMP2-FC\6-311++G(3df,3pd)\C6H10N2O1S1\TSCHNEI\17-Au
g-2011\0\# mp2/6-311++g(3df,3pd) counterpoise=2\CI_1_opt_counterpoise\0,1\C,0,1.2
843,-0.342106,1.154437\C,0,2.200417,-0.327235,-1.076309\S,0,0.981128,-1.215729,-0.26
8587\H,0,0.692503,-0.497213,2.04048\H,0,2.444721,-0.518058,-2.109952\C,0,2.29465,0.
564573,0.926587\N,0,2.810392,0.576164,-0.335168\H,0,2.679914,1.250637,1.665668\O,
0,-1.773228,-0.006696,1.362312\C,0,-2.149965,0.011993,0.196068\H,0,-3.497462,-0.775
899,-1.329689\H,0,-2.562357,-1.97446,-0.420038\N,0,-1.734857,0.946488,-0.697267\C,0,
-3.097721,-1.028862,-0.350227\H,0,-3.914553,-1.159083,0.353889\H,0,-2.045296,0.8602
14,-1.648652\C,0,-0.751523,1.957695,-0.368536\H,0,-0.730338,2.060393,0.711891\H,0,-
1.033582,2.907173,-0.817401\H,0,0.244525,1.676612,-0.712385\\Version=AM64L-G03R
evC.02\State=1-A\HF=-247.0983779\MP2=-248.0562544\RMSD=3.768e-
09\Thermal=0.\PG=C01 [X(C6H10N2O1S1)]\
```

4.6 References

1. a) Davidson, B. S. *Chem. Rev.* **1993**, *93*, 1771; b) Wipf, P. *In Alkaloids: Chemical and Biological Perspectives*, Pelletier, S. W., Ed.; Pergamon: New York, **1998**, 187; c) Wipf, P.; Uto, Y. *J. Org. Chem.* **2000**, *65*, 1037, and references cited therein; d) Bertram, A.; Pattenden, G. *Nat. Prod. Rep.* **2007**, *24*, 18; e) Bagley, M. C.; Dale, J. W.; Merritt, E. A.; Xiong, X. *Chem. Rev.* **2005**, *105*, 685; f) Yeh, V. S. C. *Tetrahedron* **2004**, *60*, 11995; g) Roy, R. S.; Gehring, A. M.; Milne, J. C.; Belshaw, P. J.; Walsh, C. T. *Nat. Prod. Rep.* **1999**, *16*, 249 h) Houssen, W. E.; Jaspars, M. *ChemBioChem* **2010**, *11*, 1803; i) Bertram, A.; Blake, A. J.; de Turiso, F. G. L.; Hannam, J. S.; Jolliffe, K. A.; Pattenden, G.; Skae, M. *Tetrahedron* **2003**, *59*, 6979; (j) Haberhauer, G.; Drosdow, E.; Oeser, T.; Rominger, F. *Tetrahedron* **2008**, *64*, 1853 and references cited therein.
2. a) Sohda, K.; Hiramoto, M.; Suzumura, K.; Takebayashi, Y.; Suzuki, K.; Tanaka, A. *J. Antibiot.* **2004**, *58*, 32; b) Linington, R. G.; Gonzalez, J.; Urena, L.-D.; Romero, L. I.; Ortega-Barria, E.; Gerwick, W. H. *J. Nat. Prod.* **2007**, *70*, 397; c) Tan, L. T.; Williamson, R. T.; Gerwick, W. H.; Watts, K. S.; McGough, K.; Jacobs, R. *J. Org. Chem.* **2000**, *65*, 419; d) Roy, R. S.; Gehring, A. M.; Milne, J. C.; Belshaw, P. J.; Walsh, C. T. *Nat. Prod. Rep.* **1999**, *16*, 249; e) Li, Y.-M.; Milne, J. C.; Madison, L. L.; Koller, R.; Walsh, C. T. *Science* **1996**, *274*, 1188.
3. a) Michael, J. P.; Pattenden, G. *Angew. Chem. Int. Ed.* **1993**, *32*, 1; b) Bertram, A.; Pattenden G., *Nat. Prod. Rep.* **2007**, *24*, 18.
4. a) Williams, A. B.; Jacobs, R. S. *Cancer Lett.* **1993**, *71*, 97; b) Ogino, J.; Moore, R. E.; Patterson, G. M. L.; Smith, C. D. *J. Nat. Prod.* **1996**, *59*, 581 c) Pucci, M. J.; Bronson, J. J.; Barrett, J. F.; DenBleyker, K. L.; Discotto, L. F.; Fung-Tome, J. C.; Ueda, Y. *Antimicrob. Agents Chemother.* **2004**, *48*, 3697; d) Sohda, K. Y.; Hiramoto, M.; Suzumura, K. I.; Takebayashi, Y.; Suzuki, K. I.; Tanaka, A. *J. Antibiot.* **2004**, *58*, 32; e) Wagner, B.; Schumann, D.; Linne, U.; Koert, U.; Marahiel, M. A. *J. Am. Chem. Soc.* **2006**, *128*, 10513; f) Lentzen, G.; Klinck, R.; Matassova, N.; Aboul-ela, F.; Murchie, A. I. H. *Chem. Biol.* **2003**, *10*, 769; g) Linington, R. G.; Gonzalez, J.; Urena, L. D.; Romero, L. I.; Ortega-Barria, E.; Gerwick, W. H. *J. Nat. Prod.* **2007**, *70*, 397; h) Tan, L. T.; Williamson, R. T.; Gerwick, W. H.; Watts, K. S.; McGough, K.; Jacobs, R. *J. Org. Chem.* **2000**, *65*, 419; i) Portmann, C.; Blom, J. F.; Gademann, K.; Juttner, F. *J. Nat. Prod.* **2008**, *71*,

- 1193; j) Wipf, P.; Venkatraman, S.; Miller, C. P.; Geib, S. J. *Angew. Chem., Int. Ed.* **1994**, *33*, 1516; k) Wipf, P.; Miller, C. P.; Grant, C. M. *Tetrahedron* **2000**, *56*, 9143; l) Bertram, A.; Hannam, J. S.; Jolliffe, K. A.; González-Lo'pez de Turiso, F.; Pattenden, G. *Synlett* **1999**, 1723; m) Downing, S. V.; Aguilar, E.; Meyers, A. I. *J. Org. Chem.* **1999**, *64*, 826; n) Aguilar, E.; Meyers, A. I. *Tetrahedron Lett.* **1994**, *35*, 2477; o) Bertram, A.; Pattenden, G. *Heterocycles* **2002**, *58*, 521.
5. a) Fairlie, D. P.; West, M. W.; Wong, A. K.; *Curr. Med. Chem.* **1998**, *5* 29; b) Lucke, A. J.; Tyndall, J. D. A.; Singh, Y.; Fairlie, D. P. *J. Mol. Graph. Model.* **2003**, *21*, 341; (c) Singh, Y.; Sokolenko, N.; Kelso, M. J.; Gahan, L. R.; Abbenante, G.; Fairlie, D. P. *J. Am. Chem. Soc.* **2001**, *123*, 333; (d) Singh, Y.; Stoermer, M. J.; Lucke, A. J.; Guthrie, T.; Fairlie, D. P. *J. Am. Chem. Soc.* **2005**, *127*, 6563.
6. a) Reichardt, C. *Solvents and Solvent Effects in Organic Chemistry*; VCH: New York, 1990. b) Williams, C.; Bochar, F.; Frisch, H. L. *Annu. Rev. Phys. Chem.* **1981**, *32*, 433; c) Singer, P. T.; Smalas, A.; Carty, R. P.; Mangel, W. F.; Sweet, R. M. *Science* **1993**, *259*, 669; d) Berne, B. J.; Weeks, J. D.; Zhou, R. H. *Annu. Rev. Phys. Chem.* **2009**, *60*, 85. e) Cheng, Y. K.; Rossky, P. J. *Nature* **1998**, *392*, 696.
7. a) Burdick, D.; Soreghan, B.; Kwon, M.; Kosmoski, J.; Knauer, M.; Henschen, A.; Yates, J.; Cotman, C.; Glabe, C. *J. Biol. Chem.* **1992**, *267*, 546. b) Cruz, L.; Urbanc, B.; Borreguero, J. M.; Lazo, N. D.; Teplow, D. B.; H. Eugene Stanley, H. E. *Proc. Natl. Acad. Sci. U.S.A.* **2005**, *102*, 18258. c) Coles, M.; Bicknell, W.; Watson, A. A.; Fairlie, D. P.; Craik, D. J. *Biochemistry* **1998**, *37*, 11064.
8. a) Lansbury, P. T.; Costa, P. R.; Griffiths, J. M.; Simon, E. J.; Auger, M.; Halverson, K. J.; Kocisko, D. A.; Hendsch, Z. S.; Ashburn, T. T.; Spencer, R. G. S.; Tidor, B.; Griffin, R. G. *Nat. Struct. Biol.* **1995**, *2*, 990; b) Petkova, A. T.; Leapman, R. D.; Guo, Z. H.; Yau, W. M.; Mattson, M. P.; Tycko, R. *Science* **2005**, *307*, 262; c) Luhrs, T.; Ritter, C.; Adrian, M.; Riek-Loher, D.; Bohrmann, B.; Dobeli, H.; Schubert, D.; Riek, R. *Proc. Natl. Acad. Sci. U.S.A.* **2005**, *102*, 17342.
9. a) Gazit, E. *Chem. Soc. Rev.* **2007**, *36*, 1263; b) Matson, J. B.; Zha, R. H.; Stupp, S. I. *Curr. Opin. Solid State Mater. Sci* **2011**, *15*, 225; c) Matson, J. B.; Stupp, S. I. *Chem. Commun.* **2012**, *48*, 26.
10. Hirst, A. R.; Escuder, B.; Miravet, J. F.; Smith, D. K. *Angew. Chem., Int. Ed.* **2008**, *47*, 8002.
11. Mooibroek, T. J.; Gamez, P.; Reedijk, J. *CrystEngComm* **2008**, *10*, 1501.

12. a) Jeffrey, G. A. *An Introduction to Hydrogen Bonding*; Oxford University Press: New York, 1997. b) Desiraju, G. R.; Steiner, T. *The Weak Hydrogen Bond in Structural Chemistry and Biology*; Oxford Science Publications: Oxford, 1999. c) Hobza, P.; Havlas, Z. *Chem. Rev.* **2000**, *100*, 4253; d) Desiraju, G. R. *Angew. Chem., Int. Ed.* **2007**, *46*, 8342; e) Gu, Y.; Kar, T.; Scheiner, S. *J. Am. Chem. Soc.* **1999**, *121*, 9411.
13. a) Alcock, N. W. *Adv. Inorg. Chem. Radiochem.* **1972**, *15*, 1; b) Angyan, J. G.; Poirier, R. A.; Kucsman, A.; Csizmadia, I. G. *J. Am. Chem. Soc.* **1987**, *109*, 2237; c) Bürgi, H.-B.; Dunitz, J. D. *J. Am. Chem. Soc.* **1987**, *109*, 2924. d) Minkin, V. I.; Minyaev, R.M. *Chem. Rev.* **2001**, *101*, 1247; e) Bleiholder, C.; Werz, D. B.; Köppel, H.; Gleiter, R. *J. Am. Chem. Soc.* **2006**, *128*, 2666; f) Nagao, Y.; Miyamoto, S.; Miyamoto, M.; Takeshige, H.; Hayashi, K.; Sano, S.; Shiro, M.; Yamaguchi, K.; Sei, Y. *J. Am. Chem. Soc.* **2006**, *128*, 9722; g) Sanz, P.; Yanez, M.; Mo, O. *Chem. Eur. J.* **2003**, *9*, 4548; h) Bleiholder, C.; Gleiter, R.; Werz, D. B.; Köppel, H. *Inorg. Chem.* **2007**, *46*, 2249; i) Iwaoka, M.; Takemoto, S.; Tomoda, S. *J. Am. Chem. Soc.* **2002**, *124*, 10613; j) Nagao, Y.; Hirata, T.; Goto, S.; Sano, S.; Kakehi, A.; Iizuka, K.; Shiro, M. *J. Am. Chem. Soc.* **1998**, *120*, 3104; k) Wu, S.; Greer, A. *J. Org. Chem.* **2000**, *65*, 4883; l) Tripathi, S. K.; Patel, U.; Roy, D.; Sunoj, R.B.; Singh, H. B.; Wolmershauser, G.; Butcher, R. J. *J. Org. Chem.* **2005**, *70*, 9237; m) Gonzalez, F. V.; Jain, A.; Rodriguez, S.; Saez, J.A.; Vicent, C.; Peris, G. *J. Org. Chem.* **2010**, *75*, 5888.
14. a) Werz, D. B.; Gleiter, R.; Rominger, F. *J. Am. Chem. Soc.* **2002**, *124*, 10638; b) Werz, D. B.; Staeb, T. H.; Benisch, C.; Rausch, B. J.; Rominger, F.; Gleiter, R. *Org. Lett.* **2002**, *4*, 339; c) Werz, D. B.; Gleiter, R.; Rominger, F. *J. Org. Chem.* **2002**, *67*, 4290; d) Werz, D. B.; Rausch, B. J.; Gleiter, R. *Tetrahedron Lett.* **2002**, *43*, 5767; e) Werz, D. B.; Gleiter, R.; Rominger, F. *Organometallics* **2003**, *22*, 843; f) Gleiter, R.; Werz, D. B.; Rausch, B. J. *Chem. Eur. J.* **2003**, *9*, 2676; g) Schulte, J. H.; Werz, D. B.; Rominger, R.; Gleiter, R. *Org. Biomol. Chem.* **2003**, *1*, 2788; h) Werz, D. B.; Gleiter, R. *J. Org. Chem.* **2003**, *68*, 9400; i) Werz, D. B.; Gleiter, R.; Rominger, F. *J. Org. Chem.* **2004**, *69*, 2945; j) Gleiter, R.; Werz, D. B. *Chem. Lett.* **2005**, *34*, 126; k) Werz, D. B.; Gleiter, R.; Rominger, F. *J. Organomet. Chem.* **2004**, *689*, 627; l) Werz, D. B.; Fischer, F. R.; Kornmayer, S. C.; Rominger, F.; Gleiter, R. *J. Org. Chem.* **2008**, *73*, 8021; m) Gleiter, R.; Werz, D. B. *Chem. Rev.* **2010**, *110*, 4447.

15. Taylor, J. C.; Markham, G. D. *J. Biol. Chem.* **1999**, *274*, 32909.
16. a) Li, H.; Hallows, W. H.; Punzi, J. S.; Marqued, V. E.; Carrell, H. L.; Pankiewicz, L. K. W.; Watanabe, K. A.; Goldstein, B. M. *Biochemistry* **1994**, *33*, 23; b) Burling, F. T.; Goldstein, B. M. *J. Am. Chem. Soc.* **1992**, *114*, 2313 c) Franchetti, P.; Cappellacci, L.; Grifantini, M.; Barzi, A.; Nocentini, G.; Yang, H.; OConnor, A.; Jayaram, H. N.; Carrell, C.; Goldstein, B. M. *J. Med. Chem.* **1995**, *38*, 3829 d) Goldstein, B. M.; Li, H.; Hallows, W. H.; Langs, D. A.; Franchetti, P.; Cappellacci, L.; Grifantini, M. *J. Med. Chem.* **1994**, *37*, 1684; e) Goldstein, B. M.; Takusagawa, F.; Berman, H. M.; Srivastava, P. C.; Robinst, R. K. *J. Am. Chem. Soc.* **1983**, *105*, 7416.
17. Iwaoka, M.; Takemoto, S.; Tomoda, S. *J. Am. Chem. Soc.* **2002**, *124*, 10613.
18. Wu, S.; Greer, A. *J. Org. Chem.* **2000**, *65*, 4883.
19. a) Møller, C.; Plesset, M. S. *Phys. Rev.* **1934**, *46*, 618; b) Pople, J. A.; Seeger, R.; Krishnan, R. *Int. J. Quantum Chem. Symp.* **1977**, *11*, 149; c) Pople, J. A.; Binkley, J. S.; Seeger, R. *Int. J. Quantum Chem. Symp.* **1976**, *10*, 1.
20. a) Krishnan, R.; Binkley, J. S.; Seeger, R.; Pople, J. A. *J. Chem. Phys.* **1980**, *72*, 650; b) McLean, A. D.; Chandler, G. S. *J. Chem. Phys.* **1980**, *72*, 5639; c) Curtiss, L. A.; McGrath, M. P.; Blaudeau, J.-P.; Davis, N. E.; Binning, R. C., Jr.; Radom, L. *J. Chem. Phys.* **1995**, *103*, 6104; d) Clark, T.; Chandrasekhar, J.; Spitznagel, G. W.; Schleyer, P. V. R. *J. Comput. Chem.* **1983**, *4*, 294.
21. Pople J. A.; et al. *Gaussian03*, Revision B.03; Gaussian, Inc.: Wallingford, CT, 2004.
22. Foster, J. P.; Weinhold, F. *J. Am. Chem. Soc.* **1980**, *102*, 7211.
23. SAINT v4 software reference manual. Madison, Wisconsin, USA: Siemens Analytical X-Ray Systems, Inc.; 2000.
24. Sheldrick, G. M. SADABS, program for empirical absorption correction of area detector data, Universität Göttingen (Germany) 2000.
25. SHELXS-97: Sheldrick, G. M. *Acta Crystallogr. Sect A* **1990**, *46*, 467; b) Sheldrick, G. M., SHELXL-97, Universität Göttingen (Germany) 1997.

4.7 Appendix I: Characterization Data of Synthesized Compounds

Designation	Description	Page
Boc-Phe-Thz-OEt (2)	¹ H NMR (400 MHz)	248
Boc-Phe-Thz-OEt (2)	¹³ C NMR (400 MHz)	248
Cyclic tripeptide-Phe-Thz (4)	¹ H NMR (400 MHz)	249
Cyclic tripeptide-Phe-Thz (4)	¹³ C NMR (400 MHz)	249
Cyclic tripeptide-Tyr-Thz (6)	¹ H NMR (400 MHz)	250
Cyclic tripeptide-Tyr-Thz (6)	¹³ C NMR (400 MHz)	250

